MODELING OF A THIN-LIQUID FALLING-FILM IN ABSORPTION COOLING SYSTEMS

BY

Kamilu Moradeyo ODUNFA

B.Sc. (Hons) Mechanical Engineering (Ibadan)

M. Sc. Mechanical Engineering (Ibadan)

M. Phil. Mechanical Engineering (Ibadan)

(Matriculation Number: 44113)

A thesis in the Department of

MECHANICAL ENGINEERING

Submitted to Faculty of Technology in partial fulfillment

of the requirement for the Degree of DOCTOR OF PHILOSOPHY

of the

UNIVERSITY OF IBADAN

Mechanical Engineering Department,

University of Ibadan,

Ibadan.

MARCH 2012

UNIVERSITY OF IBADAN

ABSTRACT

Absorption refrigeration systems are generally characterized by low Coefficient of Performance (COP). Absorption enhancement is an effective way of improving the COP of refrigeration systems. Literature is sparse on the use of magnetic field for the enhancement of absorption refrigeration systems despite its cheapness and environmental friendliness as compared with other enhancement methods. Although the method has recently been employed on ammonia solution, its influence on lithium bromide (LiBr) and lithium chloride (LiCl) solutions is yet to be fully studied. In this study a numerical model for the magnetic field enhancement of the absorption cooling-system using LiBr and LiCl solutions was developed and evaluated.

The flow within the film thickness to the absorber wall was considered as a two-dimensional steady laminar flow. A Finite Difference model was developed based on conservation of mass, momentum, energy equations and mass transport relationship. The model was validated using data from the literature on ammonia solution. Standard parameters including absorber wall length (1 m), film thickness (10^{-3} m), magnetic field vacuum permeability (1.257 x 10^{-6} $kgmA^{-2}s^{-2}$), magnetic mass susceptibilities and magnetic induction intensities were used for LiBr and LiCl solutions' modeling. Changes in their concentrations, both in the direction of falling film and across its thickness, were investigated. Data were analysed using descriptive statistics and Student's t-test (p=0.05).

The concentration distribution for ammonia solution within the film thickness was not significantly different from results in the literature. For the magnetic induction range of 0.0 and 3.0 Tesla, the concentration distribution of LiBr solution in the direction of falling film was between 54.9% and 60.0%, while that of LiCl solution ranged between 39.9% - 45.0%. Meanwhile, across the film thickness and for the same range of magnetic induction of 0.0 and 3.0 Tesla, the concentration distribution for LiBr solution was between 0.0 and 0.19 and those of LiCl solution were between 0.0 and 0.13. The concentration of LiBr solution increased from 0.0 to 4.7 and 0.0 to 21.7 when magnetic induction was increased from 0.0 to 1.4 and 0.0 to 3.0 Tesla, respectively. Similarly for LiCl solution, increased values of 0.0 to 3.3 and 0.0 to 15.5 were obtained when magnetic induction was increased from 0.0 to 1.4 and 0.0 to 3.0 Tesla, respectively. In both cases, it implies higher cooling effect. Relative to 0.0 Tesla, the COP of LiBr and LiCl solutions

UNIVERSITY OF IBADAN

absorption refrigeration systems was increased by 0.1% when magnetic induction was 1.4 Tesla, while increment of 0.3% and 0.2% respectively were obtained when magnetic induction was 3.0 Tesla. The percentage increments in COP of LiBr solution were not significantly different from that of the LiCl solution.

Magnetic field enhanced the absorption performance in the lithium bromide and lithium chloride solutions; hence can be used in typical absorption refrigeration systems.

Keywords: Magnetic field, Refrigeration, Thin-liquid Falling-film, Absorption cooling-Systems

Word count: 457

UNIVERSITY OF IBADAN

DEDICATION

To all

Who fear God and acknowledge the power of His might,

The doer of His word

Through our Lord Jesus Christ

This work

Is dedicated

UNIVERSITY OF IBADAN

ACKNOWLEDGEMENT

To God be the glory honor and power for His mercy and kindness who out of His marvelous light discovered and set me free from the power of darkness and oppression. He clothed my nakedness, opened my eyes and established my going academically, professionally and in every other ramification of my life. God has been so wonderful to me, He gives me life, strength and sound health even throughout the first frustrating seven years of my imprisonment and entanglement in my first aborted M. Phil degree programme. He did not leave or forsakes me in my successful M. Phil degree programme even up to this end, indeed He is a shelter in time of storm.

I must appreciate my supervisor Prof. R.O Fagbenle for being so kind to me. In my state of academic hopelessness, he assured me of greater hope. For allowing himself to be used of the Lord to gather my battered and shattered academic life, I say a big thank you Sir. In deed you are a builder of life, especially for the young ones, you are also a template of a good Professor; an excellent father academically, professionally and in every other facet of human life, I prophesy onto your life Sir, it shall be well with you and your family. You will continue to be a vessel of honor in God's mansion. Throughout your life you will not sorrow, the joy of the Lord will continue to be your strength.

I am grateful to Prof. A. E Oluleye, the present Dean of the Faculty of Technology, University of Ibadan. He is such a loving and caring father, a template of a Dean in the citadel of learning. He enthusiastically took interest in the progress and development of young ones myself inclusive. Words can not be enough to express my gratitude to you for this. I can only pray that God in His infinite mercies reward you with

UNIVERSITY OF IBADAN

blessings. The Lord will satisfy you with long life and sound health, you will live to eat the fruits of your labour.

I must equally express my gratitude to entire staff of the Department of Mechanical Engineering, University of Ibadan, whose love and concern to see me to the end of this programme was intoxicating. I must specifically thank the immediate and the present head of the Department Dr. O. Oluwole and Dr. M.O Oyewola respectively for helping me throughout, your constant encouragement on this programme has been of tremendous help. God will continue to bless you all. My specific appreciation also goes to Dr. Dare, Dr. T.A.O Salau, Engr. R. Abu, Dr. Ismail, Dr. I.F, Odesola and Dr. Fadare for their supports in one form or the other. To Dr.(Mrs) F,O Akintayo of Civil Engineering Department, I say thank you. The Dean of Postgraduate School Prof. Olorunnisola, you are highly appreciated Sir, Dr. Victor Oladokun and all other heads of the Departments in the Faculty of Technology, I appreciate you all, God will continue to bless you.

I specifically express my appreciation to the past Faculty Sub-Dean Post graduate Dr. Falade of the Department of Food Technology, University of Ibadan. He is such a loving and caring colleague, he enthusiastically took interest in my research work. Words can not be enough to express my gratitude to you for your assistance and support. I can only pray that God in His infinite mercies will reward you with more blessings. The Lord will satisfy you with long life and sound health, you will live to eat the fruits of your labour. Immediate past and present Faculty Sub-Deans Postgraduate Dr. Ogunjuyigbe and Dr. Ewemoje, you are all highly appreciated. My special appreciation also goes to the present Sub-Dean Postgraduate School Dr. J.O Babalola of Chemistry Department and

UNIVERSITY OF IBADAN

immediate past ASUU Chairman, University of Ibadan, Dr Ademola Aremu; May the Lord God continue to lift you all higher and higher.

I must thank specially my loving wife, an Estate Surveyor per excellent Mrs. Victoria Oluwafunmike Odunfa (a.k.a Peace). Indeed you have demonstrated your name by allowing yourself to be the channel of the peace of the Lord to my life. I thank you for your moral support and continued endurance. You have been a vessel of honor in God's mansion, so you will continue to be, I pray that God will continually make you a light to many generations. I am grateful to my God-given children, Victoria, Esther and Victor; in deed you are children of signs and wonder to me. The Lord will build around you the wall of fire that will continually separate you from the dangers of both day and night. You will live to continue to declare the glory of God in the land of the living. I must also appreciate Ojo Temitope O, my able research and engineering assistant, you have been so wonderful and helpful to me in this work, May the Lord God grant you your heart desire.

I am also grateful to the present President of the Gospel Fellowship Incorporated Bro. Abel Aro for his care and concern, and his spiritual support throughout the period of this programme, I say thank you Sir. I am appreciative to the University for the Improved Internet Facilities that have made it possible to have a better grip of the subject of study. There are many others whom I may not be able to mention, but have contributed in one way or the other towards the success of this work. I am grateful to all and wish you success in your endeavours.

K.M Odunfa

UNIVERSITY OF IBADAN

TABLE OF CONTENTS

UNIVERSITY OF IBADAN

UNIVERSITY OF IBADAN

LIST OF FIGURES Page

UNIVERSITY OF IBADAN

UNIVERSITY OF IBADAN

UNIVERSITY OF IBADAN

UNIVERSITY OF IBADAN

UNIVERSITY OF IBADAN

UNIVERSITY OF IBADAN

UNIVERSITY OF IBADAN

UNIVERSITY OF IBADAN

UNIVERSITY OF IBADAN

UNIVERSITY OF IBADAN

UNIVERSITY OF IBADAN

LIST OF TABLES

UNIVERSITY OF IBADAN

UNIVERSITY OF IBADAN

UNIVERSITY OF IBADAN

LIST OF SYMBOLS

	Unit
μ = film dynamic viscosity……	kg/m/s
υ_o = mean velocity……	m/s
α = thermal diffusivity……..……	m^2/s
k = thermal conductivity of fluid …….....	W/m K
ρ = liquid density……..	kg/m^3
D = species diffusivity…… ……	m^2/s
β = cubic expansivity of fluid ……..	K^{-1}
T_w = dimensional wall temperature……	^0C
T_{in} = inlet refrigerant temperature…….	^0C
C_{in} = initial absorbent concentration ……....	%
C_{eq} = equilibrium absorbent concentration……..	%
g = gravity…….	m/s^2
h_0 = mean film thickness……	m
ν = kinematic viscosity of fluid…….	m^2/s
Ha = heat of absorption……...	kJ/kg
Pv = absorbent vapour pressure……....	mm. Hg
R_{ef} = film Reynolds number	
Γ = film mass flow rate	

UNIVERSITY OF IBADAN

CERTIFICATION

I certify that this research work was carried out by Mr. K.M. Odunfa in the Department of Mechanical Engineering, University of Ibadan, Ibadan, Nigeria.

_____

Research Supervisor,

Prof. R. O. Fagbenle. FNSE
B.S.M.E. (Urbana-Champaign), M.S.M.E. (Iowa State), PhD (Urbana-Champaign), R.Engr.
Professor
Department of Mechanical Engineering,
University of Ibadan,
Ibadan, Nigeria.

UNIVERSITY OF IBADAN

CHAPTER ONE

INTRODUCTION

1.1 General Background

In recent years, the terms energy conservation and environmental safety have become a thing of global concern due to the increasing energy prices, energy security and environmental impact of energy prospecting, processing and utilization. In time past, not much emphasis was placed on the issue as it is now. The worldwide attention to Climate Change phenomenon and its impacts which have been conclusively linked to fossil energy use has prompted the emergence of the new technologies in many areas of global economy, such as in cooling system development sector. Cooling system basically may be divided into two categories; Vapour compression system and sorption system. Sorption system is further sub-divided into absorption and adsorption systems. Vapour compression system involves the use of a compressor for the compression process; An absorption system is simply the replacement of the traditional compression with a thermo chemical fluid lifting process. In other words it is the mixture of a gas in a liquid, the two fluids present a strong affinity to form a solution, while adsorption is a process that occurs when a gas or liquid solute accumulates on the surface of a solid or, more rarely, a liquid (adsorbent), forming a molecular or atomic film (the adsorbate).

In the manufacturing of cooling machine/system, for the increasing interest in the efficient use of energy at minimum environmental cost has necessitated the increased demand for absorption refrigeration systems driven by waste heat or solar thermal energy instead of conventional systems driven by fossil-energy derived or conventional. The current imbalance of energy demand and supply coupled with the environmental degradation in many developing countries such as Nigeria has further increased the urgent need for highly efficient and sustainable energy technologies.

In the absorption process, heat and mass transfer usually take place within a thin-liquid falling-film. Heat and mass transfer in thin-liquid falling film absorption process has received the attention of many researchers over the years especially in the last two decades. This is as a result of its wider application in many modern devices such as absorption air-conditioners, absorption chillers, absorption heat pumps etc Yang and Wood (1992). Absorption enhancement is another aspect in this area that has also attracted the attention of researchers. Absorption enhancement is an effective way to improve the performance of absorption refrigeration systems. Generally,

UNIVERSITY OF IBADAN

there are three kinds of methods in absorption enhancement (Kim et al.,2006).The first kind falls under the category of mechanical methods, which improve the performance by modifying the shape, surface and structure of the heat transfer tubes (Chen et al.,2006). The second kind comprise chemical methods which involve the addition of surfactant in the absorbent while the third kind is the addition of nano-particles in the absorbing solution e.g Cu, CuO and Al_2O_3 nano-particles added into ammonia-water solution (Kim et al., 2007a and 2007b), Fe and Carbon nano-tubes (CNT) in lithium bromide-water solution (Yong Tae Kang et al.,2007). Research on nano-fluids / nano-particles in absorbent are categorized into five groups(1) stability analysis and experiments; (2)property measurement such as thermal conductivity and viscosity;(3)convective and boiling heat transfer;(4)mass transfer in binary nanofluids; and (5)theoretical analysis and model development.

However, the effect of magnetic field on absorption refrigeration system is seldom mentioned in the literature apart from its established influence on the absorption process in ammonia vapour into ammonia-water solution absorption refrigeration system (Niu et al., 2006). The magnetic field may therefore also have certain influence on the absorption process in other absorption refrigeration systems such as water vapour into lithium bromide-water solution and water vapour into lithium chloride-water solution absorption system.

In previous studies without any form of enhancement, Andberg (1982), Grossman (1983) and Andberg and Vliet (1983) have employed the modeling technique. Modeling is categorized into two namely (i) Numerical and (ii) Experimental.

Numerical methods have been used over many decades and continue to be developed to effectively tackle many engineering problems. Some of these numerical methods include Finite Element method, finite difference method, boundary element method, Monte Carlo technique and Vortex Method. These methods may be categorized into two: probabilistic approach and deterministic approach. Probabilistic methods generally make constant recourse to random numbers, and Monte Carlo and Vortex element techniques fall into this category while Finite Element, Finite difference and boundary element techniques are deterministic in nature.

In absorption process modeling either unenhanced or enhanced, experimental modeling has been extensively employed, while the numerical modeling of the problem has been rather difficult due to the presence of waves in the falling liquid film. However, the smooth film absorption assumption has allowed successful modeling of the problem even though without any

UNIVERSITY OF IBADAN

form of enhancement. One of the earliest of such models was developed by G. Grossman (1983), later followed by other researchers such as Andberg and Vliet (1983) and Yang and Wood, B.D (1992).

In the area of numerical modeling of enhanced absorption system, Xiao Feng Niu et al. (2006) established the mathematical model for magnetic field enhanced absorption process for ammonia-water solution on a falling-film. The changes in physical properties of ammonia-water solution in absorption, the variation of falling film and the convection in the direction of thickness of liquid film were considered in the modeling; Distribution of some parameters in falling–film absorption, such as velocity, temperature and concentration; in the application of magnetic field was obtained. Numerical results obtained show that magnetic field can improve the performance of ammonia-water falling-film absorption, and the absorption strengthening effect increases with the enhancement of magnetic induction intensity. The strengthening effect is limited within the magnetic field intensity of 0-3 T, but there are trends of increasing strengthening effect in stronger magnetic fields. In both unenhanced and enhanced absorption system studies, several working fluids have been investigated, some of which are Lithium bromide-water (LiBr-H_2O), Lithium-Chloride Water (LiCl-H_2O) and Ammonia-water (NH_3-H_2O) all of which are popularly used in single-stage and advanced absorption air-conditioning/heat pump technology.

Xiao Feng Niu et al. (2009) experimentally studied the effect of external magnetic field on falling film absorption for ammonia-water system. The study established the following findings: (i) An external magnetic field acting in the same direction as falling film has an enhancing effect on absorption of ammonia-water process, and the absorption enhancement is more greater in stronger magnetic field. When external magnetic field with the same direction as the falling film is exerted, several absorption variables, including the concentration of the ammonia-water solution after absorption, the outlet temperature of the cooling water, the absorption heat and absorption mass in the external magnetic field, are higher than those without external magnetic field exerted. Moreover, the four absorption variables increase with the increase in magnetic induction intensity, (ii) Not all magnetic fields can enhance the ammonia-water absorption process. When an external magnetic field acting against the direction of falling film is exerted, the absorption variables in magnetic field are all smaller than those in conventional absorption without magnetic field exerted. The magnetic field opposing the

UNIVERSITY OF IBADAN

direction of the falling film weakens the absorption of ammonia-water (iii) The absorption can be more intense if the external magnetic field is combined with optimal operating conditions. Experimental results show that the changes in the outlet cooling water temperature, absorption heat and absorption mass with and without external magnetic field exerted, are larger when the inlet solution concentration is lower. Larger cooling water flow rate, lower cooling water temperature and smaller solution flow rate are beneficial to absorption in magnetic field as they do in conventional absorption.

The finite difference method has been applied much more than the finite element method in the analysis of absorption/adsorption systems. The finite element method sometimes described as a versatile and powerful numerical method is a piecewise approximation method. It approximates a problem described by a system of differential equations by a number of algebraic equations relating a finite number of variables (unknowns). These algebraic equations are then solved on the digital computer (for large systems) using an appropriate solution technique. The fundamental concept of the method is that any continuous field quantity (e.g. temperature and concentration) in a continuum can be approximated by a discrete model composed of a set of piecewise continuous parameter functions defined over a finite number of sub-domains. These sub-domains which are referred to as finite elements are connected at discrete points called nodes. The parameter functions must satisfy specific compatibility and completeness requirements.

In engineering problems, either probabilistic or deterministic methods could be used depending on the degree of accuracy required of the solution in comparison with experimentally data or analytic solution. Absorption process enhancement under magnetic field apart for its established effect on ammonia-water absorption process (Xiao Feng Niu et al.(2006), (2009)) as earlier mentioned, magnetic field effect is seldom used and to the best of the knowledge of the researcher, it has not been used in either lithium bromide-water or lithium chloride-water absorption system. This present work therefore investigates the effect of a magnetic field enhanced absorption process on a smooth thin-liquid falling-film in a cooling system using lithium bromide-water (LiBr-H_2O) and (LiCl- H_2O) refrigerants/absorbents combinations. A model of the problem is first developed from the resulting differential equations and solved using the finite difference method. Such an investigation would reveal sections of the absorber that

UNIVERSITY OF IBADAN

need to be redesigned and its material re-specified, e.g for optimal efficiency of refrigerant absorption by the absorbent.

Statement of the Problem

In the manufacturing of modern absorption devices such as absorption air-conditioners, chillers and heat pumps, the most popularly used refrigerant/absorbent combination or working fluids are Lithium-Water Bromide (LiBr-H_2O), Lithium Chloride-Water (LiCl-H_2O), Ammonia-water (NH_3–H_2O), Pentafluoroethane (HFC-125) and Trifluoroethane (HFC-143a). Due to the zero ozone depletion potential (ODP) and zero global warming potential (GWP) of NH_3-H_2O and H_2O-LiBr) Fagbenle et al. (1994), these two refrigerant/absorbent combination are relatively environmentally friendly. Ammonia-water solution is however incompatible with copper, the popular tubing material for transporting refrigerants, for this reason, it is less popularly used than the other working fluids.

The other working fluids such as Halogenated Chlorofluorocarbons (HCFCs), and Azeotropic mixtures (R-500 and R-502) that were popularly used in the past have been declared non-environmentally friendly following the Montreal Protocol and subsequent London and Copenhagen meetings of 1990 and 1992, Fagbenle et al. (1994). This is because of their high Ozone Depletion Potential (ODP) and high Global Warming Potential (GWP) coupled with their roles in the green house effect (either directly through the fluids used or indirectly through the energy consumption in systems using fossil-energy) and as such they are no more in use.

Numerical modeling of the absorption process on a thin-liquid falling-film generally has been difficult due to complication arising from the presence of waves. The Odunfa (2008), approached this issue by considering waves as a second order effect, thereby, appropriating the flow as a smooth falling-film. The degree to which ignoring the second-order effect affects the results by using a thin-liquid falling-film approximation to the absorption process was investigated in his work using lithium bromide-water and lithium chloride-water as working fluids. The results obtained then compared well with the existing experimental results. This research work thus aims at further investigating and establishing the influence of the magnetic field on the absorption process in a smooth thin-liquid falling-film for a cooling system using (LiBr-H_2O) and (LiCl-H_2O) refrigerants/absorbents.

UNIVERSITY OF IBADAN

Justification

Energy conservation and environmental concerns are increasingly attracting global attentions, due to the increasing energy prices and environmental impact of energy prospecting, processing and utilization. As such conventional refrigeration systems are gradually giving way to newer technologies such as absorption cooling systems. Since the major concern in absorption refrigeration systems hinges largely on the energy conservation, environmental issues and efficient cooling system which the present work is to be addressed, hence the justification for this work.

Aims and Objectives

The present work aims and objectives are (i) to develop and evaluate a numerical model for the magnetic field enhancement of the absorption cooling systems using lithium bromide (LiBr) and lithium chloride (LiCl) water solution. (ii) to establish absorption system's performance improvement with increment in magnetic induction intensity enhancement on the two investigated fluids and (iii) to establish the enhancement of the Coefficient of Performance (COP) of both fluids with magnetic field.

Expected practical application of this work includes the design of efficient absorption plant components such as absorbers, evaporators, condensers and generators. Also in this study, key factors such as refrigerant/absorbent combination's parameters and film velocity which influence the improvement level in the absorption performance under magnetic field enhancement would be established.

UNIVERSITY OF IBADAN

CHAPTER TWO

LITERATURE REVIEW

2.1: **Introduction**

The production of cold temperature has application in many fields of human endeavour, e.g. for preservation of perishable products, in the food processing industry, in the air conditioning sector and for the preservation of pharmaceutical products. Based on the cooling temperature requirement, the applications of the absorption systems/machines can be broadly classified into three categories; air-conditioning (8-15^{o}C) for space cooling, refrigeration (0-8^{o}C) for food and vaccine storage and freezing (< 0^{o}C) for ice making purposes.

2.1.1: Cooling Technology

Cooling technology is classified into two broad systems; vapour compression and absorption cooling systems. Based on the cooling temperature requirement, either of the two classifications can be further broken down into the three categories mentioned above.

2.1.2: Advantages and Disadvantages of Vapour Compression and Absorption Refrigeration

i. **The amount of power required**: The compressor of the vapor compression cycle requires large amount of power for its operation and it increases as the size of the refrigeration system increases. In case of the vapor absorption refrigeration system, the pump power required to circulate the absorber-absorbent fluids is relatively very small.

ii. Running cost: The vapor compression refrigeration system can run only on electric power, and they require large amount of power. In case of the absorption refrigeration system only small pump is required whose electric power consumption is generally quite low. Thus the running cost of the absorption refrigeration system is much smaller than for the vapor compression system.

iii. **Foundations required and noise**: The compressor of the vapour compression system is operated at very high speeds and with consequent vibrations and noise. It also requires very strong foundation to withstand the vibrations. In the absorption refrigeration system, there are no

UNIVERSITY OF IBADAN

major moving parts hence they do not vibrate and make no noise. The absorption refrigeration system operates silently with no vibration

iv. **Maintenance**: The compressor is a key component of the compression cycle having a number of moving parts. Thus the compression system generally requires a lot maintenance attention. In the absorption refrigeration system the only moving part is the small pump that fails rarely making the system to be robust and requiring little or no maintenance.

v. **Type of refrigerant used and its cost**: The refrigerant used by the absorption refrigeration system is environmentally friendly; easily and cheaply available. In the case of the vapour compression refrigeration system, halocarbons that are been used as the refrigerants are not environmentally friendly and also very expensive.

vi. **Leakage of the refrigerant:** In the absorption refrigeration system leakage of the refrigerant seldom occurs while the refrigerant itself is relatively inexpensive. Thus refrigerant recharging costs is minimal. In vapour compression systems, leakages of the refrigerant occurs quite often requiring regular refrigerant recharge of the system usually at a relatively high cost.

vii. **Greenhouse effect:** Most of the halocarbon refrigerants used in the compression refrigeration system has a high GWP. Following the Montreal Protocol, their use has to stop completely by the year 2020. In the absorption refrigeration system, refrigerants have very low or zero GWP and they are not in any exclusion list.

2.1.3: Vapour compression System

Fig. 2a is a typical vapour compression system (Chiller) York model. The following major components can be identified in the figure: compressor, condenser coil, evaporator and fans. Other minor components such as filter drier, oil line and other accessories are also shown in the figure.

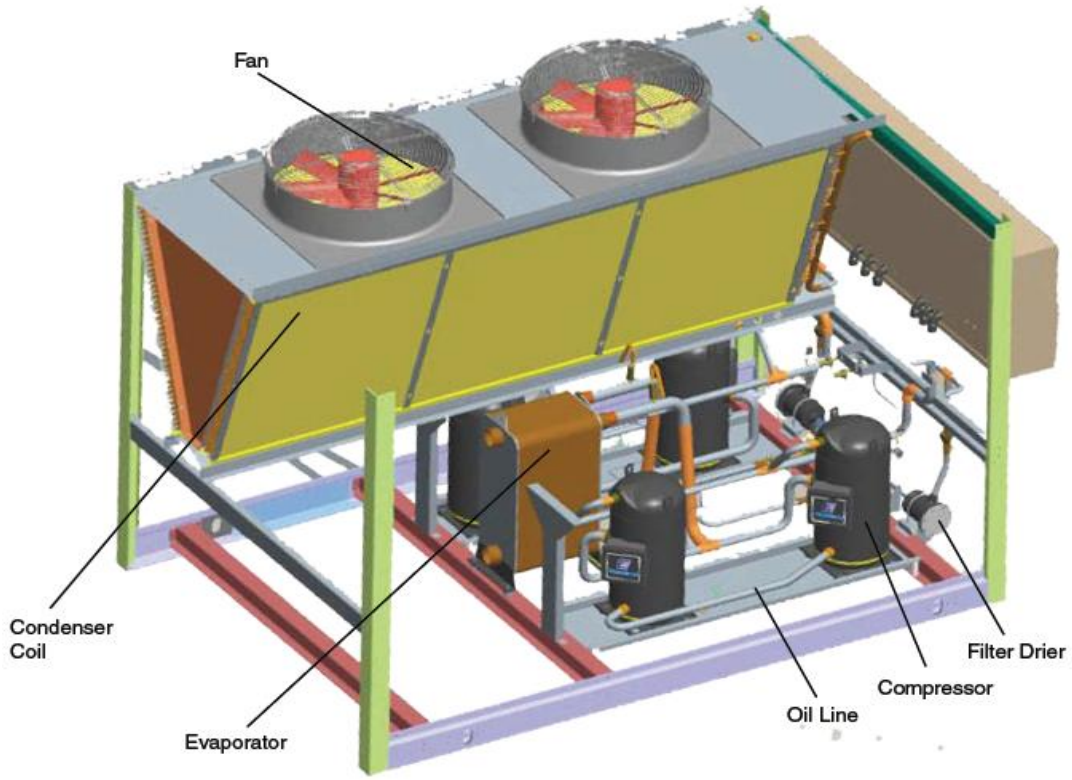

Fig.2a. Vapour Compression Chiller-three stage Compressor

2.1.4: Vapour compression cycle

Fig 2b shows the typical schematic diagram of a single stage compression system containing a compressor, a condenser, an evaporator and an expansion valve. The two- stage compression system shown in fig 2c contains a flash chamber, and two compressors instead of one as in the single-stage system.

UNIVERSITY

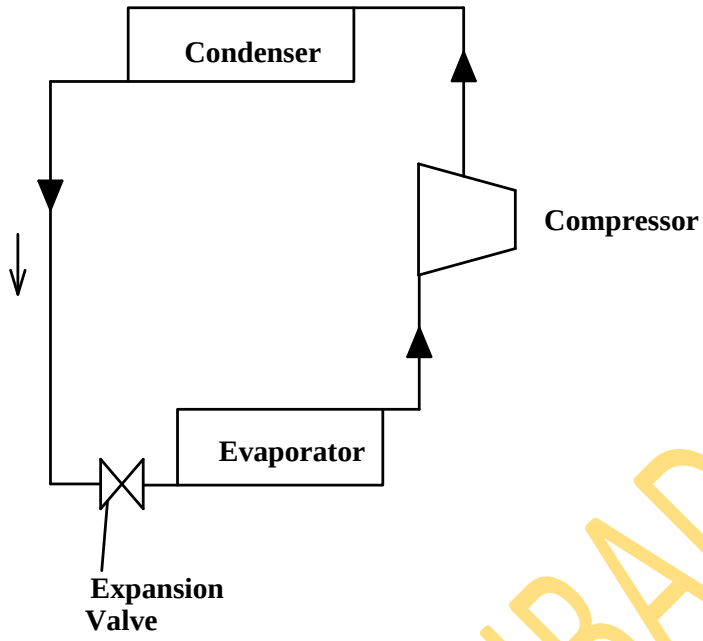

Fig.2b. Basic Vapour Compression cycle- Single Stage

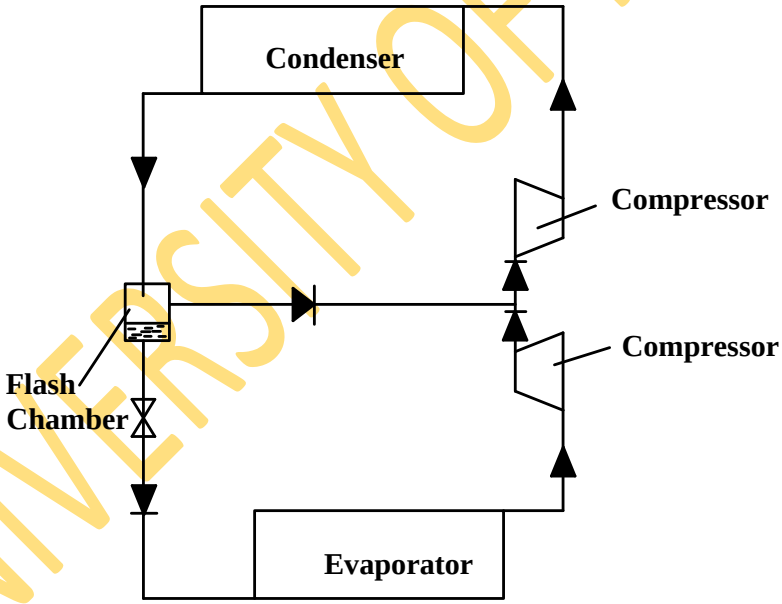

Fig.2c. Basic Vapour Compression cycle - Two-stage Compressor and a flash chamber

UNIVERSITY OF IBADAN

2.1.5: Absorption System

Fig. 2d is a typical two-stage absorption system (Chiller). It contains two generators (G1& G2), two condensers (C1& C2), an absorber, and an evaporator. Other components such as pump, an expansion valves and solution heat exchanger (SHE) are also in the figure. The line diagram of the two-stage absorption refrigeration cycle appears in fig 2f.

Fig. 2d.Typical two-stage Absorption Chiller

2.1.6: Principle of operation of Absorption system

The working fluid in an absorption refrigeration system is a binary solution consisting of refrigerant and absorbent. In the **fig. 2e** below, two evacuated vessels are connected to each

other. The left vessel contains liquid refrigerant while the right vessel contains a binary solution of absorbent/refrigerant. The solution in the right vessel will absorb refrigerant vapour from the left vessel causing pressure to reduce. While the refrigerant vapour is being absorbed, the temperature of the remaining refrigerant will reduce as a result of its vaporization. This causes a refrigeration effect to occur inside the left vessel. At the same time, solution inside the right vessel becomes more dilute because of the higher content of refrigeration absorbed. This is called the "absorption process". Normally, the absorption process is an exothermic process, therefore it must reject heat out to the surrounding in order to maintain its absorption capability. Whenever the solution cannot continue with the absorption process because of saturation of the refrigerant, the refrigerant must be separated out from the diluted solution. Heat is normally the key for this separation process. It is applied to the right vessel in order to dry the refrigerant from the solution as shown in **fig. 2e(b)** below. The refrigerant vapour will be condensed by transferring heat to the surroundings. With these processes, the refrigeration effect can be produced by using heat energy. However, the cooling effect cannot be produced continuously as the process cannot be done simultaneously. Therefore, an absorption refrigeration cycle is a combination of these two processes as shown in **fig. 2f.** As the separation process occurs at a higher pressure than the absorption process, a circulation pump is required to circulate the solution. Coefficient of performance of an absorption refrigeration system is obtained from;

$$\text{COP} = \frac{\text{cooling capacity obtained at evaporator}}{\text{heat input for the generator} + \text{work input for the pump}}$$

The work input for the pump is negligible relative to the heat input at the generator; therefore, the pump work is often neglected in the evaluation of the COP.

UNIVERSITY OF IBADAN

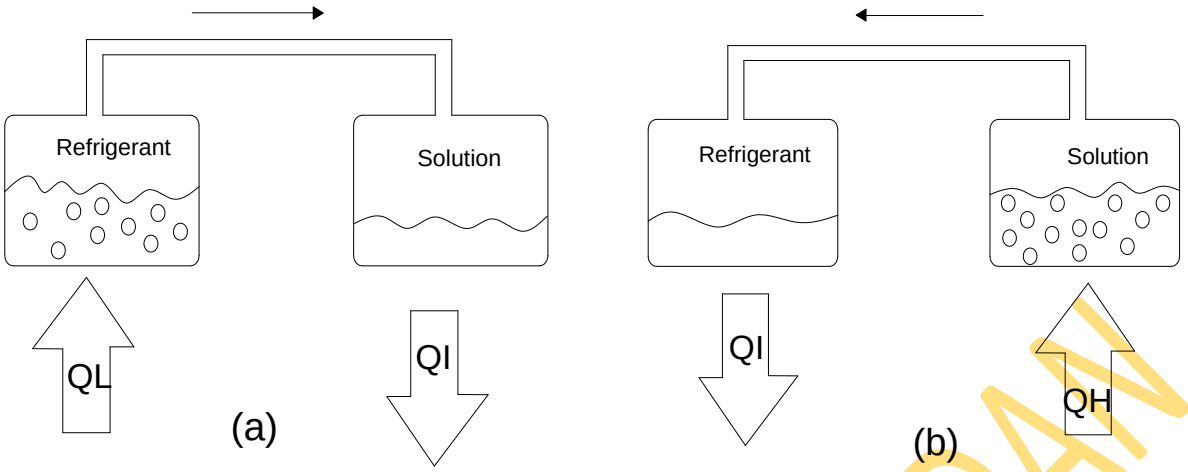

Fig. 2e: An intermittent Absorption Cycle

. **(a)** Absorption process occurs in right vessel causing cooling effect in the other,
(b) Refrigerant separation process occurs

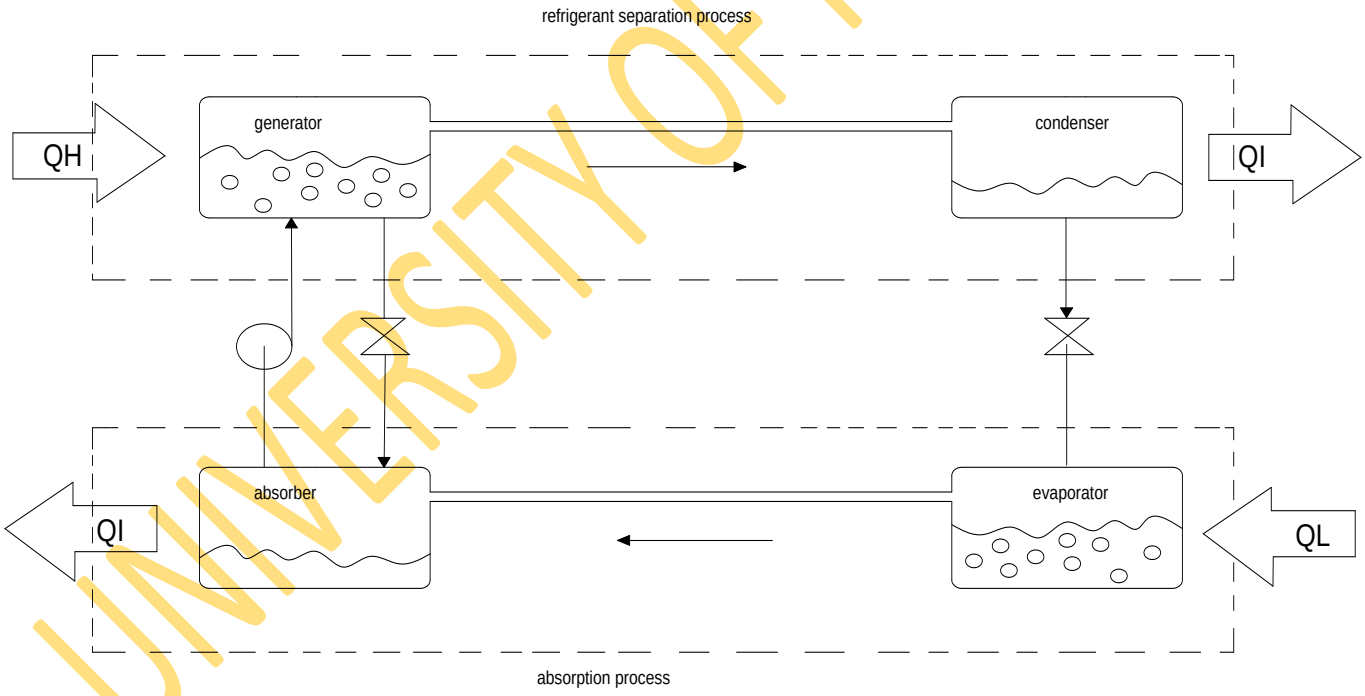

Fig. 2f: A continuous absorption refrigeration cycle composes of two processes mentioned in the earlier figure.

UNIVERSITY OF IBADAN

2.1.7: Working fluids/Refrigerants

A review of literature carried out on the refrigerants used in air-conditioning and refrigerating systems reveals that fully halogenated chlorofluoro carbon (CFCs) and halon compounds, carbon tetra chloride (CCL_4), 1,1, l-trichloride ethane (Methyl Chloroform CH_3CCl_3) and methyl bromide (CH_3Br) are the commonly used refrigerants in the industrial and commercial compression cooling systems. Following the scientific findings on the above mentioned refrigerants that they have high ozone depletion potential (ODP) and global warming potential (GWP), the 1987 Montreal Protocol was made in 1990 and amended in Copenhagen in 1992 to phase out or ban these refrigerants from usage by the year 2015. Ever since this protocol, the search for replacement chemicals has been exclusively in the developed countries, because the bulk of the production and consumption of these restricted chemicals is in these countries. Furthermore the technical expertise, research infrastructure and the direct and allied economic investment are all in these countries.

Researchers in this field of study worldwide have intensified efforts towards finding alternative refrigerants to the CFC's which will not only be environmentally friendly, but which will also be energy efficient. A survey of absorption fluids provided by Marcriss et al.(1988) suggests that, there are some 40 refrigerant compounds and 200 absorbent compounds available. However, the most common working fluids are water lithium bromide (H_2O–LiBr), water lithium Chloride (H_2O–LiCl) and Ammonia–water (NH_3–H_2O) solutions. Heat and mass transfer analysis of cooling systems has been continuously undertaken by researchers such as Yang and Wood (1992), Muhsin et al.(2004), Fernandez et al.(2005), Xu et al.(2006) and Gu et al.(2007) in order to improve on plant and component design and efficiencies. Water lithium bromide (H_2O–LiBr) and water lithium chloride (H_2O-LiCl) solutions remain the most popularly used refrigerant-absorbent pairs in absorption cooling systems and as such the present work employs these two working fluids, albeit with magnetic field enhancement.

2.1.8: Various designs of absorption refrigeration cycles

Pongsid Srikhirin et al. (2001) in his review of absorption refrigeration technologies established the following designs of absorption refrigeration cycles: the single-effect absorption system (Fig.2g), the absorption heat transformer (Fig.2h), the double-effect water/LiBr absorption cycle (Fig.2i), the double-effect absorption cycle operates with two pressure levels

UNIVERSITY OF IBADAN

(Fig.2j), a triple-effect absorption cycle operates at four pressure levels (Fig.2k), the dotted loop shows secondary fluid used for transferring heat from high the temperature section in the absorber to low temperature section in the generator (Fig.2l), The cycle with absorber heat recovery (Fig. 2m), A half – effect absorption cycle (Fig. 2n), Combined vapour absorption/compression heat pump (Fig. 2o), Double effect absorption –compression cycle, (Fig. 2p), A combined cycle proposed by Caccoila et al (Fig.2q, A resorption cycle proposed by Altenkirch (Fig. 2r), Solar driven dual cycle absorption (Fig. 2s), A modified double effect combined ejector – absorption refrigeration cycle (Fig. 2t), A combined ejector/absorption system using DMETEG/R22 and DMETEG/R21 as working fluids (Fig**.** 2u), A combined ejector/absorption proposed by Aphornratana and Eames (Fig. 2v), A combined cycle proposed by Eames and Wu (Fig. 2w**),** osmotic-membrane absorption cycle (Fig.2x), and diffusion absorption refrigeration system DAR) (Fig.2y).

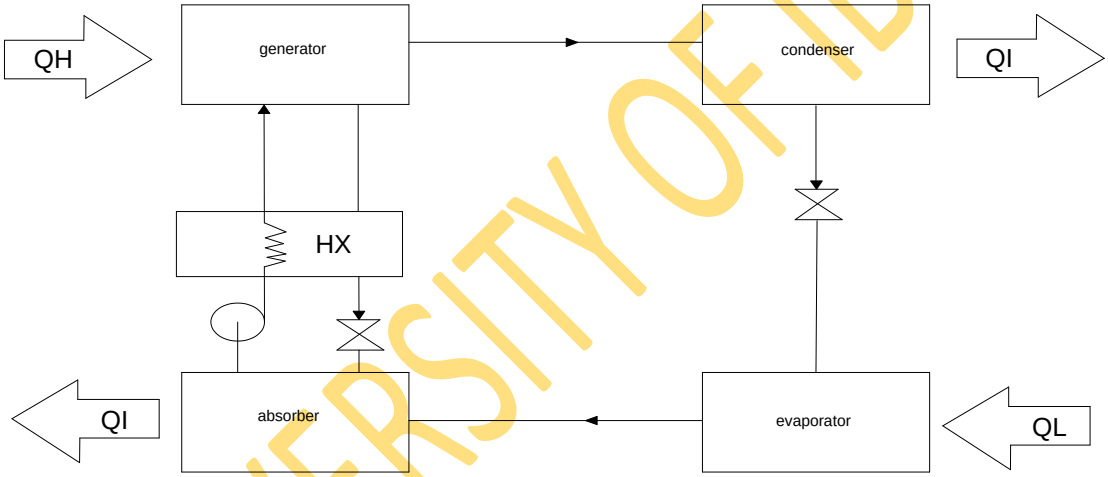

Fig.2g: A Single–effect LiBr/water absorption refrigeration system with a solution heat exchanger (HX) that helps decrease heat input at the generator

UNIVERSITY OF IBADAN

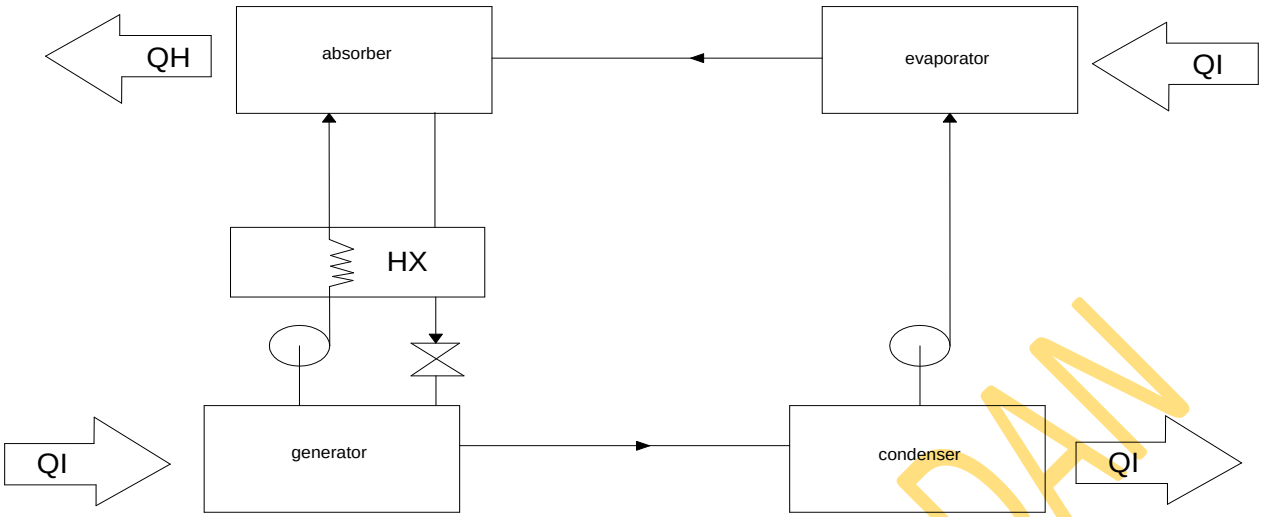

Fig.2h: Absorption heat transformer absorbs waste heat at the generator. Liquid refrigerator is pumped to the evaporator to absorb waste heat. High temperature useful heat from the absorber is heat of absorption.

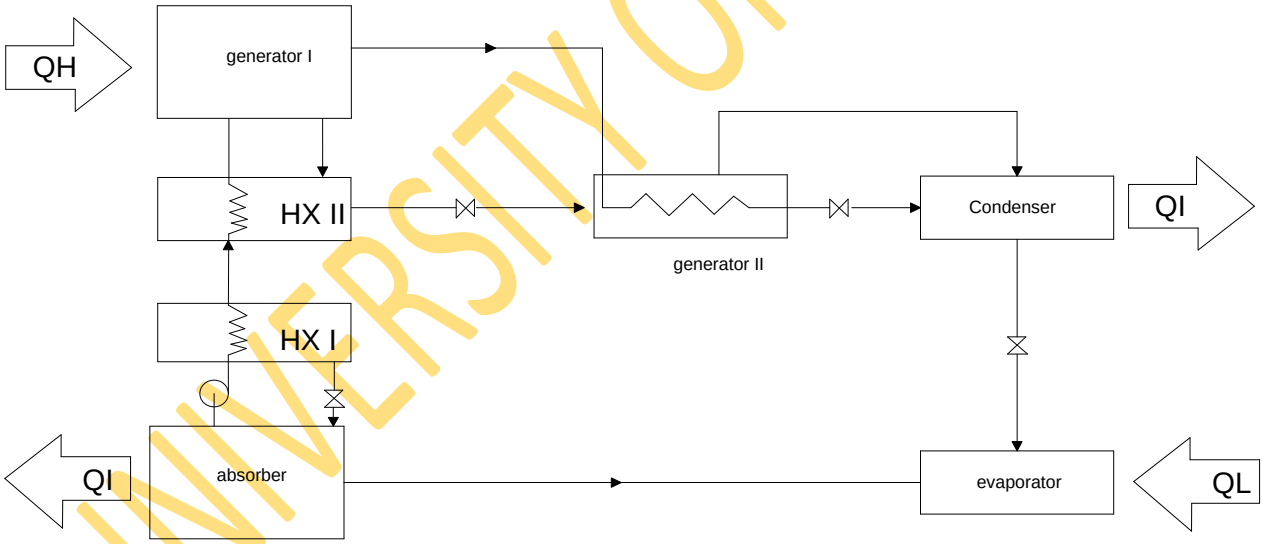

Fig.2i: A double – effect water/LiBr absorption cycle. Heat released from the condensation of refrigerant vapour is used as heat input in generator II. This cycle is operated with 3 pressure levels i.e high, moderate and low pressure.

UNIVERSITY OF IBADAN

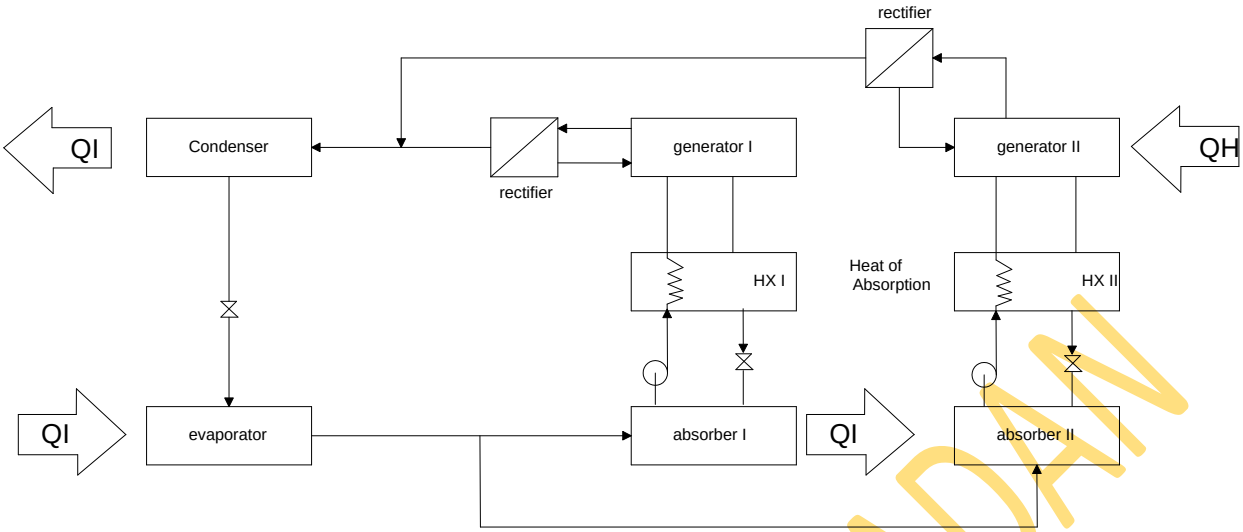

Fig. 2j: A double – effect absorption cycle operates with two pressure levels. Heat of absorption from Absorber II is supplied to the Desorber I for the refrigerant separation process.

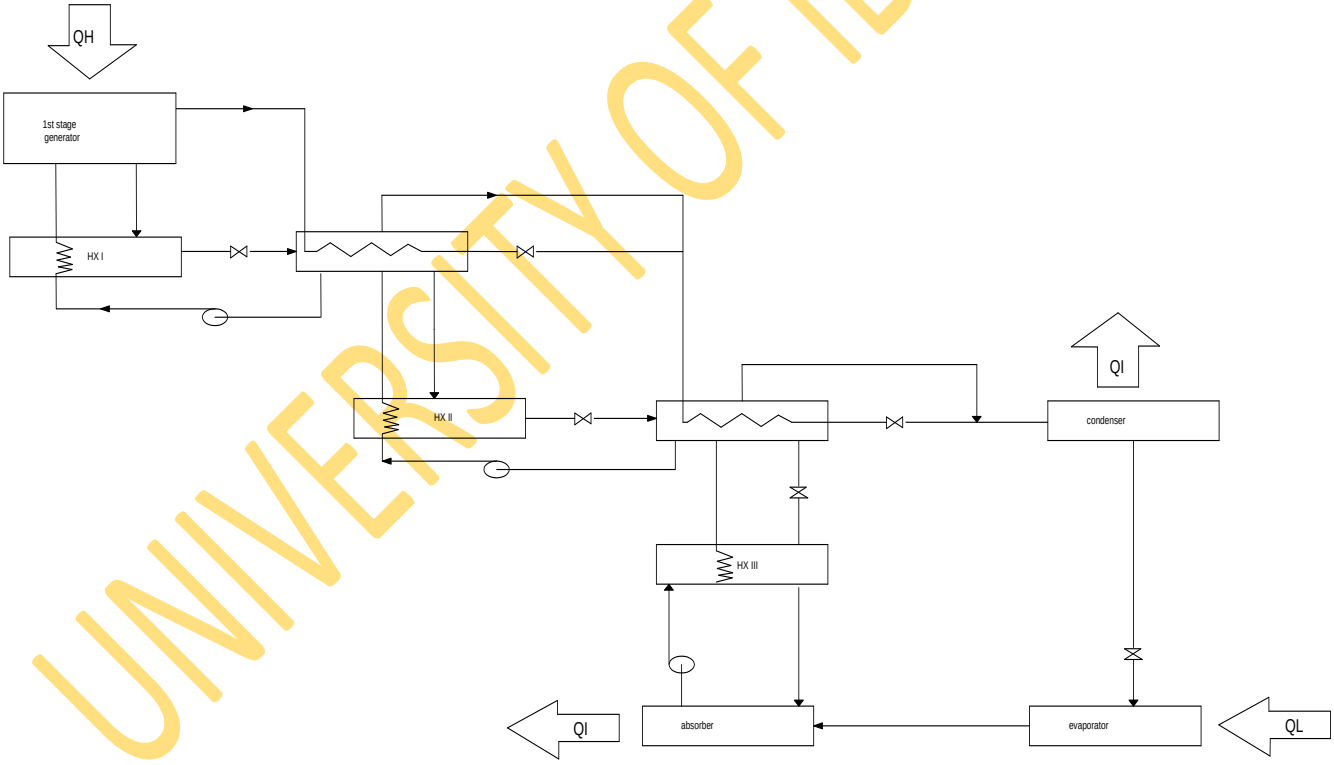

Fig. 2k: A triple – effect absorption cycle operates at four pressure levels. Heat of condensation from the higher – pressure stage is used for refrigerant separation in the lower pressure stage.

UNIVERSITY OF IBADAN

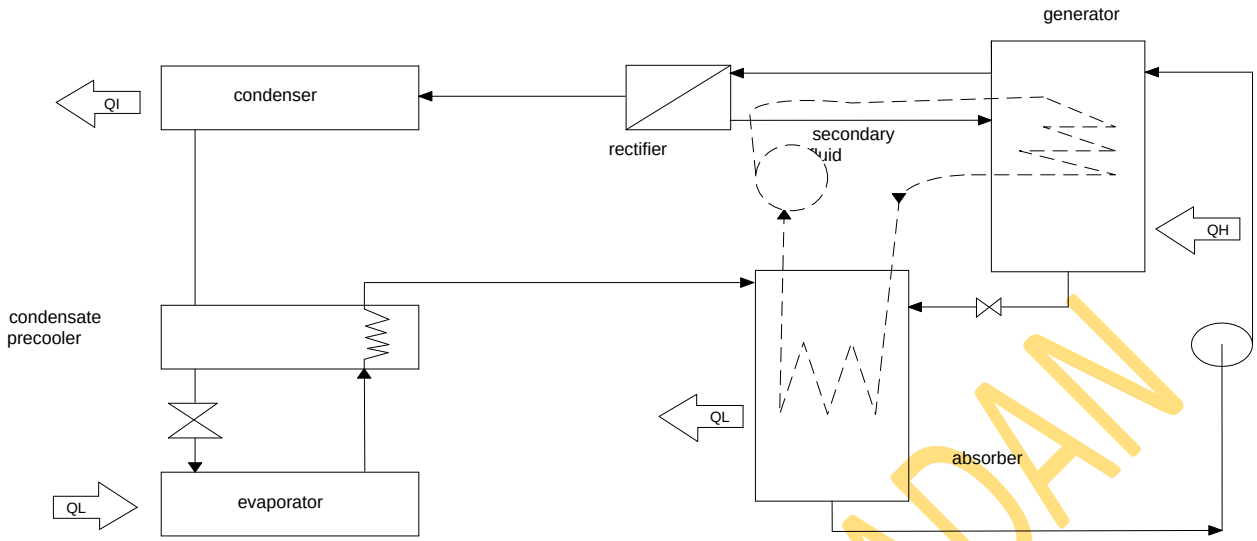

Fig. 2l: The dotted loop shows secondary fluid used for transferring heat from high temperature section in the absorber to low temperature section in the generator.

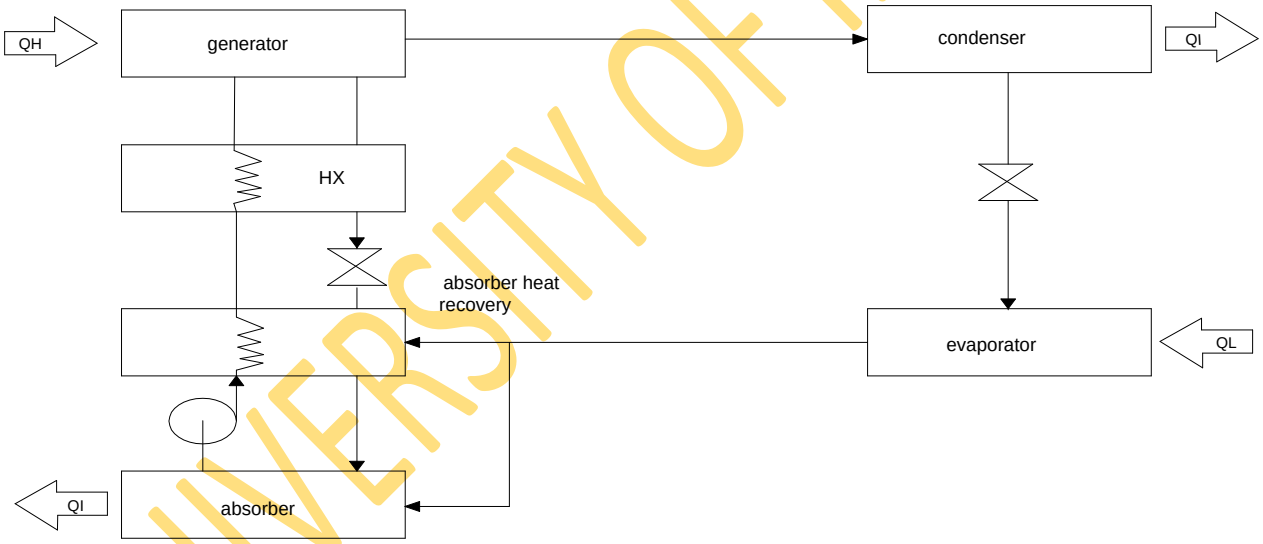

Fig. 2m: The cycle with absorber heat recovery uses heat of absorption of preheat the outgoing stream from the absorber to the generator.

UNIVERSITY OF IBADAN

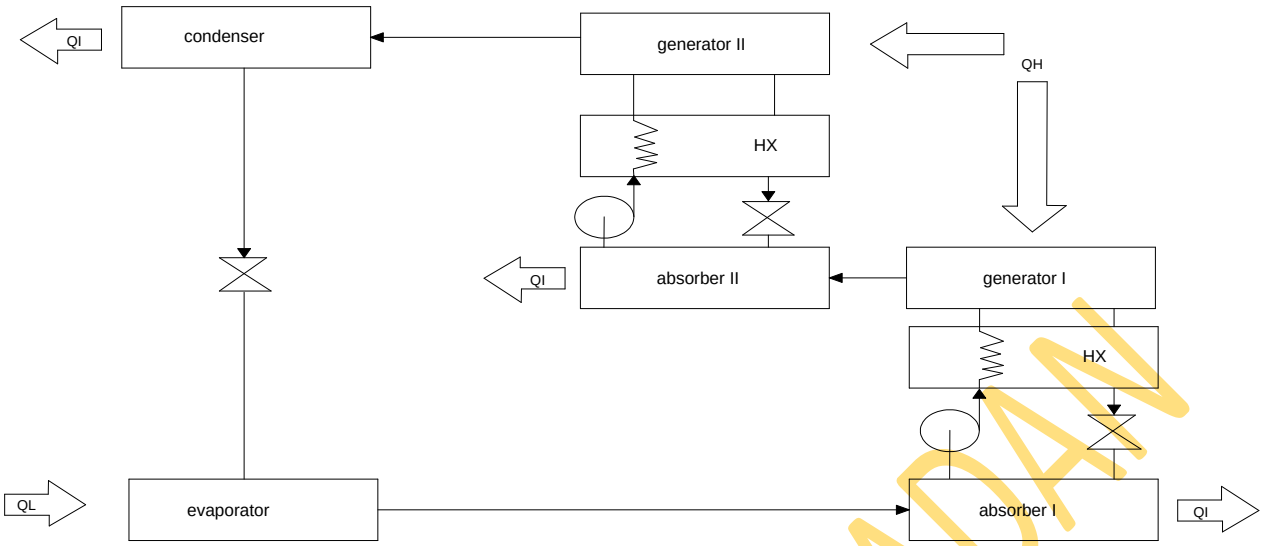

Fig. 2n: A half – effect absorption cycle is a combination of two single – effect cycles but working at different pressure levels. Letting heat source temperature be lower than the minimum temperature is necessary for a single – effect cycle working at the same pressure level.

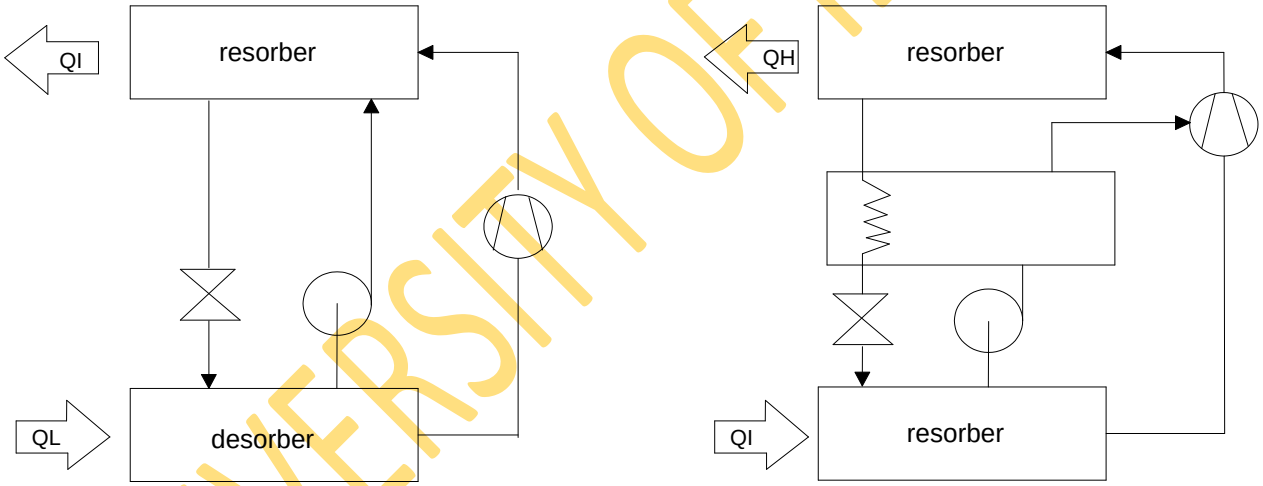

Fig. 2o: Combined vapour absorption/compression heat pump.

UNIVERSITY OF IBADAN

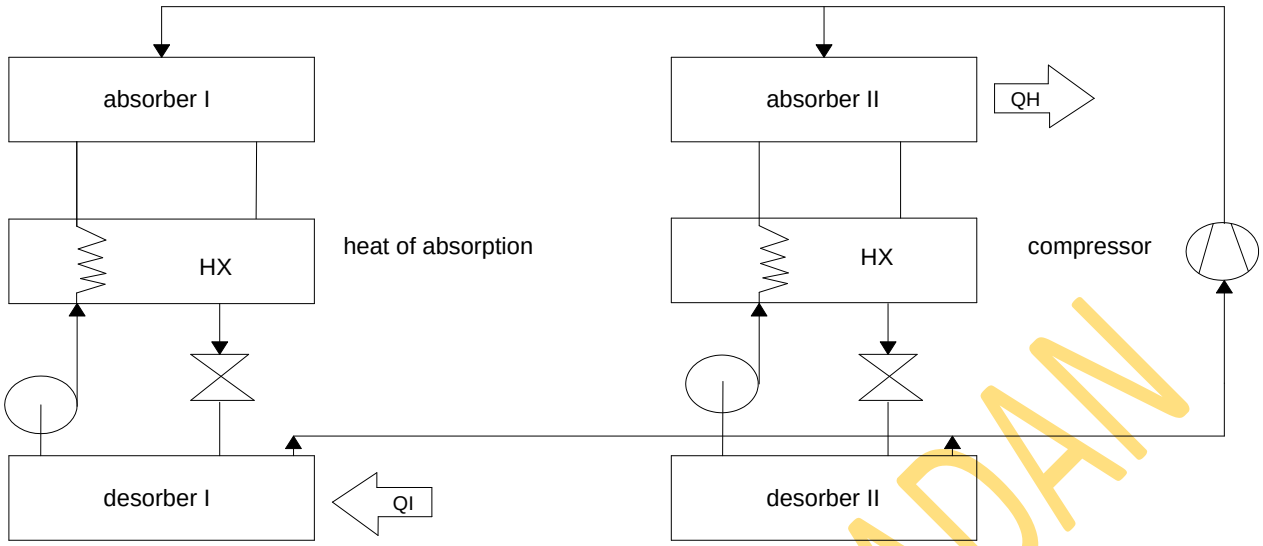

Fig. 2p: Double effect absorption –compression cycle is configured as a heat pump. Heat of absorption in the first stage will be supplied to the second stage for refrigerant separation.

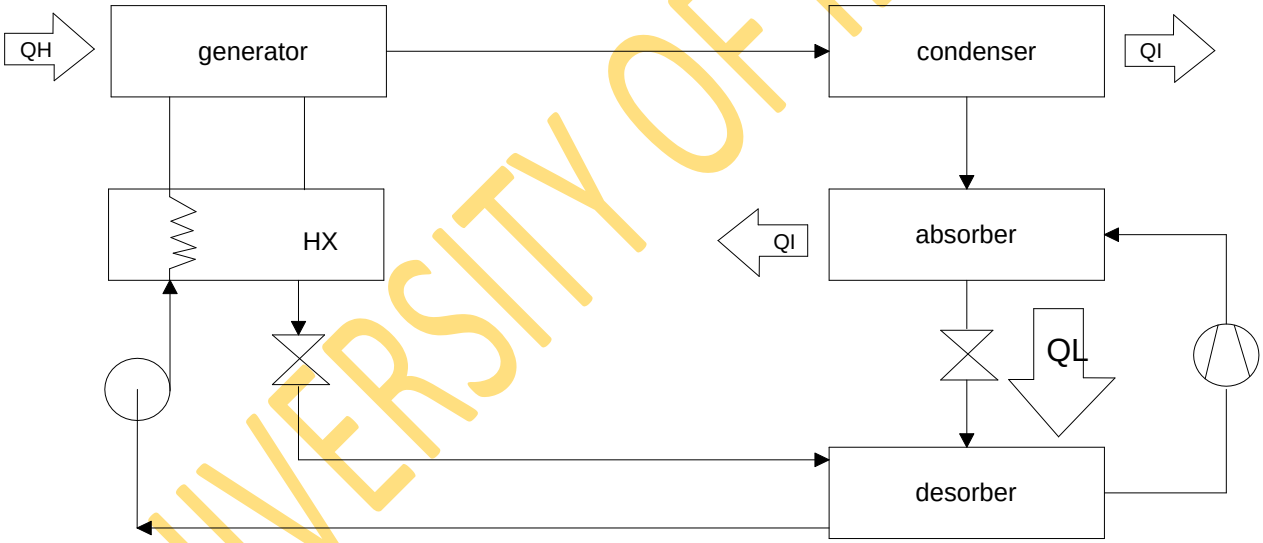

Fig.2q: A combined cycle proposed by Caccoila et al.(86), employing two combinations of working fluids ie. $NH_4/H_2O/KHO$. The rectifier is absent and also the highest pressure is decreased.

UNIVERSITY OF IBADAN

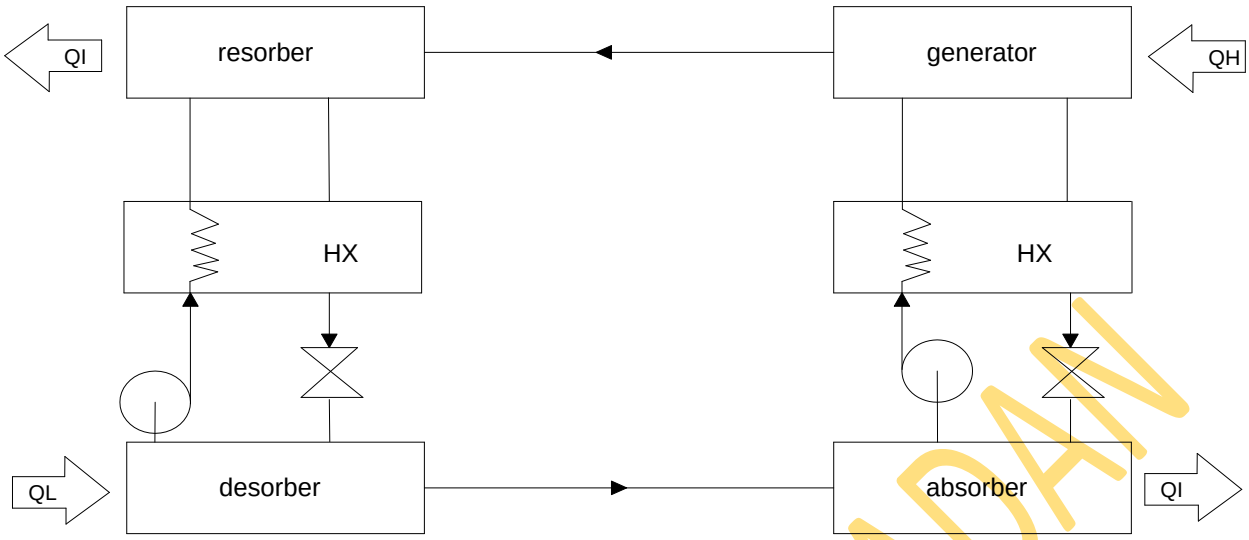

Fig. 2r: A resorption cycle proposed by Altenkirch uses two solution circuits.

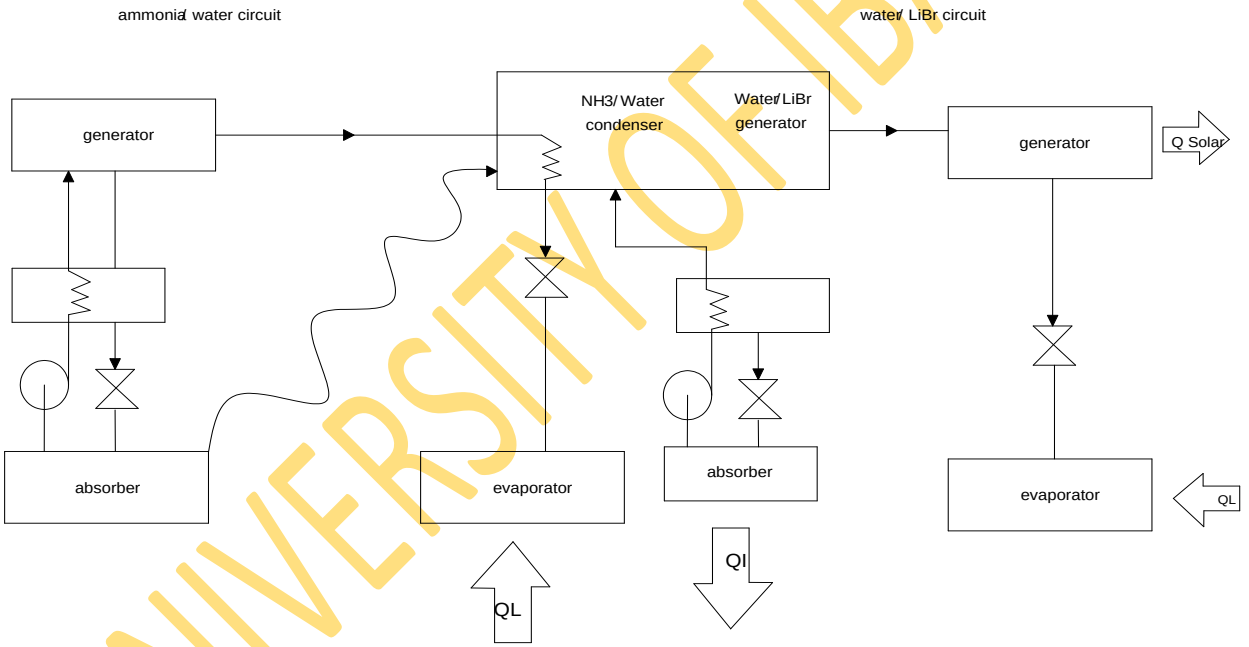

Fig. 2s: Solar driven dual cycle absorption employs to different working fluids i.e NH_3/water and water/LiBr. Heat of absorption and condensation from NH_3/water cycle are supplied to the generator of water/LiBr cycle.

UNIVERSITY OF IBADAN

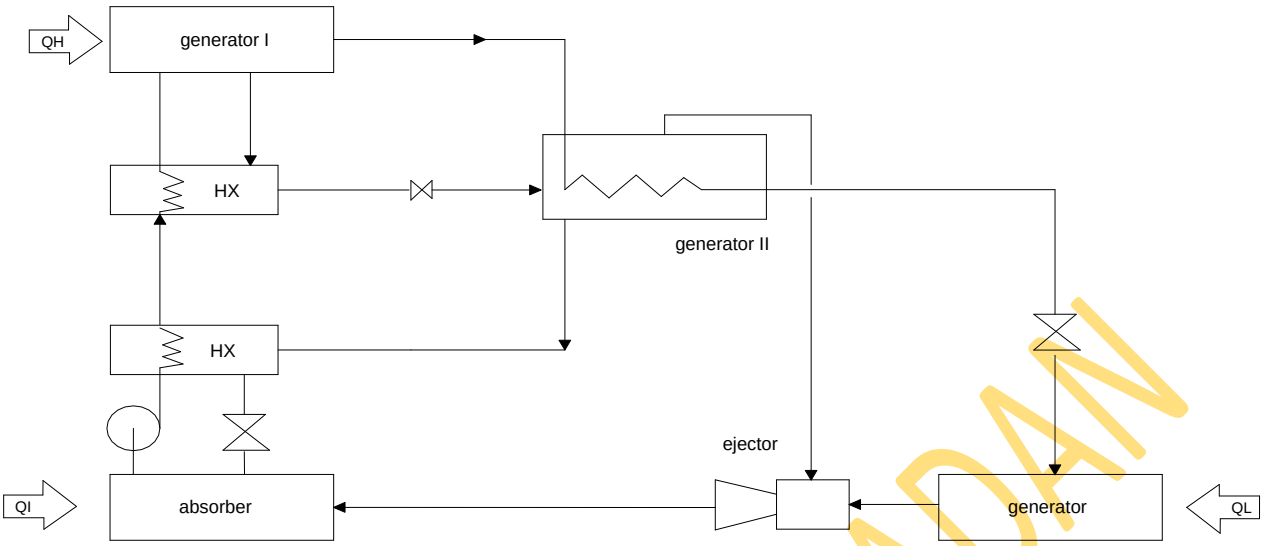

Fig. 2t: A modified double effect combined ejector – absorption refrigeration cycle where there is no condenser included.

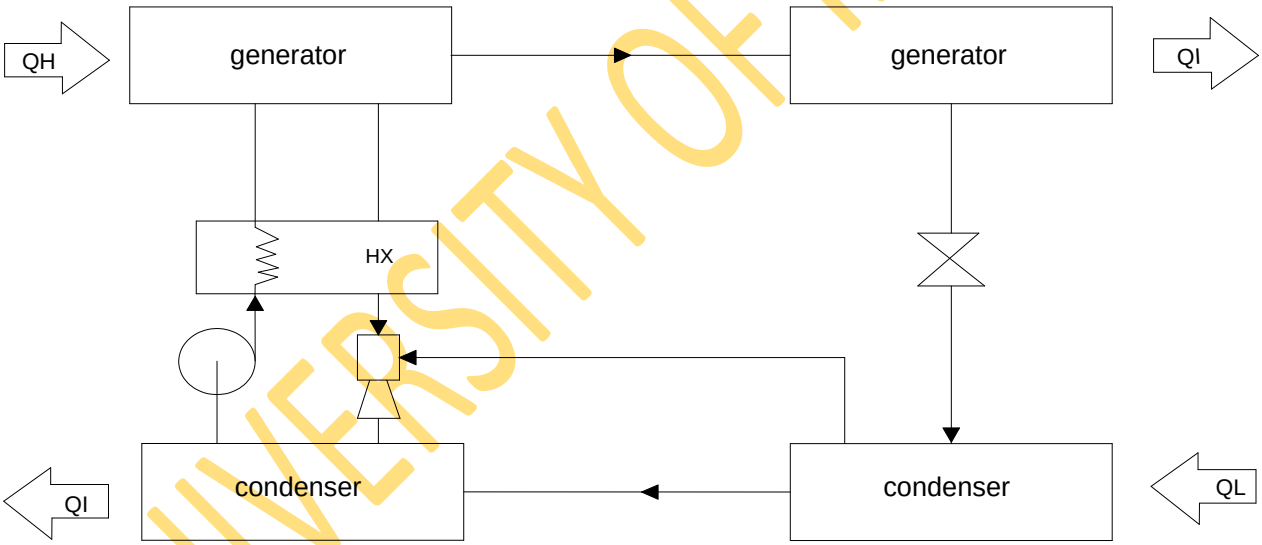

Fig. 2u: A combined ejector/absorption system using DMETEG/R22 and DMETEG/R21 as working fluids. The strong solution in the returning leg from generator serves as primary fluid and refrigerant vapour from evaporator as second fluid.

UNIVERSITY OF IBADAN

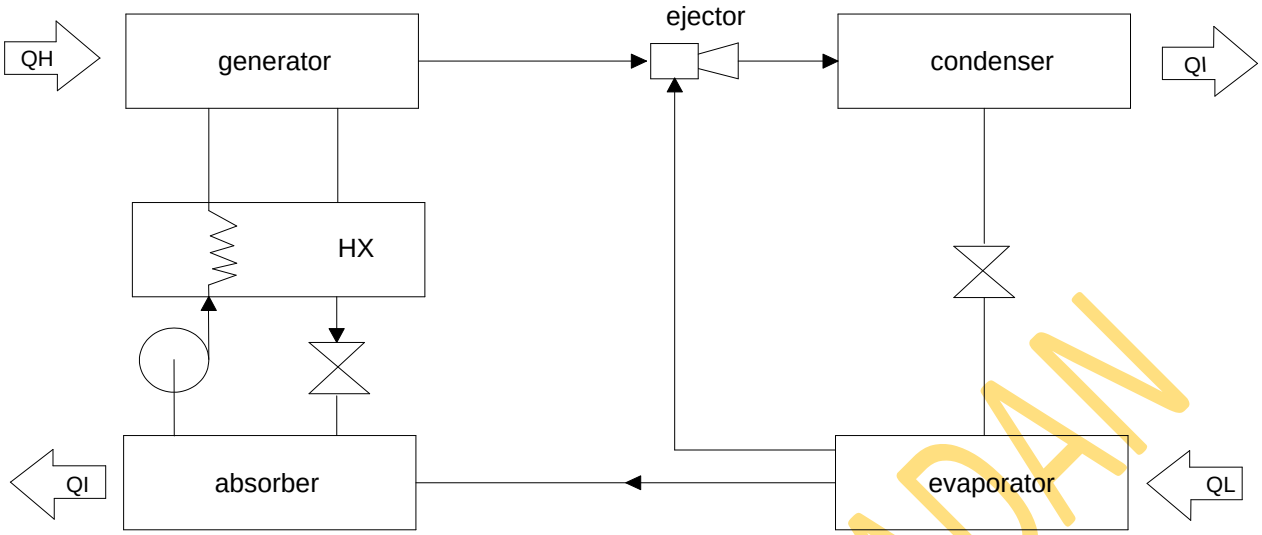

Fig. 2v: A combined ejector/absorption proposed by Aphornratana and Eames, was invented. High pressure refrigerant vapour from the generator enters the ejector as motive fluid to carry the refrigerant vapour from the evaporator.

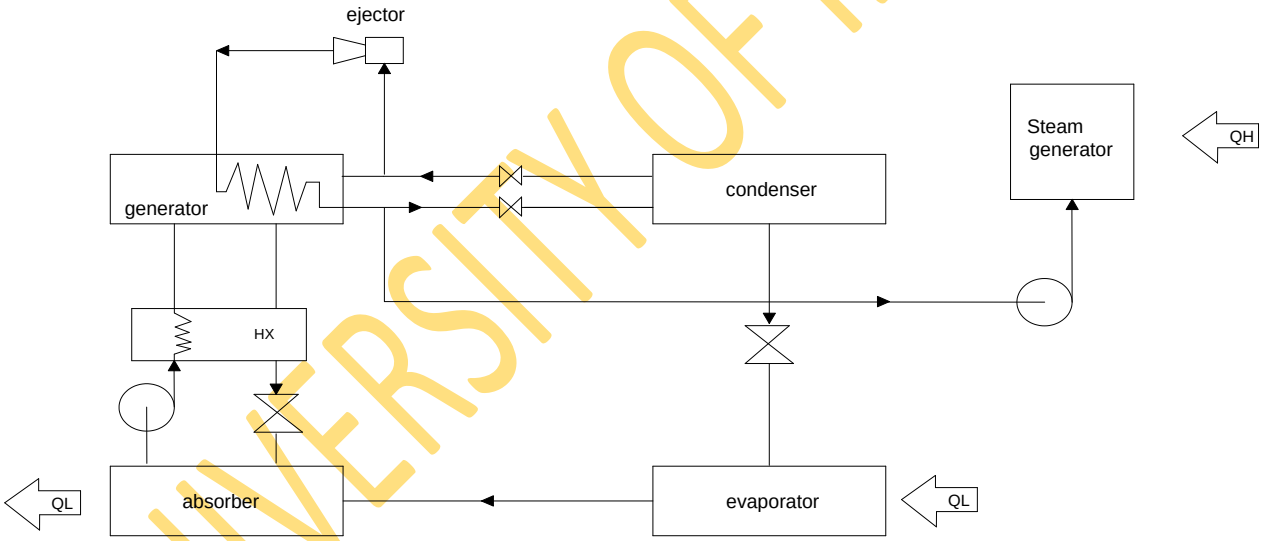

Fig. 2w: A combined cycle proposed by Eames and Wu (93). The highest solution circuit temperature ia maintained at about 18C. So the corrosion problem is alleviated.

UNIVERSITY OF IBADAN

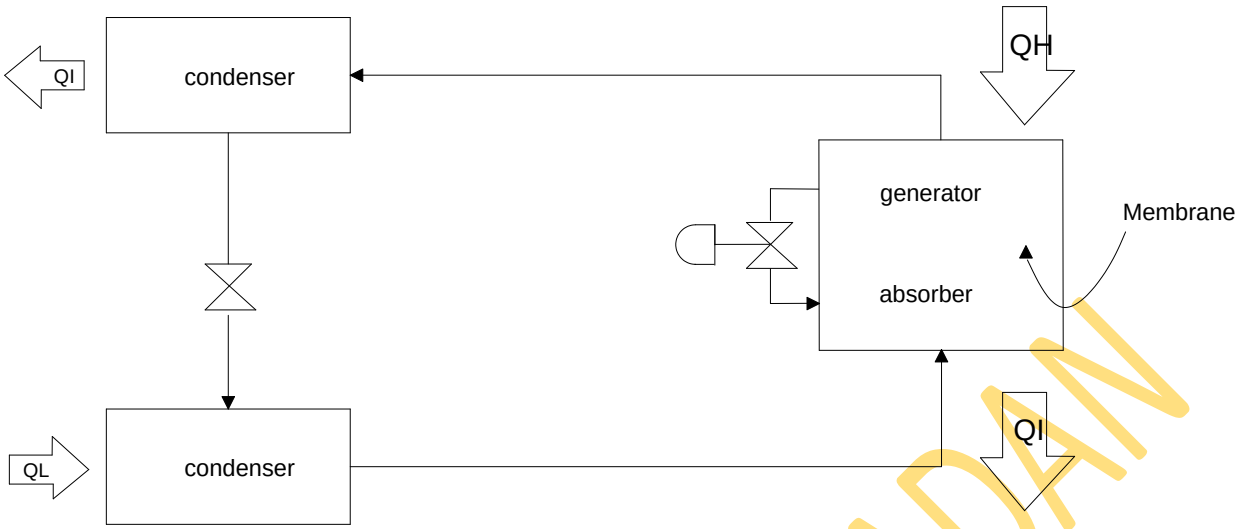

Fig. 2x: An osmotic membrane absorption cycle employs heat for refrigerant separation and producing pressure within the system.

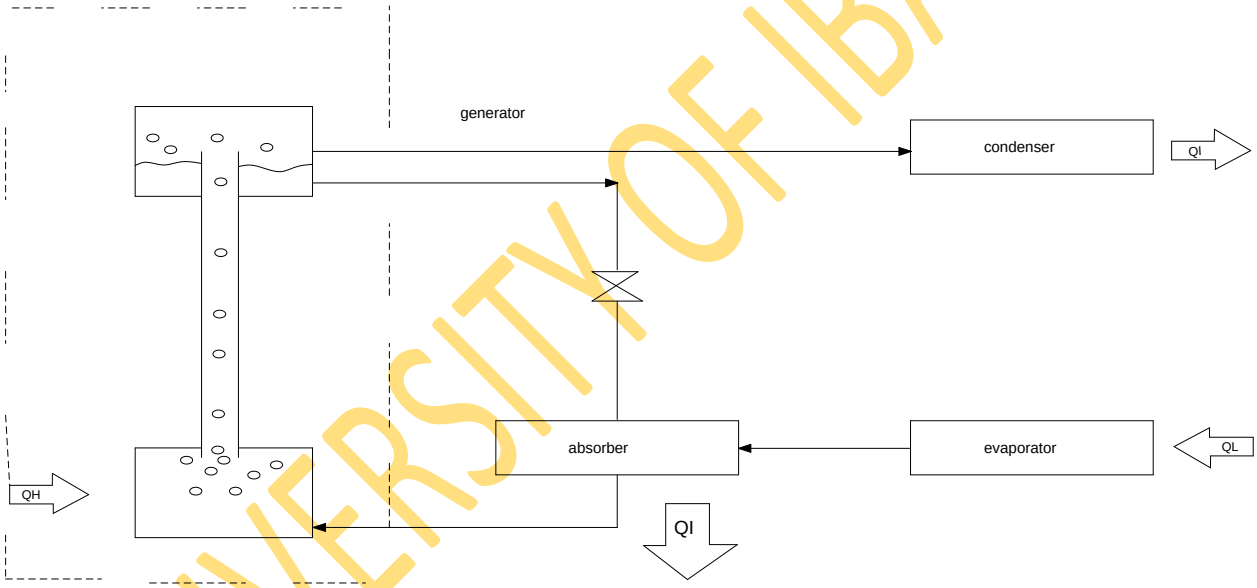

Fig. 2y: The diagram shows a bubble pump in the generator module. Heat input to the generator is used for both circulation of working fluid and evaporation of refrigeration.

2.1.9: Practical Absorption Cycle

Fig. 2zi is a basic absorption cycle that uses a lithium bromide and water solution as an absorbent and water as refrigerant. The single-stage fundamental absorption refrigeration system (ARS) contains a generator, an absorber, a condenser, an evaporator, a solution pump, expansion valves or restrictors, and a solution heat exchanger (SHE). The flow path is shown in the figure with arrows.

UNIVERSITY OF IBADAN

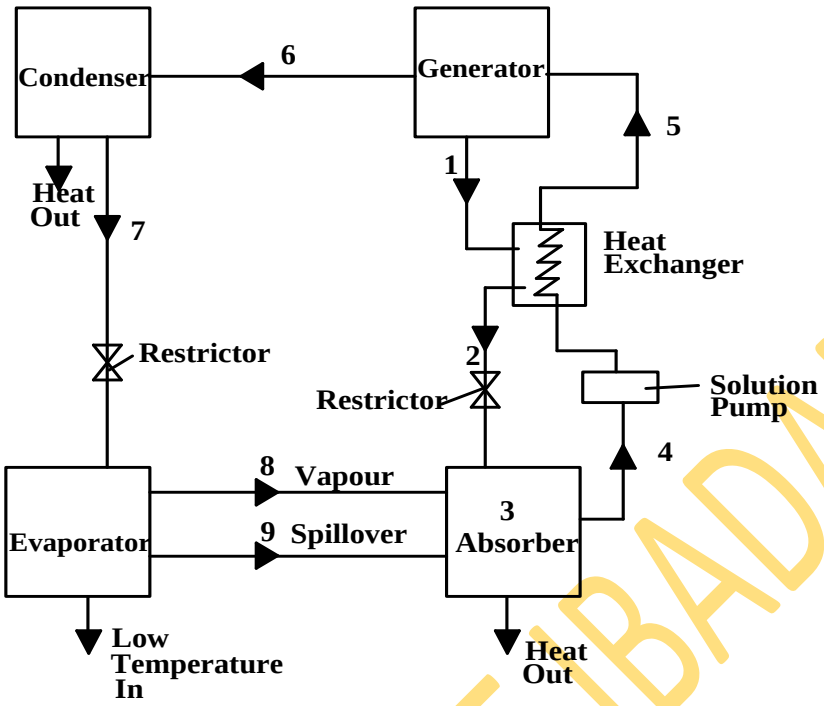

Fig.2zi. Lithium bromide-water single-stage absorption Refrigeration cycle

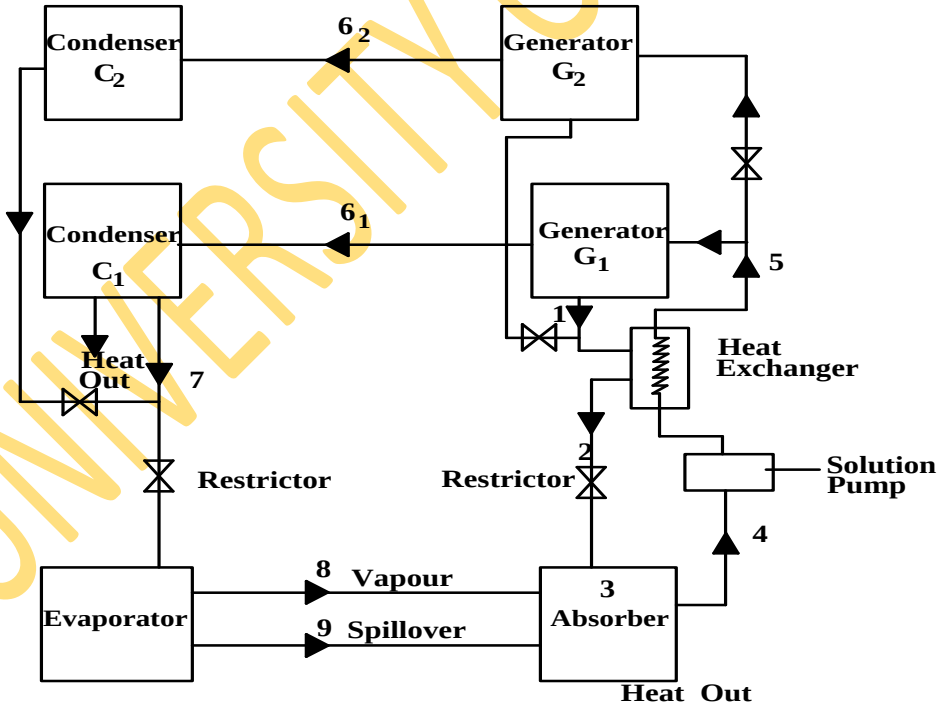

Fig. 2zii. Lithium bromide-water two-stage absorption Refrigeration cycle

UNIVERSITY OF IBADAN

2.3: Numerical Modeling

Experimental modeling of heat and mass transfer on thin-liquid falling film in unenhanced and enhanced absorption has been extensively studied, while there are relatively few studies on numerical modeling of the problem. In experimental unenhanced absorption process modeling, Ali et al. (2002) investigated the technical feasibility of driving a lithium chloride-water solution absorption-cooling unit by a low-temperature heat source (such as solar energy using a simple flat-plate collector) for air-conditioning applications. The operating characteristics of the unit were extensively investigated and the C.O.P of the unit was found to be 19% as against the design value of 21%. Safarik et al. (2004) also carried out an experimental modeling on a solar power absorption chiller with low capacity using lithium bromide-water solution as the working fluid. The field test carried out at three sites in the summer of 2003 after the prototype test in this experimental modeling showed that the absorption chiller performed reliably and flexibly over a wide range of external conditions. Abdelmessih et al. (2005) experimentally investigated the use of non-traditional absorbent/refrigerant pairs such as ethylene glycol-water on a designed and built absorption refrigeration cycle. The investigation was successful in replacing traditional hazardous absorbent/refrigerant pairs with ethylene glycol-water pair. The working fluids chosen are safe, unlike the commercial absorbent/refrigerant pairs. Yaxiu et al. (2007) also examined experimentally a compact solar pump-free lithium bromide absorption refrigeration system equipped with a second generator, a falling-film absorber, a falling-film evaporator and an efficient luminate thermosiphon elevation tube. The experiment confirmed a 48.5% increase in the COP.

Since the numerical modeling of both unenhanced and enhanced absorption process is complicated by the presence of the waves in the falling liquid-film, the smooth falling film unenhanced absorption approximation has been more popularly investigated, the earliest of such being the work of Grossman and Andberg (1983). This was even considered complicated in formulation due to the restriction of the model to the case with the inlet absorbent temperature being equal to that of the wall. In the same year Andberg and Vliet (1983) also investigated the smooth falling-film absorption under laminar flow using a different model from his research model, this was also considered quite sophisticated and somewhat too complicated in formulation.

UNIVERSITY OF IBADAN

Yang and Wood (**1992)** investigated a numerical model of the absorption process on a smooth liquid falling-film in lithium bromide water and a lithium chloride water solution system. Yang et al. (1992) developed a numerical absorption model of a simple smooth-film of LiCl-H_2O and LiBr-H_2O systems with Reynolds number of 2.7, 27 and 100 using finite difference solution approach. The solutions obtained were similar to the results of the earlier work of Grossman et al. (1983) and generally agreed with available experimental data. Argiriou et al. (2004) conducted a numerical investigation on a prototype low capacity solar assisted lithium bromide absorption heat pump coupled with a sub-floor system using the commercial simulator known as TRNSYS. The results indicated that the estimated energy savings against a conventional cooling system using a compression type heat pump was in the range of 20-27%. Xu et al. (2006) simulated an absorption process in an advanced energy storage system. The latest of the modeling in this area was on a two-stage absorption chiller driven at two-temperature levels using thermodynamic modeling technique by Gustavo et al. (2007). The study established that the machine can operate in summer as a double-stage chiller driven by heat at 170 ^{0}C from natural gas, as a single-stage chiller driven by heat at 90 ^{0}C from solar energy, or simultaneously in combined mode at both temperatures. It also established the capability of operating in winter in "double-lift" mode for heating with a driving heat at 170 ^{0}C from natural gas.

Ghaddar et al. (1996) modeled solar lithium bromide absorption system performance in Beirut using a simulated computer program. The results shows that for each ton of refrigeration it is required to have a minimum collector area of 23.3m^2 with an optimal water storage tank capacity ranging from 1000 to 1500 litres for the system to operate solely on solar energy for about seven hours a day. The energy use in cooling was also found to be of function of solar collector area and storage tank capacity. Based on the economic assessment performed on the current cost of conventional cooling system, it was also found that the solar cooling system is marginally competitive only when combined with domestic water heating.

Bruno et al (2004) modeled Ammonia-water-sodium hydroxide mixtures absorption refrigeration plant using a commercial process simulator "Aspen Plus 2003". It was found that the system performance is notably increased (lower driving temperature and higher COP).

Fernandez et al. (2005) also modeled an absorption processes taking place in Ammonia-water absorption system using finite difference approach. The simultaneous heat and mass transfer set

UNIVERSITY OF IBADAN

of nonlinear differential equations were solved using the above mentioned approach. The results established the expected typical range of values of $x_{vb} < z < \infty$.or $-\infty < z < x_{Lb}$ and $x_{Lb} < z < x_{vi}$ for mass transfer against temperature variations in different components of the plant such as absorber and evaporator where x, z, b, L, i and v are defined as ammonia molar concentration, ammonia to net molar flux transferred ratio, bulk conditions, liquid, liquid-vapour interface and vapour respectively.

Icksoo et al. (2006) developed a water-lithium bromide absorption process model over a horizontal tube using finite difference approach. The model predicts that significant absorption takes place in the drop formation regime with a considerable variation of temperature and mass fraction. Xu et al. (2006) simulated aqueous lithium bromide (LiBr-H_2O) advanced energy storage system using finite difference method. The result predicts the dynamic characteristics and performance of the system, including the temperature and concentration of the working fluid, the mass and energy in the storage tanks, the compressor intake mass or volume flow rate, discharge pressure, compression ratio, power and consumption work, the heat loads of heat exchanger devices in the system and so on. The result also indicated that the integrated coefficient of performance (COP_{int}) of the system was 3.09 and 3.26 respectively as against the expected value of 3.0 under the two storage strategies, while the isentropic efficiency of water vapour compressor was set as 0.6. These results were found to be very helpful in understanding and evaluating the system as well as for system design, operation and control.

Gustavo et al. (2007) studied a two-stage LiBr-water absorption chiller driven at two temperature levels using thermodynamic modeling technique. The study established that the machine can operate in summer as a double-stage chiller driven by heat at 170 ^{0}C from natural gas, as a single-stage chiller driven by heat at 90 ^{0}C from solar energy, or simultaneously in combined mode at both temperatures. It also established the capability of operating in winter in "double-lift" mode for heating with a driving heat at 170 ^{0}C from natural gas. Balghouthi et al. (2007) conducted both experimental and numerical modeling on solar water-lithium bromide absorption air conditioning in Tunisian climatic conditions (36^0 Latitude and 10^0 longitude, 400cal/cm^{2}day average solar irradiation, and 3700h/year and 350 total insolation period and sunny days per year respectively) using the TRNSYS and 'EES' Engineering Equation Solver programs in the study. The model established that absorption solar air-conditioning system was suitable under Tunisian conditions. Despite the initial high cost and almost zero maintenance

UNIVERSITY OF IBADAN

cost, this system could help to minimize fossil fuel-based energy use, reduce electricity demand on the national grid especially at peak demand periods in summer and eliminate the use of CFCs.

In experimental enhanced absorption process study, Wen-long Cheng et al. (2003) investigated experimentally the effect of additive on falling film absorption of water vapour in aqueous LiBr. The experimental results showed that small amounts of additive can enhance the heat transfer of absorption process significantly, and the enhancement degree is influenced by additive concentration and Reynolds number. Based on a dimensionless analysis of the Navier-Stokes equations applied to the falling film absorption process, a new dimensionless parameter, surface renewal number Rn was introduced, and a semi-empirical equation of enhancement factor of additive was obtained, which shows that the enhancement effect of additive on Nusset number of absorption process is determined by the absorption Marangoni number Ma, the surface Marangoni number Ma_A, the surface renewal number Rn, the adsorption number η, and the Reynolds number Re. It was proved that the semi-empirical equation can agree with the experimental results well by introduction of the parameters related to surface tension into the equation. The study concluded as follows: i.There is an optimum additive concentration in which the enhancement effect of additive is strongest, ii.The Marangoni number Ma, the surface Marangoni number Ma_A, and the surface renewal number Rn enlarge the enhancement of the heat transfer during absorption, iii. The adsorption number η reduces the heat transfer of absorption, and iv. The enhancement factor decreases as the Reynolds number increases. Yong Tae Kang et al. (2006) in their experimental study also obtained the following results: (i). The vapour absorption rate increases with increasing solution mass flow rate and the concentration of Fe nanoparticles and CNT. The effect of coolant mass flow rate on the vapour absorption rate is not significant under the experimental conditions, (ii). The heat transfer rate increases with increasing the solution mass flow rate while it is not much affected by the concentration of nanoparticles, (iii). The mass transfer enhancement is much more significant than the heat transfer enhancement in the binary nanofluids with Fe nanoparticles and CNT, and (iv). The mass transfer enhancement from the CNT (average 2.16 for 0.01 wt % and average 2.48 for 0.1 wt %) becomes higher than that from the Fe nanoparticles (average 1.71 for 0.01 wt % and average 1.90 for 0.1 wt %). Therefore, the CNT is a better candidate than Fe nanoparticles for performance enhancement in H_2O/LiBr absorption system.

UNIVERSITY OF IBADAN

In numerical enhanced absorption refrigeration study, Staicovici et al. (2005) modeled water-lithium bromide absorption/generation processes in a Marangoni Convection (applied practical method by the thermal absorption technology in the past decades to significantly improve the absorption process) Cell using the Two-Point theory (TPT) of mass and heat transfer. The model established the capability of (TPT) approach in the Marangoni convection assisted water-lithium bromide absorption process following the successful modeling of the ammonia-water absorption process. It also confirms Marangoni convection basic mechanism explanation in the case of the water-lithium bromide medium. Xohar et al. (2005) investigated the influence of diffusion in the ammonia-water diffusion absorption refrigeration (DAR) cycle configuration on the system performance using a computer simulator known as 'EES' Engineering Equation Solver. The result reveals that DAR cycle without condensate sub-cooling shows higher COP of 14-20% compared with the DAR cycle with the condensate sub-cooling, but it occurs at higher evaporator temperature of about 15^0C.

Niu et al. (2006) performed a numerical analysis of falling film ammonia-water absorption in a magnetic field using a computer program known as TDMA due to the tri-diagonal matrix formation of the equations after discretization. It was found that when the magnetic induction intensity at the solution's inlet was 3Tesla (T), the increment in concentration of ammonia-water solution at outlet was 1.3% and the absorbability increased by 5.9%. The COP of the absorption refrigeration system increased by 4.7% and the decrement in circulation ratio was 8.3%. This establishes a positive effect on the ammonia-water falling film absorption to some degree.

From the above review, it is evident that the finite difference approach has received much attention in the existing literature thereby establishing its popularity and reliability. In addition the review also established some works done in enhanced absorption refrigeration study most especially using additives or nano-fluids / nano-particles in both ammonia-water and water-lithium bromide (H_2O-LiBr) solution. However to the best of knowledge of the researcher, only magnetic field enhanced ammonia-water falling film absorption has been worked upon while none on this type of enhancement has been done on either water-lithium bromide (H_2O-LiBr) or water-lithium chloride (H_2O-LiCl) pairs. This present work therefore uses the finite difference method in an application of the falling film magnetic field enhanced absorption model to the 2-D flow over a vertical flat surface. The two working fluids to be investigated under this magnetic

UNIVERSITY OF IBADAN

field enhancement are lithium chloride-water ($LiCl-H_2O$) and lithium bromide-water ($LiBr-H_2O$) pairs.

UNIVERSITY OF IBADAN

CHAPTER THREE

METHODOLOGY

3.1 Assumptions

In developing the governing equations for this flow modeling the absorption process in a smooth thin-liquid film, the following assumptions are made.

i. The flow is a fully developed steady laminar flow as shown in fig. 3.1a hence velocity (v) in Y-direction is zero

ii. The fluid properties are constant and not varying with temperature and concentration.

iii. The mass rate of vapour absorbed is very small compared to the solution flow rate such that the film thickness and flow velocities can be treated as constant.

iv. Heat transfer in the vapor phase is negligible.

v. Vapor pressure equilibrium exists between the vapour and liquid at the interface.

vi. The Peclet numbers are large enough such that the diffusion in the flow direction can be neglected.

vii. Diffusion thermal effects are negligible.

viii. The magnetic induction intensity descends linearly along the flow of falling-film.

ix. The shear stress at the liquid–vapor interface is negligible

The model coordinate system is as shown in Fig. 3.1a Yang and Wood (1992) where U is the velocity in the film in X-direction.

3.2: **Governing equations**

Niu et al. (2006) in his study of magnetic field enhancement effect on absorption process of ammonia-water solution, the first of its kind, utilized model governing equations (1a) through (1e). The study was done on non-smooth thin-liquid falling film. The equations are as follows; the heat transfer energy equation (1a), continuity equation (1b), momentum equation (1c) and quality or mass transfer equation (1e).

UNIVERSITY OF IBADAN

$$\rho C_p u \frac{\partial T}{\partial x} + \rho C_p v \frac{\partial T}{\partial y} = \frac{\partial}{\partial y}\left(\lambda \frac{\partial T}{\partial y}\right) \quad (1a)$$

$$\frac{\partial(\rho u)}{\partial x} + \frac{\partial(\rho v)}{\partial y} = 0 \quad (1b)$$

$$\rho u \frac{\partial u}{\partial x} + \rho v \frac{\partial u}{\partial y} = \frac{\partial}{\partial y}\left(\mu \frac{\partial u}{\partial y}\right) + \rho g + \int_{mag} \quad (1c)$$

$$\rho u \frac{\partial \xi}{\partial x} + \rho v \frac{\partial \xi}{\partial y} = \frac{\partial}{\partial y}\left(\rho D_m \frac{\partial \xi}{\partial y}\right) \quad (1d)$$

Where $\int_{mag}$ (Li, G.D (1999)) in the above equation is the magnetic force which the falling-film solution experienced per unit volume. It is in the direction of downward vertically.

$$\int_{mag} = \frac{\rho \chi^{B^2}}{l.\mu_0} \quad (1e)$$

where χ is the magnetic mass susceptibility of either Lithium bromide and or Lithium chloride water solution, B is the magnetic induction intensity, l is the length of falling-film flows, and μ_0 is the vacuum's permeability.

Odunfa (2008) utilized the following heat transfer, mass transfer, continuity equation and the velocity field equation in smooth thin-liquid falling film (Bird et al (1960) and Yang and Wood (1992)). The study was done on a smooth thin-liquid falling film. The equations are as follows; the energy conservation equation (2a), continuity equation (2b), conservation of linear momentum equation Bird et al (1960) (2c) and quality or mass transfer equation (2d).

UNIVERSITY OF IBADAN

$$\rho C_p u \frac{\partial T}{\partial x} + \rho C_p v \frac{\partial T}{\partial y} = \frac{\partial}{\partial y}\left(\lambda \frac{\partial T}{\partial y}\right) \quad (2a)$$

$$\frac{\partial(\rho u)}{\partial x} + \frac{\partial(\rho v)}{\partial y} = 0 \quad (2b)$$

$$U = \frac{3}{2} V_0 \left[2\frac{y}{h_0} - \left(\frac{y}{h_0}\right)^2 \right] \quad (2c)$$

$$\rho u \frac{\partial \xi}{\partial x} + \rho v \frac{\partial \xi}{\partial y} = \frac{\partial}{\partial y}\left(\rho D_m \frac{\partial \xi}{\partial y}\right) \quad (2d)$$

A closer inspection of the utilized set of equations in the two cases mentioned above i.e non smooth falling-film Niu et al. (2006) and smooth thin-liquid falling-film Odunfa (2008) reveals that the equations in both cases are similar, only with the exception of equation (1c) of the first case and equation (2c) in the latter one. The first case non-smooth falling-film but enhanced magnetically, while the second case is smooth falling-film, but not enhanced magnetically. The present work is on a smooth thin-liquid falling-film which is to be enhanced magnetically. Towards achieving this, a magnetic field enhanced velocity field model equation in smooth thin liquid falling-film, using mass transport relationship was developed as shown in appendix A. This developed enhanced velocity model equation (xxi) in the appendix A was used to replace equation (2c), thus the model set of magnetic enhanced velocity, heat and mass transfer equations on a smooth thin-liquid falling-film corresponding to the coordinate system shown in fig. 3.1a will now be:

$$u \frac{\partial T}{\partial x} - \alpha \frac{\partial^2 T}{\partial y^2} = 0 \quad (3a)$$

$$\partial \frac{(\rho u)}{\partial x} = 0 \quad (3b)$$

$$\frac{\partial^2 u}{\partial y^2} + 3\frac{v_0}{h^2{}_0} + \rho g + \frac{\rho \chi B^2}{l \mu_0} = 0 \quad (3c)$$

$$u \frac{\partial \xi}{\partial x} - D_m \frac{\partial^2 \xi}{\partial y^2} = 0 \quad (3d)$$

UNIVERSITY OF IBADAN

The final developed model magnetic enhanced velocity field, heat and mass transfer equations on a smooth thin-liquid falling-film in a cooling system are:

$$\frac{\partial^2 u}{\partial y^2} + 3\frac{v_0}{h^2{}_0} + \rho g + \frac{\rho \chi B^2}{l\mu_0} = 0 \qquad (4a)$$

$$u\frac{\partial T}{\partial x} - \alpha\frac{\partial^2 T}{\partial y^2} = 0 \qquad (4b)$$

$$u\frac{\partial \xi}{\partial x} - D_m\frac{\partial^2 \xi}{\partial y^2} = 0 \qquad (4c)$$

where χ is the magnetic mass susceptibility, B is the magnetic induction intensity, l is the length of falling-film flows, μ_0 is the vacuum permeability, T is temperature, ξ is concentration (absorbent), α is thermal diffusivity, D_m is species diffusivity, V_0 is the average velocity within the film thickness and h_0 is the film thickness

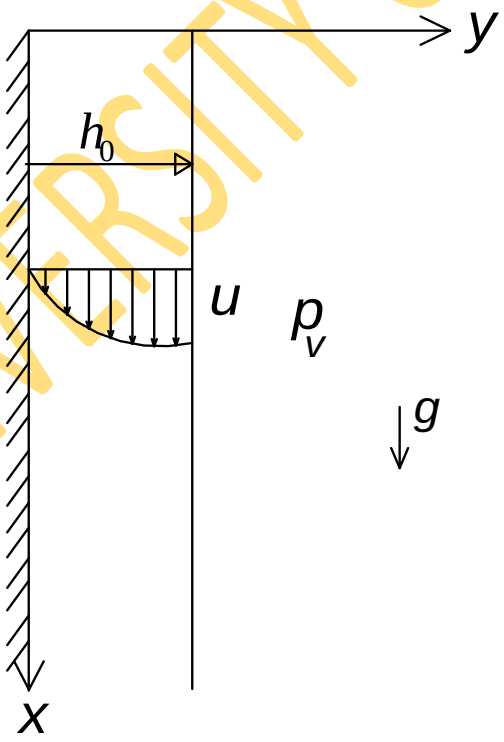

Fig. 3.1a: 2-d representation of a thin-liquid falling-film

UNIVERSITY OF IBADAN

Boundary Conditions

At x = 0; u = u_{in}, T = T_{in} and $\xi = \xi_{equil}$ - (5a)

At y = 0; (non permeable wall);

u = 0, $T = T_w$, $\frac{\partial \xi}{\partial y} = 0$ - (5b)

At $y = h_0$; $-K\frac{\partial T}{\partial y} = \rho D_m \frac{\partial \xi}{\partial y} H_a$ $\xi = \xi_{equil}(T, P_v)$ (5c)

At the vapour-liquid interface, $y = h_0$; $\left(\frac{\partial u}{\partial y}\right)_{y=0} = 0, P_v = (T_s, \xi_s) = const.$

Where H_a = Heat of absorption, T_w = Wall temperature P_v = Vapour pressure and

$\xi_{equil}(T, P_v)$ = equilibrium concentration at the interface temperature and ambient vapour pressure.

3.3: Finite Difference formulation of the governing equations

The general finite difference formulation or approximation of the first derivative of a function $F_{(x, y)}$ with respect to x is given as

$$\frac{dF}{dx} = \frac{F(x + \Delta x, y) - F(x, y)}{\Delta x} \quad - \quad (6a) \text{ and}$$

$$\frac{d^2F}{dx^2} = \frac{d}{dx}\left(\frac{dF}{dx}\right) = \frac{\left(\frac{F(x + \Delta x + \Delta x, y) - F(x + \Delta x, y)}{\Delta x} - \frac{F(x + \Delta x, y) - F(x, y)}{\Delta x}\right)}{\Delta x} \quad - \quad (6b)$$

Similarly the first derivative of a function F(x, y) with respect to y is also given as

$$\frac{dF}{dy} = \frac{F(x, y + \Delta y) - F(x, y)}{\Delta y} \quad - \quad (7a) \quad \text{and}$$

UNIVERSITY OF IBADAN

$$\frac{d^2F}{dy^2} = \frac{d}{dy}\left(\frac{dF}{dy}\right) = \frac{\dfrac{F(x, y+\Delta y+\Delta y) - F(x, y+\Delta y)}{\Delta y} - \dfrac{F(x, y+\Delta y) - F(x, y)}{\Delta y}}{\Delta y} \quad \text{- (7b)}$$

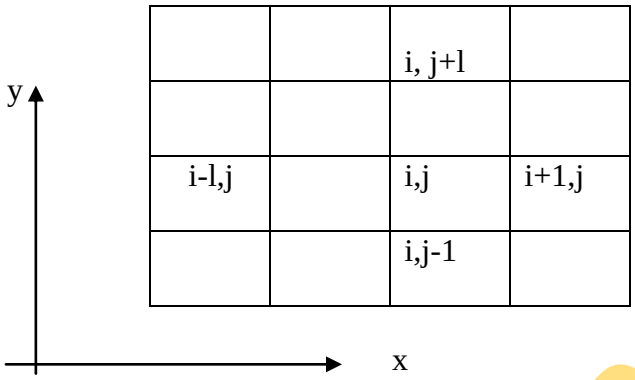

Fig. 3.1b: Finite difference diagram

Using a central finite difference approximation in fig. 3.1b then equation (6b) become

$$\frac{d^2F}{dx^2} = \frac{F(x+\Delta x, y) - 2F(x, y) + F(x-\Delta x, y)}{\Delta x^2} \quad (8a)$$

$$= \frac{F_{i+1,j} - 2F_{i,j} + F_{i-1,j}}{\Delta x^2} \quad (8b)$$

Similarly equation (7b) become

$$\frac{d^2F}{dy^2} = \frac{F(x, \Delta y+\Delta y) - 2F(x, y) + F(x, y-\Delta y)}{\Delta y^2} \quad (9a)$$

$$= \frac{F_{i,j+1} - 2F_{i,j} + F_{i,j-1}}{\Delta y^2} \quad (9b)$$

Relating the above derived equation to the heat transfer equation (1)

$$U\frac{\partial T}{\partial x} - \alpha\frac{\partial^2 T}{\partial y^2} = U\frac{F_{i+1,j} - F_{i,j}}{\Delta x} - \alpha\frac{F_{i,j+1} - 2F_{i,j} + F_{i,j-1}}{\Delta y^2} \quad (10)$$

If $\Delta x = \Delta y = h$

UNIVERSITY OF IBADAN

$$U\frac{\partial T}{\partial x}-\alpha\frac{\partial^2 T}{\partial y^2}=\mathrm{U}\left[F_{i+1,j}-F_{i,j}\right]h-\alpha\left[F_{i,j+1}-2F_{i,j}+F_{i,j-1}\right]=0 \qquad (10b)$$

For $F_{i,j}=T_{i,j}$

$$U\frac{\partial T}{\partial x}-\alpha\frac{\partial^2 T}{\partial y^2}=\mathrm{U}\left(T_{i+1,j}-T_{i,j}\right)h-\alpha\left(T_{i,j+1}-2T_{I,J}+T_{i,j-1}\right)=0 \qquad 10c$$

Therefore $\mathrm{U}\left(T_{i+1,j}-T_{i,j}\right)h-\alpha\left(T_{i,j+1}-2T_{I,J}+T_{i,j-1}\right)=0$ - 10d

Similarly for the same laminar flow, relating the derived equations (8a – 9b) to the mass transfer equation (3d)

$$u\frac{\partial \xi}{\partial x}-D_m\frac{\partial^2 \xi}{\partial y^2}=u\frac{F_{i+1,j}-F_{i,j}}{\Delta x}-D_m\frac{F_{i,j+1}-2F_{i,j}+F_{i,j-1}}{\Delta y^2} \qquad (11a)$$

again if $\Delta x = \Delta y = \mathrm{h}$

$$u\frac{\partial \xi}{\partial x}-D_m\frac{\partial^2 \xi}{\partial y^2}=u\left(F_{i+1,j}-F_{i,j}\right)-D_m\left(F_{i,j+1}-2F_{i,j}+F_{i,j-1}\right) \quad - \qquad (11b)$$

$$F_{i,j}=\xi_{i,j}$$

$$\therefore u\frac{\partial \xi}{\partial x}-D_m\frac{\partial^2 \xi}{\partial y^2}=u\left(\xi_{i+1,j}-\xi_{i,j}\right)-D_m\left(\xi_{i,j+1}-2\xi_{i,j}+\xi_{i,j-1}\right)=0 \quad - \qquad (11c)$$

$$\therefore\ u\left(\xi_{i+1,j}-\xi_{i,j}\right)-D_m\left(\xi_{i,j+1}-2\xi_{i,j}+\xi_{i,j-1}\right)=0 \quad - \qquad (11d)$$

Equations (12a and 12b) depict the basic general finite difference equations for heat and mass transfer.

$$u\left(T_{i+1,j}-T_{i,j}\right)-\alpha\left(T_{i,j+1}-2T_{i,j}+T_{i,j-1}\right)=0 \quad - \qquad (12a)$$

$$u\left(\xi_{i+1,j}-\xi_{i,j}\right)-D_m\left(\xi_{i,j+1}-2\xi_{i,j}+\xi_{i,j-1}\right)=0 \quad - \qquad (12b)$$

UNIVERSITY OF IBADAN

3.4: Formulation of the magnetic field enhanced finite difference model of the governing equations

The thin liquid falling-film thickness is far too small compared to the entire length of the absorber wall. The film thickness is similar to the boundary layer thickness in heat transfer analysis, therefore the above general finite difference formulation of the governing equations cannot be applied for the internal thin film regime. Therefore the required model finite difference formulation of the governing equations will be as follows:

For the model, Δx is not equal Δy , therefore

$$\frac{\partial^2 u}{\partial y^2} + 3\frac{v_0}{h_0^2} + \rho g + \frac{\rho\chi\beta^2}{l\mu_0} = [\frac{F_{i,j+1} - 2F_{i,j} + F_{i,j-1}}{\Delta y^2}] + 3\frac{v_0}{h_0^2} + \rho g + \frac{\rho\chi\beta^2}{l\mu_0} = 0 \qquad (13a)$$

For $F_{i,j} = u_{i,j}$

$$\frac{\partial^2 u}{\partial y^2} + 3\frac{v_0}{h_0^2} + \rho g + \frac{\rho\chi\beta^2}{l\mu_0} = (u_{i,j+1} - 2u_{i,j} + u_{i,j-1}) + \frac{3v_0\Delta y^2}{h_0^2} + \rho g\Delta y^2 + \Delta y^2\frac{\rho\chi\beta^2}{l\mu_0} = 0$$

Therefore, $(u_{i,j+1} - 2u_{i,j} + u_{i,j-1}) + \frac{3v_0\Delta y^2}{h_0^2} + \rho g\Delta y^2 + \Delta y^2\frac{\rho\chi\beta^2}{l\mu_0} = 0 \qquad (13b)$

$$u\frac{\partial T}{\partial x} - \alpha\frac{\partial^2 T}{\partial y^2} = \mathrm{u}[\Delta y]^2\left[F_{i+1,j} - F_{i,j}\right] - [\Delta x]\alpha\left[F_{i,j+1} - 2F_{i,j} + F_{i,j-1}\right] = 0 \qquad (13c)$$

For $F_{i,j} = T_{i,j}$

$$u\frac{\partial T}{\partial x} - \alpha\frac{\partial^2 T}{\partial y^2} = \mathrm{u}[\Delta y]^2\left(T_{i+1,j} - T_{i,j}\right) - \alpha\left(T_{i,j+1} - 2T_{i,j} + T_{i,j-1}\right)\Delta x = 0 \qquad (13d)$$

Therefore $\mathrm{u}[\Delta y]^2\left(T_{i+1,j} - T_{i,j}\right) - \alpha\left(T_{i,j+1} - 2T_{i,j} + T_{i,j-1}\right)\Delta x = 0$ - (14a)

$$u\frac{\partial \xi}{\partial x} - D_m\frac{\partial^2 \xi}{\partial y^2} = u[\Delta y]^2\left[F_{i+1,j} - F_{i,j}\right] - D_m[\Delta x]\left[F_{i,j+1} - 2F_{i,j} + F_{i,j-1}\right] \qquad (14b)$$

$F_{i,j} = \xi_{i,j}$

UNIVERSITY OF IBADAN

$$\therefore u\frac{\partial \xi}{\partial x} - D_m \frac{\partial^2 \xi}{\partial y^2} = u[\Delta y]^2\left(\xi_{i+1,j} - \xi_{i,j}\right) - D_m\left(\xi_{i,j+1} - 2\xi_{i,j} + \xi_{i,j-1}\right)\Delta x = 0 \quad (15a)$$

$$\text{Therefore} \therefore \; u[\Delta y]^2\left(\xi_{i+1,j} - \xi_{i,j}\right) - D_m\left(\xi_{i,j+1} - 2\xi_{i,j} + \xi_{i,j-1}\right)\Delta x = 0 \quad - \quad (15b)$$

Equations (12b) and (13b); the finite difference model equations satisfied at each node in the interior face of the domain R for heat and mass transfer.

$$(u_{i,j+1} - 2u_{i,j} + u_{i,j-1}) + \frac{3\nu_0 \Delta y^2}{h_0^2} + \rho g \Delta y^2 + \Delta y^2 \frac{\rho \chi \beta^2}{l\mu_0} = 0 \quad - \quad (16a)$$

$$u[\Delta y]^2\left(T_{i+1,j} - T_{i,j}\right) - \alpha\left(T_{i,j+1} - 2T_{i,j} + T_{i,j-1}\right)\Delta x = 0 \quad - \quad (16b)$$

$$u[\Delta y]^2\left(\xi_{i+1,j} - \xi_{i,j}\right) - D_m\left(\xi_{i,j+1} - 2\xi_{i,j} + \xi_{i,j-1}\right)\Delta x = 0 \quad - \quad (16c)$$

3.5: Boundary conditions

At the boundary, usually the parameters such as temperature and concentration are known (Dirichlet conditions) or the boundary is considered to be perfectly insulated (Newmann or Adiabatic conditions). Insulated boundaries are handled by developing boundary element/nodal equations. In this model, Newmann or Adiabatic boundary condition was used along the absorber wall. Figure 3.2 shows a half element in the model lying on an insulated left boundary of the smooth film thickness portion of the absorber. The net heat flowing into this element must be equal to zero when considering steady-state condition in the film. In the boundary shown in Fig 3.2, the quantity of heat flowing into the three faces of the half element in time dt is given by the following equations:

UNIVERSITY OF IBADAN

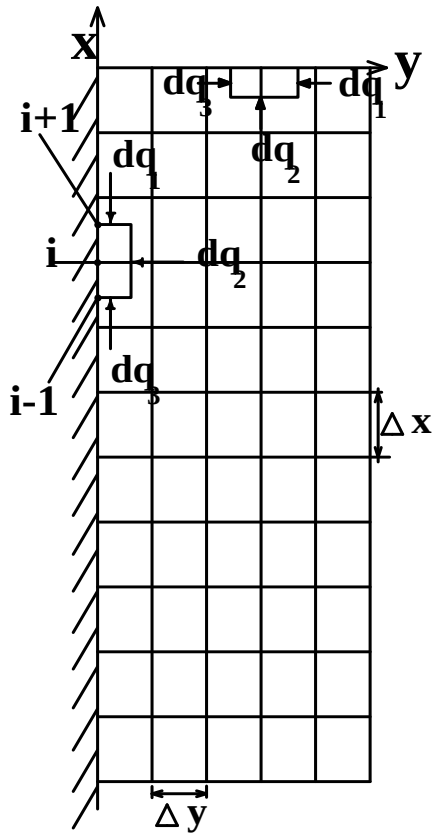

Fig. 3.2 Temperature boundary conditions analysis

From fig. 3.2, the heat balance equation for the half element is

$dq_1 + dq_2 + dq_3 = 0$ (17)

The complete boundary difference equations (xxiii to xxvi) in this study appearing in Appendix A was applied, thus

(Left) $T_{i+1,j} + 2T_{i,j+1} + T_{i-1,j} - 4T_{i,j} = 0$ (18a)

(Right) $T_{i+1,j} + 2T_{i,j-1} + T_{i-1,j} - 4T_{i,j} = 0$ (18b)

(Upper) $T_{i,j-1} + 2T\,i-1, j + T_{i,j+1} - 4T_{i,j} = 0$ (18c)

(Lower) $T_{i,j-1} + 2T_{i+1,j} + T_{i,j+1} - 4T_{i,j} = 0$ (18d)

Thus, in obtaining a solution for the steady state heat flow in the smooth film absorption medium, Eq. (17) must hold at every interior grid point and Eqs. (18a) through (18d) must be

UNIVERSITY OF IBADAN

satisfied at any appropriate known or insulated boundaries. Gaussian elimination methods or Gauss-Seidel iteration method could be employed to solve the equations accurately for the number of grid-points required.

For the steady state mass flow in the smooth film-absorption medium shown in figure 3.3, similar approach was employed to develop boundaries equations for the unknown or insulated boundaries as shown in the figure.

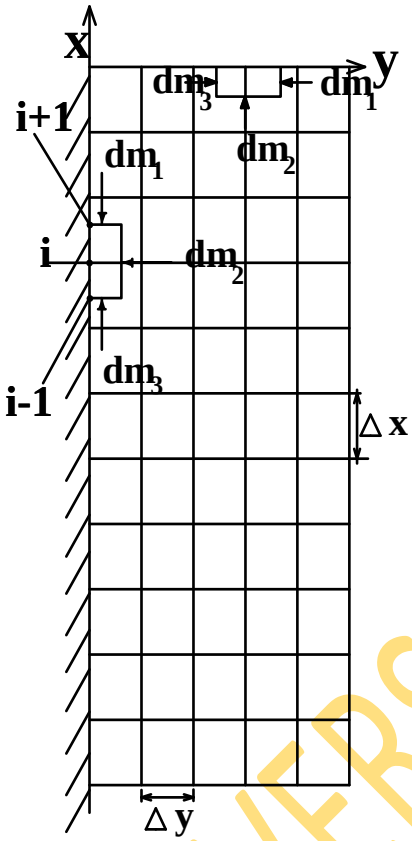

Fig. 3.3 Concentration boundary conditions analysis

The net mass flowing into this element must be equal to zero when considering steady-state condition in the liquid-film. The quantity of mass flowing into the three faces of the half-element in time dt are given by the following equations.

From fig. 3.3 the mass balance equation for the half-element is

$$dm_1 + dm_2 + dm_3 = 0 \qquad (19)$$

UNIVERSITY OF IBADAN

The complete boundary difference equations (xxviii to xxxi) in this study appearing in Appendix A was applied, thus

(Left) $\xi_{i+1,j} + 2\xi_{i,j+1} + \xi_{i-1,j} - 4\xi_{i,j} = 0$ (20a)

(Right) $\xi_{i+1,j} + 2\xi_{i,j-1} + \xi_{i-1,j} - 4\xi_{i,j} = 0$ (20b)

(Upper) $\xi_{i,j-1} + 2\xi_{i-1,j} + \xi_{i,j+1} - 4\xi_{i,j} = 0$ (20c)

(Lower) $\xi_{i,j-1} + 2\xi_{i+1,j} + \xi_{i,j+1} - 4\xi_{i,j} = 0$ (20d)

Thus, in obtaining a solution for the steady state mass flow in the smooth film absorption medium, Equation (19) must hold at every interior grid point and Eqs. (20a) through (20d) must be satisfied at any appropriate known or insulated boundaries.

Equations (17) and (19) are for the interior grid points in the smooth film absorption medium while equations (18a) through (18d) and equations (20a) through (20d) are for the boundary conditions in heat and mass transfer respectively. The development of these boundary equations took due cognisance of the inlet conditions to the absorber, absorber wall and the given condition in the thin-liquid falling-film/gas or vapour interface. The two immediate adjacent nodes to each of the corner nodes of the medium are taken into consideration in the program to determine the unknowns at the corner nodes.

3.6: Solution Method

As earlier mentioned, there are many solution techniques available that are being used for solving the global finite difference matrix equations 12b and 13b coupled with the boundary equations 15 and 20 generated. Two of the most widely used methods are Gauss-Seidel iteration and Gaussian elimination method as modified by Paynes and Iron and reported by Okon, (1990).The modified Gaussian elimination method employed is given in Appendix D.

3.7: Computer Programming

The finite difference method is used to solve the governing equations (1) & (2) as given in the form of finite difference equations (16a) & (16b). The solution technique used is Gaussian

UNIVERSITY OF IBADAN

elimination scheme as modified by Paynes and Iron and reported by Okon, (1990) on the digital computer. The computer program and the subroutines are written in FORTRAN 90 language.

Main Program

The program shown in Appendix A solves equations (16a) & (16b) using modified Gaussian elimination scheme. The flow chart is shown in Fig. 3.4a. This main program utilizes two (2) different subroutines. These subroutines are written to execute various steps involved in applying the finite difference scheme. The problem data are introduced into the program in the "data block", where the input parameters can be easily modified to suit any case study. The main program, after generating the global matrix, calls subroutine "solution1", before calling subroutine "solution2". After calling a subroutine solution the results were finally "displayed.

Subroutines

These are sub-programs written to execute various steps involved in applying the finite difference method using Gaussian elimination scheme. They are called by the main program. Below are the subroutines employed to execute various steps in the main program;

Solution1 & Solution 2

These are the core sub-routines, they also perform similar functions. These subroutines perform their functions after the implementation of the boundary conditions in the global domain. Solution1 generates the temperature profile of the domain, while solution2 takes care of concentration profile within the domain.

DATA

There is a well-known cliché in the computer world-GIGO an acronym to mean "Garbage in Garbage out" i.e. the quality of the output is no better than the quality of the input. In order to obtain high quality output of temperature and concentration profiles in the domain, the input data utilized was obtained from the literature as was used for the available experimental and numerical modelings. The data utilized from the literature are as shown in Table 3.1(General data), Table 3.2 ($LiBr - H_2O$) and Table 3.3 ($LiCl - H_2O$) respectively.

UNIVERSITY OF IBADAN

Fig. 3.4a: **Main Program Flow Chart**

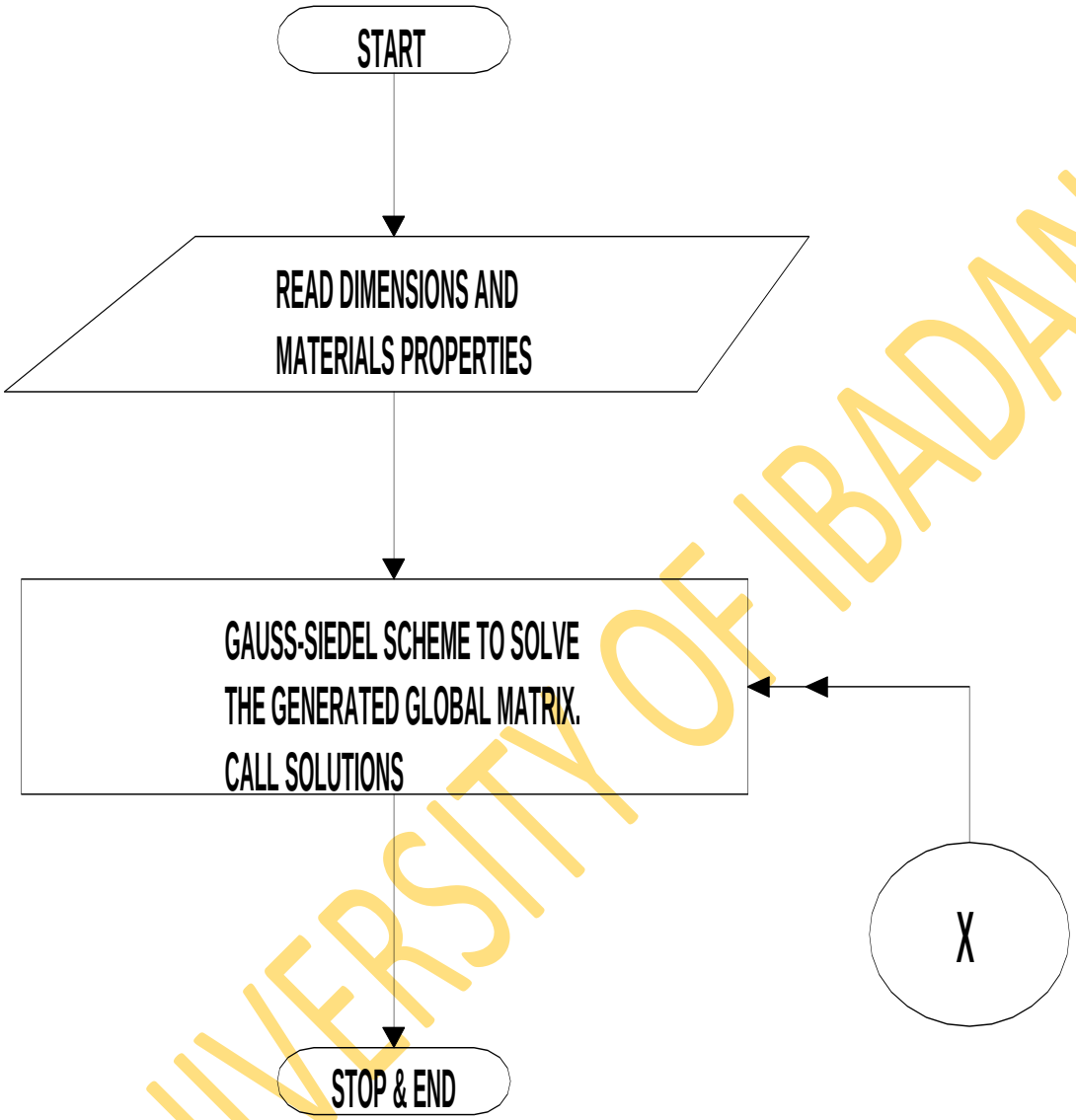

UNIVERSITY OF IBADAN

Fig. 3.4b: **Subroutine Solution Flow Chart**

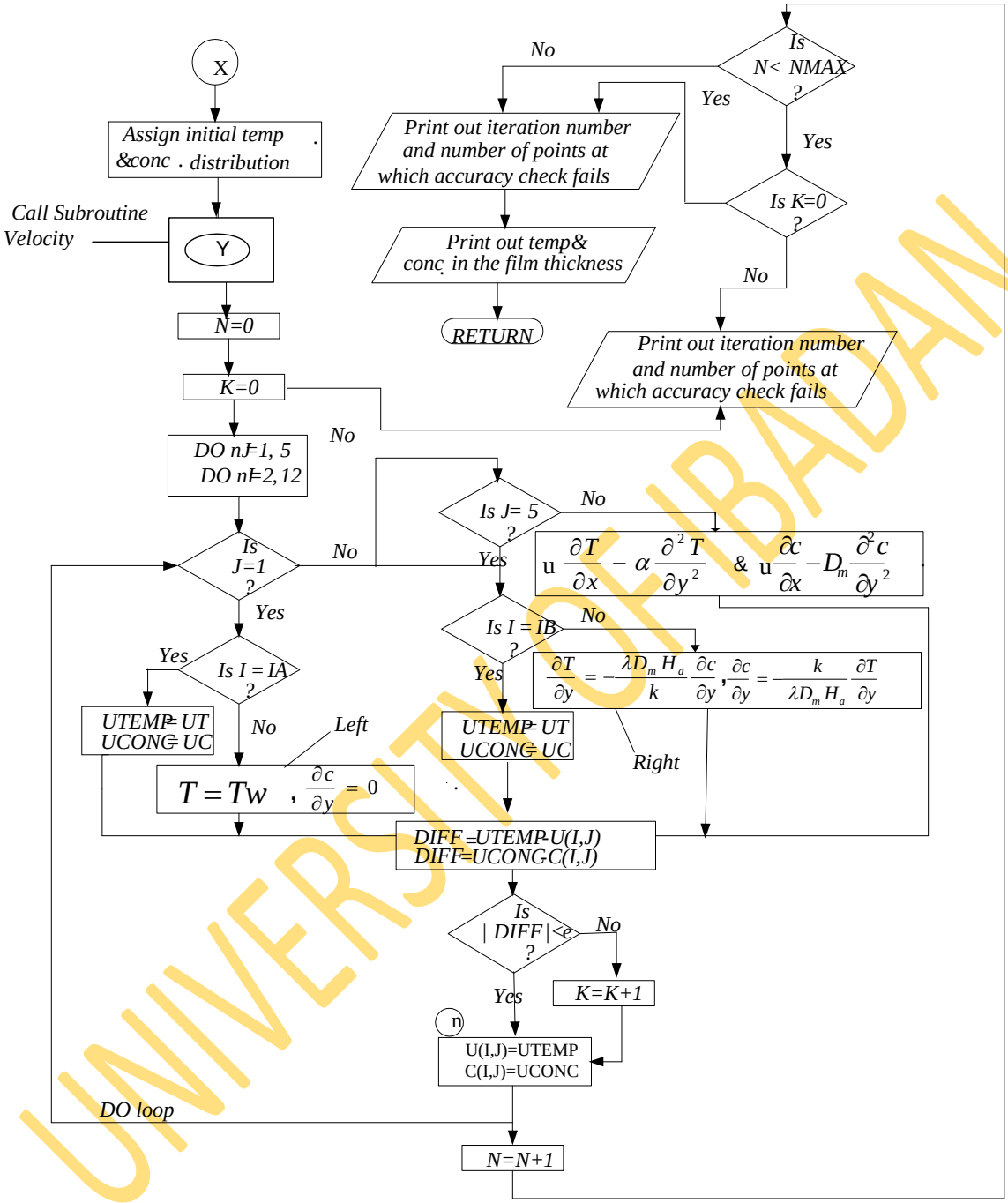

UNIVERSITY OF IBADAN

Fig. 3.4c: **Model Subroutine Velocity Flow Chart**

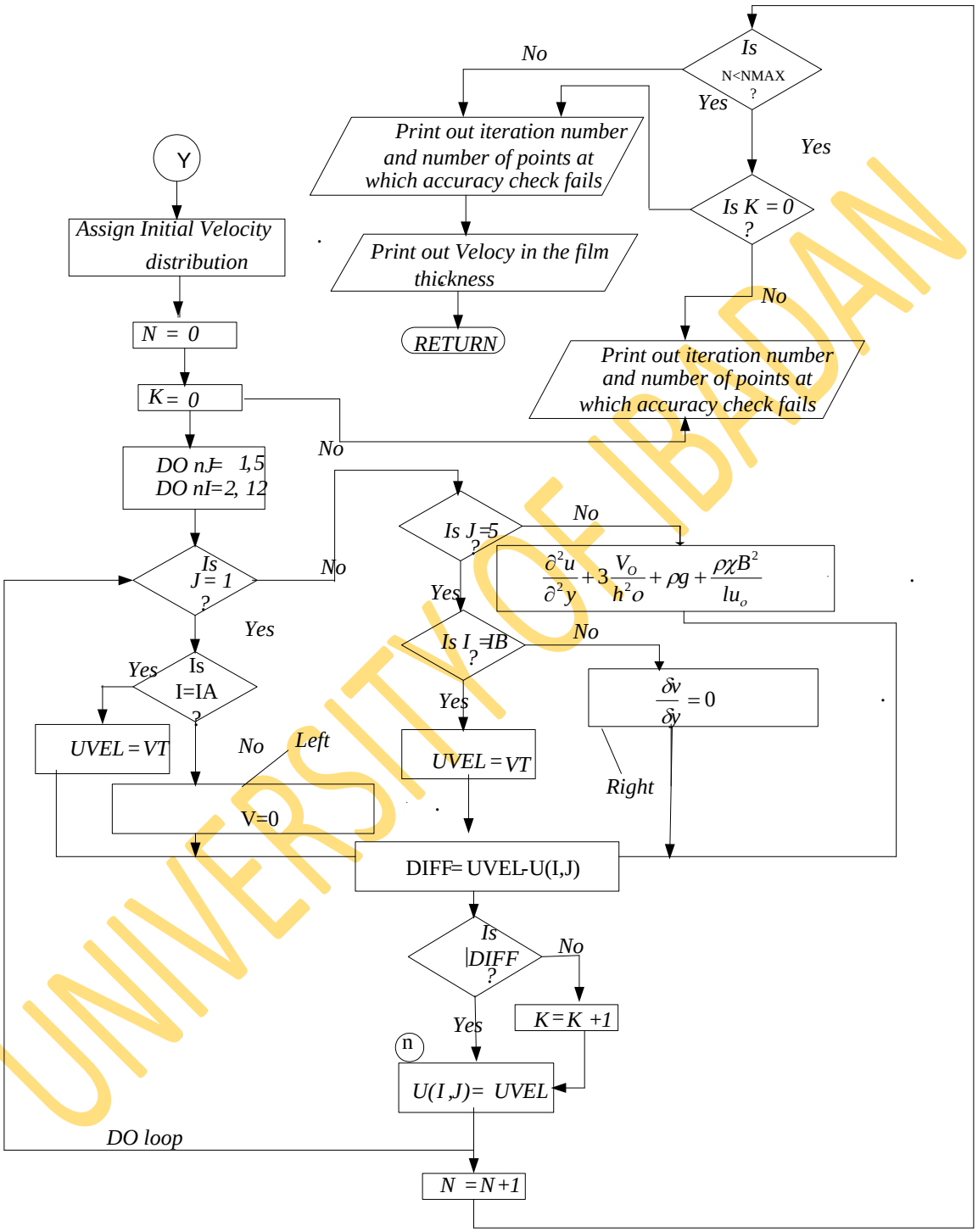

UNIVERSITY OF IBADAN

DATA

Table 3.1: **General;** Niu Xiaofeng et al. [2006]

β magnetic induction intensity at the inlet of solution	= 0, 1.4 and 3.0 Tesla
χ magnetic mass susceptibility LiBr-H_2O &LiCl-H_2O solutions	= 0.0000343, 0000243
u_{in} Initial velocity	= 0.362 ms^{-1}

Table 3.2: **NH_3-H_2O Data** Niu Xiaofeng et al. [2006]

μ film dynamic viscosity	=	$4 \times 10^{-4} kgm^{-1}s^{-1}$
μ_0 vacuum Permeability	=	$1.257 \times 10^{-6} kgmA^{-2}s^{2}$
ν_o mean velocity	=	$3.15 \times 10^{-4} ms^{-1}$
ρ Liquid density	=	$127 kgm^{-3}$
K Thermal conductivity	=	$176 Wm^{-1}K^{-1}$
T_w Wall Temperature	=	35^oC
T_{in} Inlet Temperature	=	35^oC
C_{in} Initial absorbent Conc.	=	20%
C_{eq} Equilibrium absorb. Con	=	20%
g Gravity	=	$9.8 ms^{-2}$
h_o Mean film thickness	=	$1.00 \times 10^{-3} m$
H_a Heat of absorption	=	3466kJ/kg
Pv. Absorbent Vapour Pressure	=	7.02mm.Hg
R_{ef} Film Reynolds number	=	100
I Film mass flowrate	=	$0.01 kgm^{-1}s^{-1}$

UNIVERSITY OF IBADAN

Table 3.3: **LiBr-H_2O Data** Yang et al. [1992]

μ film dynamic viscosity	=	$4 \times 10^{-4} kgm^{-1}s^{-1}$
μ_0 vacuum Permeability	=	$1.257 \times 10^{-6} kgmA^{-2}s^{2}$
ν_o mean velocity	=	$3.15 \times 10^{-4} ms^{-1}$
α Thermal diffusivity	=	$k/\rho_{cp} = 0.155 m^2 s^{-1}$
ρ Liquid density	=	$127 kgm^{-3}$
K Thermal conductivity	=	$176 Wm^{-1}K^{-1}$
D Species diffusivity	=	$1 \times 10^{-10}\ m^2 s^{-1}$
T_w Wall Temperature	=	35^oC
T_{in} Inlet Temperature	=	44.44^oC
C_{in} Initial absorbent Conc.	=	60%
C_{eq} Equilibrium absorb. Con	=	60%
g Gravity	=	$9.8 ms^{-2}$
h_o Mean film thickness	=	$1.00 \times 10^{-3} m$
H_a Heat of absorption	=	3466kJ/kg
Pv. Absorbent Vapour Pressure	=	7.02mm.Hg
R_{ef} Film Reynolds number	=	100
I Film mass flowrate	=	$0.01 kgm^{-1}s^{-1}$

UNIVERSITY OF IBADAN

Table 3.4: LiCl-H_2O Data Yang et al. [1992]

μ film dynamic viscosity	=	$4 \times 10^{-4} kgm^{-1}s^{-1}$
ν_o mean velocity	=	$3.15 \times 10^{-5} ms^{-1}$
α Thermal diffusivity	=	$k/\rho_{cp} = 0.155 m^2 s^{-1}$
ρ Liquid density	=	$1000 kgm^{-3}$
K Thermal conductivity	=	$176 Wm^{-1} K^{-1}$
D Species diffusivity	=	$2.0 \times 10^{-9} m^2 s^{-1}$
T_w Wall Temperature	=	30^oC
T_{in} Inlet Temperature	=	35^oC
C_{in} Initial absorbent Conc.	=	45%
C_{eq} Equilibrium absorb. Con	=	35.8%
g Gravity	=	$9.8 ms^{-2}$
h_o Mean film thickness	=	$1.74 \times 10^{-3} m$
H_a Heat of absorption	=	3466kJ/kg
Pv. Absorbent Vapour Pressure	=	9.2mm.Hg
R_{ef} Film Reynolds number	=	100
I Film mass flow-rate	=	$0.01 kgm^{-1}s^{-1}$

UNIVERSITY OF IBADAN

CHAPTER FOUR

COMPUTATIONAL RESULTS AND DISCUSSION

4.1 General remarks on result presentation

The continuity, momentum, energy and species mass transport equations indicated in the previous section were coded in a computer algorithm using FORTRAN programming coding language. The code was run on a personal computer with sufficient memory facilities to carry out the simulation exercise. The model run was initially executed using ammonia-water so as to validate the developed model code before using the main two working fluid pairs namely lithium bromide-water and lithium chloride-water. The parameters utilized in the literature by Andberg (1982), Yang et al (1992) and Niu Xiaofen (2006) and (2009) as shown in Tables 3.1, 3.2, 3.3 and 3.4 in two cases have been used. The domain area was divided into 13 x 5 mesh evenly spaced in both the direction of falling (x) and in the direction of film thickness (y) in this thesis. The tabulated and plotted graphical figures of the model results are presented side by side with that of the literature where available as shown in the following tables and figures. The results cover the velocity, heat and mass analysis in both the direction of falling film and that of the film thickness direction.

4.2 Numerical Results in the direction of falling film (X) for Ammonia-water, X = Absorber length

The nodal parameters distribution obtained in the direction of falling within the film thickness in the bulk for Ammonia-water (NH_3-H_2O) solution compares well with the existing literature. For instance Tables 4.1, 4.1.2, 4.1.4 and 4.1.7 and Figs 4.1 to 4.1.5 represent the distribution of average velocity, Temperature and concentration of the falling-film within the bulk in X-axis or direction of the falling film at various magnetic induction intensities in NH_3-H_2O solution. Both the table and figures established that the velocity at stronger magnetic field is larger than that of the weaker one. This established parameter distribution within the bulk when compared with the existing literature results in ammonia-water solution had the percentage velocity deviation at 0.0, 1.4 and 3.0 Tesla ranges between -1.01 to 0.15, -1.26 to 0.00 and -1.40 to 0.00 respectively. Tables 4.1.1 and 4.1.2 represent the velocity deviation analysis, upon comparison with the literature results, it has standard velocity deviations (σ) of 1.49 X 10^{-3} at 0.0Tesla, 1.78 X 10^{-3} at 1.4Tesla and **1**.90 X 10^{-3} at 3.0Tesla. The T-Test analysis results established that the velocity,

UNIVERSITY OF IBADAN

Temperature and concentration distributions for ammonia-water was not significantly difference (p=0.05) from published results in literature as shown in the Tables 4.1.3, 4.1.6, 4.1.9 and Figures 4.1, 4.1.1, 4.1.2, 4.1.3, 4.1.4 and 4.1.5.

4.3: Tabular and Graphical representation of the literature and present work's result

Table 4.1: NH_3-H_2O Velocity Distribution in the film Comparison

Absorber length X (m)	Bulk								
	Lit. Result @ 0.0 Tesla *	Present Result @ 0.0 Tesla	% Devia-tion	Lit. Result @ 1.4 Tesla *	Present. Result @ 1.4 Tesla	% Devia-tion	Lit. Result @ 3.0 Tesla *	Present Result @3.0 Tesla	% Devia-tion
0 or 10^{-6}	0.3620	0.3620	0.00	0.3620	0.3620	0.00	0.3620	0.3620	0.00
$10^{-5.5}$	0.3660	0.3660	0.00	0.3665	0.3663	-0.06	0.3680	0.3667	-0.35
10^{-5}	0.3700	0.3700	0.00	0.3710	0.3704	-0.16	0.3720	0.3713	-0.19
$10^{-4.5}$	0.3750	0.3740	-0.27	0.3751	0.3744	-0.19	0.3790	0.3756	-0.92
10^{-4}	0.3790	0.3776	-0.37	0.3810	0.3784	-0.68	0.3840	0.3798	-1.09
$10^{-3.5}$	0.3840	0.3813	-0.70	0.3860	0.3822	-0.99	0.3890	0.3837	-1.36
10^{-3}	0.3880	0.3850	-0.77	0.3900	0.3859	-1.05	0.3920	0.3875	-1.15
$10^{-2.5}$	0.3920	0.3885	-0.89	0.3940	0.3895	-1.14	0.3950	0.3911	-0.99
10^{-2}	0.3960	0.3920	-1.01	0.3980	0.3930	-1.26	0.4000	0.3944	-1.40
$10^{-1.5}$	0.3970	0.3953	-0.43	0.4000	0.3964	-0.90	0.4020	0.3976	-1.10
10^{-1}	0.3980	0.3986	0.15	0.4020	0.3997	-0.57	0.4035	0.4006	-0.72
$10^{-0.5}$	0.4020	0.4019	0.03	0.4040	0.4029	-0.27	0.4050	0.4034	-0.40
10^{0}	0.4050	0.4050	0.00	0.4060	0.4060	0.00	0.4060	0.4060	0.00

* Niu Xiaofeng et al. [2006]

UNIVERSITY OF IBADAN

Table 4.1.1:NH_3-H_2O Velocity Deviation Analysis

Absorber length X (m)	Bulk								
	Lit. Result @ 0.0 Tesla *	Present Result @ 0.0 Tesla	Deviation	Lit. Result @ 1.4 Tesla *	Present. Result @ 1.4 Tesla	Deviation	Lit. Result @ 3.0 Tesla *	Present Result @3.0 Tesla	Deviation
0 or 10^{-6}	0.3620	0.3620	0.0000	0.3620	0.3620	0.0000	0.3620	0.3620	0.0000
$10^{-5.5}$	0.3660	0.3660	0.0000	0.3665	0.3663	0.0002	0.3680	0.3667	0.0013
10^{-5}	0.3700	0.3700	0.0000	0.3710	0.3704	0.0006	0.3720	0.3713	0.0007
$10^{-4.5}$	0.3750	0.3740	0.0010	0.3751	0.3744	0.0007	0.3790	0.3756	0.0034
10^{-4}	0.3790	0.3776	0.0014	0.3810	0.3784	0.0026	0.3840	0.3798	0.0042
$10^{-3.5}$	0.3840	0.3813	0.0027	0.3860	0.3822	0.0038	0.3890	0.3837	0.0053
10^{-3}	0.3880	0.3850	0.0030	0.3900	0.3859	0.0041	0.3920	0.3875	0.0045
$10^{-2.5}$	0.3920	0.3885	0.0035	0.3940	0.3895	0.0045	0.3950	0.3911	0.0039
10^{-2}	0.3960	0.3920	0.0040	0.3980	0.3930	0.0050	0.4000	0.3944	0.0056
$10^{-1.5}$	0.3970	0.3953	0.0017	0.4000	0.3964	0.0036	0.4020	0.3976	0.0044
10^{-1}	0.3980	0.3986	-0.0006	0.4020	0.3997	0.0023	0.4035	0.4006	0.0029
$10^{-0.5}$	0.4020	0.4019	0.0001	0.4040	0.4029	0.0011	0.4050	0.4034	0.0016
10^{0}	0.4050	0.4050	0.0000	0.4060	0.4060	0.0000	0.4060	0.4060	0.0000

* Niu Xiaofeng et al. [2006]

UNIVERSITY OF IBADAN

Table 4.1.2:NH_3-H_2O Velocity Deviation Analysis

	Result @ 0.0 Tesla			Result @ 1.4 Tesla			Result @ 3.0 Tesla		
Absorber length X (m)	**Devia-tion.**	**Mean**	**Mean Dev. Square X 10^{-6}**	**Devia-tion.**	**Mean**	**Mean Dev. Square X 10^{-6}**	**Devia-tion.**	**Mean**	**Mean Dev. Square X 10^{-6}**
0 or 10^{-6}	0.0000	0.0013	1.69	0.0000	0.0022	4.84	0.0000	0.0029	8.41
$10^{-5.5}$	0.0000	0.0013	1.69	0.0002	0.0022	4.00	0.0013	0.0029	2.56
10^{-5}	0.0000	0.0013	1.69	0.0006	0.0022	2.56	0.0007	0.0029	4.84
$10^{-4.5}$	0.0010	0.0013	0.09	0.0007	0.0022	2.25	0.0034	0.0029	0.25
10^{-4}	0.0014	0.0013	0.01	0.0026	0.0022	0.16	0.0042	0.0029	1.69
$10^{-3.5}$	0.0027	0.0013	1.96	0.0038	0.0022	2.56	0.0053	0.0029	5.76
10^{-3}	0.0030	0.0013	2.89	0.0041	0.0022	3.61	0.0045	0.0029	2.56
$10^{-2.5}$	0.0035	0.0013	4.84	0.0045	0.0022	5.29	0.0039	0.0029	1.00
10^{-2}	0.0040	0.0013	7.29	0.0050	0.0022	7.84	0.0056	0.0029	7.29
$10^{-1.5}$	0.0017	0.0013	0.16	0.0036	0.0022	1.96	0.0044	0.0029	2.25
10^{-1}	-0.0006	0.0013	3.61	0.0023	0.0022	0.01	0.0029	0.0029	0.00
$10^{-0.5}$	0.0001	0.0013	1.44	0.0011	0.0022	1.21	0.0016	0.0029	1.69
10^{0}	0.0000	0.0013	1.69	0.0000	0.0022	4.84	0.0000	0.0029	8.41
$\sum$			**29.05**			**41.13**			**46.71**

@ 0.0 Tesla, Std. deviation (σ) = $\sqrt{2.9.05x10^{-6}/13}$ = 1.49 X 10^{-3}

@1.4 Tesla, Std. deviation (σ) = $\sqrt{41.13x10^{-6}/13}$ = 1.78 X 10^{-3}

@3.0 Tesla Std. deviation (σ) = $\sqrt{46.71x10^{-6}/13}$ = 1.90 X 10^{-3}

Table 4.1.3:NH_3-H_2O Velocity T- Test analysis

Independent Samples Test

		Levene's Test for Equality of Variances		t-test for Equality of Means						
									95% Confidence Interval of the Difference	
		F	Sig.	t	df	Sig. (2-tailed)	Mean Difference	Std. Error Difference	Lower	Upper
Velocity @ 0.0 Tesla	Equal variances assumed	.023	.881	.234	24	.817	.001292	.005526	-.010114	.012698
	Equal variances not assumed			.234	23.992	.817	.001292	.005526	-.010114	.012698
Velocity @ 1.4 Tesla	Equal variances assumed	.084	.775	.382	24	.706	.002192	.005745	-.009665	.014050
	Equal variances not assumed			.382	23.942	.706	.002192	.005745	-.009667	.014051
Velocity @ 3.0 Tesla	Equal variances assumed	.018	.893	.507	24	.617	.002908	.005740	-.008939	.014754
	Equal variances not assumed			.507	23.961	.617	.002908	.005740	-.008940	.014755

UNIVERSITY OF IBADAN

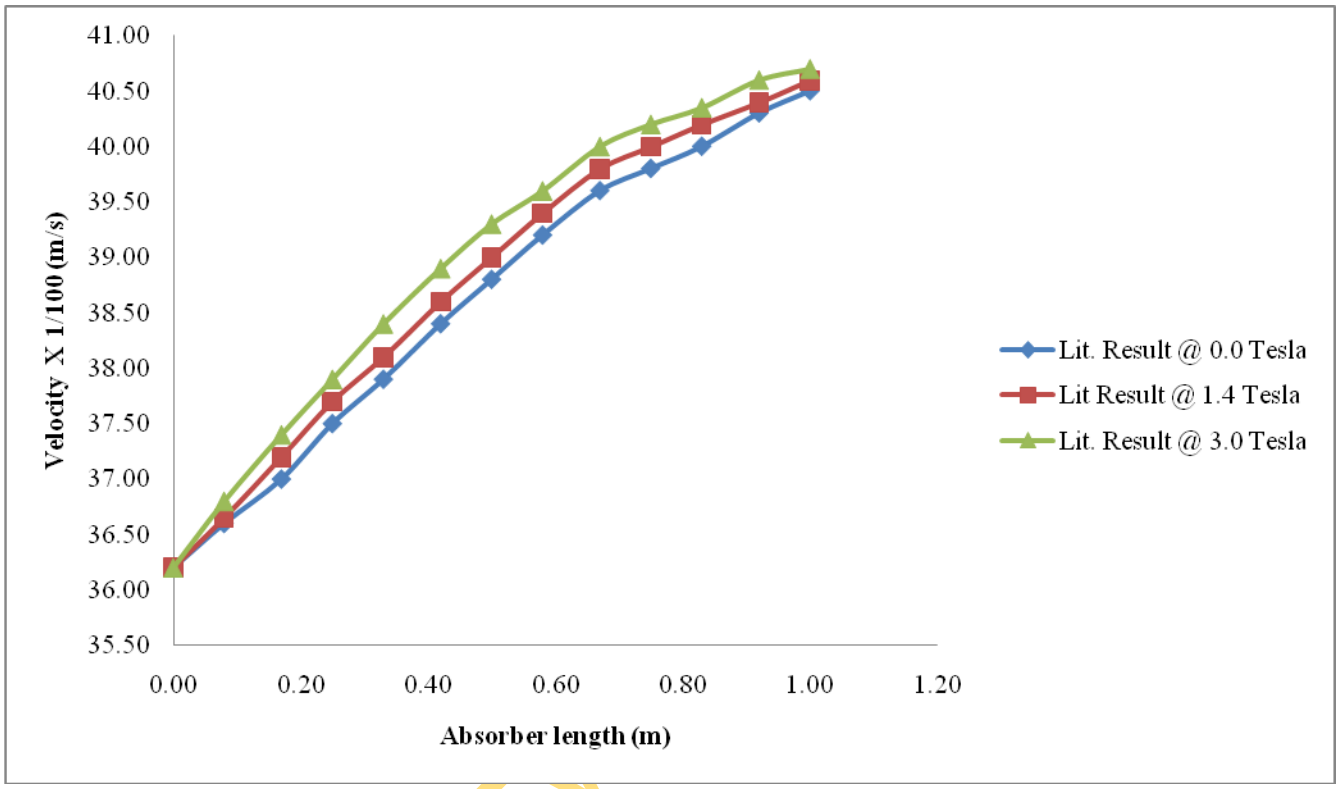

Fig.4.1: NH_3-H_2O Velocity Distribution in the film at 0.0, 1.4 and 3.0Tesla

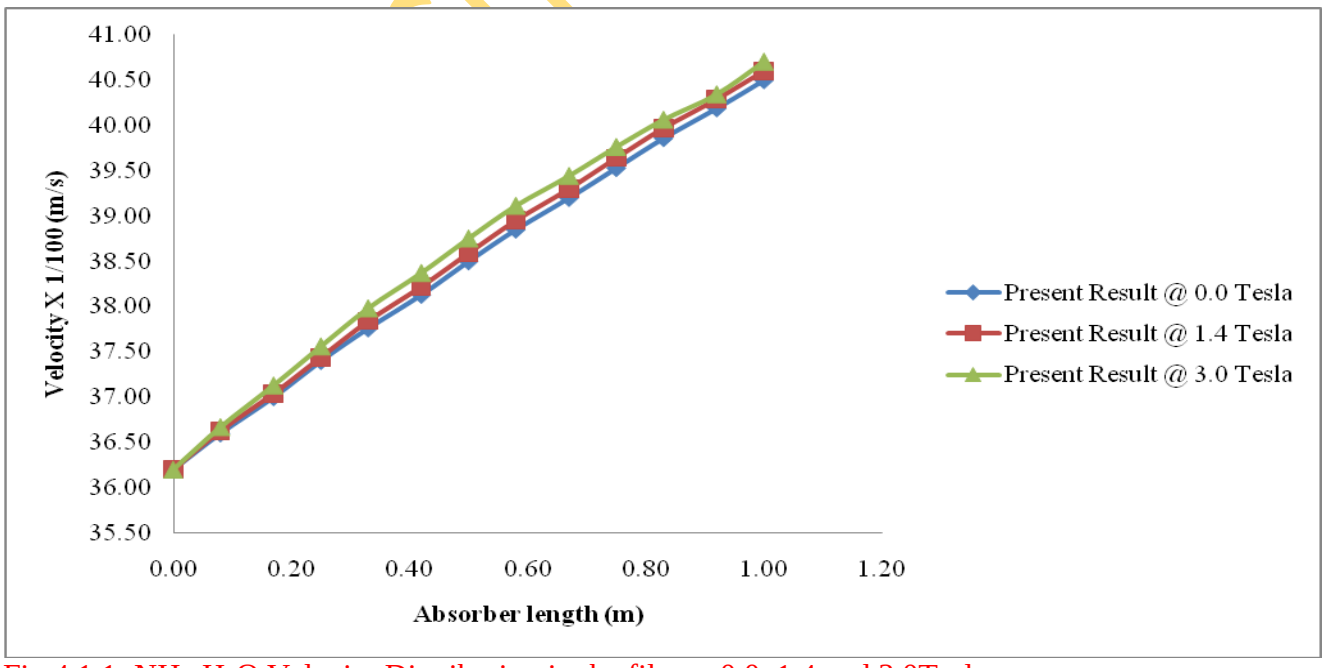

Fig.4.1.1: NH_3-H_2O Velocity Distribution in the film at 0.0, 1.4 and 3.0Tesla

Table 4.1.4:NH_3-H_2O Temperature Distribution in the film Comparison

	BULK								
Absorber length X (m)	**Lit. Result @ 0.0 Tesla ***	**Present Result @ 0.0 Tesla**	**Deviation.**	**Lit. Result @ 1.4 Tesla ***	**Present Result @ 1.4 Tesla**	**Deviation.**	**Lit. Result @ 3.0 Tesla ***	**Present Result @ 3.0 Tesla**	**Deviation.**
0 or 10^{-6}	35.00	35.00	0.00	35.00	35.00	0.00	35.00	35.00	0.00
$10^{-5.5}$	32.00	32.00	0.00	32.00	32.00	0.00	32.00	32.00	0.00
10^{-5}	29.00	30.00	-1.00	29.00	30.00	-1.00	29.00	30.00	-1.00
$10^{-4.5}$	27.00	28.00	-1.00	27.00	28.00	-1.00	27.00	28.00	-1.00
10^{-4}	26.00	26.00	0.00	26.00	26.00	0.00	26.00	26.00	0.00
$10^{-3.5}$	25.00	24.00	1.00	25.00	24.00	1.00	25.00	24.00	1.00
10^{-3}	23.00	23.00	0.00	23.00	23.00	0.00	23.00	23.00	0.00
$10^{-2.5}$	22.00	21.00	1.00	22.00	21.00	1.00	22.00	21.00	1.00
10^{-2}	21.00	20.00	1.00	21.00	20.00	1.00	21.00	20.00	1.00
$10^{-1.5}$	18.00	18.00	0.00	18.00	18.00	0.00	18.00	18.00	0.00
10^{-1}	17.00	17.00	0.00	17.00	17.00	0.00	17.00	17.00	0.00
$10^{-0.5}$	16.00	16.00	0.00	16.00	16.00	0.00	16.00	16.00	0.00
10^{0}	15.00	15.00	0.00	15.00	15.00	0.00	15.00	15.00	0.00

* Niu Xiaofeng et al. [2006]

UNIVERSITY OF IBADAN

Table 4.1.5:NH_3-H_2O Temperature Deviation Analysis

	Result @ 0.0 Tesla			Result @ 1.4 Tesla			Result @ 3.0 Tesla		
Absorber length X (m)	**Deviation.**	**Mean**	**Mean Deviation. Square**	**Deviation.**	**Mean**	**Mean Deviation. Square**	**Deviation.**	**Mean**	**Mean Deviation Square**
0 or 10^{-6}	0.00	0.0769	0.01	0.00	0.0769	0.01	0.00	0.0769	0.01
$10^{-5.5}$	0.00	0.0769	0.01	0.00	0.0769	0.01	0.00	0.0769	0.01
10^{-5}	-1.00	0.0769	1.16	-1.00	0.0769	1.16	-1.00	0.0769	1.16
$10^{-4.5}$	-1.00	0.0769	1.16	-1.00	0.0769	1.16	-1.00	0.0769	1.16
10^{-4}	0.00	0.0769	0.01	0.00	0.0769	0.01	0.00	0.0769	0.01
$10^{-3.5}$	1.00	0.0769	0.85	1.00	0.0769	0.85	1.00	0.0769	0.85
10^{-3}	0.00	0.0769	0.01	0.00	0.0769	0.01	0.00	0.0769	0.01
$10^{-2.5}$	1.00	0.0769	0.85	1.00	0.0769	0.85	1.00	0.0769	0.85
10^{-2}	1.00	0.0769	0.85	1.00	0.0769	0.85	1.00	0.0769	0.85
$10^{-1.5}$	0.00	0.0769	0.01	0.00	0.0769	0.01	0.00	0.0769	0.01
10^{-1}	0.00	0.0769	0.01	0.00	0.0769	0.01	0.00	0.0769	0.01
$10^{-0.5}$	0.00	0.0769	0.01	0.00	0.0769	0.01	0.00	0.0769	0.01
10^{0}	0.00	0.0769	0.01	0.00	0.0769	0.01	0.00	0.0769	0.01
$\sum$			**4.92**			**4.92**			**4.92**

@ 0.0 Tesla, Std. deviation (σ) = $\sqrt{4.92/13}$ = 0.62

@ 1.4 Tesla, Std. deviation (σ) = $\sqrt{4.92/13}$ = 0.62

@3.0 Tesla, Std. deviation (σ) = $\sqrt{4.92/13}$ = 0.62

Table 4.1.6:NH_3-H_2O Temperature T- test analysis

Independent Samples Test

		Levene's Test for Equality of Variances		t-test for Equality of Means						
									95% Confidence Interval of the Difference	
		F	Sig.	t	df	Sig. (2-tailed)	Mean Difference	Std. Error Difference	Lower	Upper
Temperature result at 0.0 Tesla	Equal variances assumed	.029	.865	.031	24	.975	.077	2.479	-5.039	5.193
	Equal variances not assumed			.031	23.980	.975	.077	2.479	-5.039	5.193
Temperature result at 1.4 Tesla	Equal variances assumed	.029	.865	.031	24	.975	.077	2.479	-5.039	5.193
	Equal variances not assumed			.031	23.980	.975	.077	2.479	-5.039	5.193
Temperature result at 3.0 Tesla	Equal variances assumed	.029	.865	.031	24	.975	.077	2.479	-5.039	5.193
	Equal variances not assumed			.031	23.980	.975	.077	2.479	-5.039	5.193

UNIVERSITY OF IBADAN

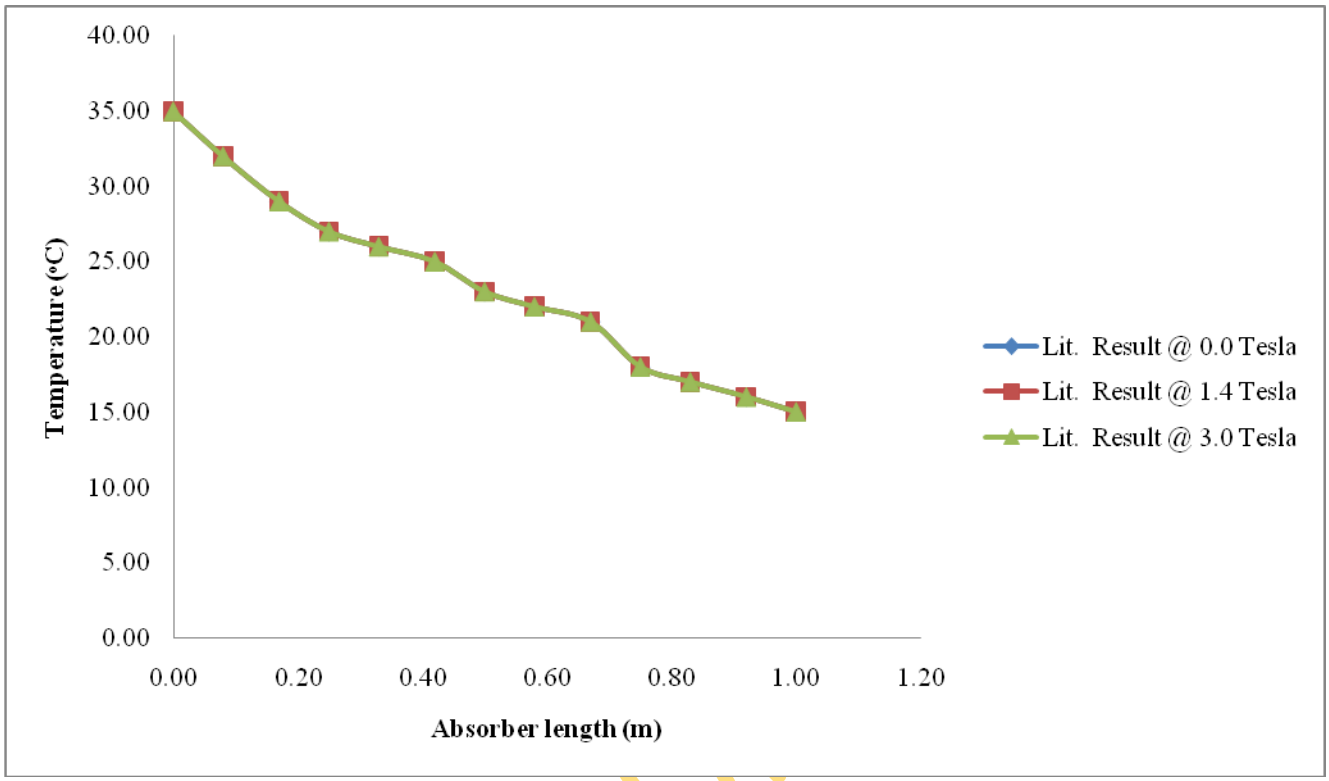

Fig. 4.1.2: NH_3-H_2O Temperature Distribution in the film from Lit. Result

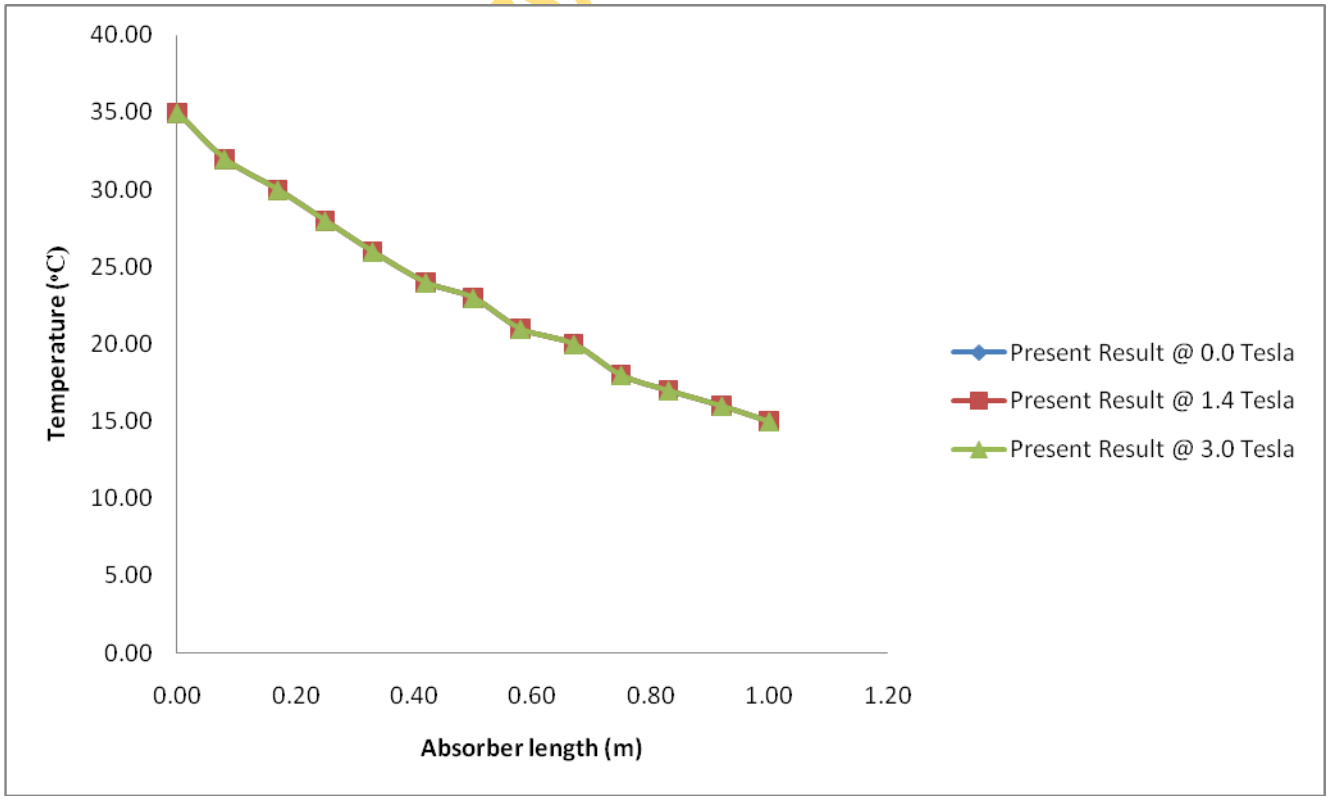

Fig. 4.1.3: NH_3-H_2O Temperature Distribution in the film from Present Result

Table 4.1.7:NH_3-H_2O Concentration Distribution in the Film Comparison

	BULK								
Absorber length X (m)	**Lit. Result @ 0.0 Tesla** *	**Present Result @ 0.0 Tesla**	**Devia-tion.**	**Lit. Result @ 1.4 Tesla** *	**Present Result @ 1.4 Tesla**	**Devia-tion.**	**Lit. Result @ 3.0 Tesla** *	**Present Result @ 3.0 Tesla**	**Devia-tion.**
0 or 10^{-6}	0.2000	0.2000	0.0000	0.2000	0.2000	0.0000	0.2000	0.2000	0.0000
$10^{-5.5}$	0.2200	0.2101	0.0099	0.2220	0.2102	0.0118	0.2250	0.2104	0.0146
10^{-5}	0.2300	0.2207	0.0093	0.2320	0.2211	0.0109	0.2400	0.2215	0.0185
$10^{-4.5}$	0.2500	0.2320	0.0180	0.2520	0.2326	0.0194	0.2620	0.2332	0.0288
10^{-4}	0.2700	0.2440	0.0260	0.2720	0.2448	0.0272	0.2800	0.2457	0.0343
$10^{-3.5}$	0.2900	0.2567	0.0333	0.2920	0.2578	0.0342	0.3000	0.2589	0.0411
10^{-3}	0.3050	0.2702	0.0348	0.3100	0.2716	0.0384	0.3200	0.2730	0.0470
$10^{-2.5}$	0.3190	0.2845	0.0345	0.3200	0.2863	0.0337	0.3300	0.2880	0.0420
10^{-2}	0.3300	0.2998	0.0302	0.3320	0.3020	0.0300	0.3410	0.3040	0.0370
$10^{-1.5}$	0.3380	0.3160	0.0220	0.3400	0.3186	0.0214	0.3500	0.3211	0.0289
10^{-1}	0.3500	0.3334	0.0166	0.3550	0.3365	0.0185	0.3610	0.3394	0.0216
$10^{-0.5}$	0.3550	0.3518	0.0032	0.3600	0.3555	0.0045	0.3650	0.3590	0.0060
10^{0}	0.3600	0.3600	0.0000	0.3680	0.3650	0.0030	0.3750	0.3700	0.0050

* Niu Xiaofeng et al. [2006]

UNIVERSITY OF IBADAN

Table 4.1.8 NH_3-H_2O Concentration Deviation Analysis

	Result @ 0.0 Tesla			Result @ 1.4 Tesla			Result @ 3.0 Tesla		
Absorber length X (m)	**Deviation.**	**Mean**	**Mean Deviation. Square X 10^{-4}**	**Deviation.**	**Mean**	**Mean Deviation. Square X 10^{-4}**	**Deviation.**	**Mean**	**Mean Deviation. Square X 10^{-4}**
0 or 10^{-6}	0.0000	0.0183	3.35	0.0000	0.0195	3.80	0.0000	0.0250	6.25
$10^{-5.5}$	0.0099	0.0183	0.71	0.0118	0.0195	0.59	0.0146	0.0250	1.08
10^{-5}	0.0093	0.0183	0.81	0.0109	0.0195	0.74	0.0185	0.0250	0.42
$10^{-4.5}$	0.0180	0.0183	0.00	0.0194	0.0195	0.00	0.0288	0.0250	0.14
10^{-4}	0.0260	0.0183	0.59	0.0272	0.0195	0.59	0.0343	0.0250	0.86
$10^{-3.5}$	0.0333	0.0183	2.25	0.0342	0.0195	2.16	0.0411	0.0250	2.59
10^{-3}	0.0348	0.0183	2.72	0.0384	0.0195	3.57	0.0470	0.0250	4.84
$10^{-2.5}$	0.0345	0.0183	2.62	0.0337	0.0195	2.02	0.0420	0.0250	2.89
10^{-2}	0.0302	0.0183	1.42	0.0300	0.0195	1.10	0.0370	0.0250	1.44
$10^{-1.5}$	0.0220	0.0183	0.14	0.0214	0.0195	0.04	0.0289	0.0250	0.15
10^{-1}	0.0166	0.0183	0.03	0.0185	0.0195	0.01	0.0216	0.0250	0.12
$10^{-0.5}$	0.0032	0.0183	2.28	0.0045	0.0195	2.25	0.0060	0.0250	3.61
10^{0}	0.0000	0.0183	3.35	0.0030	0.0195	2.72	0.0050	0.0250	4.00
$\sum$			**20.27**			**19.60**			**28.40**

@ 0.0 Tesla, Std. deviation (σ) = $\sqrt{20.27x10^{-4}/13} = 1.25x10^{-2}$

@ 1.4 Tesla, Std. deviation (σ) = $\sqrt{19.60x10^{-4}/13} = 1.23x10^{-2}$

@3.0 Tesla, Std. deviation (σ) = $\sqrt{28.40x10^{-4}/13} = 1.48x10^{-2}$

Table 4.1.9 NH_3-H_2O Concentration T- test analysis

Independent Samples Test

		Levene's Test for Equality of Variances		t-test for Equality of Means						
									95% Confidence Interval of the Difference	
		F	Sig.	t	df	Sig. (2-tailed)	Mean Difference	Std. Error Difference	Lower	Upper
Concentration @ 0.0 Tesla	Equal variances assumed	.015	.904	.857	24	.400	.0183	.0213	-.0257	.0623
	Equal variances not assumed			.857	23.993	.400	.0183	.0213	-.0257	.0623
Concentration @ 1.4 Tesla	Equal variances assumed	.013	.911	.888	24	.383	.0195	.0219	-.0258	.0647
	Equal variances not assumed			.888	23.993	.383	.0195	.0219	-.0258	.0647
Concentration @ 3.0 Tesla	Equal variances assumed	.009	.924	1.113	24	.277	.0250	.0225	-.0214	.0713
	Equal variances not assumed			1.113	23.994	.277	.0250	.0225	-.0214	.0713

UNIVERSITY OF BRADFORD

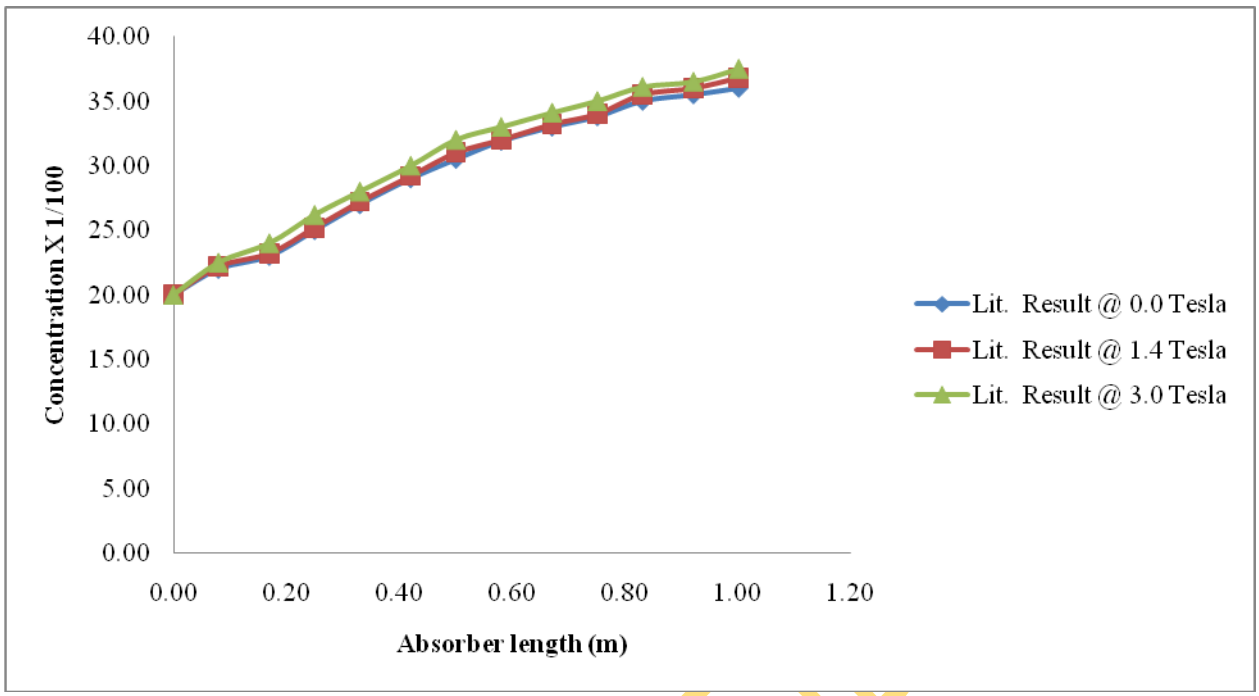

Fig. 4.1.4: NH_3-H_2O Concentration Distribution in the film from Lit. Result

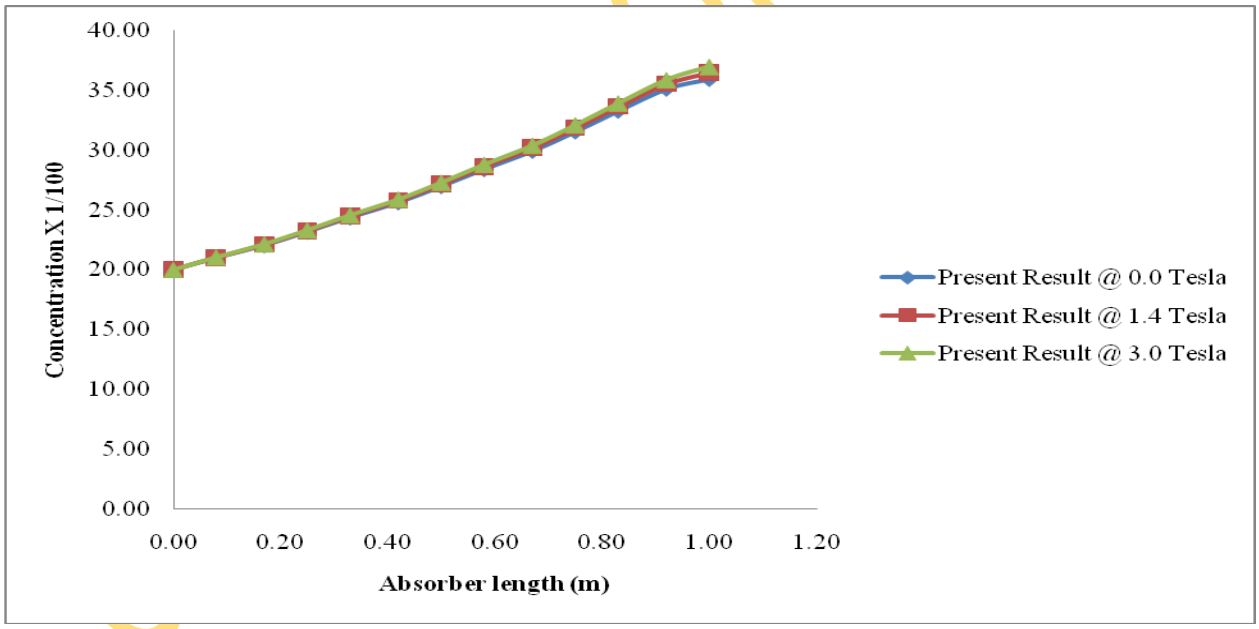

Fig. 4.1.5: NH_3-H_2O Concentration Distribution in the film from Present Result

4.4 Numerical Results in the direction of falling film (X) for Lithium bromide and Lithium Chloride Solution, X = Absorber length.

Tables 4.2 to 4.2.3, 4.3.4, 4.3.7, 4.4.4 and 4.4.5 and Figs 4.1.6 to 4.2.5 and 4.5.3, 4.7.5 to 4.8.2 represent the distribution of average velocity of the falling-film both in the bulk and the interface in the X-axis or direction of the falling film at various magnetic induction intensities in both Lithium bromide and Lithium chloride solutions. Both the tables and figures establish that the velocity at stronger magnetic field is larger than that of the weaker one. This is because the magnetic field force solution suffered is in the same direction with the gravity and increases with the growing of magnetic induction intensity. Moreover, it is found that the velocity u increases gradually at a fixed magnetic induction intensity, which may be attributed to the resultant force of magnetic force and gravity in the direction of falling both within the bulk and at the interface. However, as the frictional force decreases and the increase in falling velocity is slowed down within the bulk. The percentage velocity changes for LiBr-H_2O within the bulk in X-direction when magnetic intensities was increased from 0.0 to 1.4 Tesla increased from 0.00 – 1.15 up to 2/3length of the absorber wall before decrease to 0.0 at the solution surface. When increased from 0.0 to 3.0 Tesla, the percentage velocity change increased from 0.00 to 4.81 to the same absorber length and finally decreases to 0.0 percent at the end of the absorber length (10^0m). For LiCl solution, the percentage velocity changes within the bulk in X-direction when magnetic intensity was increased from 0.0 to 1.4 Tesla increases from 0.00 to 0.85 up to the 2/3 length of absorber wall and decreases down to 0.0 at the end of the absorber length (1 m). When increased from 0.0 to 3.0 Tesla it increases from 0.0 to 3.44 up to the middle length of the absorber and finally decreases to 0.0 at the end of the absorber length (1 m).

UNIVERSITY OF IBADAN

4.4: Tabular and Graphical representation of the literature and present work results

Table 4.2: LiBr-H_2O Velocity Distribution in the film

Absorber length X (m)	Bulk								
	Lit. Result @ 0.0 Tesla	Present Result @ 0.0 Tesla	% Devia	Lit. Result @ 1.4 Tesla	Present. Result @ 1.4 Tesla	% Devia	Lit. Result @ 3.0 Tesla	Present Result @3.0 Tesla	% Devia
0 or 10^{-6}	N/A	0.3620		N/A	0.3620		N/A	0.3620	
$10^{-5.5}$	"	0.3662		"	0.3674		"	0.3718	
10^{-5}	"	0.3702		"	0.3726		"	0.3840	
$10^{-4.5}$	"	0.3742		"	0.3774		"	0.3879	
10^{-4}	"	0.3780		"	0.3818		"	0.3944	
$10^{-3.5}$	"	0.3818		"	0.3860		"	0.3997	
10^{-3}	"	0.3854		"	0.3898		"	0.4039	
$10^{-2.5}$	"	0.3889		"	0.3933		"	0.4070	
10^{-2}	"	0.3924		"	0.3965		"	0.4090	
$10^{-1.5}$	"	0.3957		"	0.3994		"	0.4099	
10^{-1}	"	0.3989		"	0.4019		"	0.4097	
$10^{-0.5}$	"	0.4020		"	0.4041		"	0.4084	
10^{0}	N/A	0.4050		N/A	0.4060		N/A	0.4060	

** Absorber length (m)

UNIVERSITY OF IBADAN

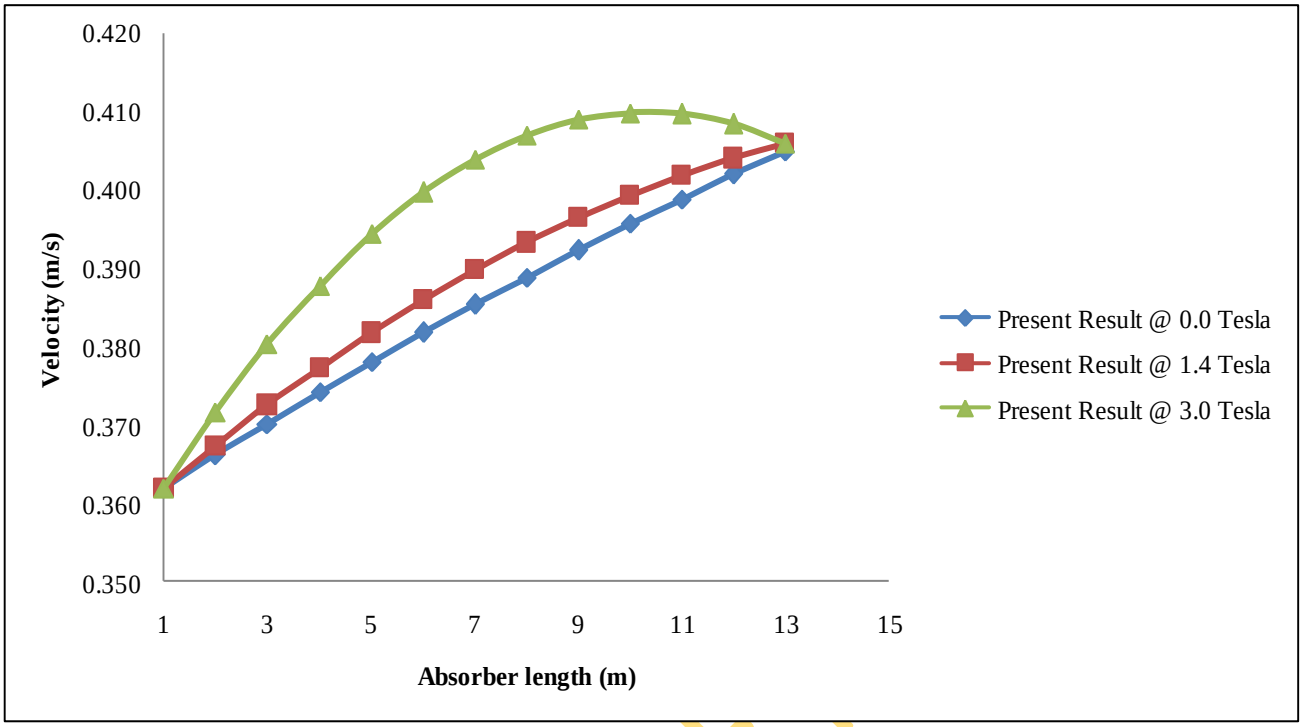

Fig. 4.1.6: Velocity Distribution in the Film at 0.0, 1.4 and 3.0Tesla for LiBr- H_2O

Table 4.2.1: LiBr-H_2O Velocity Changes within the film in X-direction, X = Absorber length.

Absorber length X (m)	Bulk					
	Present Result @ 0.0 Tesla	Present. Result @ 1.4 Tesla	% Changes in X-dir	Present Result @ 0.0 Tesla	Present Result @3.0 Tesla	% Changes in X-dir
0 or 10^{-6}	0.3620	0.3620	0.00	0.3620	0.3620	0.00
$10^{-5.5}$	0.3662	0.3674	0.35	0.3662	0.3718	1.53
10^{-5}	0.3702	0.3726	0.63	0.3702	0.3840	2.75
$10^{-4.5}$	0.3742	0.3774	0.85	0.3742	0.3879	3.68
10^{-4}	0.3780	0.3818	1.01	0.3780	0.3944	4.33
$10^{-3.5}$	0.3818	0.3860	1.11	0.3818	0.3997	4.70
10^{-3}	0.3854	0.3898	1.15	0.3854	0.4039	4.81

UNIVERSITY OF

$10^{-2.5}$	0.3889	0.3933	1.13	0.3889	0.4070	4.65
10^{-2}	0.3924	0.3965	1.06	0.3924	0.4090	4.25
$10^{-1.5}$	0.3957	0.3994	0.93	0.3957	0.4099	3.61
10^{-1}	0.3989	0.4019	0.76	0.3989	0.4097	2.72
$10^{-0.5}$	0.4020	0.4041	0.53	0.4020	0.4084	1.60
10^{0}	0.4050	0.4060	0.25	0.4050	0.4060	0.25

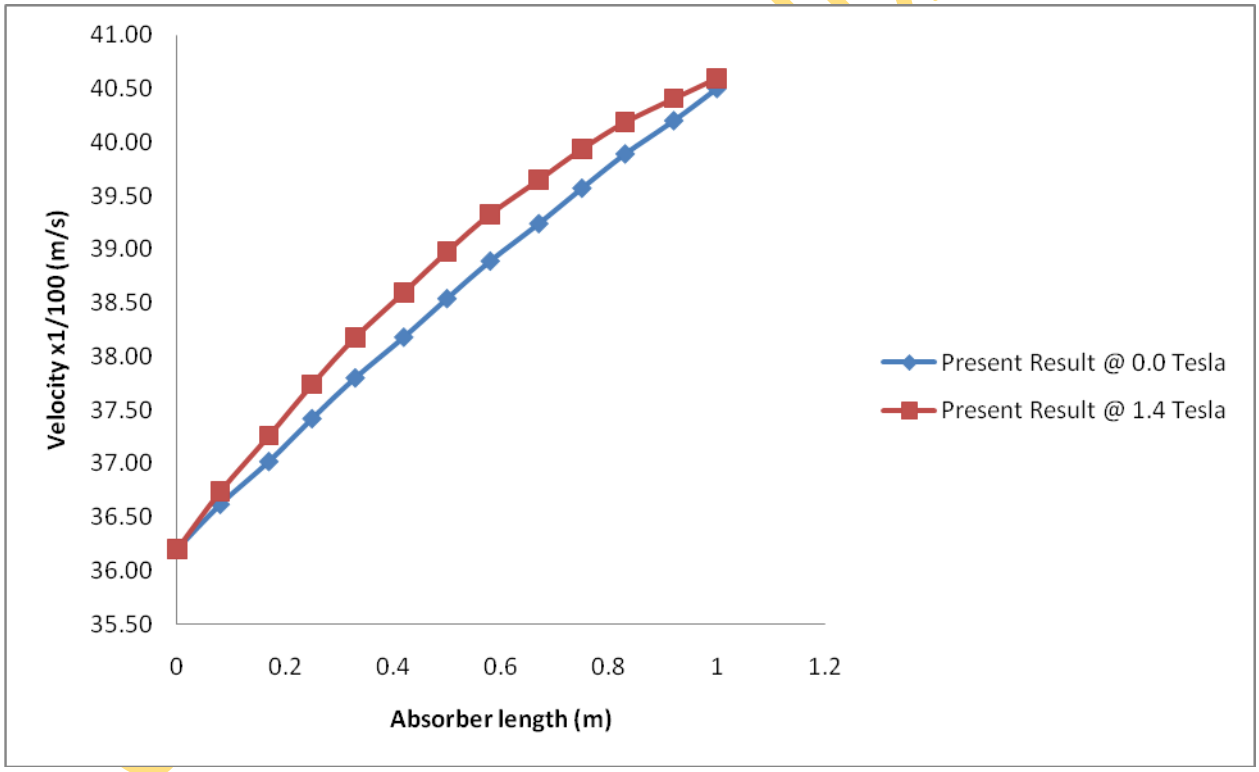

Fig. 4.1.7: Velocity Changes within the Film in X-Direction at 0.0 & 1.4 Tesla, X = Absorber length.

IBADAN

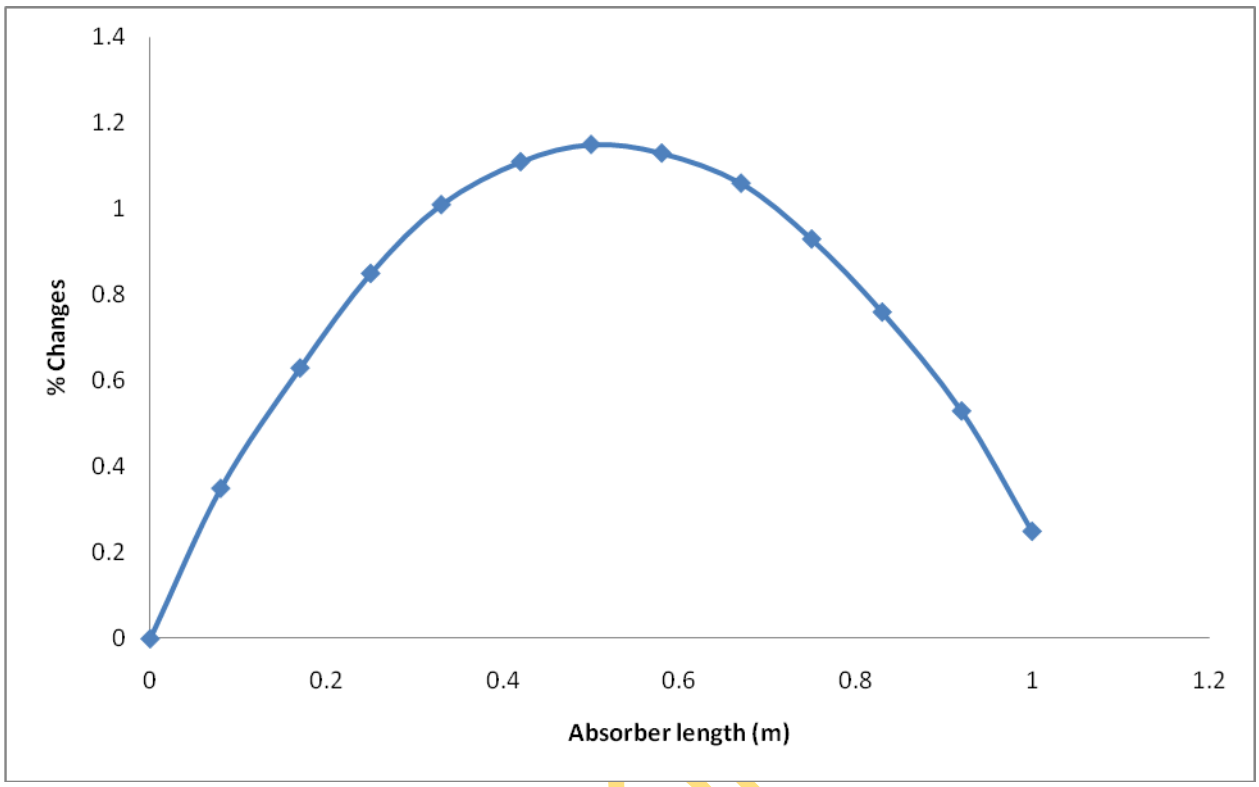

Fig. 4.1.8: % Velocity Changes within the Film in X-Direction from 0.0 & 1.4Tesla, X = Absorber length.

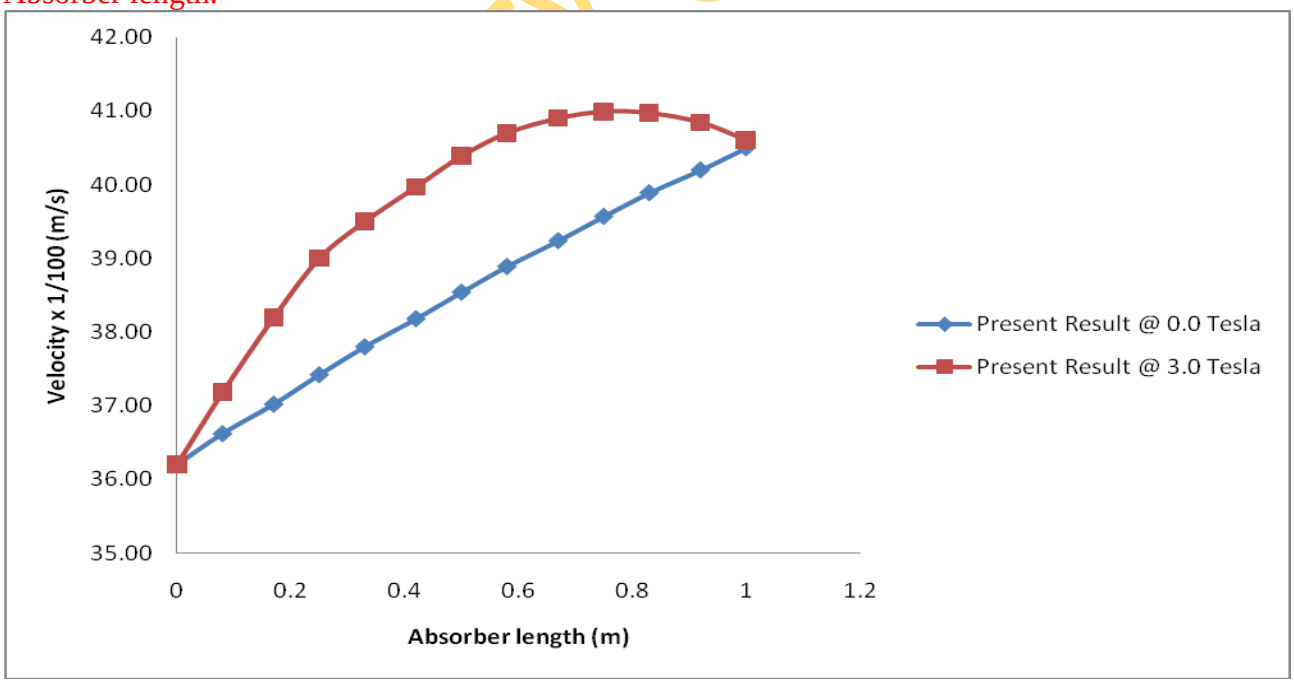

Fig. 4.1.9: Velocity Changes within the Film in X-Direction at 0.0 & 3.0 Tesla, X = Absorber length.

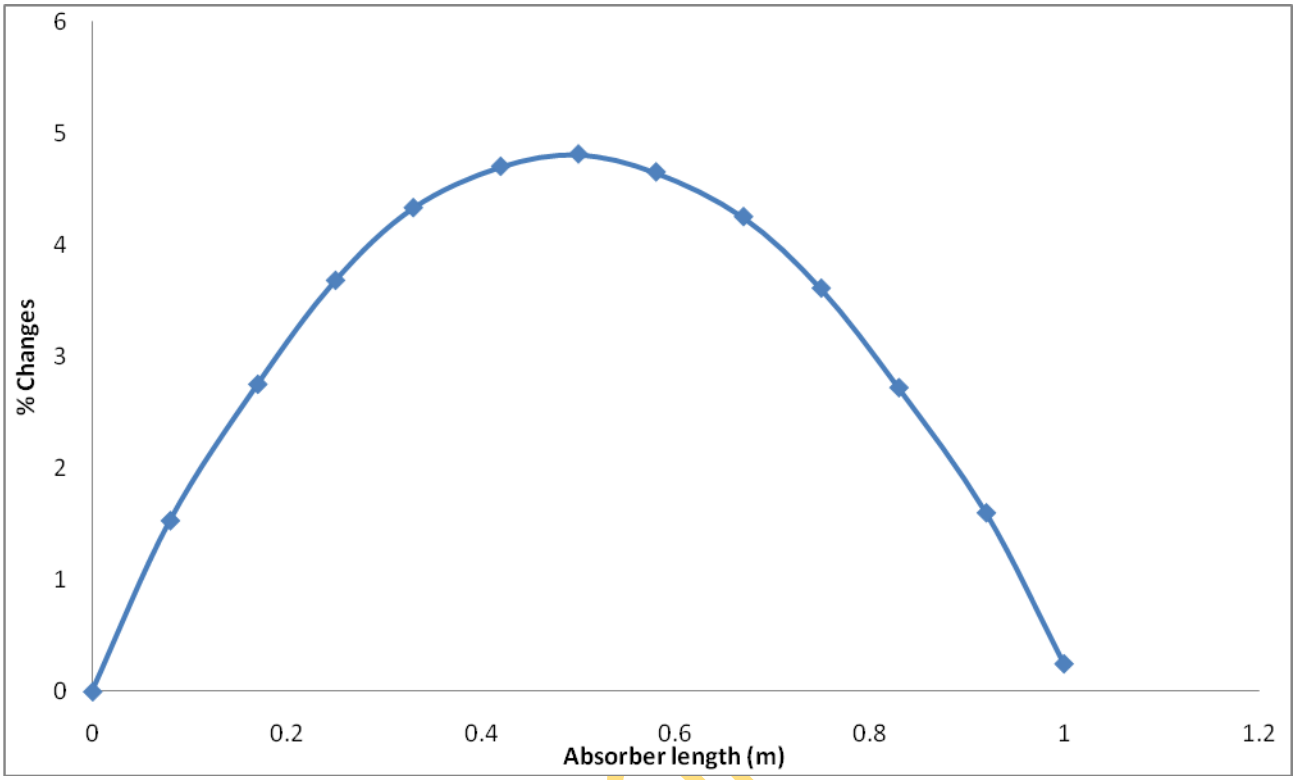

Fig.4.2: % Velocity Changes within the Film in X-direction from 0.0 & 3.0Tesla, X = Absorber length.

Table 4.2.2: LiBr-H_2O Velocity Distribution in the film

Absorber length X (m)	Interface								
	Lit. Result @ 0.0 Tesla	Present Result @ 0.0 Tesla	% Devia-tion	Lit. Result @ 1.4 Tesla	Present. Result @ 1.4 Tesla	% Devia-tion	Lit. Result @ 3.0 Tesla	Present Result @3.0 Tesla	% Devia-tion
0 or 10^{-6}	N/A	0.3620		N/A	0.3620		N/A	0.3620	
$10^{-5.5}$	"	0.3662		"	0.3674		"	0.3718	
10^{-5}	"	0.3662		"	0.3674		"	0.3718	
$10^{-4.5}$	"	0.3662		"	0.3674		"	0.3718	
10^{-4}	"	0.3662		"	0.3674		"	0.3718	

UNIVERSITY OF

$10^{-3.5}$	"	0.3662		"	0.3674		"	0.3718	
10^{-3}	"	0.3662		"	0.3674		"	0.3718	
$10^{-2.5}$	"	0.3662		"	0.3674		"	0.3718	
10^{-2}	"	0.3662		"	0.3674		"	0.3718	
$10^{-1.5}$	"	0.3662		"	0.3674		"	0.3718	
10^{-1}	"	0.3662		"	0.3674		"	0.3718	
$10^{-0.5}$	"	0.3662		"	0.3674		"	0.3718	
10^{0}	N/A	0.4050		N/A	0.4060		N/A	0.4060	

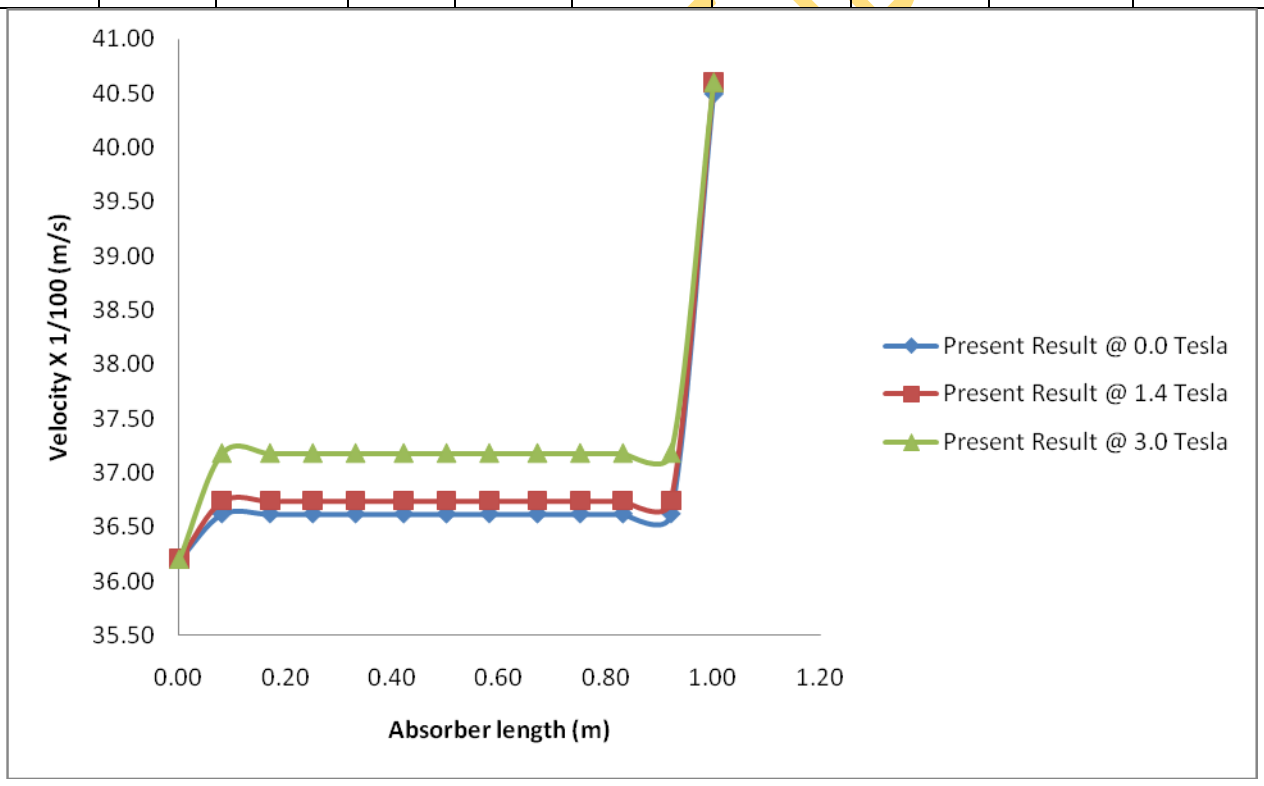

Fig. 4.2.1: **LiBr-H_2O** Velocity Distribution in the Film at the Interface

IBADAN

Table 4.2.3: LiBr-H_2O Velocity Changes within the film in X-direction at the interface, X = Absorber length.

Absorber length X (m)	Interface					
	Present Result @ 0.0 Tesla	**Present. Result @ 1.4 Tesla**	**% Changes in X-dir**	**Present Result @ 0.0 Tesla**	**Present Result @3.0 Tesla**	**% Changes in X-dir**
0 or 10^{-6}	0.3620	0.3620	0.00	0.3620	0.3620	0.00
$10^{-5.5}$	0.3662	0.3674	0.35	0.3662	0.3718	1.53
10^{-5}	0.3662	0.3674	0.35	0.3662	0.3718	1.53
$10^{-4.5}$	0.3662	0.3674	0.35	0.3662	0.3718	1.53
10^{-4}	0.3662	0.3674	0.35	0.3662	0.3718	1.53
$10^{-3.5}$	0.3662	0.3674	0.35	0.3662	0.3718	1.53
10^{-3}	0.3662	0.3674	0.35	0.3662	0.3718	1.53
$10^{-2.5}$	0.3662	0.3674	0.35	0.3662	0.3718	1.53
10^{-2}	0.3662	0.3674	0.35	0.3662	0.3718	1.53
$10^{-1.5}$	0.3662	0.3674	0.35	0.3662	0.3718	1.53
10^{-1}	0.3662	0.3674	0.35	0.3662	0.3718	1.53
$10^{-0.5}$	0.3662	0.3674	0.35	0.3662	0.3718	1.53
10^{0}	0.4050	0.4060	0.25	0.4050	0.4060	0.25

UNIVERSITY OF IBADAN

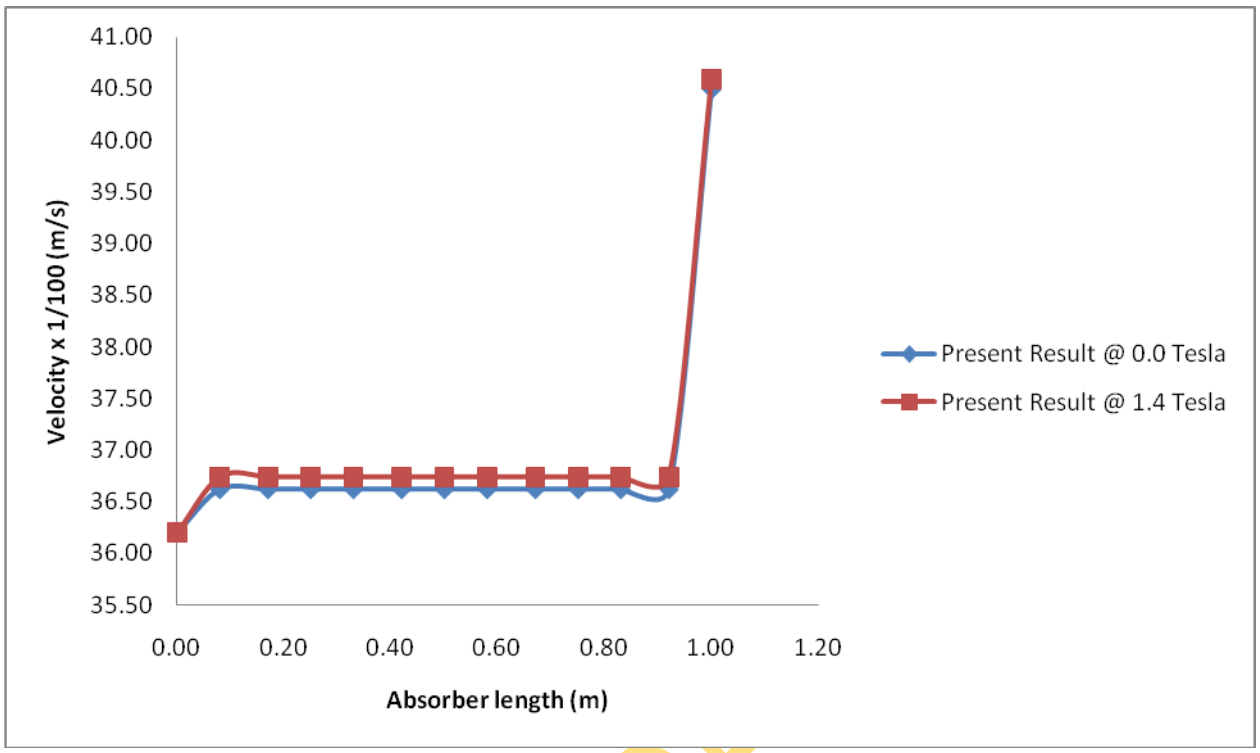

Fig. 4.2.2: LiBr-H_2O Velocity Changes at the Interface in X-direction at 0.0 and 1.4Tesla, X = Absorber length.

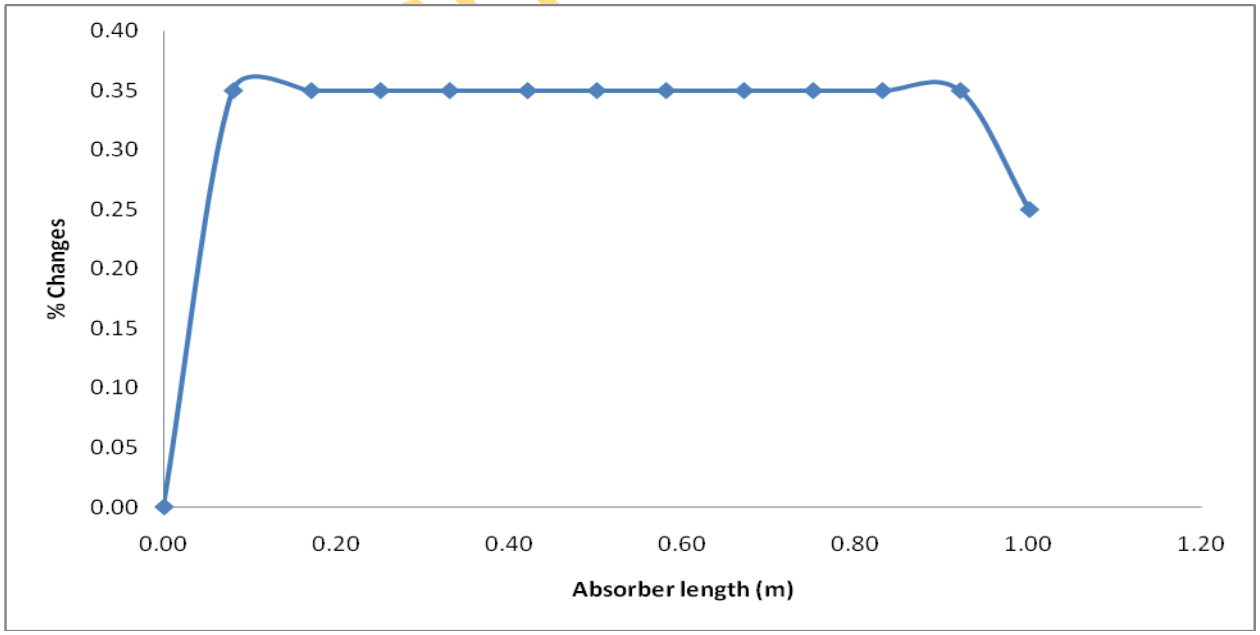

Fig. 4.2.3: % Velocity Changes at the Interface in X-Direction from 0.0 to1.4Tesla, X = Absorber length.

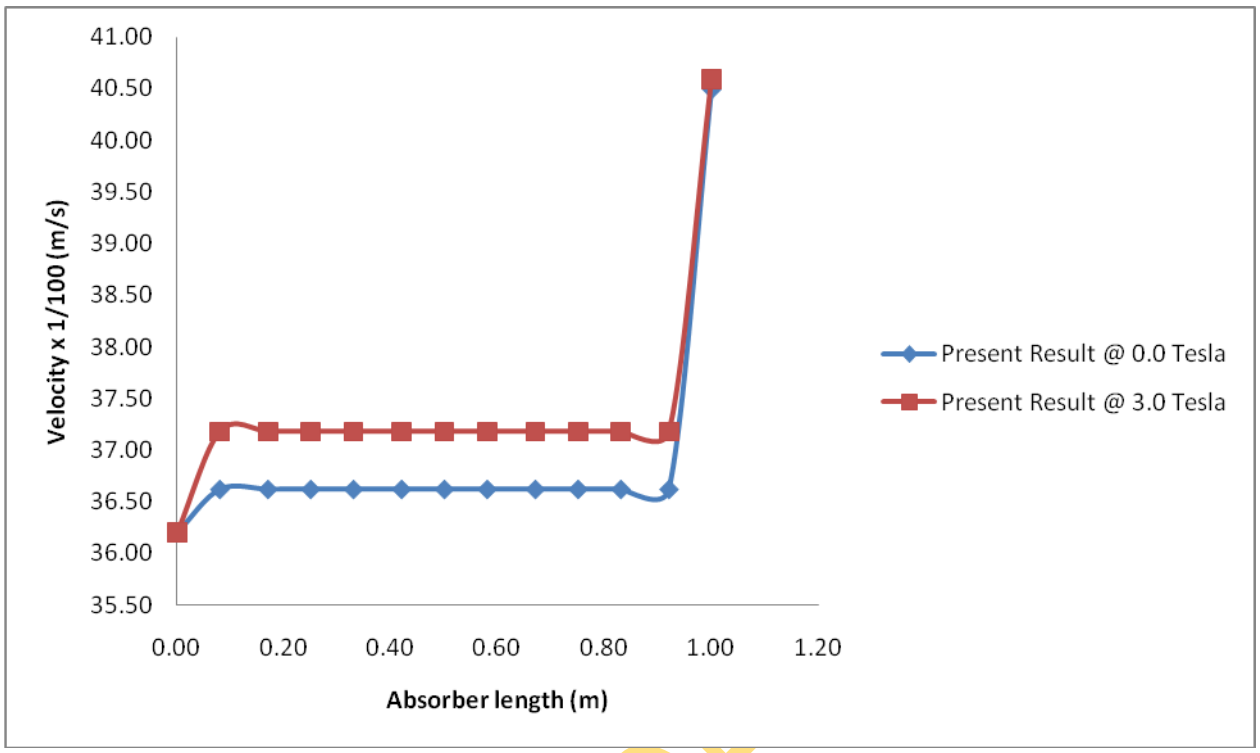

Fig. 4.2.4: Velocity Changes at the Interface in X-Direction from 0.0 & 3.0Tesla, X = Absorber length.

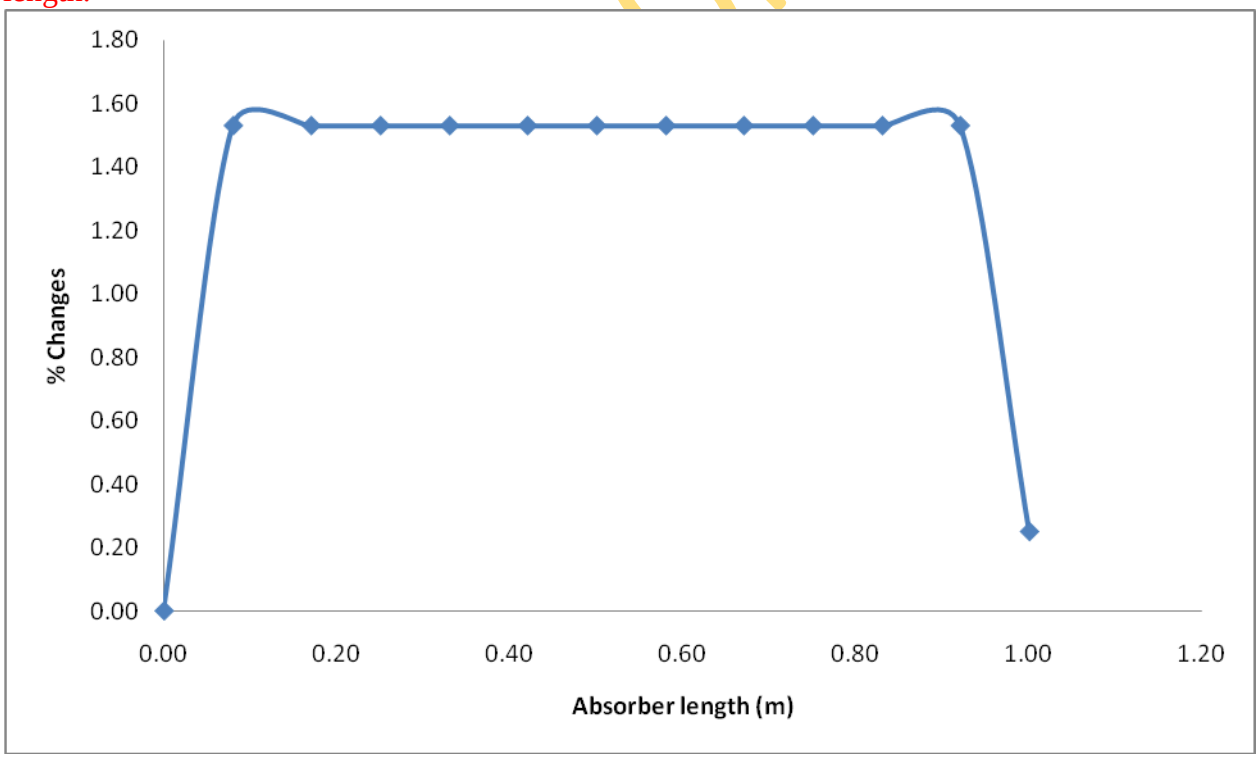

Fig. 4.2.5: % velocity Changes at the Interface in X-Direction from 0.0 to 3.0Tesla, X = Absorber length.

Table 4.2.4: LiBr-H_2O Temperature Distribution in the film Comparison

Absorber length X (m)	Bulk								
	Lit. Result @ 0.0 Tesla ***	**Present Result @ 0.0 Tesla**	**% Devia-tion**	**Lit. Result @ 1.4 Tesla**	**Present. Result @ 1.4 Tesla**	**% Devia-tion**	**Lit. Result @ 3.0 Tesla**	**Present Result @3.0 Tesla**	**% Devia-tion**
0 or 10^{-6}	44.44	44.44	0.00	N/A	44.44		N/A	44.44	
$10^{-5.5}$	43.50	44.40	2.07	"	44.40		"	44.40	
10^{-5}	43.20	43.45	0.58	"	43.45		"	43.45	
$10^{-4.5}$	43.00	42.52	-1.12	"	42.52		"	42.52	
10^{-4}	41.50	41.61	0.27	"	41.61		"	41.61	
$10^{-3.5}$	39.50	40.72	3.09	"	40.72		"	40.72	
10^{-3}	38.00	39.85	4.87	"	39.85		"	39.85	
$10^{-2.5}$	36.60	39.00	6.56	"	39.00		"	39.00	
10^{-2}	36.40	38.16	4.84	"	38.16		"	38.16	
$10^{-1.5}$	36.00	37.35	3.75	"	37.35		"	37.35	
10^{-1}	35.50	36.55	2.96	"	36.55		"	36.55	
$10^{-0.5}$	35.10	35.77	1.91	"	35.77		"	35.77	
10^{0}	35.00	35.00	0.00		35.00			35.00	

UNIVERSITY OF IBADAN

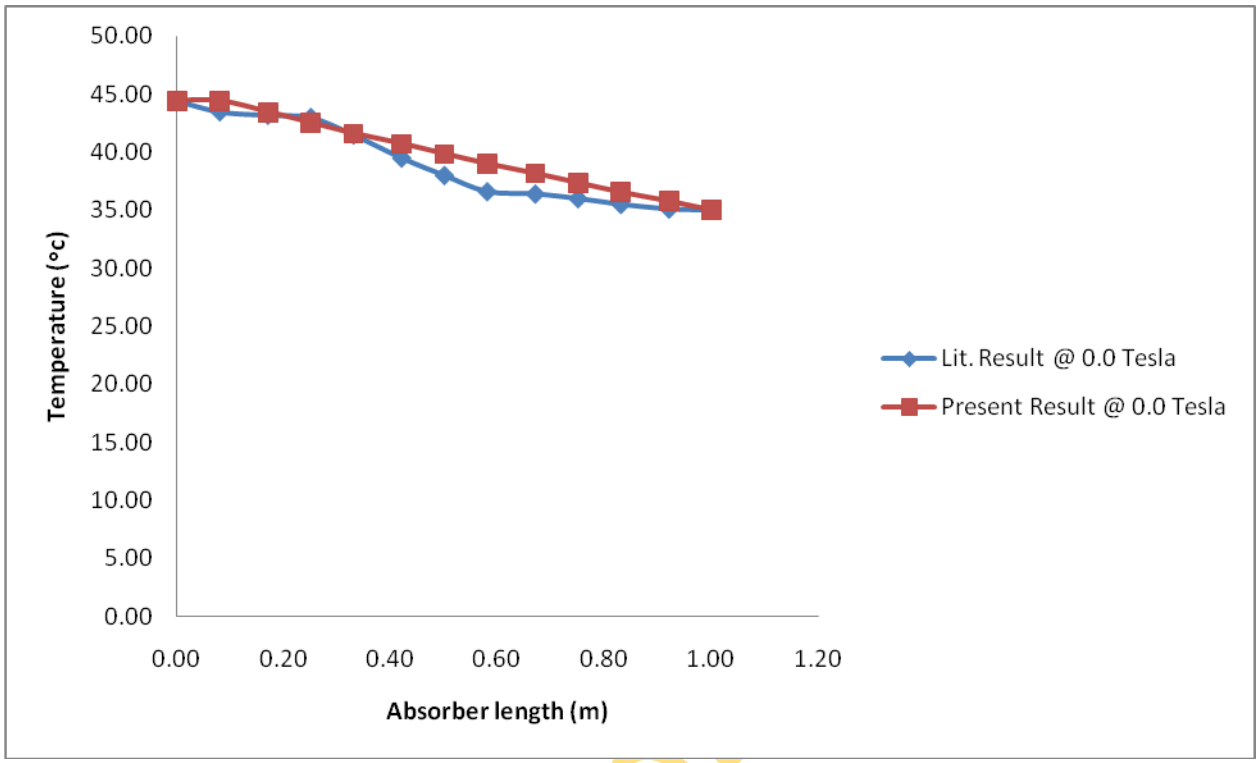

Fig. 4.2.6: LiBr-H_2O Temperature Distribution in the Film Comparison at 0.0Tesla

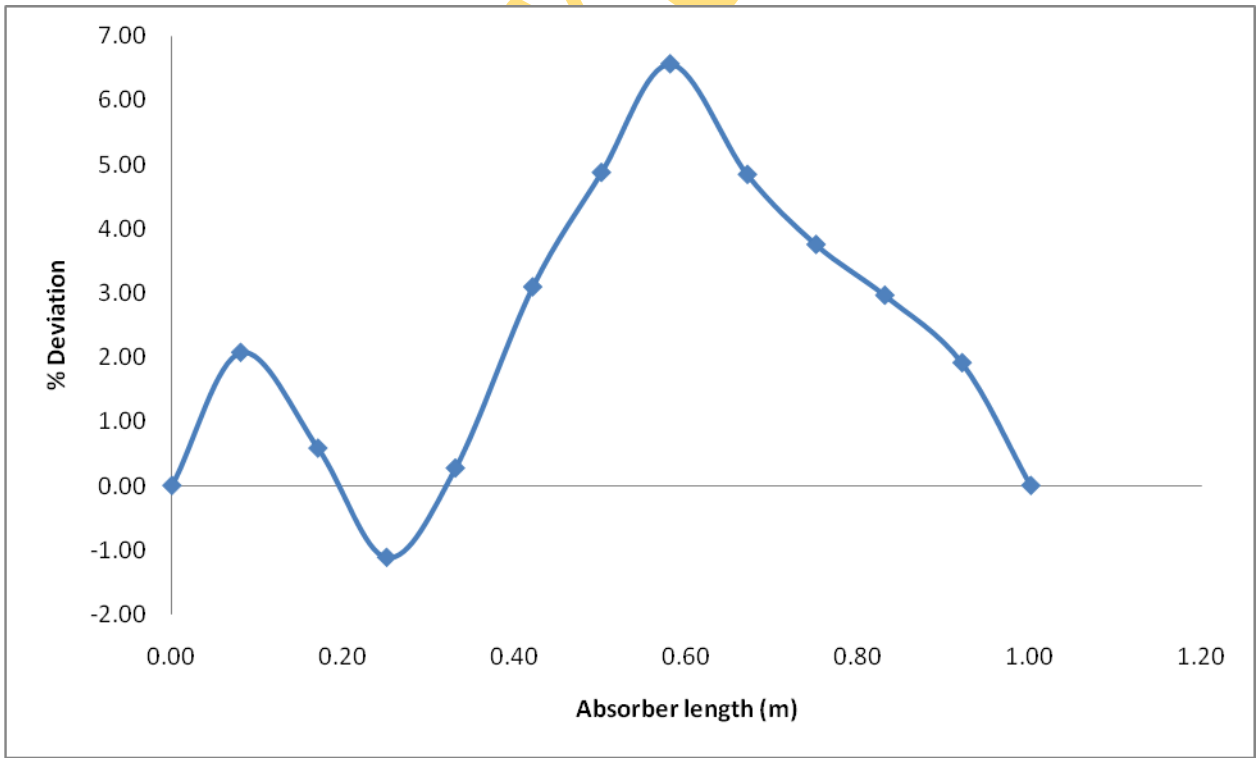

Fig. 4.2.7: % Deviation in Temperature Distribution in the Film Comparison at 0.0Tesla

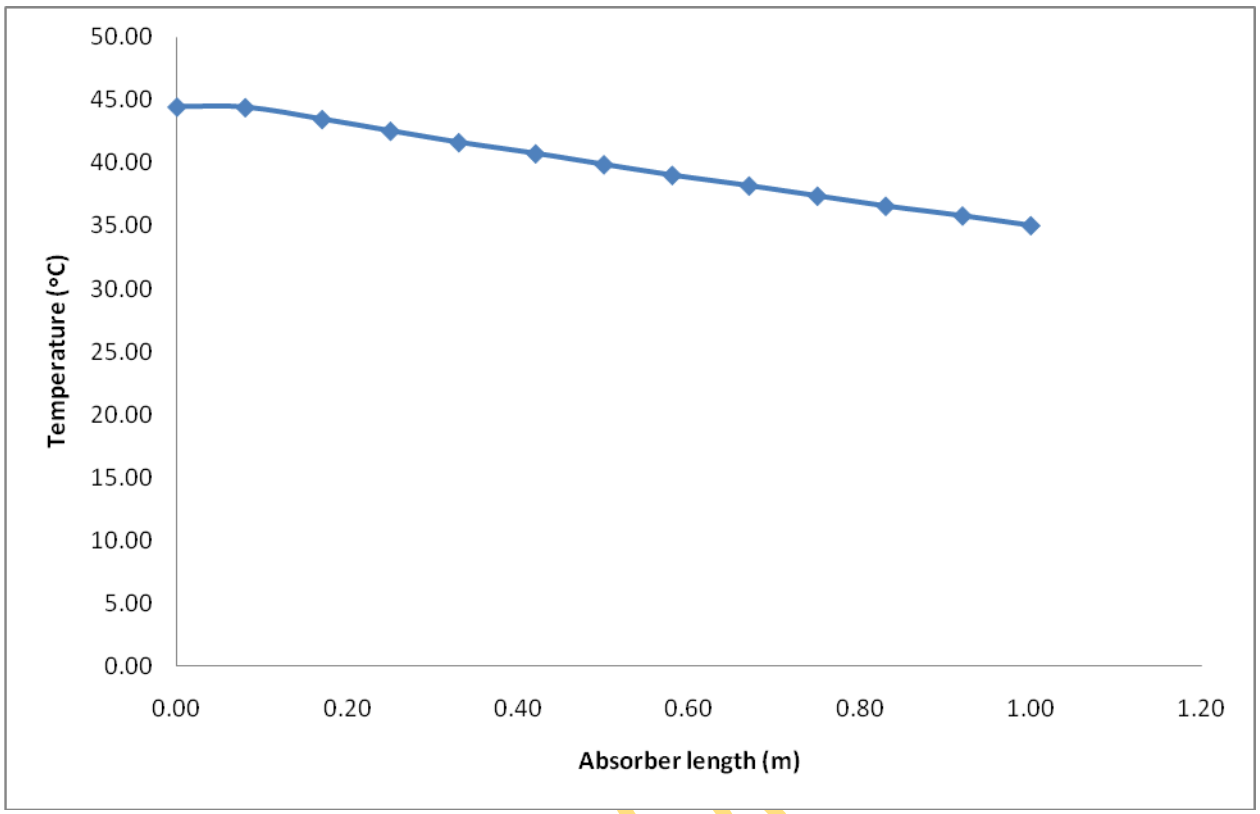

Fig. 4.2.8: Temperature Distribution in the Film at 1.4 Tesla (Present Result)

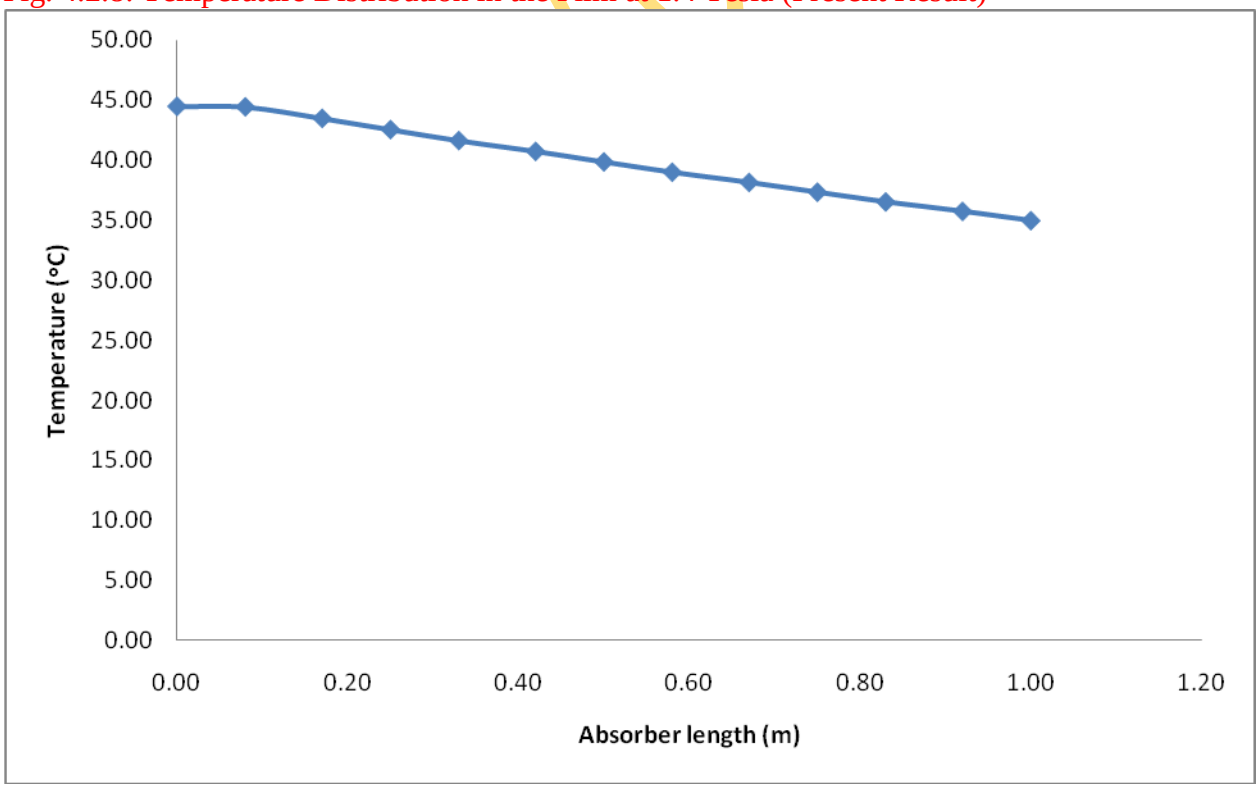

Fig.4.2.9: Temperature Distribution in the Film at 3.0 Tesla(Present Result)

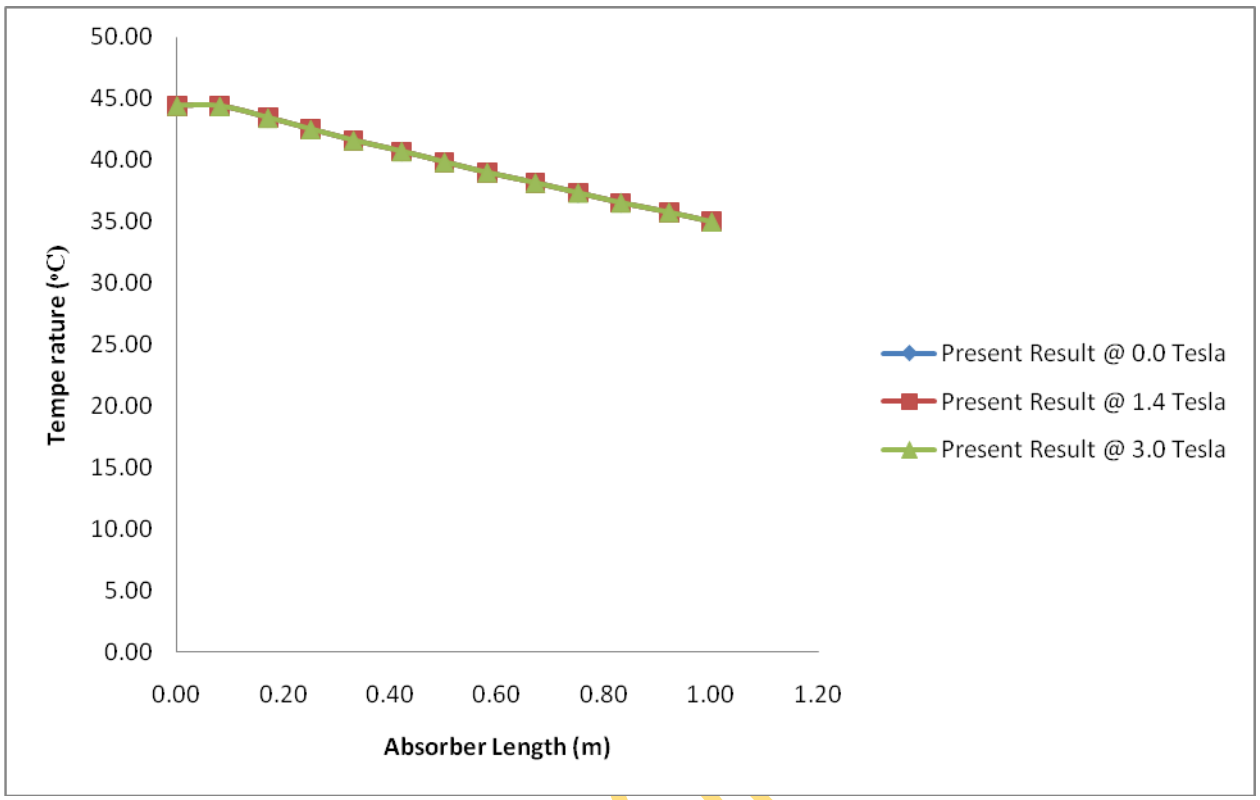

Fig.4.3: Temperature Distribution in the Thin-Liquid Smooth Falling Film (Bulk) at 0.0,1.4 and 3.0Tesla

Table 4.2.5: LiBr-H_2O Temperature Distribution in the film Comparison

Absorber length X (m)	**Interface**								
	Lit. Result @ 0.0 Tesla ***	**Present Result @ 0.0 Tesla**	**% Devia-tion**	**Lit. Result @ 1.4 Tesla**	**Present. Result @ 1.4 Tesla**	**% Devia-tion**	**Lit. Result @ 3.0 Tesla**	**Present Result @3.0 Tesla**	**% Devia-tion**
0 or 10^{-6}	44.44	44.44	0.00	N/A	44.44		N/A	44.44	
$10^{-5.5}$	44.44	44.35	-0.20	"	44.35		"	44.35	
10^{-5}	44.44	43.50	-2.12	"	43.50		"	43.50	
$10^{-4.5}$	44.44	42.65	-4.03	"	42.65		"	42.65	
10^{-4}	44.44	41.80	-5.94	"	41.80		"	41.80	
$10^{-3.5}$	44.00	40.95	-6.93	"	40.95		"	40.95	

UNIVERSITY

10^{-3}	42.00	40.10	-4.52	"	40.10		"	40.10	
$10^{-2.5}$	39.50	39.25	-0.63	"	39.25		"	39.25	
10^{-2}	38.00	38.40	1.05	"	38.40		"	38.40	
$10^{-1.5}$	37.00	37.55	1.49	"	37.55		"	37.55	
10^{-1}	36.50	36.70	0.55	"	36.70		"	36.70	
$10^{-0.5}$	36.00	35.85	2.36	"	35.85		"	35.85	
10^{0}	35.00	35.00	0.00		35.00			35.00	

*** Yang et al.(1992)

Table 4.2.6: LiBr-H_2O Temperature Deviation Analysis at the Bulk and Interface

	BULK			**INTERFACE**		
Absorber length X (m)	**Lit. Result @ 0.0 Tesla *** **	**Present Result @ 0.0 Tesla**	**Devia-tion.**	**Lit. Result @ 0.0 Tesla*****	**Present Result @ 0.0 Tesla**	**Devia-tion.**
0 or 10^{-6}	44.44	44.44	0.00	44.44	44.44	0.00
$10^{-5.5}$	43.50	44.40	0.90	44.44	44.35	0.09
10^{-5}	43.20	43.45	0.25	44.44	43.50	0.94
$10^{-4.5}$	43.00	42.52	0.48	44.44	42.65	1.79
10^{-4}	41.50	41.61	0.11	44.44	41.80	2.64
$10^{-3.5}$	39.50	40.72	1.22	44.00	40.95	3.05
10^{-3}	38.00	39.85	1.85	42.00	40.10	1.90
$10^{-2.5}$	36.60	39.00	2.40	39.50	39.25	0.25
10^{-2}	36.40	38.16	1.76	38.00	38.40	-0.40
$10^{-1.5}$	36.00	37.35	1.35	37.00	37.55	-0.55
10^{-1}	35.50	36.55	1.05	36.50	36.70	-0.20
$10^{-0.5}$	35.10	35.77	0.67	36.00	35.85	0.15
10^{0}	35.00	35.00	0.00	35.00	35.00	0.00

*** Yang et al.(1992)

UNIVERSITY OF IBADAN

Table 4.2.7: LiBr-H_2O Temperature Deviation Analysis at the Bulk and Interface

	BULK @ 0.0 Tesla			INTERFACE @ 0.0 Tesla		
Absorber length X (m)	**Deviation.**	**Mean Deviation**	**Mean Deviation. Square**	**Deviation.**	**Mean Deviation**	**Mean Deviation. Square**
0 or 10^{-6}	0.0000	0.9262	0.86	0.0000	0.7431	0.55
$10^{-5.5}$	0.9000	0.9262	0.00	0.0900	0.7431	0.43
10^{-5}	0.2500	0.9262	0.46	0.9400	0.7431	0.04
$10^{-4.5}$	0.4800	0.9262	0.20	1.7900	0.7431	1.10
10^{-4}	0.1100	0.9262	0.67	2.6400	0.7431	3.60
$10^{-3.5}$	1.2200	0.9262	0.09	3.0500	0.7431	5.32
10^{-3}	1.8500	0.9262	0.85	1.9000	0.7431	1.34
$10^{-2.5}$	2.4000	0.9262	2.17	0.2500	0.7431	0.24
10^{-2}	1.7600	0.9262	0.70	-0.4000	0.7431	1.31
$10^{-1.5}$	1.3500	0.9262	0.18	-0.5500	0.7431	1.67
10^{-1}	1.0500	0.9262	0.02	-0.2000	0.7431	0.89
$10^{-0.5}$	0.6700	0.9262	0.07	0.1500	0.7431	0.35
10^{0}	0.0000	0.9262	0.86	0.0000	0.7431	0.55
$\sum$			**7.11**			**17.39**

@ The Bulk, Std. deviation (σ) = $\sqrt{7.11/13}$ **= 0.7394**

@ The Interface, Std. deviation (σ) = $\sqrt{17.39/13}$ **= 1.1565**

UNIVERSITY OF IBADAN

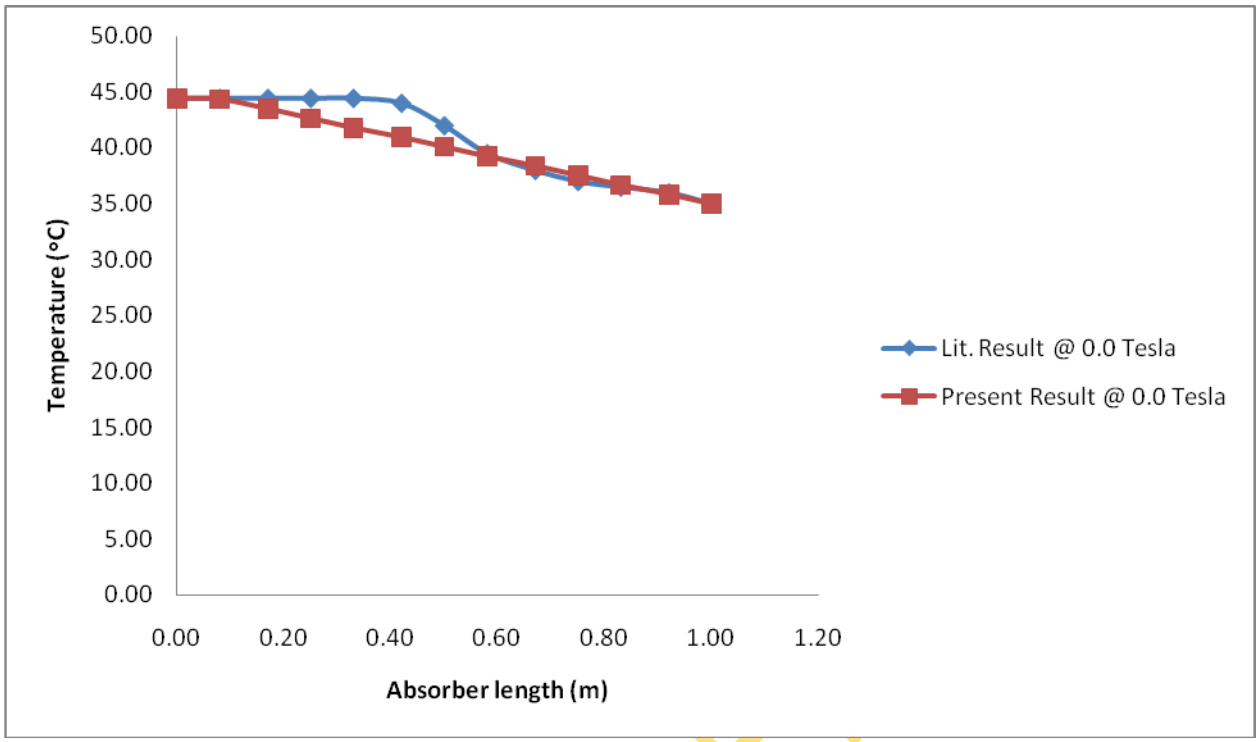

Fig4.3.1: Temperature Distribution at the Interface Comparison at 0.0 Tesla

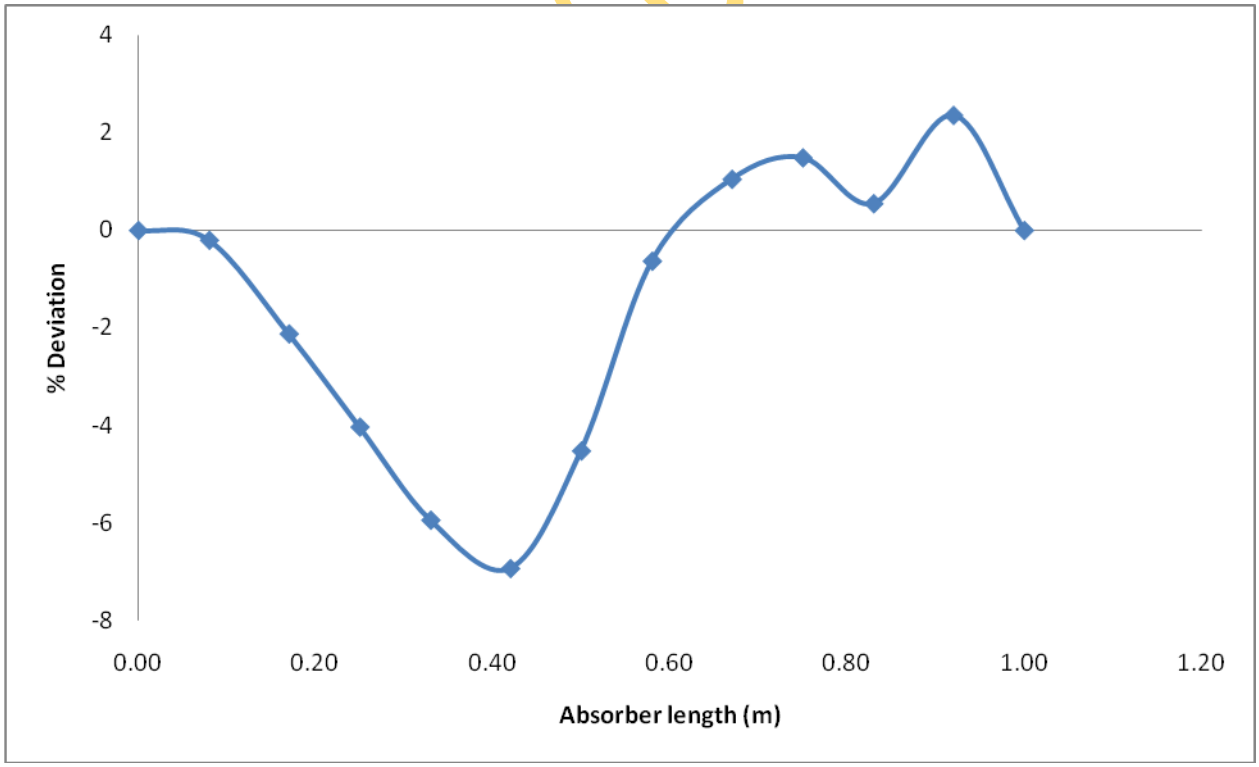

Fig. 4.3.2: %deviation in Temperature distribution at the interface Comparison at 0.0Tesla

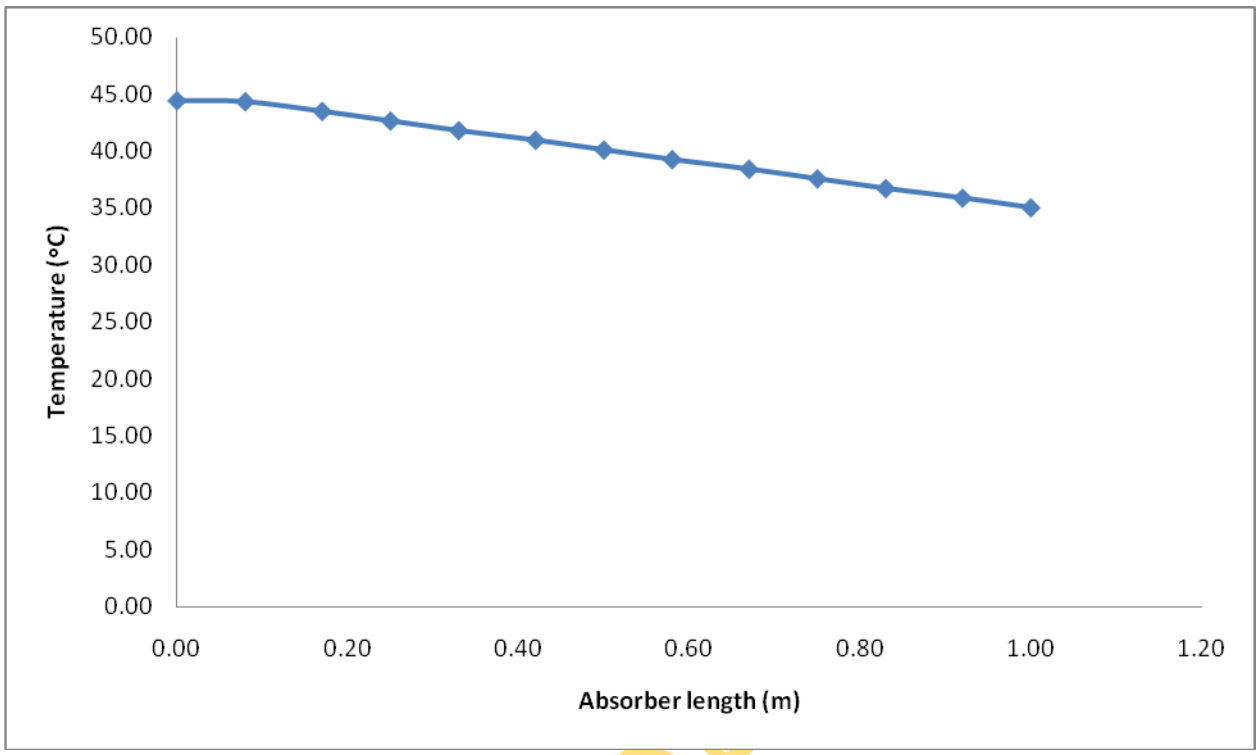

Fig4.3.3: Temperature Distribution at the Interface at 1.4 Tesla

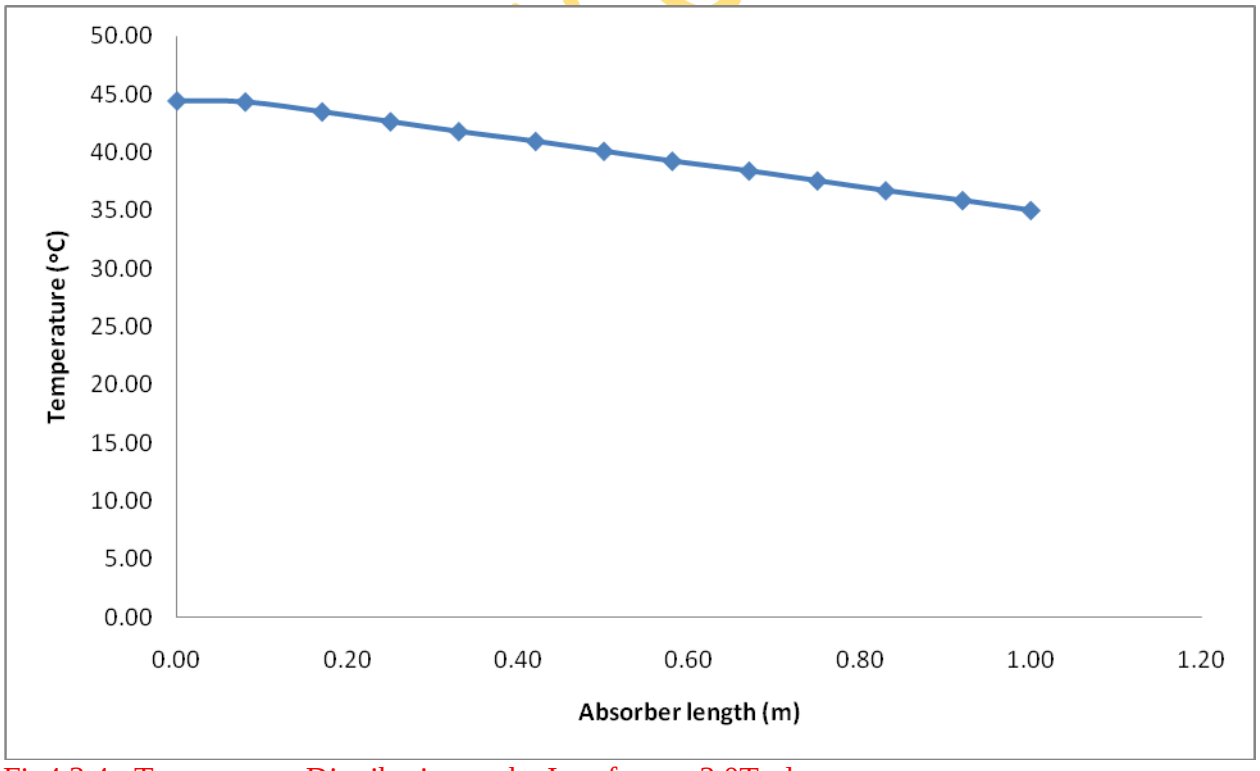

Fig4.3.4: Temperature Distribution at the Interface at 3.0Tesla

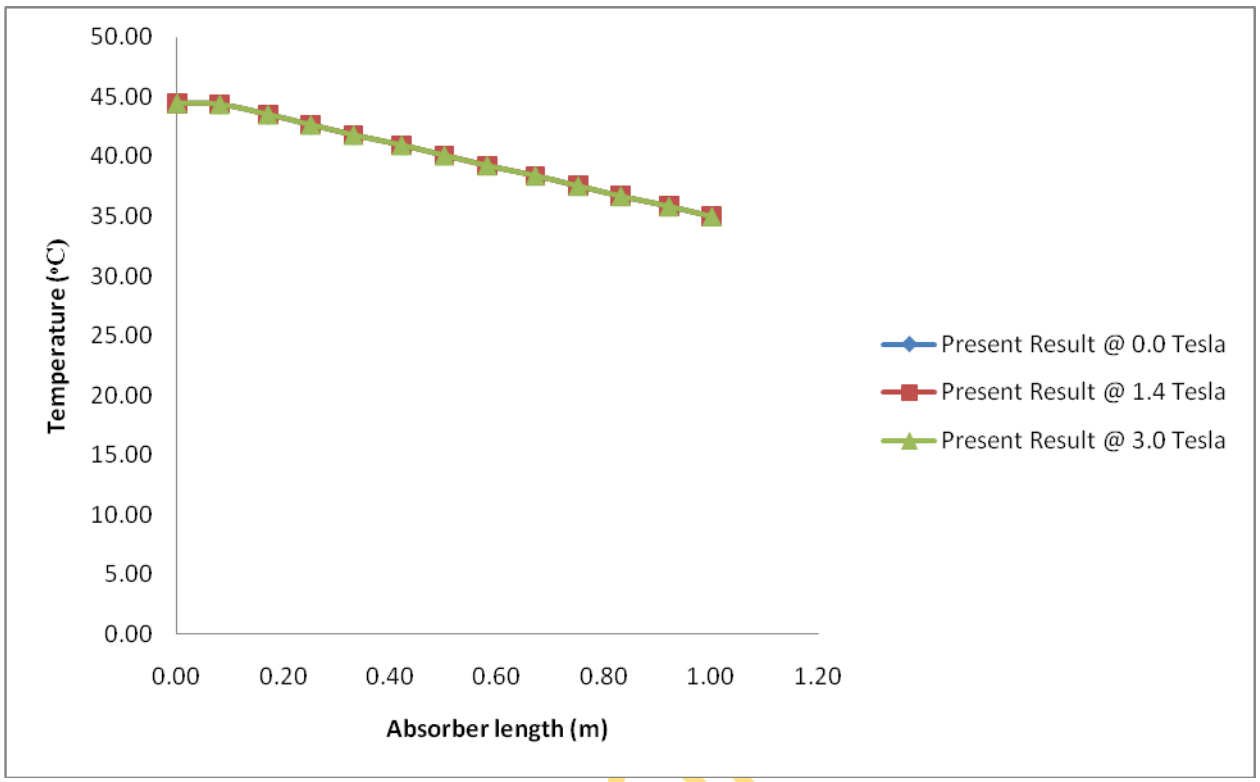

Fig4.3.5: Temperature Distribution at the Interface at 0.0, 1.4 and 3.0Tesla

Table 4.2.8: LiBr-H_2O Concentration Distribution in the film Comparison

Absorber length X (m)	Bulk								
	Lit. Result @ 0.0 Tesla ***	Present Result @ 0.0 Tesla	% Devia-tion	Lit. Result @ 1.4 Tesla	Present. Result @ 1.4 Tesla	% Devia-tion	Lit. Result @ 3.0 Tesla	Present Result @3.0 Tesla	% Devia-tion
0 or 10^{-6}	0.600	0.600	0.00	N/A	0.600		N/A	0.600	
$10^{-5.5}$	0.600	0.59545	-0.76	"	0.59547		"	0.59551	
10^{-5}	0.600	0.59090	-1.52	"	0.59094		"	0.59107	
$10^{-4.5}$	0.600	0.58635	-2.28	"	0.58642		"	0.58667	
10^{-4}	0.600	0.58180	-3.03	"	0.58191		"	0.58229	

UNIVERSITY OF

$10^{-3.5}$	0.600	0.57724	-3.79	"	0.57739		"	0.57792	
10^{-3}	0.600	0.57267	-4.56	"	0.57287		"	0.57355	
$10^{-2.5}$	0.599	0.56810	-5.16	"	0.56834		"	0.56917	
10^{-2}	0.590	0.56352	-4.49	"	0.56380		"	0.56476	
$10^{-1.5}$	0.575	0.55892	-2.80	"	0.55924		"	0.56032	
10^{-1}	0.567	0.55432	-0.01	"	0.55465		"	0.55582	
$10^{-0.5}$	0.559	0.54970	0.07	"	0.55005		"	0.55126	
10^{0}	0.545	0.54500	0.00	"	0.54500		N/A	0.54500	

*** Yang et al.(1992)

4.5: Coefficient of Performance (COP) for LiBr-water absorption Refrigeration

Coefficient of performance (COP) of an absorption refrigeration system is obtained from;

$$COP = \left(\frac{coolingcapacityobtainedatevaporator}{heatinputforthegenerator + workinputforthepump} \right)$$

Or

$$COP = \left(\frac{Concentrationattheoutlet}{Concentrationattheinlet} \right)$$

The work input for the pump is negligible relative to the heat input at the generator; therefore, the pump work is often neglected for the purposes of analysis.

From Table 4.2.9 above

At 0.0 Tesla, COP = $\frac{0.549}{0.600}$ = 0. 915

At 3.0 Tesla, COP = $\frac{0.551}{0.600}$ = 0. 918

Increment = 0.918 – 0. 915 = 0.003 = 0.3%

UNIVERSITY OF IBADAN

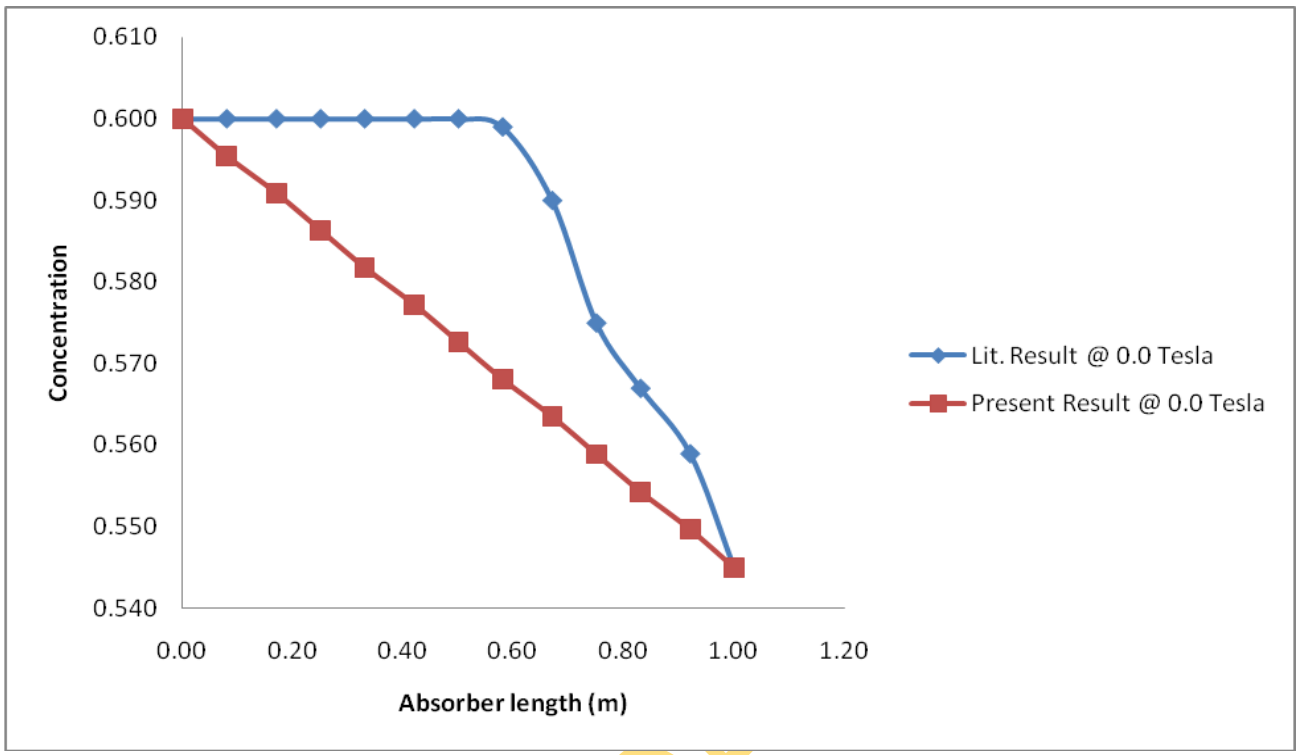

Fig. 4.3.6: LiBr-H2O Concentration Distribution in the Film Comparison at 0.0Tesla

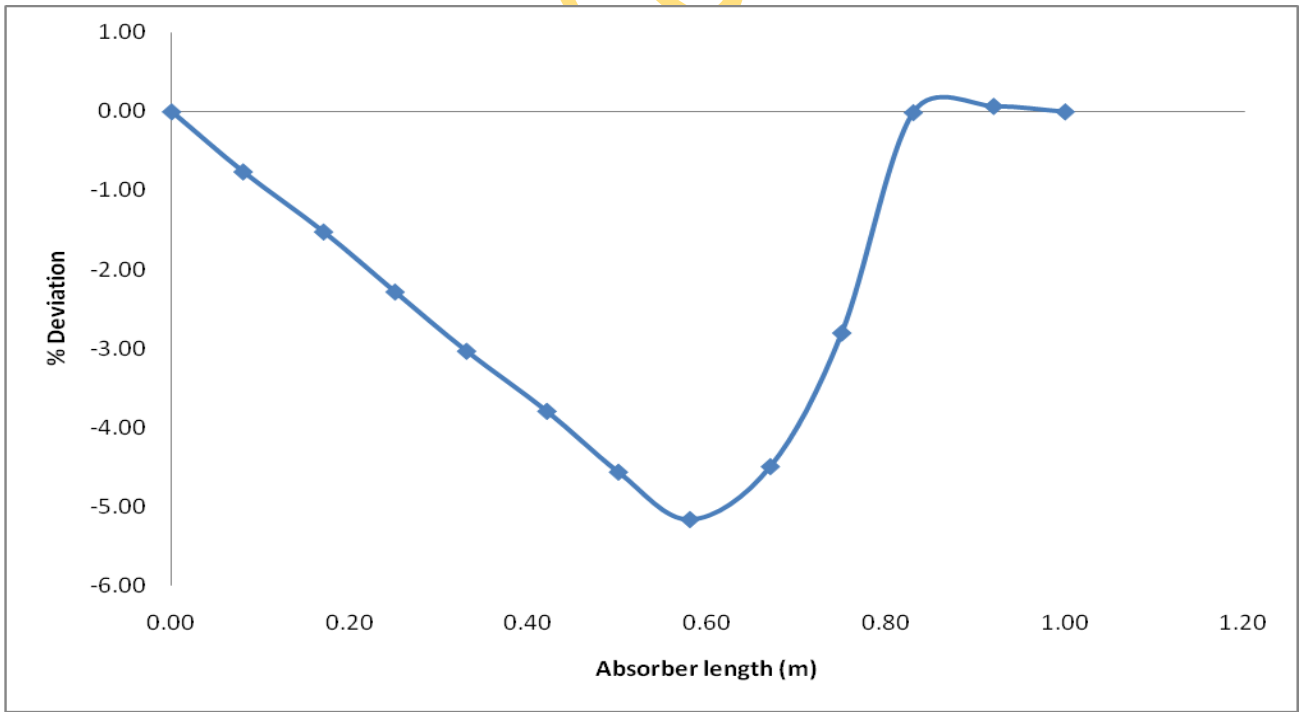

Fig 4.3.7: % Deviation in Concentration Distribution in the Film at 0.0Tesla

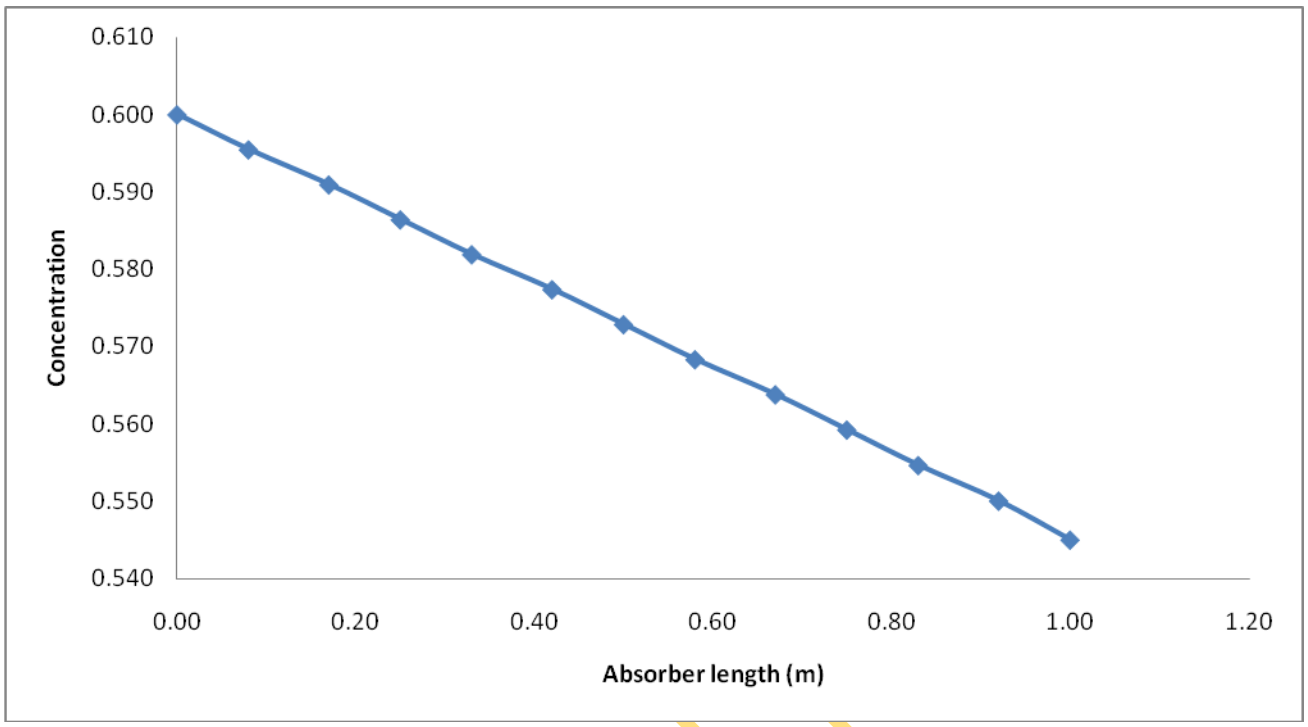

Fig. 4.3.8: LiBr-H2O Concentration Distribution in the Film at 1.4Tesla

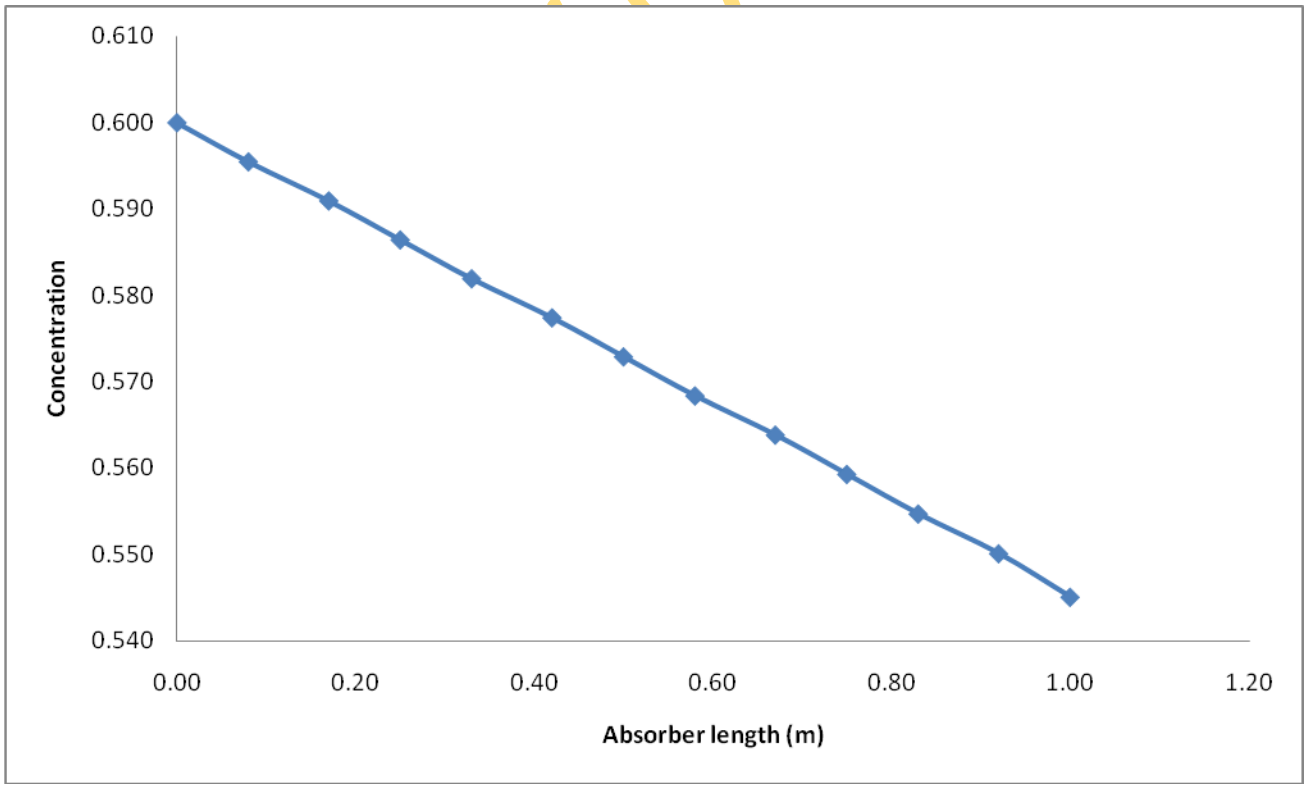

Fig. 4.3.9: LiBr-H_2O Concentration Distribution in the Film at 3.0Tesla

Table 4.2.9: LiBr-H_2O Concentration Changes within the film in X-direction, X = Absorber length.

Absorber length X (m)	Bulk					
	Present Result @ 0.0 Tesla	Present. Result @ 1.4 Tesla	% Changes in X-dir	Present Result @ 0.0 Tesla	Present Result @3.0 Tesla	% Changes in X-dir
0 or 10^{-6}	0.600	0.600	0.000	0.600	0.600	0.000
$10^{-5.5}$	0.59545	0.59547	0.003	0.59545	0.59551	0.010
10^{-5}	0.59090	0.59094	0.010	0.59090	0.59107	0.029
$10^{-4.5}$	0.58635	0.58642	0.012	0.58635	0.58667	0.055
10^{-4}	0.58180	0.58191	0.020	0.58180	0.58229	0.084
$10^{-3.5}$	0.57724	0.57739	0.026	0.57724	0.57792	0.118
10^{-3}	0.57267	0.57287	0.035	0.57267	0.57355	0.154
$10^{-2.5}$	0.56810	0.56834	0.042	0.56810	0.56917	0.188
10^{-2}	0.56352	0.56380	0.050	0.56352	0.56476	0.220
$10^{-1.5}$	0.55892	0.55924	0.057	0.55892	0.56032	0.250
10^{-1}	0.55432	0.55465	0.060	0.55432	0.55582	0.271
$10^{-0.5}$	0.54970	0.55005	0.064	0.54970	0.55126	0.284
10^{0}	0.54500	0.54500	0.000	0.54500	0.54500	0.000

UNIVERSITY OF IBADAN

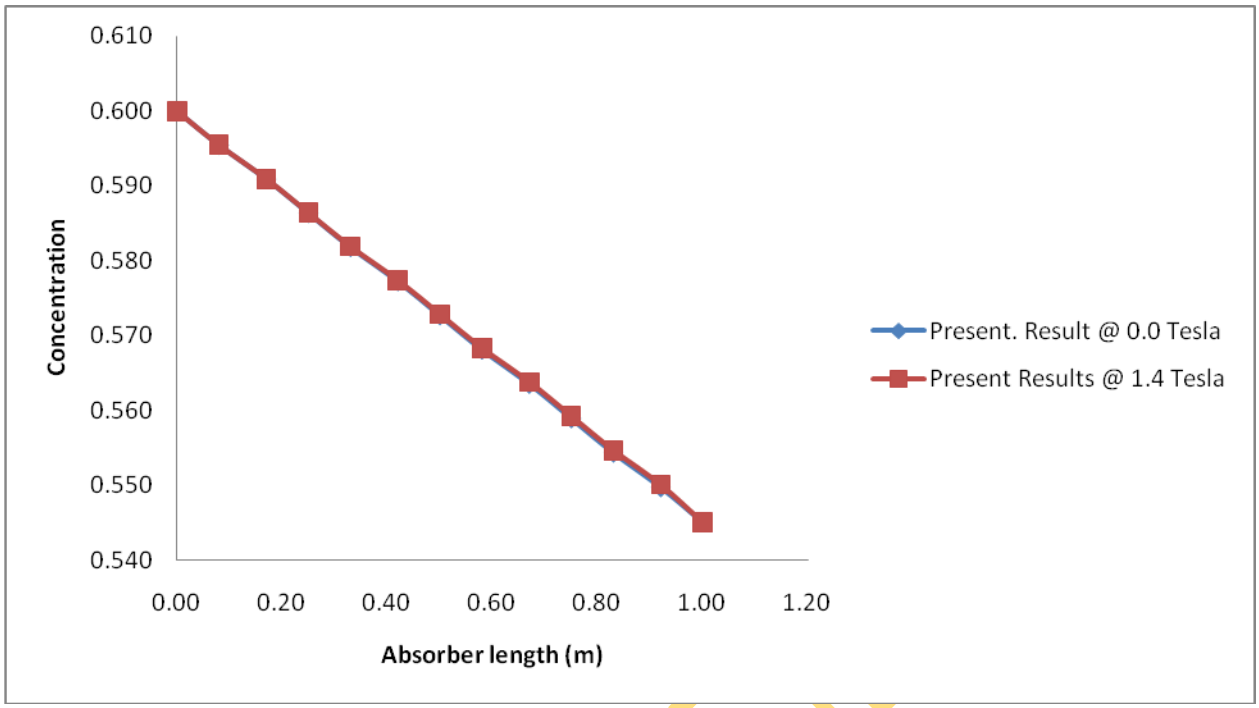

Fig 4.4: Concentration Changes within the Film in X-Direction at 0.0 and 1.4 Tesla, X = Absorber length.

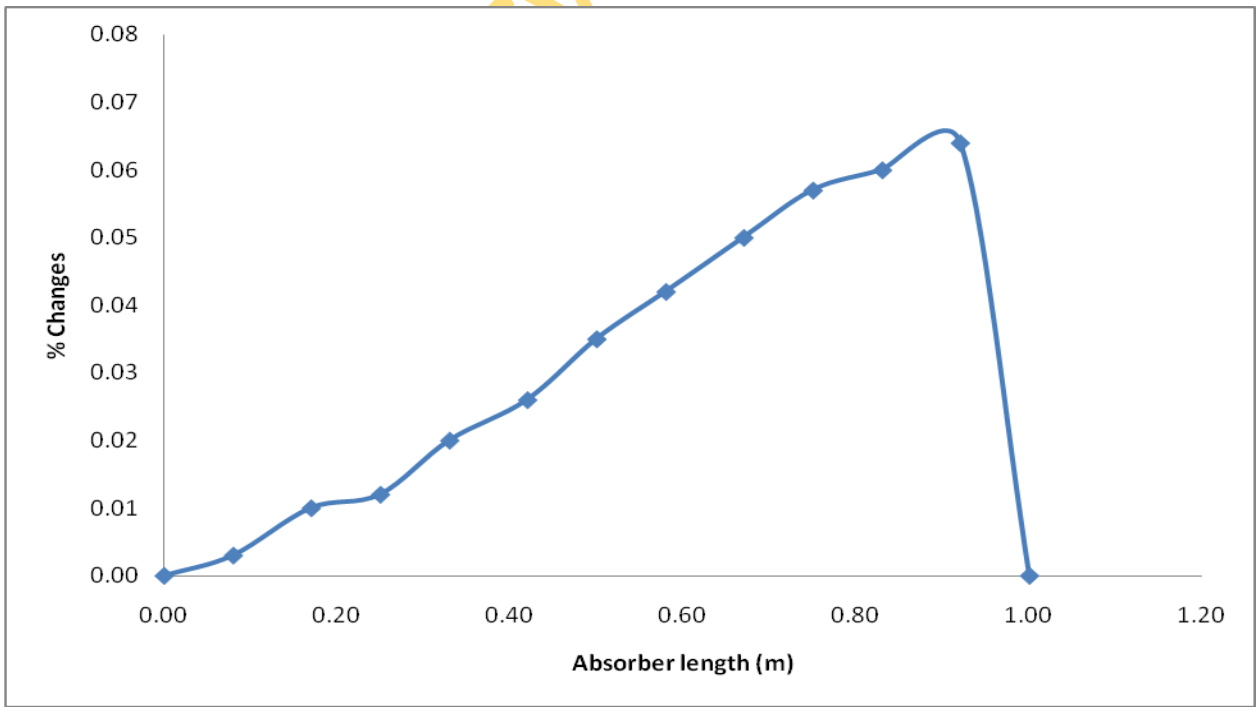

Fig 4.4.1: % Concentration Changes within the Film in X-direction at 0.0 and 1.4Tesla, X = Absorber length.

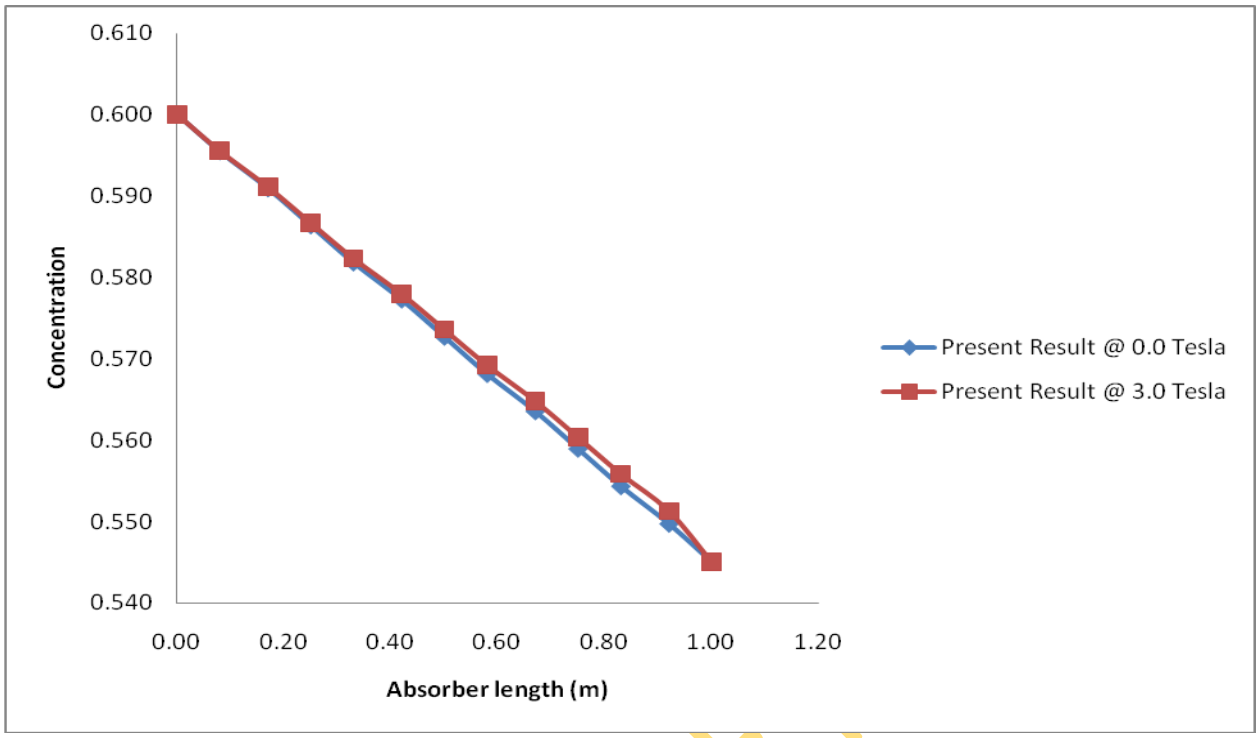

Fig 4.4.2: Concentration Changes within the Film in X-direction at 0.0 & 3.0 Tesla, X = Absorber length.

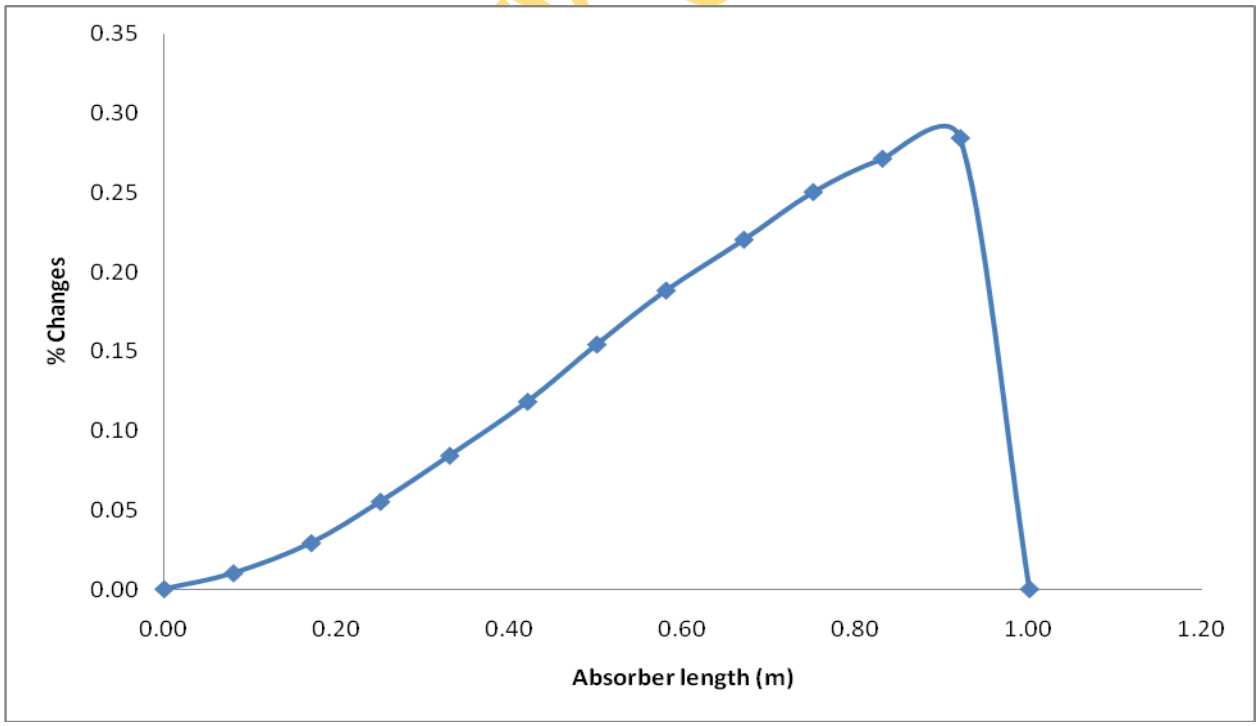

Fig 4.4.3: % Concentration Changes within the Film in X-Direction at 0.0 & 3.0Tesla, X = Absorber length.

Table 4.3: LiBr-H_2O Concentration Distribution in the film Comparison

Absorber length X (m)	Interface								
	Lit. Result @ 0.0 Tesla ***	**Present Result @ 0.0 Tesla**	**% Deviation**	**Lit. Result @ 1.4 Tesla**	**Present. Result @ 1.4 Tesla**	**% Deviation**	**Lit. Result @ 3.0 Tesla**	**Present Result @3.0 Tesla**	**% Deviation**
0 or 10^{-6}	0.599	0.600	0.17	N/A	0.600		N/A	0.600	
$10^{-5.5}$	0.599	0.59500	-0.67	"	0.59502		"	0.59507	
10^{-5}	0.599	0.59004	-1.50	"	0.59008		"	0.59019	
$10^{-4.5}$	0.599	0.58513	-2.32	"	0.58518		"	0.58535	
10^{-4}	0.599	0.58025	-3.13	"	0.58032		"	0.58054	
$10^{-3.5}$	0.591	0.57542	-2.64	"	0.57550		"	0.57577	
10^{-3}	0.580	0.57063	-1.62	"	0.57072		"	0.57105	
$10^{-2.5}$	0.570	0.56587	-0.73	"	0.56598		"	0.56636	
10^{-2}	0.560	0.56116	0.21	"	0.56128		"	0.56171	
$10^{-1.5}$	0.550	0.55648	1.18	"	0.55662		"	0.55710	
10^{-1}	0.548	0.55185	0.70	"	0.55200		"	0.55253	
$10^{-0.5}$	0.546	0.54725	0.23	"	0.54741		"	0.54799	
10^{0}	0.545	0.54500	0.00	N/A	0.54500		N/A	0.54500	

******* Yang et al.(1992)

UNIVERSITY OF IBADAN

Table 4.3.1: LiBr-H_2O Concentration Deviation Analysis at the Bulk and Interface

	BULK			INTERFACE		
Absorber length X (m)	**Lit. Result @ 0.0 Tesla *** **	**Present Result @ 0.0 Tesla**	**Devia-tion.**	**Lit. Result @ 0.0 Tesla *** **	**Present Result @ 0.0 Tesla**	**Devia-tion.**
0 or 10^{-6}	0.600	0.6000	0.0000	0.599	0.600	-0.0010
$10^{-5.5}$	0.600	0.5955	0.0045	0.599	0.595	0.0040
10^{-5}	0.600	0.5909	0.0091	0.599	0.590	0.0089
$10^{-4.5}$	0.600	0.5864	0.0136	0.599	0.585	0.0138
10^{-4}	0.600	0.5818	0.0182	0.599	0.580	0.0187
$10^{-3.5}$	0.600	0.5772	0.0227	0.591	0.575	0.0155
10^{-3}	0.600	0.5727	0.0273	0.580	0.571	0.0093
$10^{-2.5}$	0.599	0.5681	0.0309	0.570	0.566	0.0041
10^{-2}	0.590	0.5635	0.0264	0.560	0.561	-0.0011
$10^{-1.5}$	0.575	0.5589	0.0160	0.550	0.556	-0.0064
10^{-1}	0.567	0.5543	0.0126	0.548	0.552	-0.0038
$10^{-0.5}$	0.559	0.5497	0.0093	0.546	0.547	-0.0012
10^{0}	0.545	0.5450	0.0000	0.545	0.545	0.0000

*** Yang et al.(1992)

UNIVERSITY OF IBADAN

Table 4.3.2: LiBr-H_2O Concentration Deviation Analysis at the Bulk and Interface

	BULK @ 0.0 Tesla			INTERFACE @ 0.0 Tesla		
Absorber length X (m)	**Deviation.**	**Mean Deviation**	**Mean Deviation. Square** X 10^{-4}	**Deviation.**	**Mean Deviation**	**Mean Deviation. Square** X 10^{-4}
0 or 10^{-6}	0.0000	0.01425	2.03	-0.0010	0.00468	0.32
$10^{-5.5}$	0.0045	0.01425	0.95	0.0040	0.00468	0.00
10^{-5}	0.0091	0.01425	0.27	0.0089	0.00468	0.18
$10^{-4.5}$	0.0136	0.01425	0.00	0.0138	0.00468	0.83
10^{-4}	0.0182	0.01425	0.16	0.0187	0.00468	1.97
$10^{-3.5}$	0.0227	0.01425	0.71	0.0155	0.00468	1.17
10^{-3}	0.0273	0.01425	1.70	0.0093	0.00468	0.21
$10^{-2.5}$	0.0309	0.01425	2.77	0.0041	0.00468	0.00
10^{-2}	0.0264	0.01425	1.48	-0.0011	0.00468	0.33
$10^{-1.5}$	0.0106	0.01425	0.13	-0.0064	0.00468	1.23
10^{-1}	0.0126	0.01425	0.03	-0.0038	0.00468	0.72
$10^{-0.5}$	0.0093	0.01425	0.25	-0.0012	0.00468	0.35
10^{0}	0.0000	0.01425	2.03	0.0000	0.00468	0.22
Σ			**12.51**			**7.54**

@ The Bulk, Std. deviation (σ) $\sqrt{12.51x10^{-4}/13}$ **= 0.9809 X 10^{-2}**

@ The Interface, Std. deviation (σ) $\sqrt{7.54x10^{-4}/13}$ **= 0.7614 X 10^{-2}**

UNIVERSITY OF IBADAN

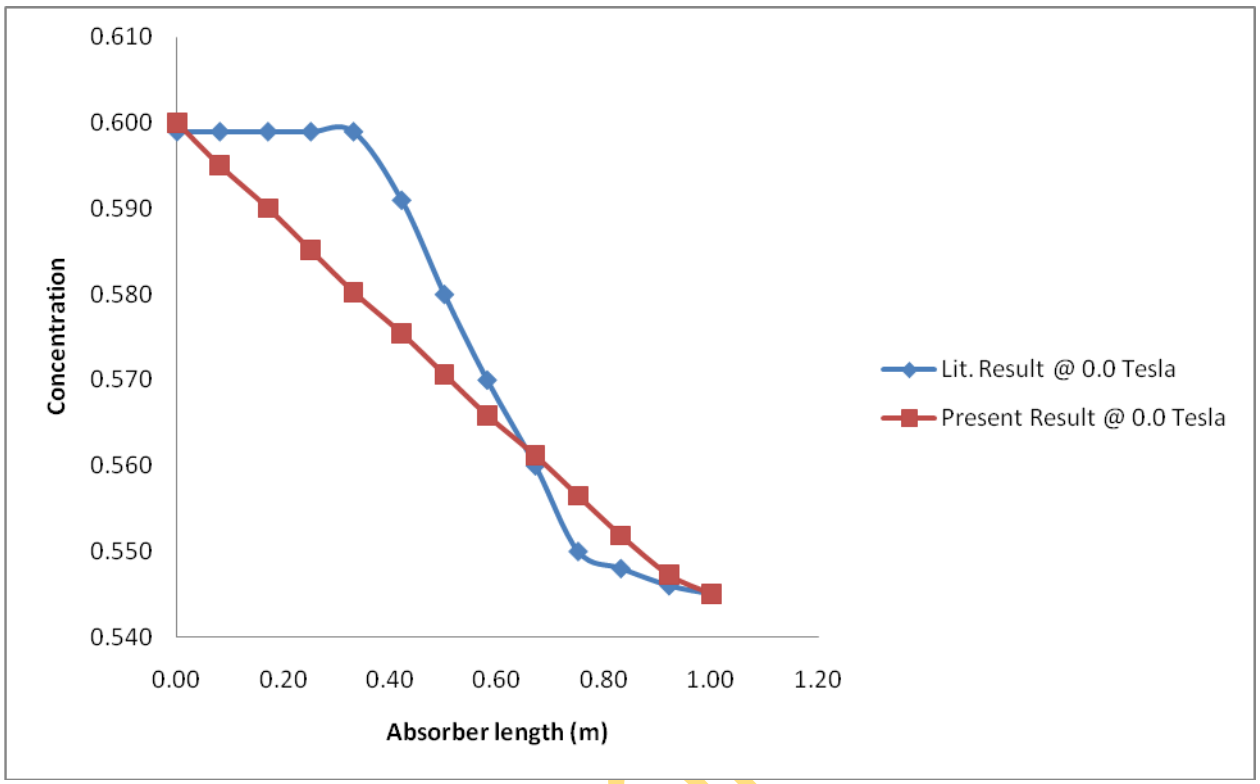

Fig 4.4.4: **LiBr-H_2O** Concentration Distribution at the Interface Comparison at 0.0Tesla

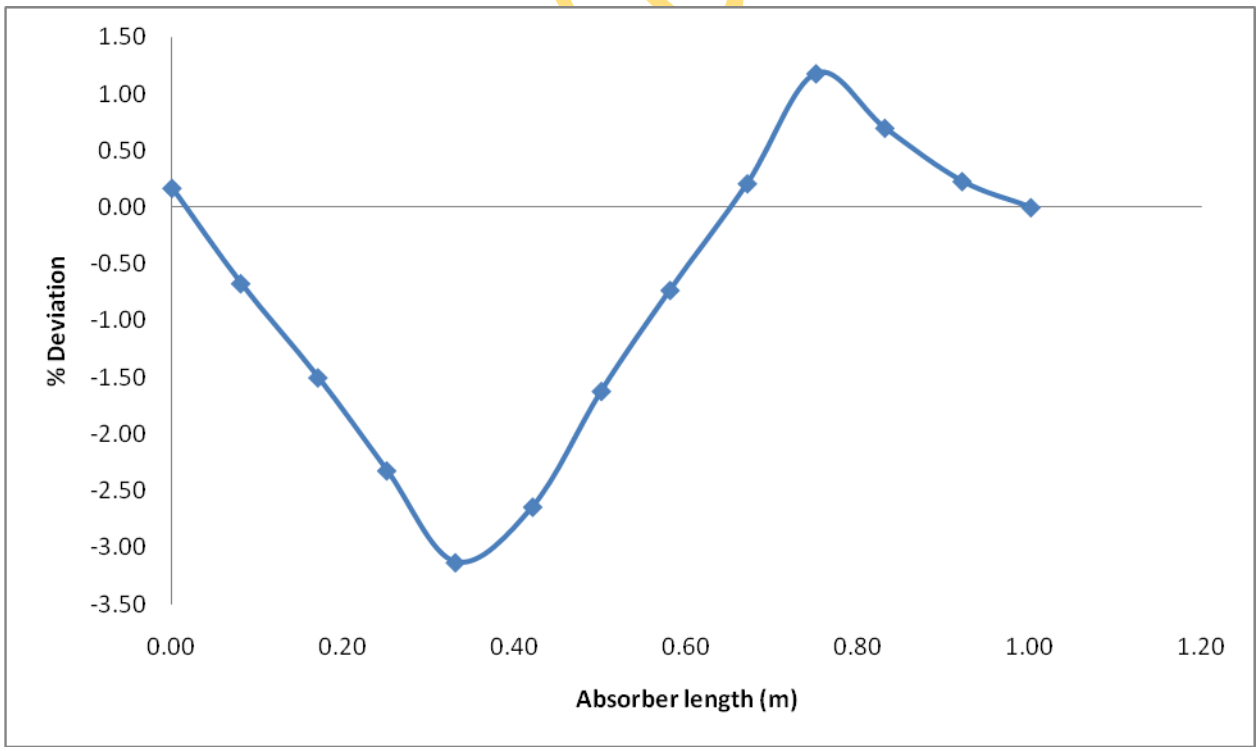

Fig 4.4.5: % Deviation in Concentration Distribution at the Interface at 0.0Tesla

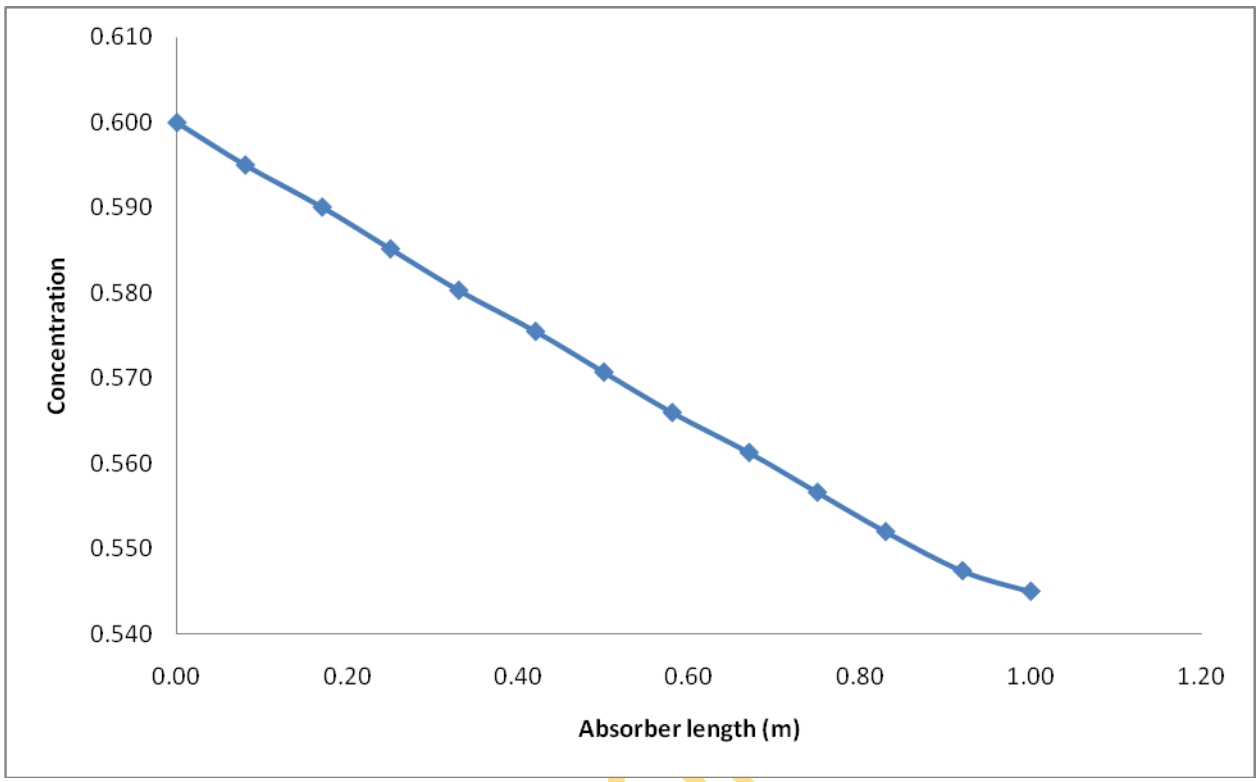

Fig 4.4.6: Concentration Distribution at the Interface at 1.4Tesla (present Result)

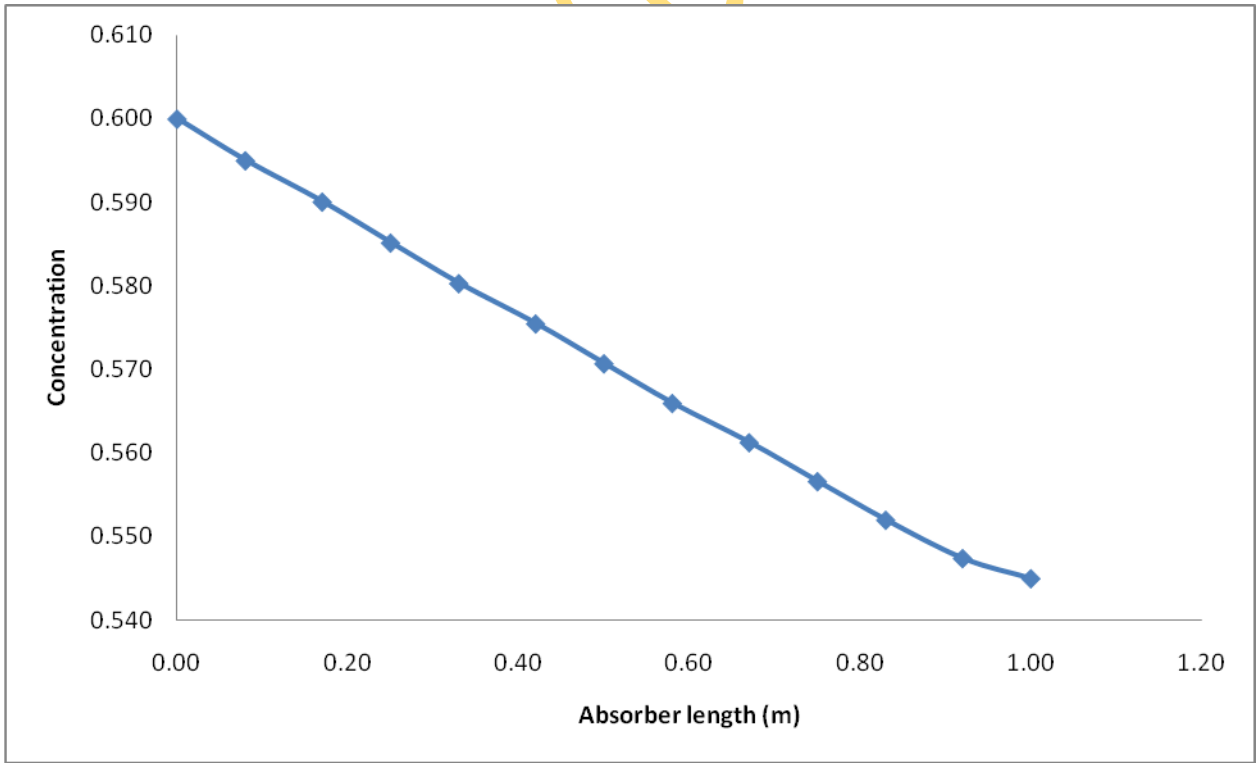

Fig 4.4.7:Concentration Distribution at the Interface at 3.0Tesla (Present Result)

Table 4.3.3: LiBr-H_2O Concentration Changes within the film in X-direction, X = Absorber length.

Absorber length X (m)	Interface					
	Present Result @ 0.0 Tesla	Present. Result @ 1.4 Tesla	% Changes in X-dir	Present Result @ 0.0 Tesla	Present Result @3.0 Tesla	% Changes in X-dir
0 or 10^{-6}	0.600	0.600	0.000	0.600	0.600	0.000
$10^{-5.5}$	0.59500	0.59502	0.003	0.59500	0.59507	0.012
10^{-5}	0.59004	0.59008	0.007	0.59004	0.59019	0.025
$10^{-4.5}$	0.58513	0.58518	0.009	0.58513	0.58535	0.038
10^{-4}	0.58025	0.58032	0.012	0.58025	0.58054	0.050
$10^{-3.5}$	0.57542	0.57550	0.014	0.57542	0.57577	0.061
10^{-3}	0.57063	0.57072	0.016	0.57063	0.57105	0.074
$10^{-2.5}$	0.56587	0.56598	0.019	0.56587	0.56636	0.087
10^{-2}	0.56116	0.56128	0.021	0.56116	0.56171	0.098
$10^{-1.5}$	0.55648	0.55662	0.025	0.55648	0.55710	0.111
10^{-1}	0.55185	0.55200	0.027	0.55185	0.55253	0.123
$10^{-0.5}$	0.54725	0.54741	0.029	0.54725	0.54799	0.135
10^{0}	0.54500	0.54500	0.000	0.54500	0.54500	0.000

UNIVERSITY OF IBADAN

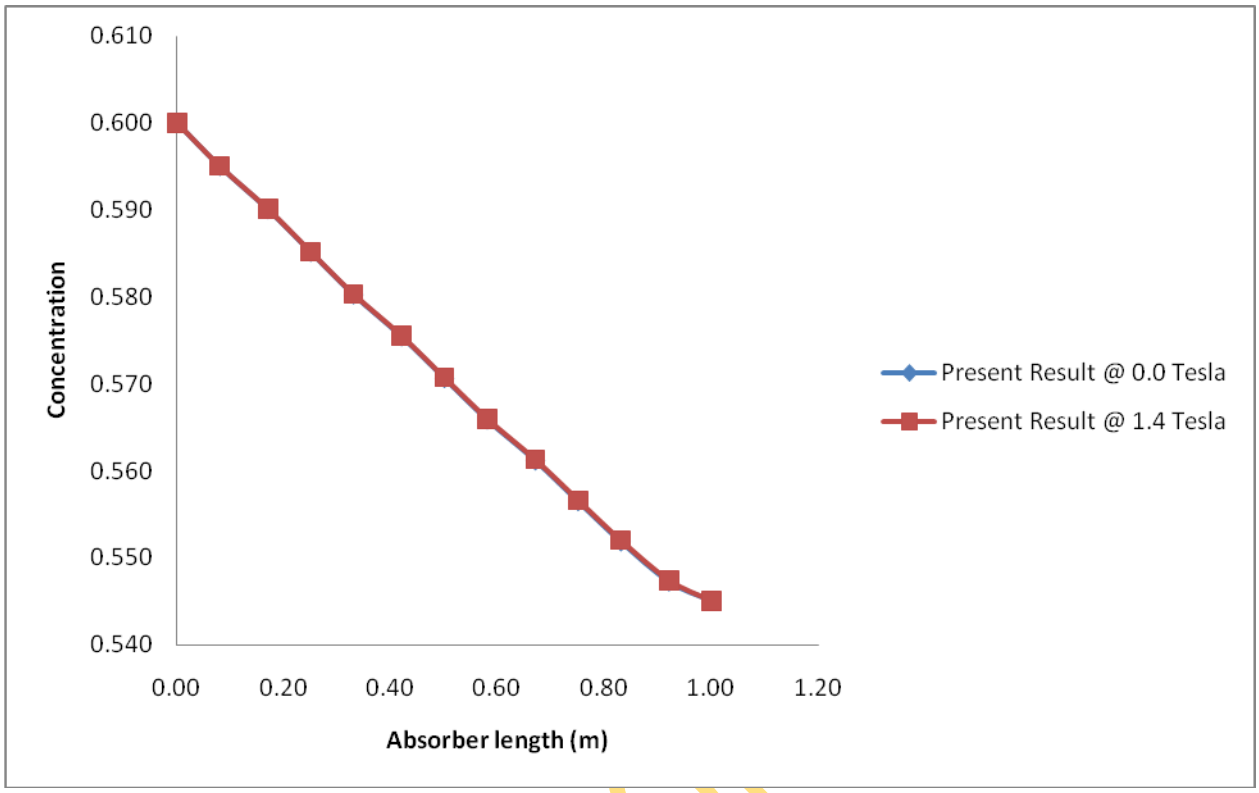

Fig 4.4.8: Concentration Changes at the interface in X-Direction from 0.0 to 1.4 Tesla, X = Absorber length.

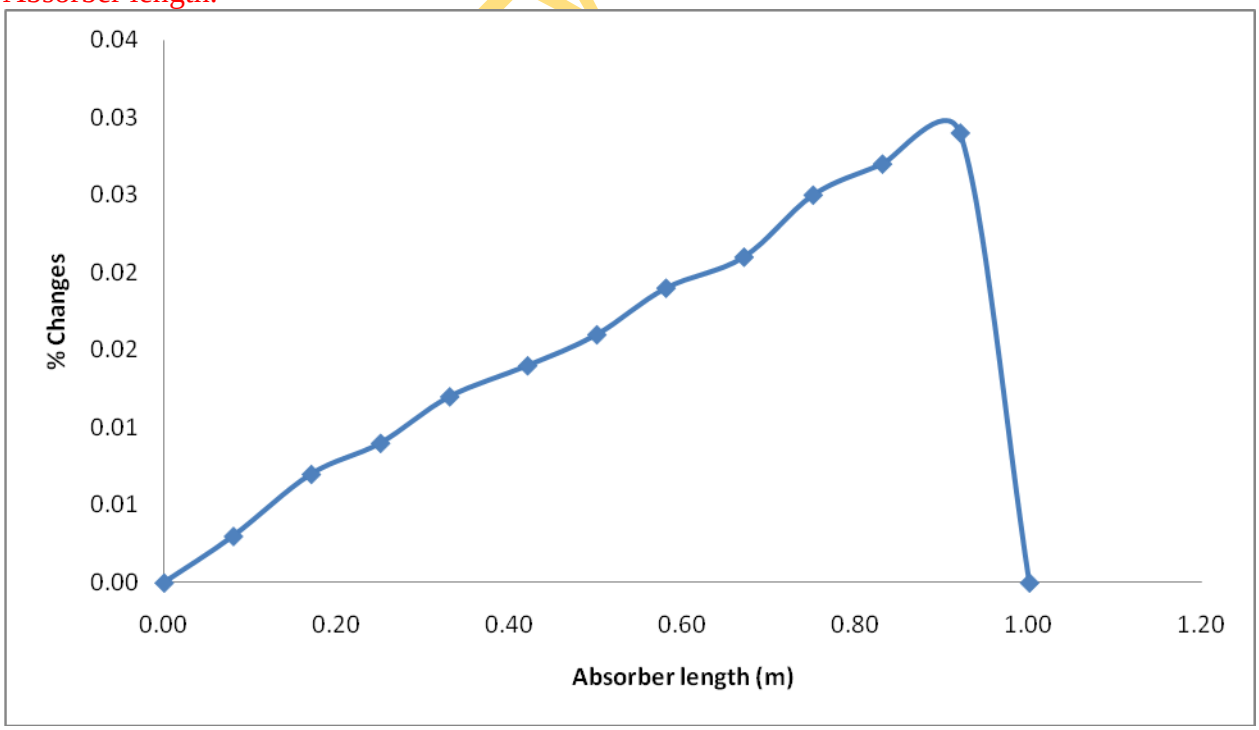

Fig 4.4.9: Concentration Changes at the interface in X-direction from 0.0 to 1.4Tesla, X = Absorber length.

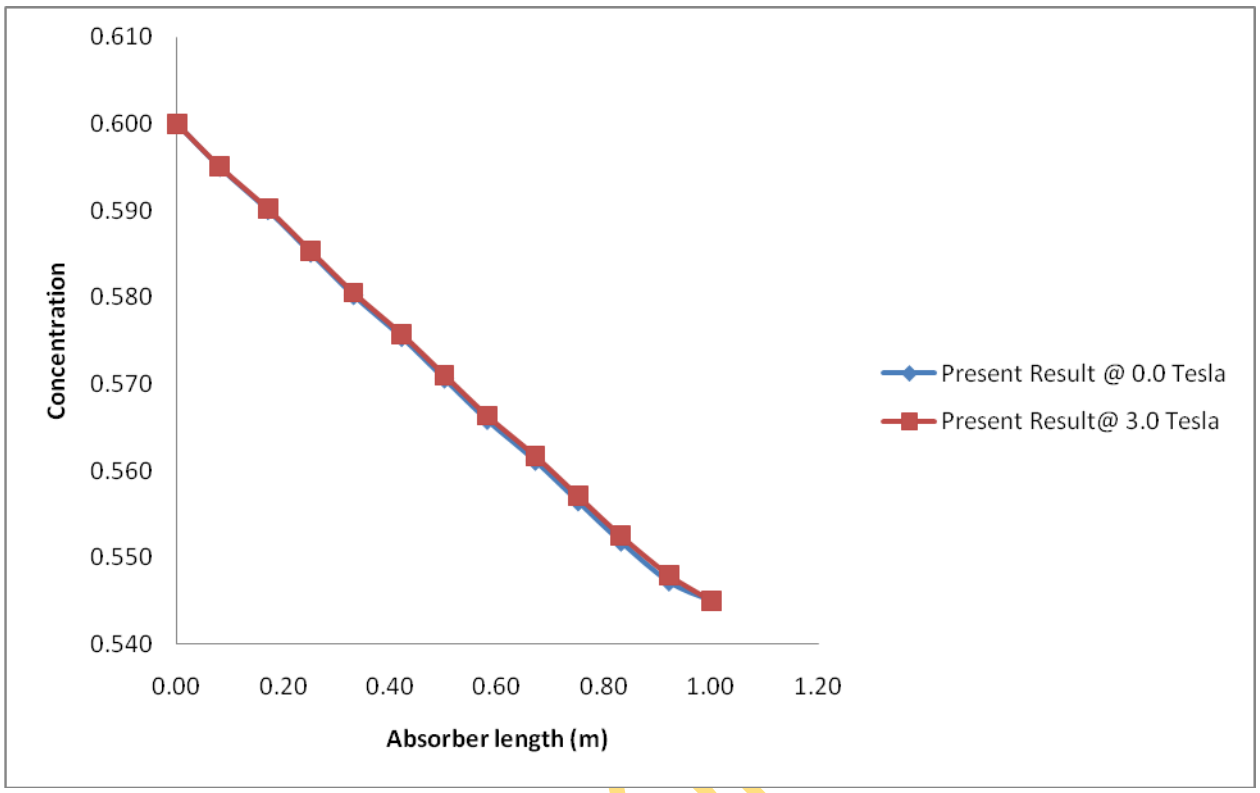

Fig 4.5: Concentration Changes at the interface in X-direction at 0.0 & 3.0 Tesla, X = Absorber length.

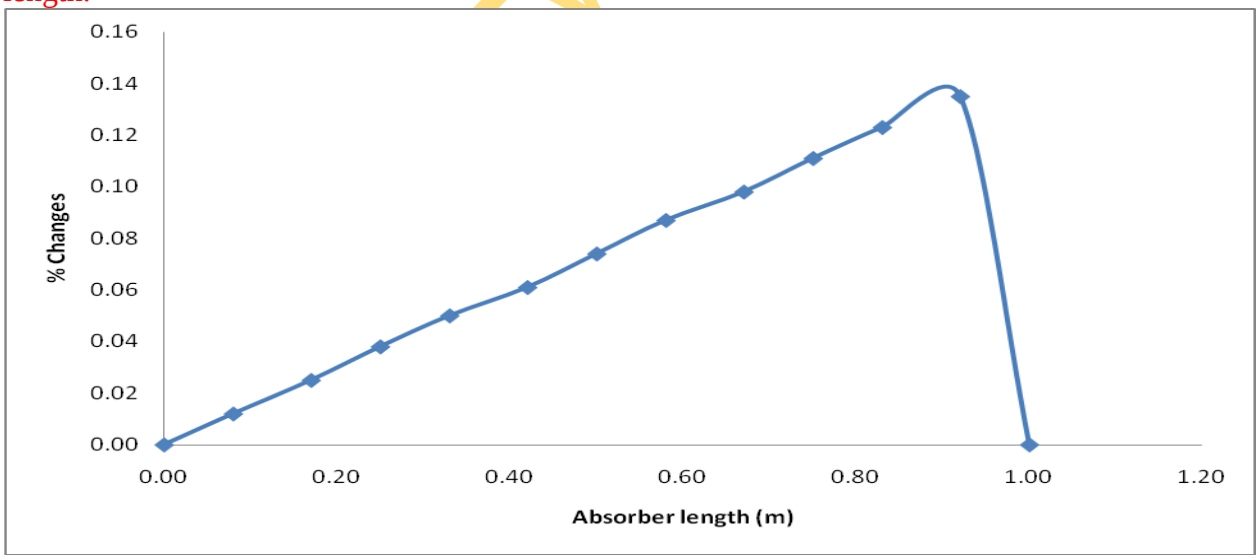

Fig 4.5.1: % Concentration Changes at the interface in X-Direction from 0.0 to 3.0Tesla, X = Absorber length.

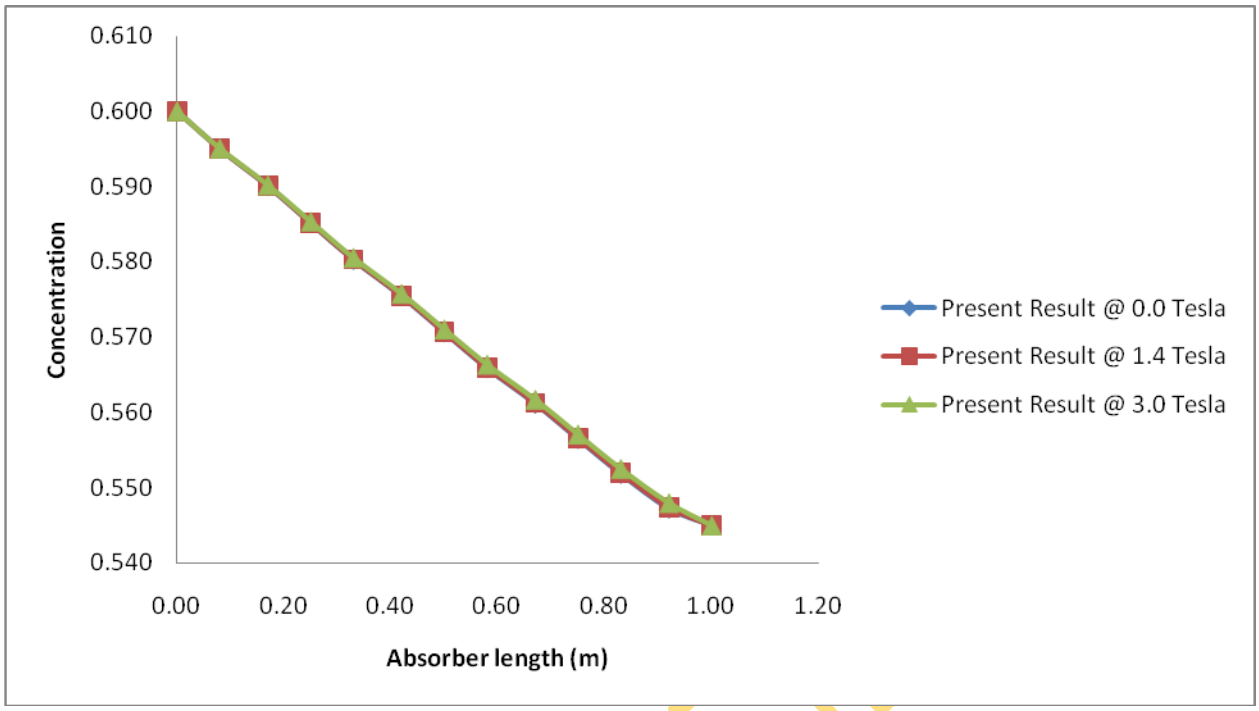

Fig 4.5.2: LiBr-H_2O Concentration Distribution at the interface in X direction at 0.0 1.4 and 3.0Tesla, X = Absorber length.

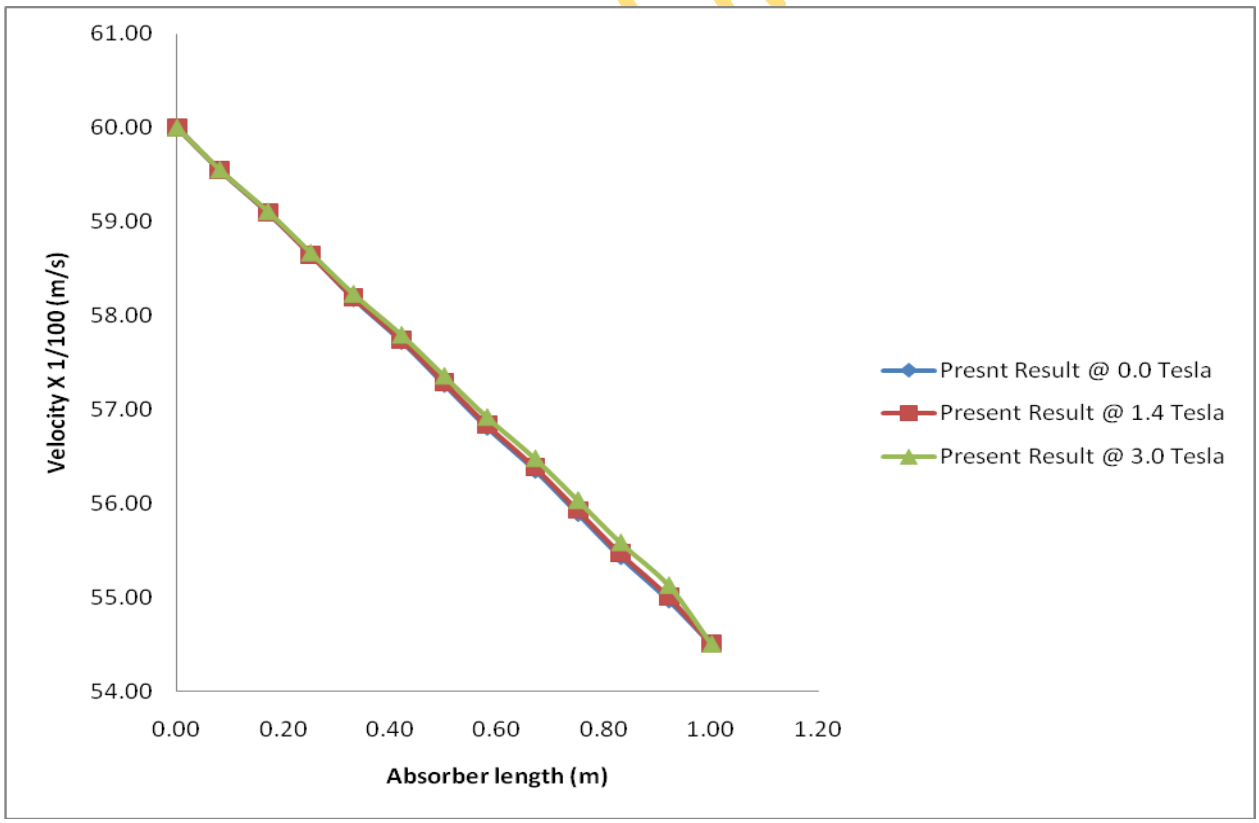

Fig 4.5.3: LiBr-H_2O Concentration Distribution in the film at 0.0 1.4 and 3.0Tesla

Table 4.3.4: LiCl-H_2O Velocity Distribution in the film

Absorber length X (m)	Bulk								
	Lit. Result @ 0.0 Tesla	Present Result @ 0.0 Tesla	% Devia -tion	Lit. Result @ 1.4 Tesla	Present. Result @ 1.4 Tesla	% Devia-tion	Lit. Result @ 3.0 Tesla	Present Result @3.0 Tesla	% Devia-tion
0 or 10^{-6}	N/A	0.3620		N/A	0.3620		N/A	0.3620	
$10^{-5.5}$	"	0.3662		"	0.3671		"	0.3702	
10^{-5}	"	0.3702		"	0.3719		"	0.3775	
$10^{-4.5}$	"	0.3742		"	0.3765		"	0.3840	
10^{-4}	"	0.3780		"	0.3808		"	0.3897	
$10^{-3.5}$	"	0.3818		"	0.3849		"	0.3946	
10^{-3}	"	0.3854		"	0.3887		"	0.3987	
$10^{-2.5}$	N/A	0.3889		N/A	0.3922		N/A	0.4019	
10^{-2}	"	0.3924		"	0.3955		"	0.4044	
$10^{-1.5}$	"	0.3957		"	0.3985		"	0.4060	
10^{-1}	"	0.3989		"	0.4013		"	0.4068	
$10^{-0.5}$	"	0.4020		"	0.4038		"	0.4068	
10^{0}	N/A	0.4050		N/A	0.4060		N/A	0.4060	

UNIVERSITY OF IBADAN

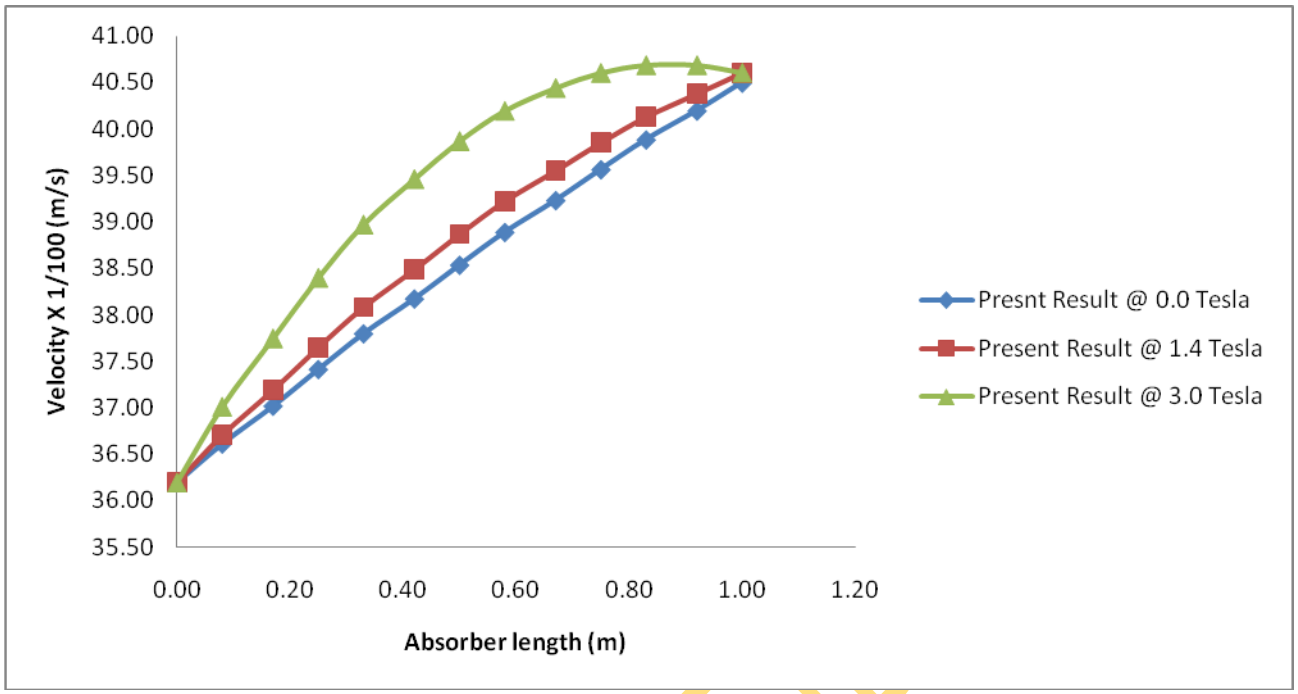

Fig 4.5.3: **LiCl-H_2O** Velocity Distribution in the Film at 0.0, 1.4 and 3.0Tesla

Table 4.3.5: LiCl-H_2O Temperature Distribution in the film Comparison

Absorber length X (m)	**Bulk**								
	Lit. Result @ 0.0 Tesla ***	**Present Result @ 0.0 Tesla**	**% Devia-tion**	**Lit. Result @ 1.4 Tesla**	**Present. Result @ 1.4 Tesla**	**% Devia-tion**	**Lit. Result @ 3.0 Tesla**	**Present Result @3.0 Tesla**	**% Devia-tion**
0 or 10^{-6}	35.00	35.00	0.00	N/A	35.00		N/A	35.00	
$10^{-5.5}$	35.00	34.74	0.00	"	34.74		"	34.74	
10^{-5}	35.00	34.49	0.00	"	34.49		"	34.49	
$10^{-4.5}$	35.00	34.23	-2.20	"	34.23		"	34.23	
10^{-4}	35.00	33.98	-2.90	"	33.98		"	33.98	
$10^{-3.5}$	35.00	33.73	-3.60	"	33.73		"	33.73	

UNIVERSITY OF

10^{-3}	35.00	33.48	-4.34	"	33.48		"	33.48	
$10^{-2.5}$	34.80	33.24	-4.48	N/A	33.24		N/A	33.24	
10^{-2}	33.90	32.99	-2.68	"	32.99		"	32.99	
$10^{-1.5}$	32.10	32.75	2.03	"	32.75		"	32.75	
10^{-1}	32.00	32.51	1.59	"	32.51		"	32.51	
$10^{-0.5}$	31.50	32.27	2.44	"	32.27		"	32.27	
10^{0}	30.00	30.00	0.00	N/A	30.00		N/A	30.00	

*** Yang et al.(1992)

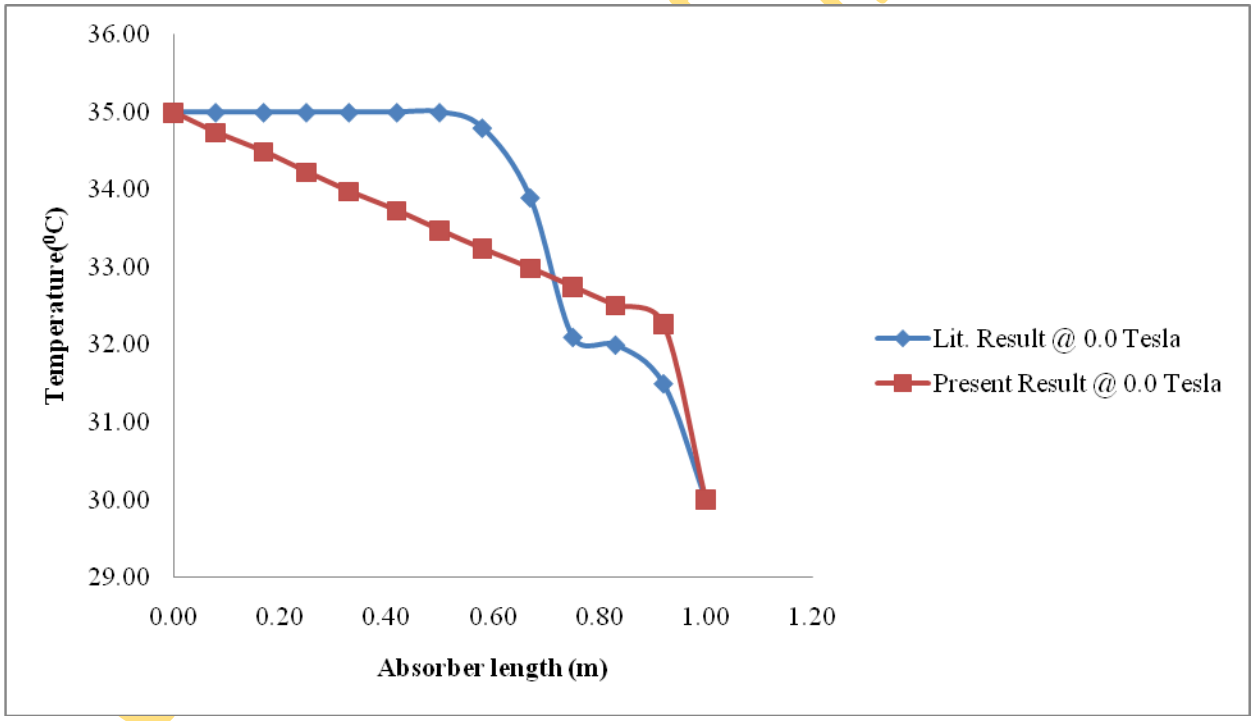

Fig 4.5.4: **LiCl-H_2O** Temperature Distribution in the Film Comparison at 0.0Tesla

- IBADAN

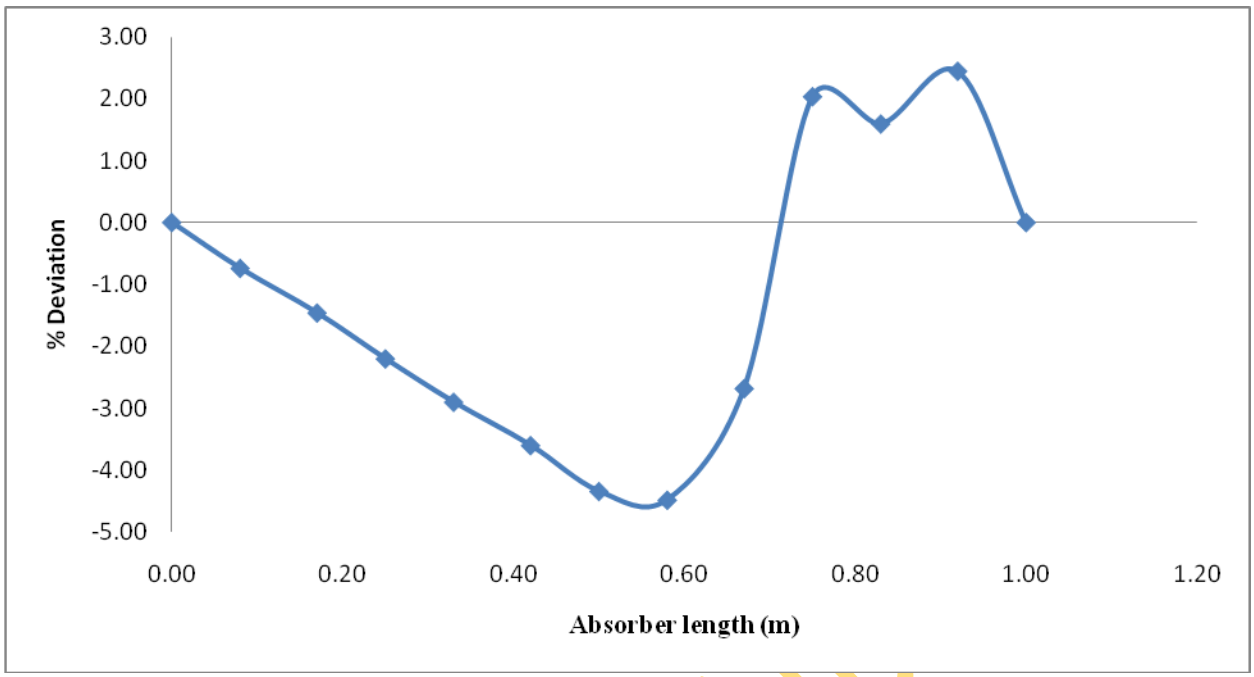

Fig. 4.5.5: % Deviation of **LiCl-H_2O** Temperature Distribution in the Film at 0.0Tesla

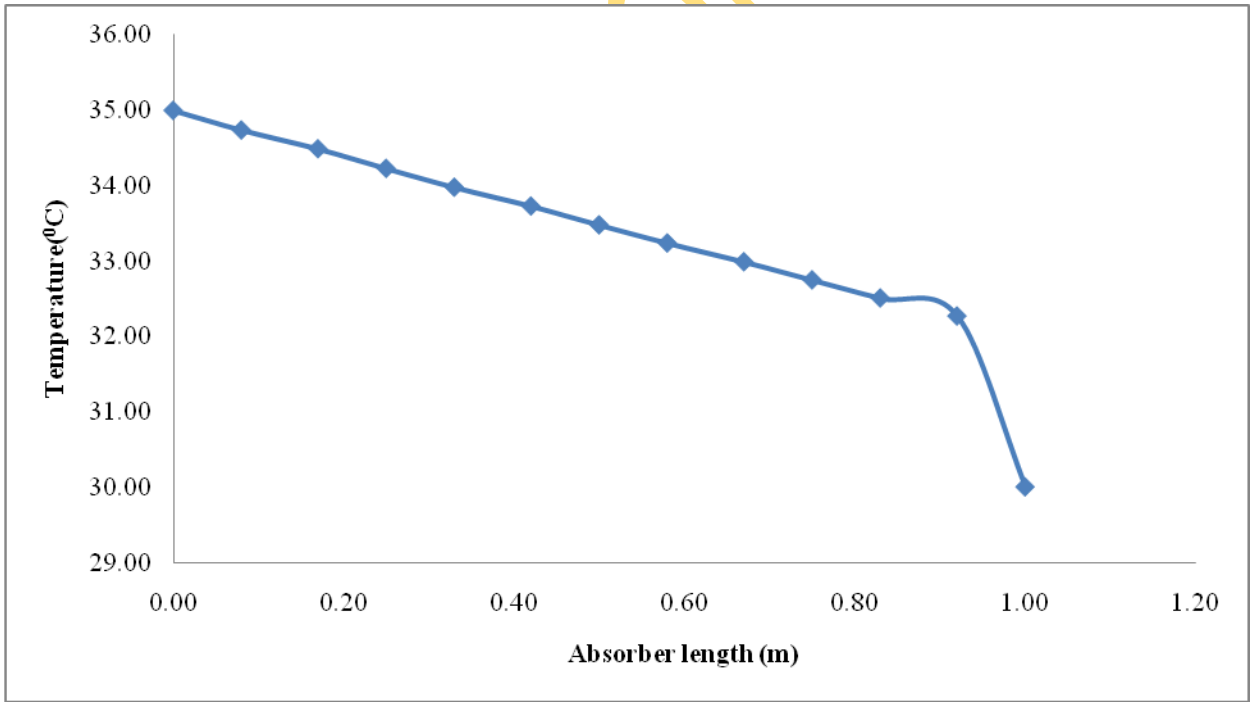

Fig. 4.5.6: Temperature Distribution in the Film at 1.4 Tesla

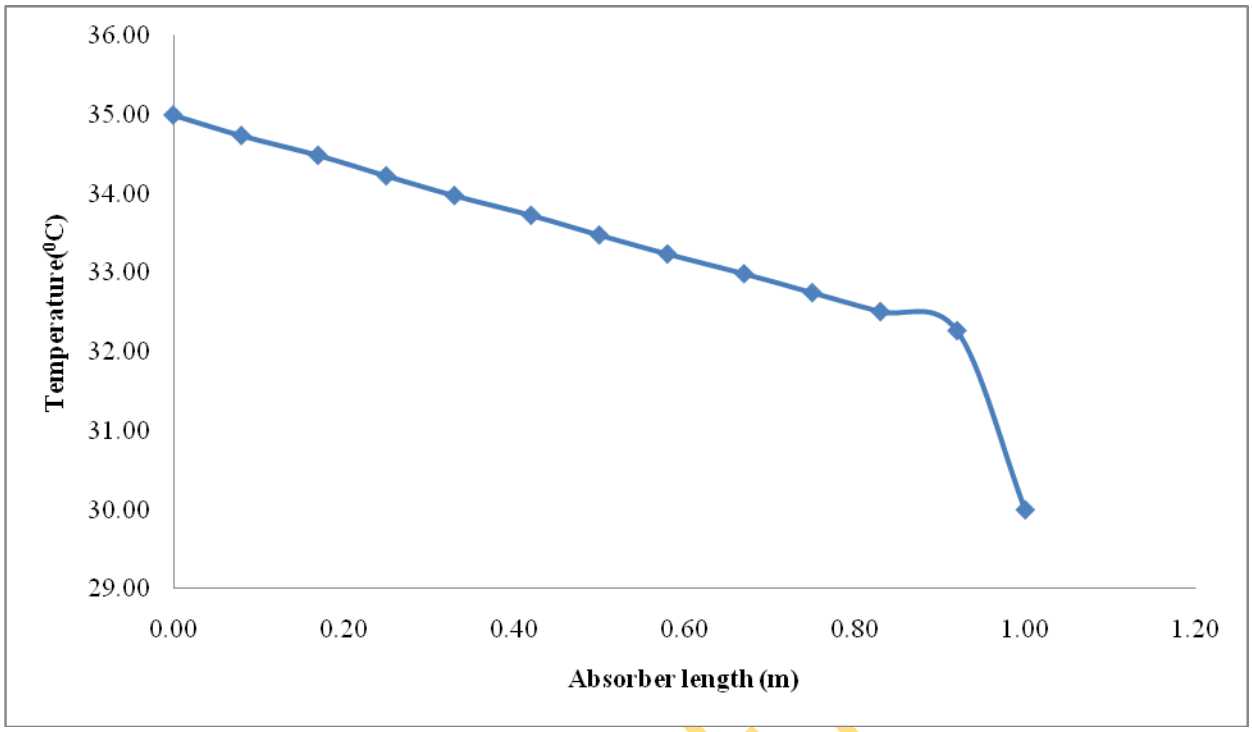

Fig 4.5.7: Temperature Distribution in the Film at 3.0Tesla

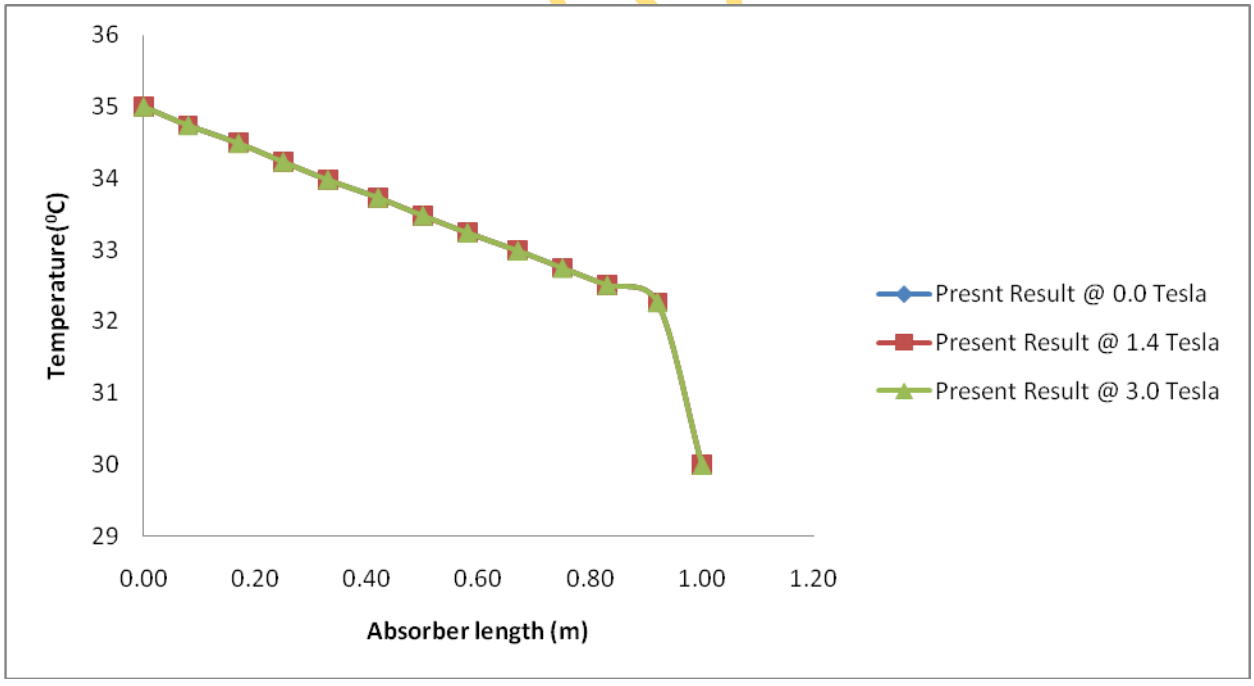

Fig. 4.5.8: **LiCl-H_2O** Temperature Distribution in the Film at 0.0, 1.4 and 3.0Tesla

Table 4.3.6: LiCl-H_2O Concentration Distribution in the film Comparison

Absorber length X (m)	Bulk								
	Lit. Result @ 0.0 Tesla ***	**Present Result @ 0.0 Tesla**	**% Deviation**	**Lit. Result @ 1.4 Tesla**	**Present. Result @ 1.4 Tesla**	**% Deviation**	**Lit. Result @ 3.0 Tesla**	**Present Result @3.0 Tesla**	**% Deviation**
0 or 10^{-6}	0.450	0.450	0.00	N/A	0.4500		N/A	0.4500	
$10^{-5.5}$	0.450	0.4453	-1.04	"	0.4453		"	0.4454	
10^{-5}	0.450	0.4406	-2.08	"	0.4407		"	0.4408	
$10^{-4.5}$	0.450	0.4360	-3.12	"	0.4361		"	0.4362	
10^{-4}	0.450	0.4313	-4.15	"	0.4314		"	0.4317	
$10^{-3.5}$	0.450	0.4267	-5.18	"	0.4268		"	0.4272	
10^{-3}	0.448	0.4221	-5.79	"	0.4222		"	0.4227	
$10^{-2.5}$	0.440	0.4174	-5.13	N/A	0.4177		N/A	0.4183	
10^{-2}	0.440	0.4128	-6.18	"	0.4131		"	0.4138	
$10^{-1.5}$	0.430	0.4082	-5.07	"	0.4085		"	0.4093	
10^{-1}	0.420	0.4036	-3.91	"	0.4039		"	0.4047	
$10^{-0.5}$	0.390	0.3990	2.30	"	0.3993		"	0.4001	
10^{0}	0.358	0.3580	0.00	N/A	0.3580		N/A	0.3580	

******* Yang et al.(1992)

UNIVERSITY OF IBADAN

Coefficient of Performance (COP) for LiCl-water absorption Refrigeration

From Table 4.3.6 above

At 0.0 Tesla, COP = $\frac{0.399}{0.450}$ = 0. 887

At 3.0 Tesla, COP = $\frac{0.400}{0.450}$ = 0.889

Increment = 0.889 – 0.887 = 0.002= 0.2%

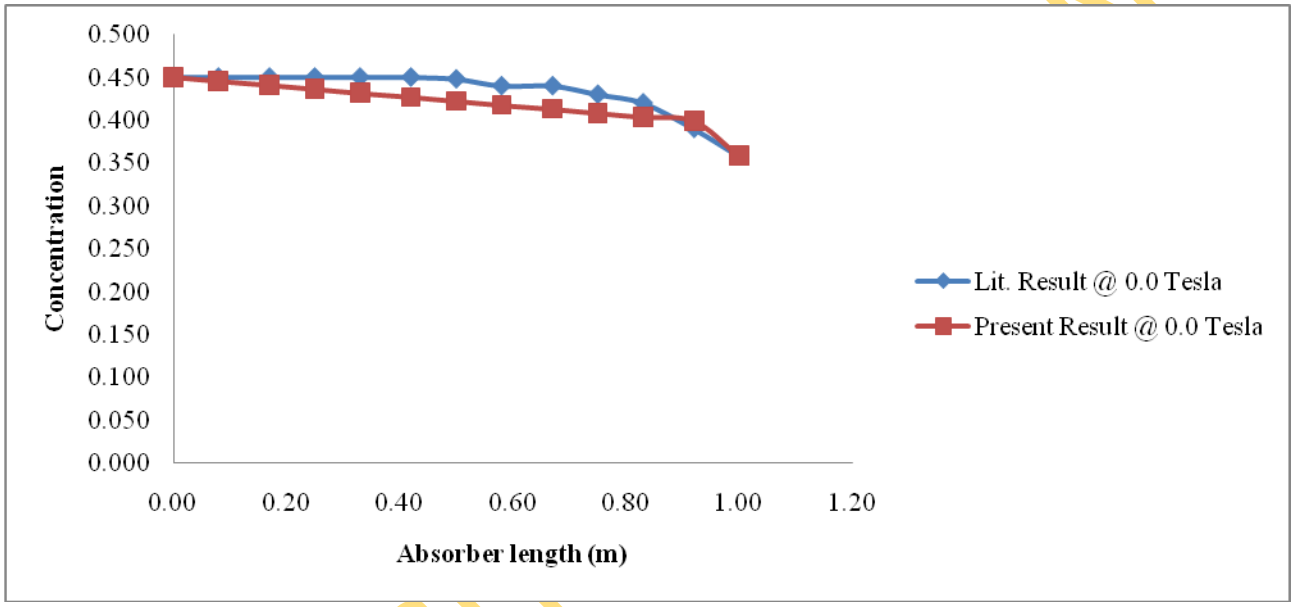

Fig. 4.5.9: **LiCl-H_2O** Concentration Distribution in the Film Comparison at 0.0 Tesla

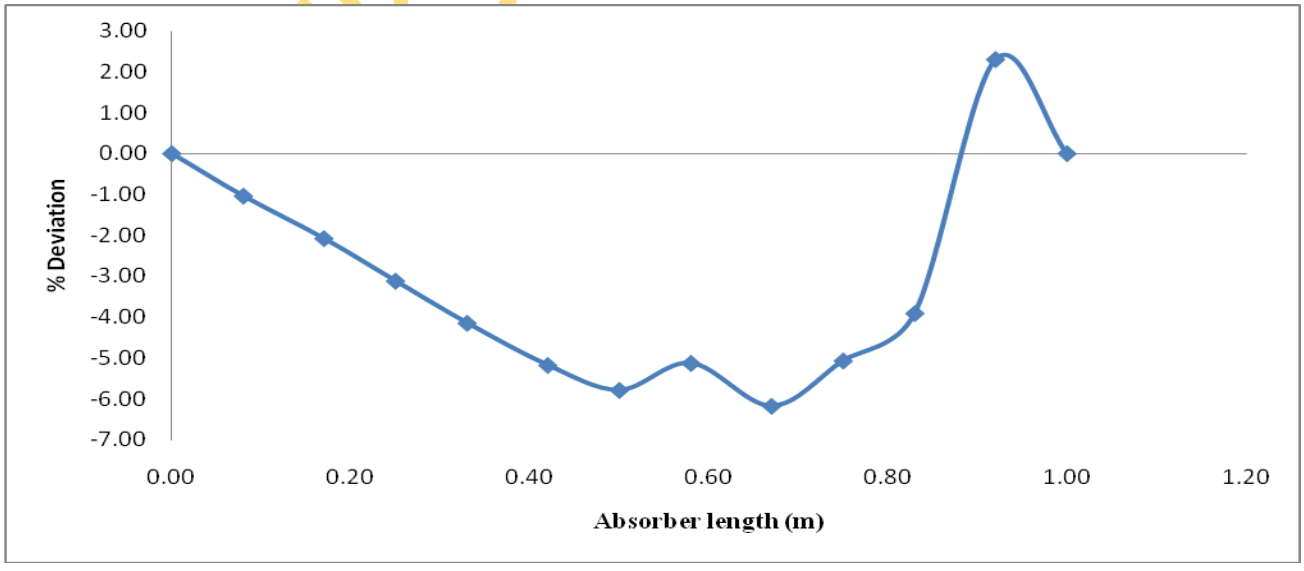

Fig. 4.6: **LiCl-H_2O** % Deviation Concentration Distribution in the Film at 0.0 Tesla

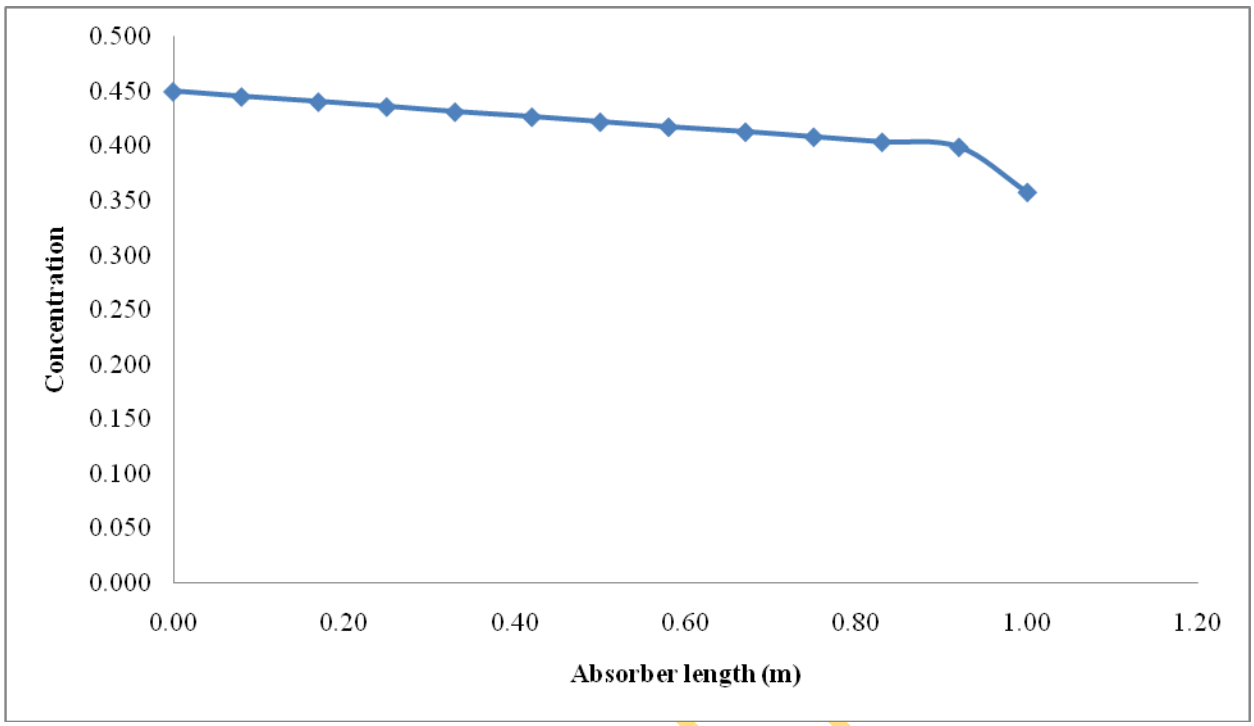

Fig. 4.6.1: **LiCl-H_2O** Concentration Distribution in the Film at 1.4 Tesla

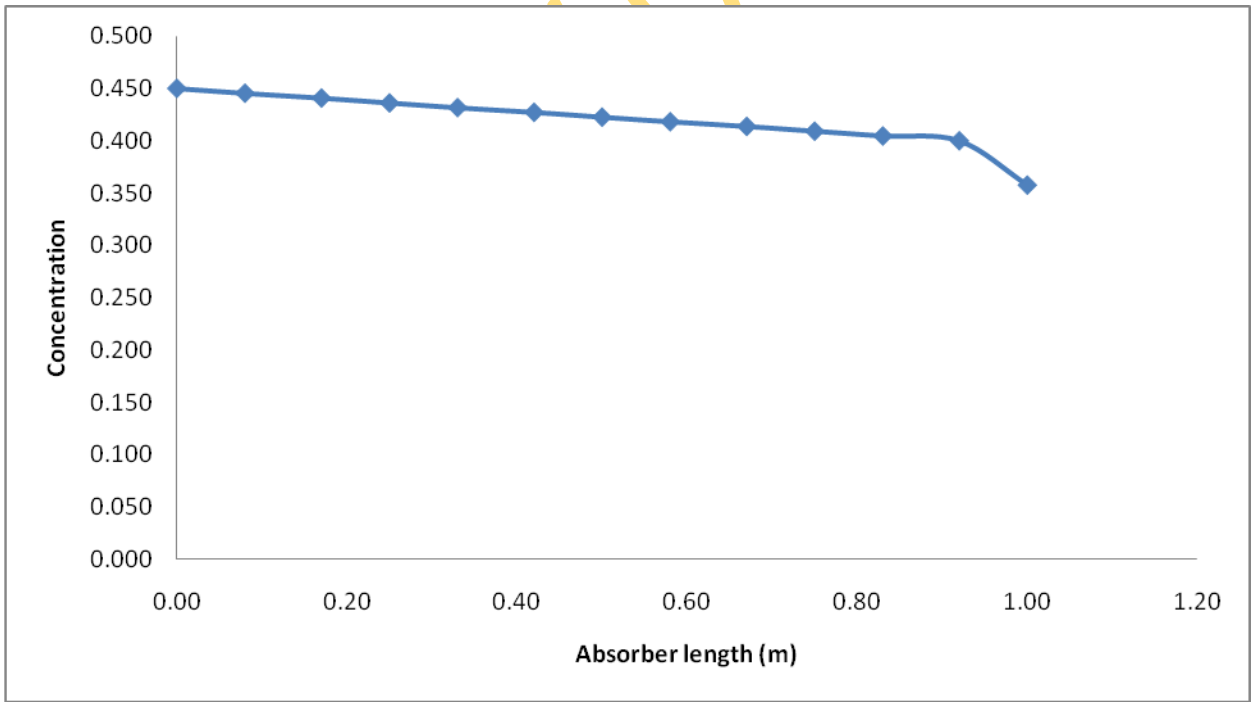

Fig. 4.6.2: Concentration Distribution in the Film at 3.0 Tesla

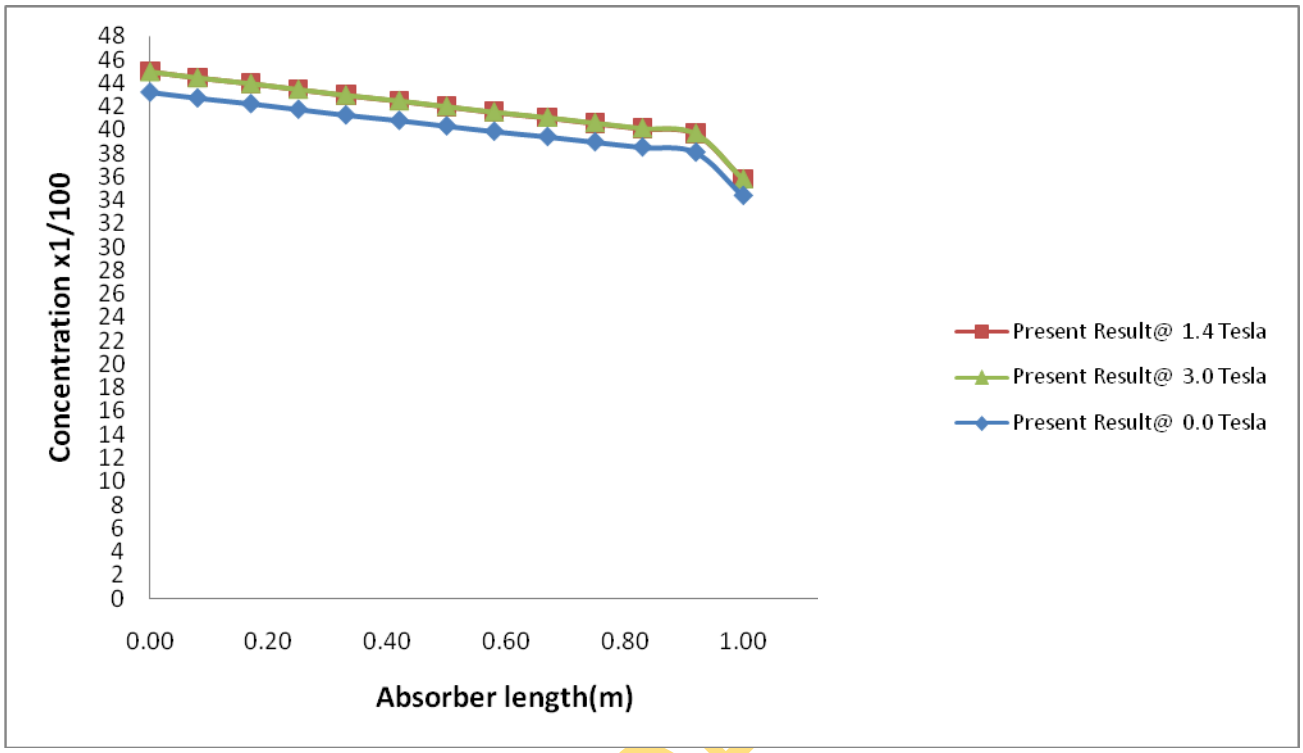

Fig. 4.6.3: LiCl-H_2O Concentration Distribution in the film at 0.0 1.4 and 3.0Tesla

Tables 4.2.8 to 4.3.3, 4.3.6, 4.4.1 to 4.4.3, 4.4.8 to 4.4.9 and Figures 4.3.6 to 4.5.2 and 4.5.9 to 4.6.3, 4.7 to 4.7.4 and 4.8.5 to 4.9.2 are the average concentration distribution both within the bulk and the interface along the falling orientation in different magnetic fields for both LiBr and LiCl solution. It can been seen that increase of magnetic induction intensity causes an increase in the concentration of LiBr-water and LiCl-water solution which indicates that magnetic field enhances the absorption process. In addition, the concentration is decreasing constantly along the falling film. The concentration distribution within the bulk and at the interface when compare with the existing literature where it exists or available, it compares well. The percentage deviation within the bulk and interface in LiBr-water solution at 0.0Tesla ranges between -5.16 - 0.07 and -3.13 – 1.18 while for the case of 1.4 and 3.0 Tesla, there was no existing literature results to compare with. For LiCl-water solution, the percentage deviation ranges between -6.18 to 2.30 and 0.0-12.50 respectively with no existing literature results available for comparison in the case of 1.4 and 3.0 Tesla.

For LiBr-H_2O, when magnetic intensity increases from 0 to 1.4Tesla, the percentage concentration changes within the bulk in the X-direction is from 0.0 to 0.064 at the end of the absorber. When the magnetic intensity increases from 0.0 to 3.0 Tesla, percentage concentration

UNIVERSITY OF

increases from 0.0 to 0.284 at the end of the absorber. For LiCl-water solution, when magnetic intensity increases from 0 to 1.4Tesla, the percentage concentration changes within the bulk in the X-direction is from 0.0 to 0.078 at the end of the absorber. When the magnetic intensity increased from 0 to 3.0Tesla, percentage concentration increases from 0.0 to 0.293 at the end of the absorber length. This observation accounts for the condensation of the refrigerant vapour towards the end of the absorber length.

Table 4.3.7: LiCl-H_2O Velocity Distribution in the film

Absorber length X (m)	**Interface**								
	Lit. Result @ 0.0 Tesla	**Present Result @ 0.0 Tesla**	**% Devia -tion**	**Lit. Result @ 1.4 Tesla**	**Present. Result @ 1.4 Tesla**	**% Devia-tion**	**Lit. Result @ 3.0 Tesla**	**Present Result @3.0 Tesla**	**% Devia-tion**
0 or 10^{-6}	N/A	0.3620		N/A	0.3620		N/A	0.3620	
$10^{-5.5}$	"	0.3662		"	0.3671		"	0.3702	
10^{-5}	"	0.3662		"	0.3671		"	0.3702	
$10^{-4.5}$	"	0.3662		"	0.3671		"	0.3702	
10^{-4}	"	0.3662		"	0.3671		"	0.3702	
$10^{-3.5}$	"	0.3662		"	0.3671		"	0.3702	
10^{-3}	"	0.3662		"	0.3671		"	0.3702	
$10^{-2.5}$	"	0.3662		"	0.3671		"	0.3702	
10^{-2}	"	0.3662		"	0.3671		"	0.3702	

UNIVERSITY OF IBADAN

$10^{-1.5}$	"	0.3662		"	0.3671		"	0.3702	
10^{-1}	"	0.3662		"	0.3671		"	0.3702	
$10^{-0.5}$	"	0.3662		"	0.3671		"	0.3702	
10^{0}	N/A	0.4050		N/A	0.4060		N/A	0.4060	

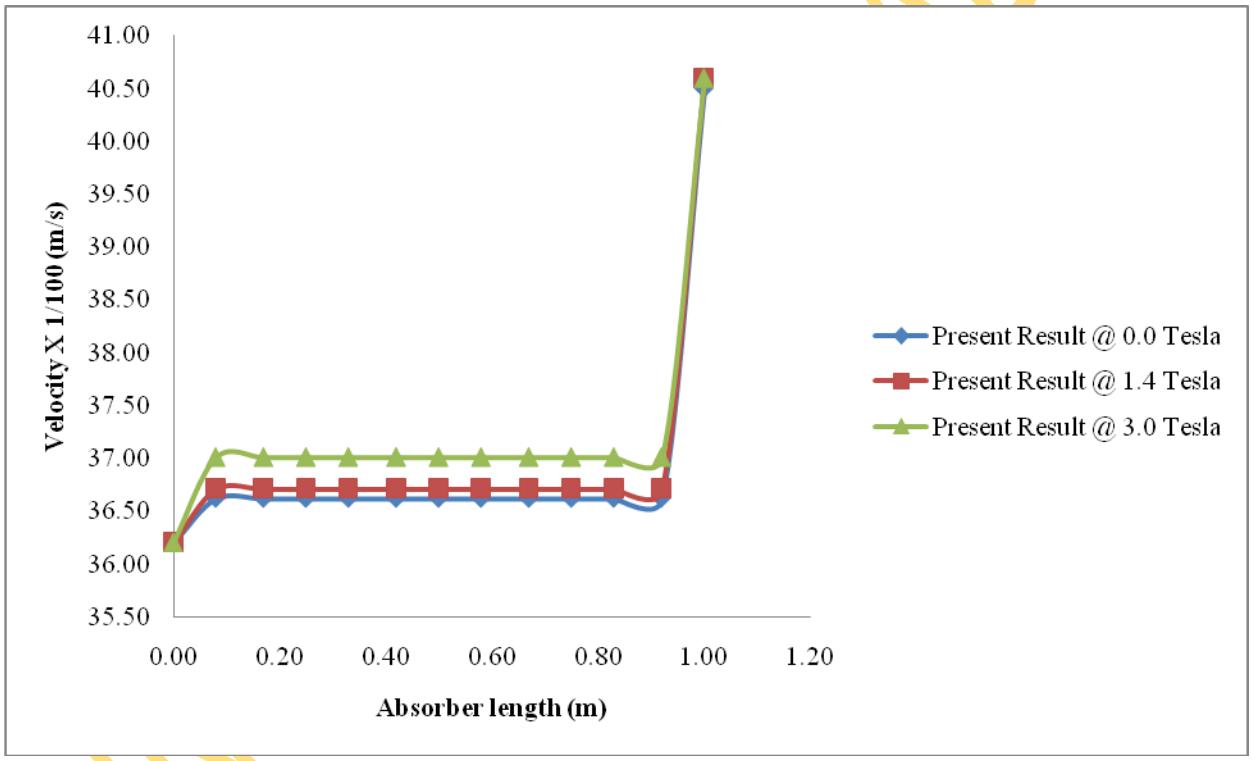

Fig. 4.6.4: Velocity Distribution at the Interface

Table 4.3.8: LiCl-H_2O Temperature Distribution in Comparison at the interface

Absorber length X (m)	Interface								
	Lit. Result @ 0.0 Tesla * **	**Present Result @ 0.0 Tesla**	**% Devia-tion**	**Lit. Result @ 1.4 Tesla**	**Present. Result @ 1.4 Tesla**	**% Devia-tion**	**Lit. Result @ 3.0 Tesla**	**Present Result @3.0 Tesla**	**% Devia-tion**
0 or 10^{-6}	36.00	35.00	-2.78	N/A	35.00		N/A	35.00	
$10^{-5.5}$	36.25	38.25	5.52	"	38.25		"	38.25	
10^{-5}	37.00	37.50	1.35	"	37.50		"	37.50	
$10^{-4.5}$	37.60	36.75	-2.26	"	36.75		"	36.75	
10^{-4}	38.00	36.00	-5.26	"	36.00		"	36.00	
$10^{-3.5}$	38.20	35.25	-7.72	"	35.25		"	35.25	
10^{-3}	38.20	34.50	-9.69	"	34.50		"	34.50	
$10^{-2.5}$	37.00	33.75	-8.78	N/A	33.75		N/A	33.75	
10^{-2}	36.00	33.00	-8.33	"	33.00		"	33.00	
$10^{-1.5}$	34.50	32.25	-6.52	"	32.25		"	32.25	
10^{-1}	33.00	31.50	-4.55	"	31.50		"	31.50	
$10^{-0.5}$	31.90	30.75	-3.61	"	30.75		"	30.75	
10^{0}	30.00	30.00	0.00	N/A	30.00		N/A	30.00	

*** Yang et al.(1992)

UNIVERSITY OF IBADAN

Table 4.3.9: LiCl-H_2O Temperature Deviation Analysis at the Bulk and Interface

	BULK			INTERFACE		
Absorber length X (m)	**Lit. Result @ 0.0 Tesla *** **	**Present Result @ 0.0 Tesla**	**Deviation.**	**Lit. Result @ 0.0 Tesla*** **	**Present Result @ 0.0 Tesla**	**Deviation.**
0 or 10^{-6}	35.00	35.00	0.00	36.00	35.00	1.00
$10^{-5.5}$	35.00	34.74	0.26	36.25	38.25	-2.03
10^{-5}	35.00	34.49	0.51	37.00	37.50	-0.50
$10^{-4.5}$	35.00	34.23	0.77	37.60	36.75	0.85
10^{-4}	35.00	33.98	1.02	38.00	36.00	2.00
$10^{-3.5}$	35.00	33.73	1.27	38.20	35.25	2.95
10^{-3}	35.00	33.48	1.52	38.20	34.50	3.70
$10^{-2.5}$	34.80	33.24	1.56	37.00	33.75	3.25
10^{-2}	33.90	32.99	0.91	36.00	33.00	3.00
$10^{-1.5}$	32.10	32.75	-0.65	34.50	32.25	2.25
10^{-1}	32.00	32.51	-0.51	33.00	31.50	1.50
$10^{-0.5}$	31.50	32.27	0.77	31.90	30.75	1.15
10^{0}	30.00	30.00	0.00	30.00	30.00	0.00

*** Yang et al.(1992)

UNIVERSITY OF IBADAN

Table 4.4: LiCl-H_2O Temperature Deviation Analysis at the Bulk and Interface

	BULK @ 0.0 Tesla			INTERFACE @ 0.0 Tesla		
Absorber length X (m)	**Deviation.**	**Mean Deviation**	**Mean Deviation. Square**	**Deviation.**	**Mean Deviation**	**Mean Deviation. Square**
0 or 10^{-6}	0.00	0.5715	0.33	1.00	1.4708	0.22
$10^{-5.5}$	0.26	0.5715	0.10	-2.03	1.4708	12.26
10^{-5}	0.51	0.5715	0.00	-0.50	1.4708	3.88
$10^{-4.5}$	0.77	0.5715	0.04	0.85	1.4708	0.39
10^{-4}	1.02	0.5715	0.20	2.00	1.4708	0.28
$10^{-3.5}$	1.27	0.5715	0.49	2.95	1.4708	2.19
10^{-3}	1.52	0.5715	0.90	3.70	1.4708	4.97
$10^{-2.5}$	1.56	0.5715	0.98	3.25	1.4708	3.17
10^{-2}	0.91	0.5715	0.11	3.00	1.4708	2.34
$10^{-1.5}$	-0.65	0.5715	1.49	2.25	1.4708	0.61
10^{-1}	-0.51	0.5715	1.17	1.50	1.4708	0.00
$10^{-0.5}$	0.77	0.5715	0.04	1.15	1.4708	0.10
10^{0}	0.00	0.5715	0.33	0.00	1.4708	2.16
Σ			**6.17**			**32.56**

@ The Bulk, Std. deviation (σ) $\sqrt{6.17/13}$ **= 0.69**

@ The Interface, Std. deviation (σ) $\sqrt{32.56/13}$ **= 1.58**

UNIVERSITY OF IBADAN

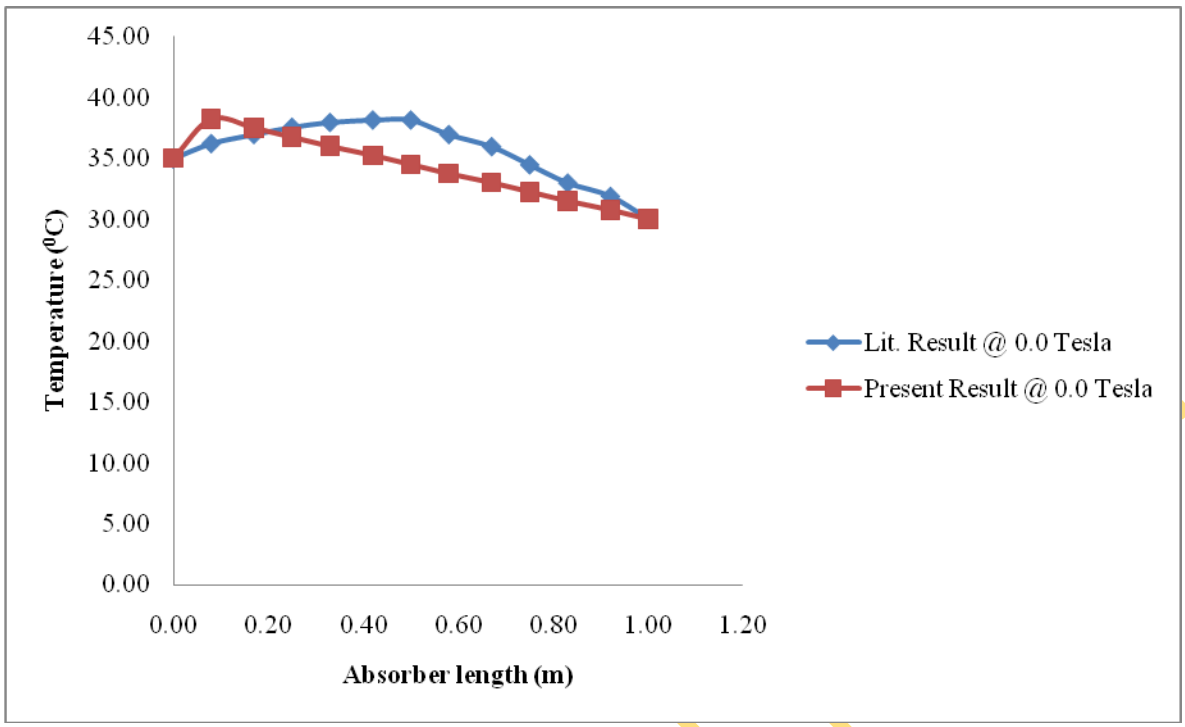

Fig 4.6.5: Temperature Distribution at the Interface Comparison at 0.0Tesla

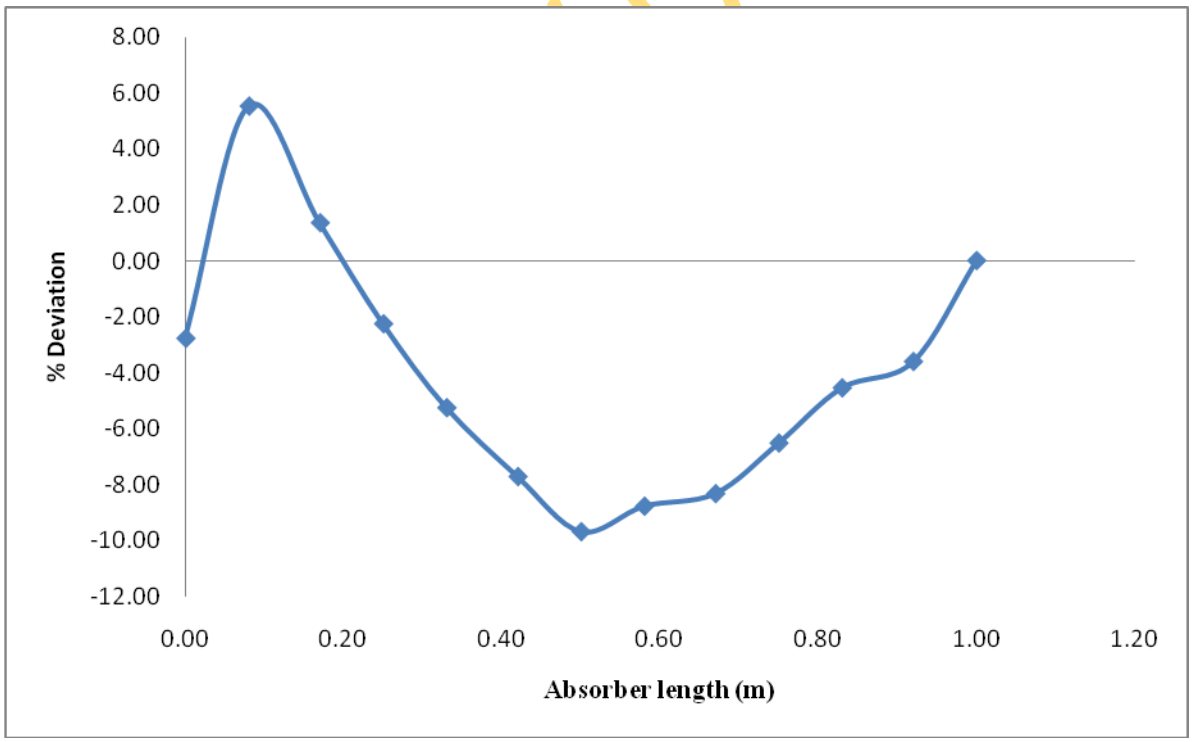

Fig 4.6.6: % deviation Temperature Distribution at the Interface at 0.0Tesla

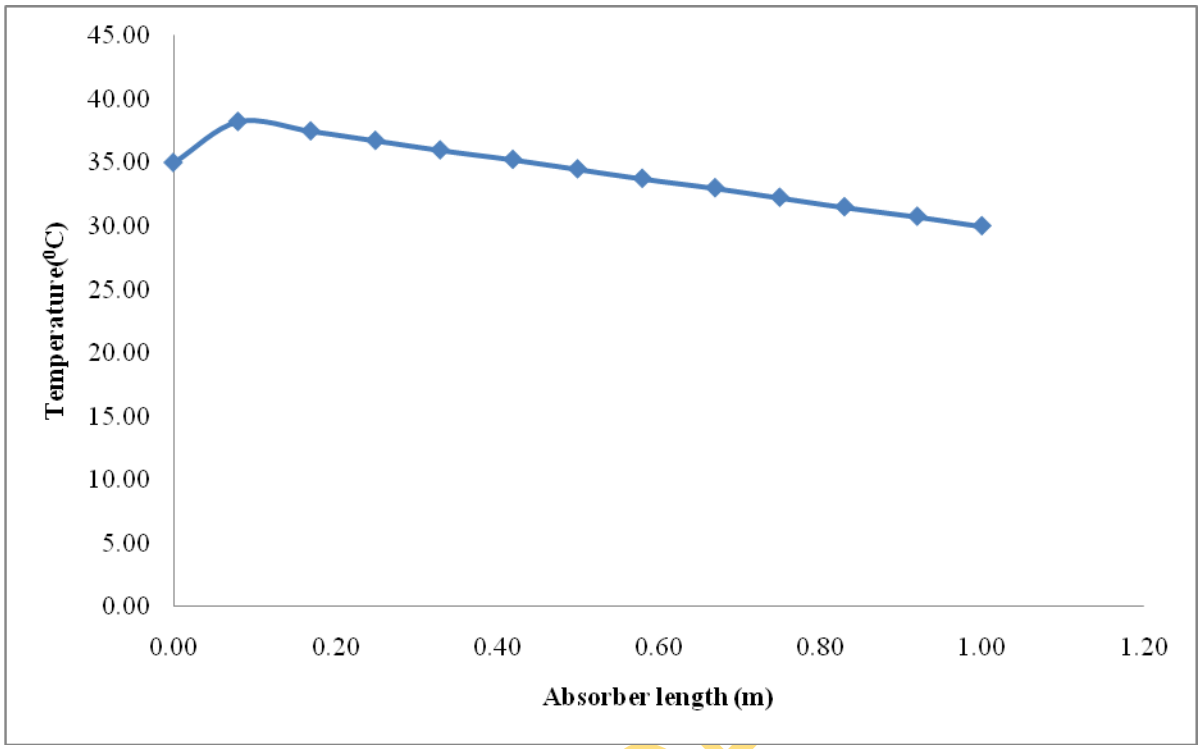

Fig. 4.6.7: **LiCl-H_2O** Temperature Distribution at the Interface at 1.4Tesla

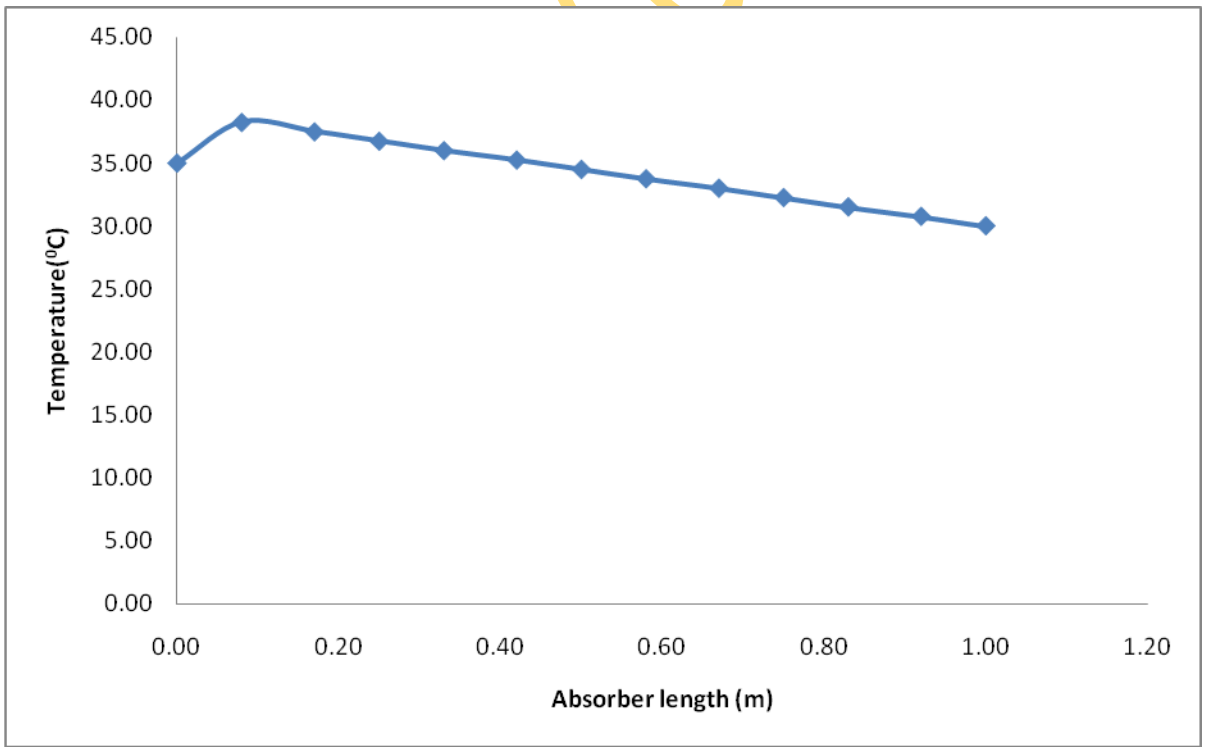

Fig. 4.6.8: **LiCl-H_2O** Temperature Distribution at the Interface at 3.0 Tesla

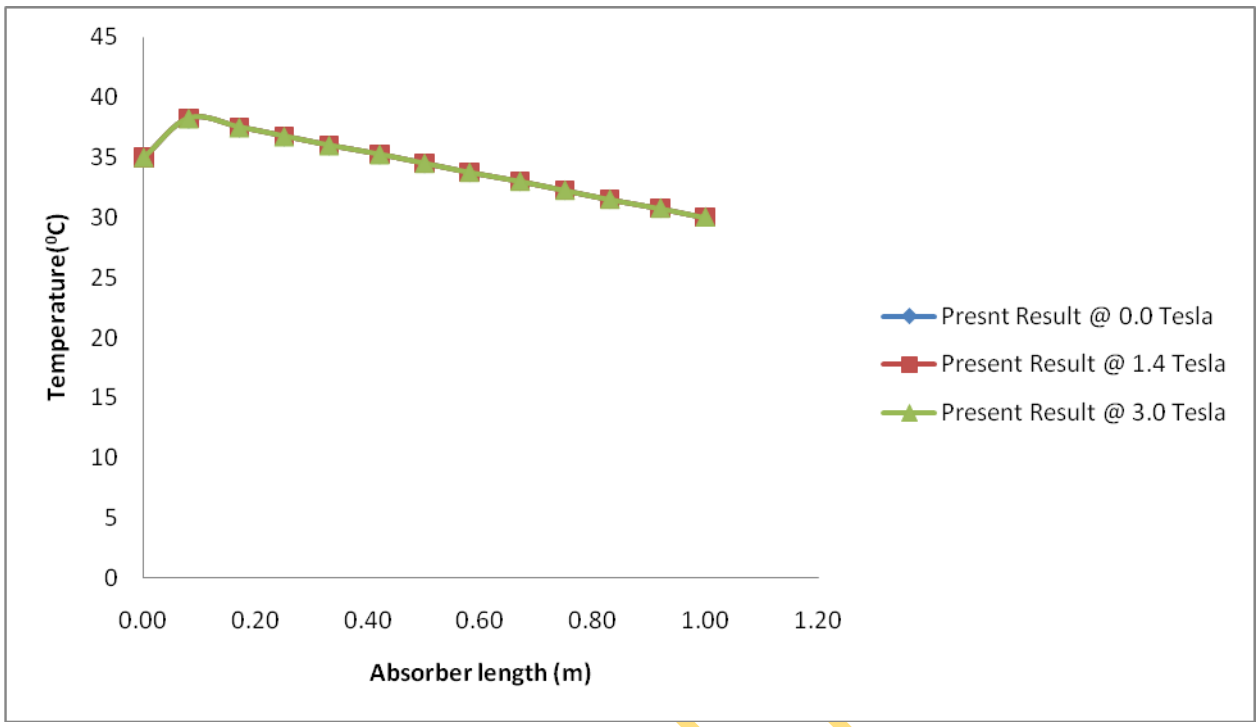

Fig.4.6.9: **LiCl-H_2O** Temperature Distribution at the interface at 0.0, 1.4 and 3.0Tesla

Table 4.4.1: LiCl-H_2O Concentration Distribution in the film Comparison

Absorber length X (m)	**Interface**								
	Lit. Result @ 0.0 Tesla ***	**Present Result @ 0.0 Tesla**	**% Devia-tion**	**Lit. Result @ 1.4 Tesla**	**Present. Result @ 1.4 Tesla**	**% Devia-tion**	**Lit. Result @ 3.0 Tesla**	**Present Result @3.0 Tesla**	**% Devia-tion**
0 or 10^{-6}	0.400	0.450	12.50	N/A	0.4500		N/A	0.4500	
$10^{-5.5}$	0.402	0.44486	10.66	"	0.44487		"	0.44491	
10^{-5}	0.405	0.43978	8.59	"	0.43980		"	0.43989	
$10^{-4.5}$	0.410	0.43476	6.04	"	0.43479		"	0.43492	
10^{-4}	0.414	0.42979	3.81	"	0.42984		"	0.43000	
$10^{-3.5}$	0.414	0.42488	2.63	"	0.42494		"	0.42514	

UNIVERSITY OF

10^{-3}	0.414	0.42003	1.46	"	0.42010		"	0.42034	
$10^{-2.5}$	0.400	0.41523	3.81	"	0.41531		"	0.41559	
10^{-2}	0.390	0.41049	5.25	"	0.41058		"	0.41089	
$10^{-1.5}$	0.380	0.40580	6.79	"	0.40590		"	0.40625	
10^{-1}	0.370	0.40116	8.42	"	0.40128		"	0.40166	
$10^{-0.5}$	0.365	0.39658	8.65	"	0.39671		"	0.39712	
10^{0}	0.358	0.35800	0.00	N/A	0.35800		N/A	0.35800	

******* Yang et al.(1992)

Table 4.4.2: LiCl-H_2O Concentration Deviation Analysis at the Bulk and Interface

	BULK			**INTERFACE**		
Absorber length X (m)	**Lit. Result @ 0.0 Tesla*****	**Present Result @ 0.0 Tesla**	**Deviation.**	**Lit. Result @ 0.0 Tesla*****	**Present Result @ 0.0 Tesla**	**Deviation.**
0 or 10^{-6}	0.450	0.4500	0.0000	0.400	0.4500	-0.0500
$10^{-5.5}$	0.450	0.4453	0.0047	0.402	0.4449	-0.0428
10^{-5}	0.450	0.4406	0.0095	0.405	0.4398	-0.0347
$10^{-4.5}$	0.450	0.4360	0.0140	0.410	0.4348	-0.0247
10^{-4}	0.450	0.4313	0.0187	0.414	0.4298	-0.0157
$10^{-3.5}$	0.450	0.4267	0.0233	0.414	0.4249	-0.0108
10^{-3}	0.448	0.4221	0.0259	0.414	0.4200	-0.0060
$10^{-2.5}$	0.440	0.4174	0.0226	0.400	0.4152	-0.0152
10^{-2}	0.440	0.4128	0.0272	0.390	0.4105	-0.0204
$10^{-1.5}$	0.430	0.4082	0.0218	0.380	0.4058	-0.0258
10^{-1}	0.420	0.4036	0.0164	0.370	0.4012	-0.0311
$10^{-0.5}$	0.390	0.3990	-0.0090	0.365	0.3966	-0.0315
10^{0}	0.358	0.3580	0.0000	0.358	0.3580	0.0000

*******Yang et al.(1992)

UNIVERSITY OF IBADAN

Table 4.4.3: LiCl-H_2O Concentration Deviation Analysis at the Bulk and Interface

	BULK @ 0.0 Tesla			INTERFACE @ 0.0 Tesla		
Absorber length X (m)	**Deviation.**	**Mean Deviation**	**Mean Deviation. Square X 10^{-4}**	**Deviation.**	**Mean Deviation**	**Mean Deviation. Square X 10^{-4}**
0 or 10^{-6}	0.0000	0.01347	1.81	-0.0500	-0.0237	6.92
$10^{-5.5}$	0.0047	0.01347	0.77	-0.0428	-0.0237	3.65
10^{-5}	0.0095	0.01347	0.16	-0.0347	-0.0237	1.21
$10^{-4.5}$	0.0140	0.01347	0.00	-0.0247	-0.0237	0.01
10^{-4}	0.0187	0.01347	0.27	-0.0157	-0.0237	0.64
$10^{-3.5}$	0.0233	0.01347	0.97	-0.0108	-0.0237	1.66
10^{-3}	0.0259	0.01347	1.55	-0.0060	-0.0237	3.13
$10^{-2.5}$	0.0226	0.01347	0.83	-0.0152	-0.0237	0.72
10^{-2}	0.0272	0.01347	1.89	-0.0204	-0.0237	0.11
$10^{-1.5}$	0.0218	0.01347	0.69	-0.0258	-0.0237	0.04
10^{-1}	0.0164	0.01347	0.09	-0.0311	-0.0237	0.55
$10^{-0.5}$	-0.0090	0.01347	5.05	-0.0315	-0.0237	0.61
10^{0}	0.0000	0.01347	1.81	0.0000	-0.0237	5.62
$\sum$			**15.89**			**24.87**

@ The Bulk, Std. deviation (σ) $\sqrt{15.89x10^{-4}/13}$ **= 1.11 X 10^{-2}**

@ The Interface, Std. deviation (σ) $\sqrt{24.87x10^{-4}/13}$ **= 1.38 X 10^{-2}**

UNIVERSITY OF IBADAN

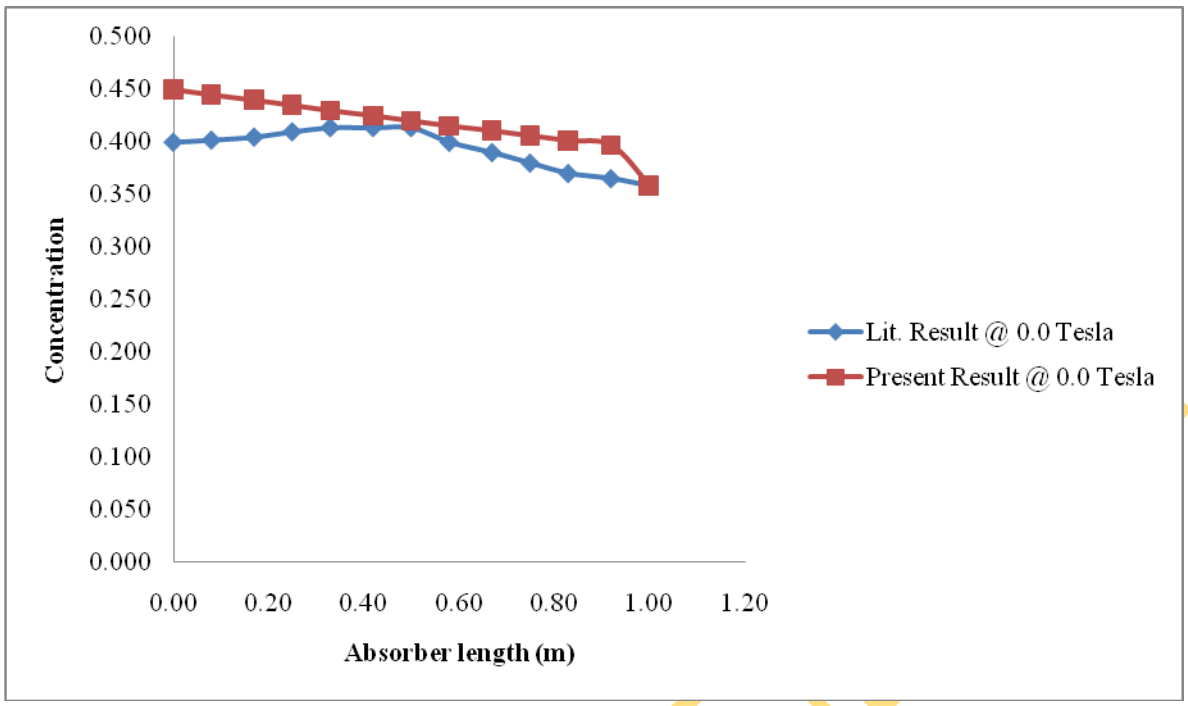

Fig. 4.7: Concentration Distribution at the Interface Comparison at 0.0 Tesla

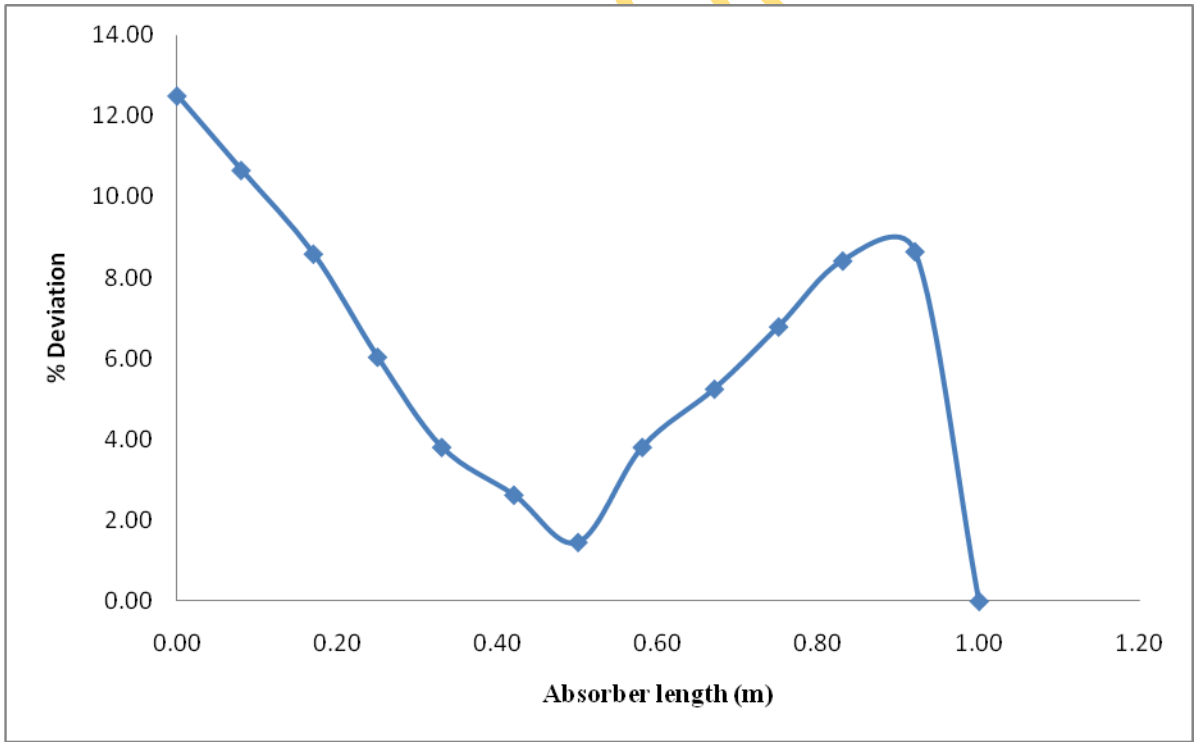

Fig.4.7.1: % Deviation of Concentration at the Interface at 0.0Tesla

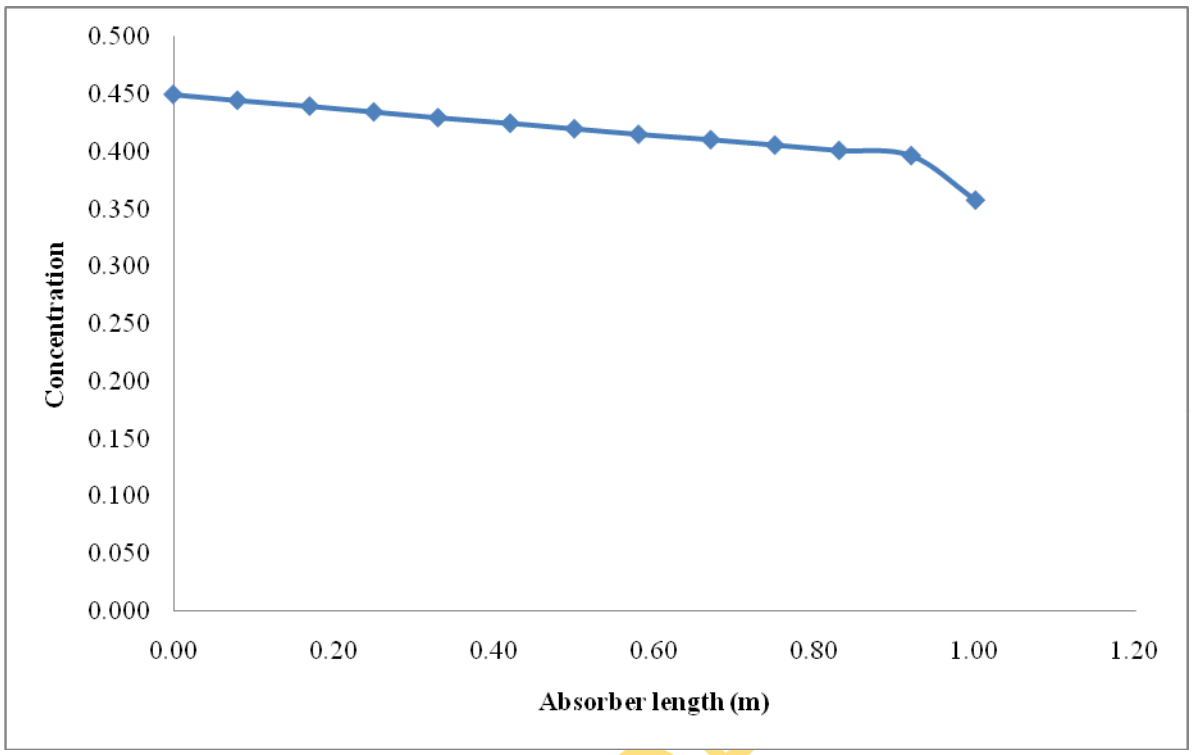

Fig.4.7.2: Concentration Distribution at the Interface at 1.4 Tesla

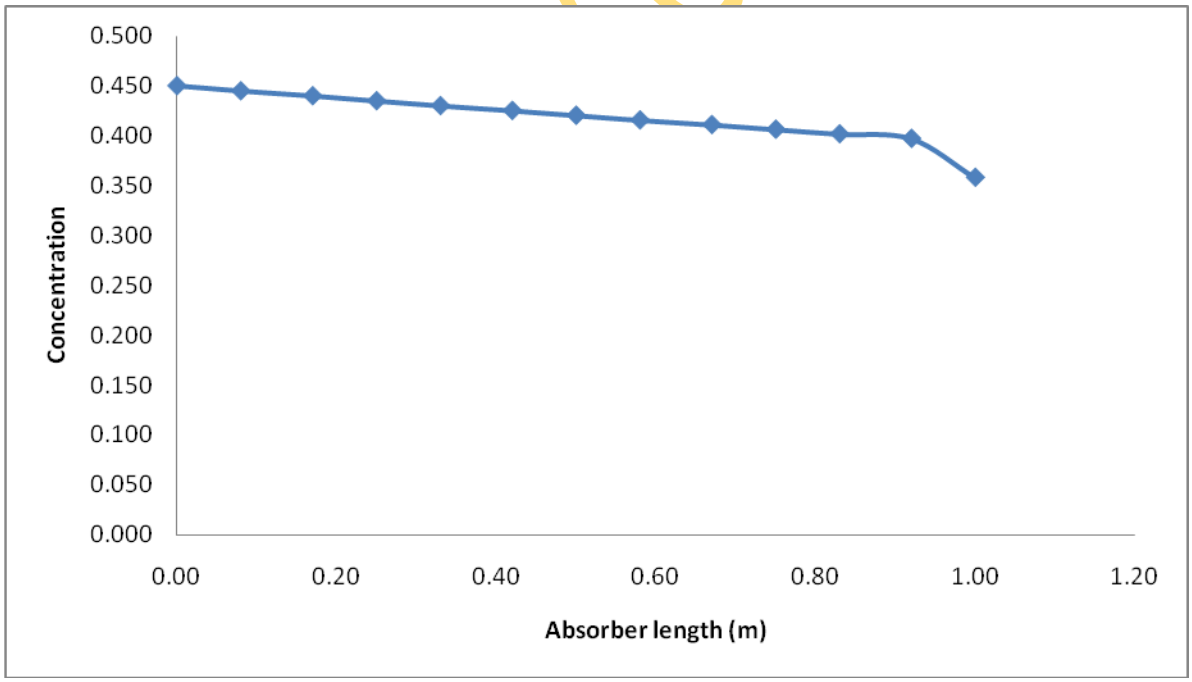

Fig.4.7.3: Concentration Distribution at the Interface at 3.0 Tesla

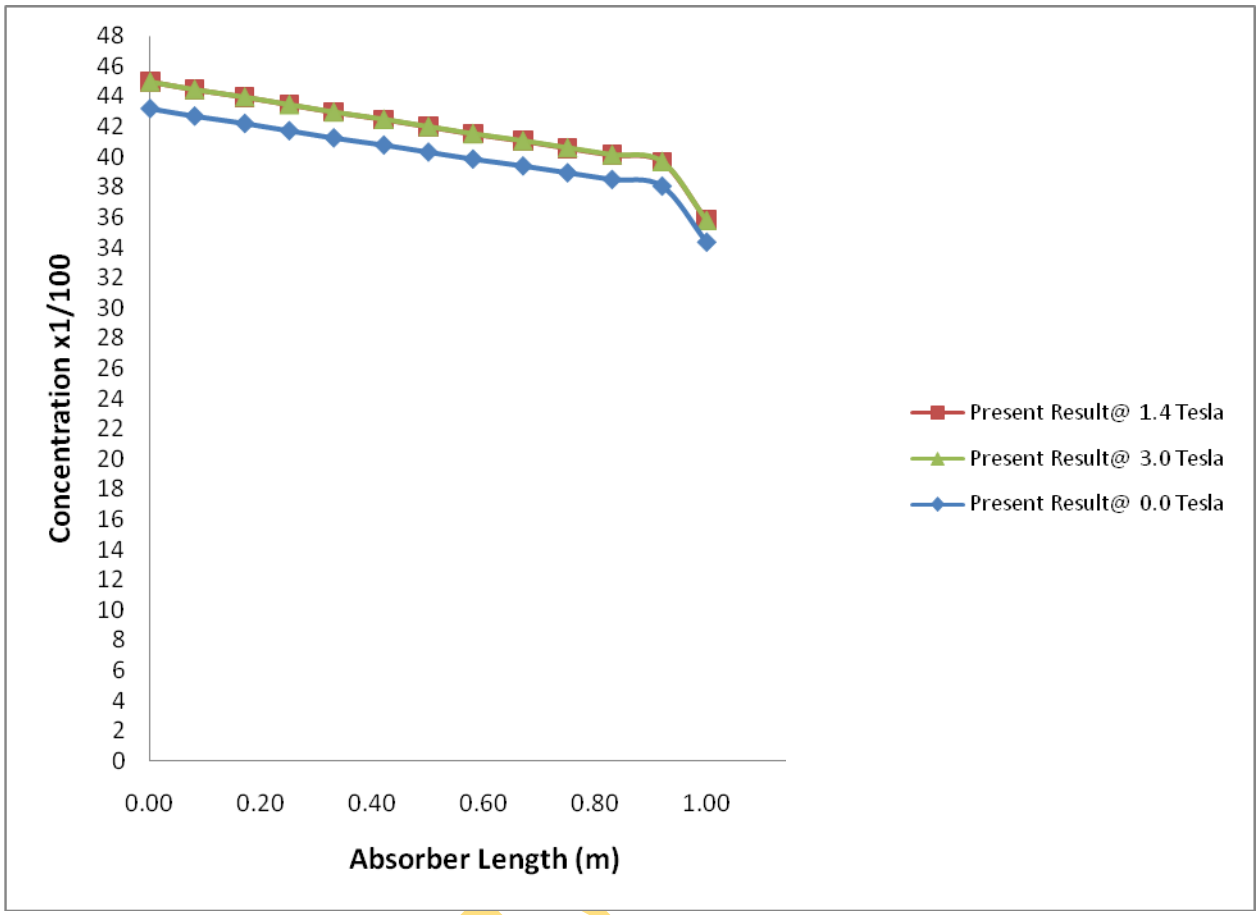

Fig. 4.7.4: LiCl-H_2O Concentration Distribution at the Interface at 0.0 1.4 and 3.0Tesla

Temperature Distribution within the bulk at various magnetic intensity

As seen in Tables 4.2.4 to 4.2.7, 4.3.5, 4.3.8 to 4.4, 4.4.6 to 4.4.7 couple with Figs 4.2.6 to 4.3.5, 4.5.4 to 4.5.8, 4.6.5 to 4.6.9 and 4.8.3 to 4.8.4 the average temperature changes varies very slightly with various values of the magnetic induction, and the temperature of solution film is higher at the inlet than within the bulk at the beginning of absorption process. For the case of LiBr-H_2O the driving force of mass transfer is relatively greater at the inlet of solution, a great amount of absorbing heat is generated. On the other hand, the cooling water's temperature is higher at the inlet of solution because of counter current flow. Both these contribute to the higher temperature at the entrance of falling solution. The temperature distribution within the bulk and interface for the two working fluids under consideration when compare with the existing available literature results, compare well. The percentage deviation for LiBr-H_2O at 0.0Tesla ranges from -1.12-6.56 in the bulk and -6.93 – 2.36 at the interface while at 1.4 and 3.0 Tesla there was no existing literature results for comparison. For LiCl-H_2O at 0.0 Tesla percentage

deviation ranges from -4.48 to 2.44 in the bulk and -9.69 to 5.52 at the interface while at 1.4 and 3.0 Tesla, there was also no existing literature results both experimental and numerical for comparison with. For both LiBr-H_2O and LiCl-H_2O solution, there was no percentage temperature change in X-direction at both the bulk and interface.

Table 4.4.4: LiCl-H_2O Velocity Changes within the film in X-direction, X = Absorber length.

Absorber length X (m)	Bulk					
	Present Result @ 0.0 Tesla	**Present. Result @ 1.4 Tesla**	**% Changes in X-dir**	**Present Result @ 0.0 Tesla**	**Present Result @3.0 Tesla**	**% Changes in X-dir**
0 or 10^{-6}	0.3620	0.3620	0.00	0.3620	0.3620	0.00
$10^{-5.5}$	0.3662	0.3671	0.26	0.3662	0.3702	1.09
10^{-5}	0.3702	0.3719	0.46	0.3702	0.3775	1.96
$10^{-4.5}$	0.3742	0.3765	0.62	0.3742	0.3840	2.63
10^{-4}	0.3780	0.3808	0.74	0.3780	0.3897	3.09
$10^{-3.5}$	0.3818	0.3849	0.82	0.3818	0.3946	3.36
10^{-3}	0.3854	0.3887	0.85	0.3854	0.3987	3.44
$10^{-2.5}$	0.3889	0.3922	0.85	0.3889	0.4019	3.34
10^{-2}	0.3924	0.3955	0.80	0.3924	0.4044	3.06
$10^{-1.5}$	0.3957	0.3985	0.72	0.3957	0.4060	2.61
10^{-1}	0.3989	0.4013	0.60	0.3989	0.4068	1.99
$10^{-0.5}$	0.4020	0.4038	0.44	0.4020	0.4068	1.20
10^{0}	0.4050	0.4060	0.25	0.4050	0.4060	0.25

UNIVERSITY OF IBADAN

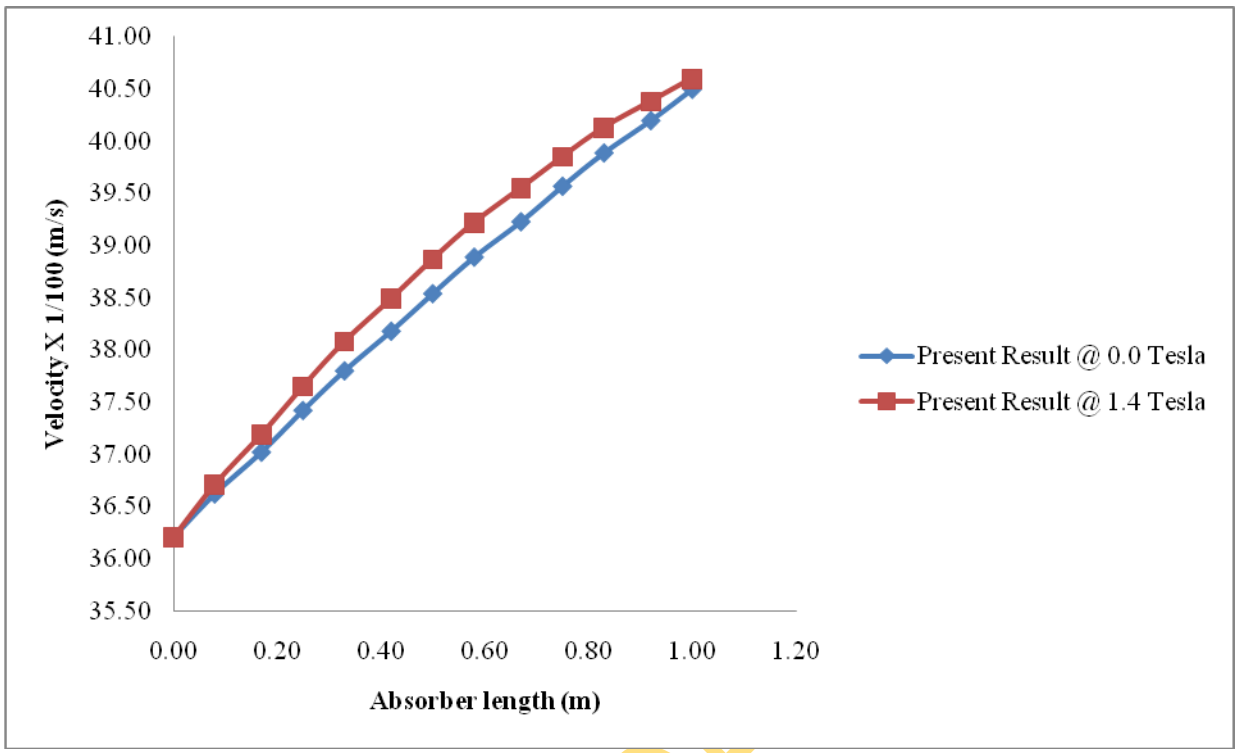

Fig. 4.7.5: Velocity Changes within the Film in X-direction at 0.0 &1.4Tesla, X = Absorber length.

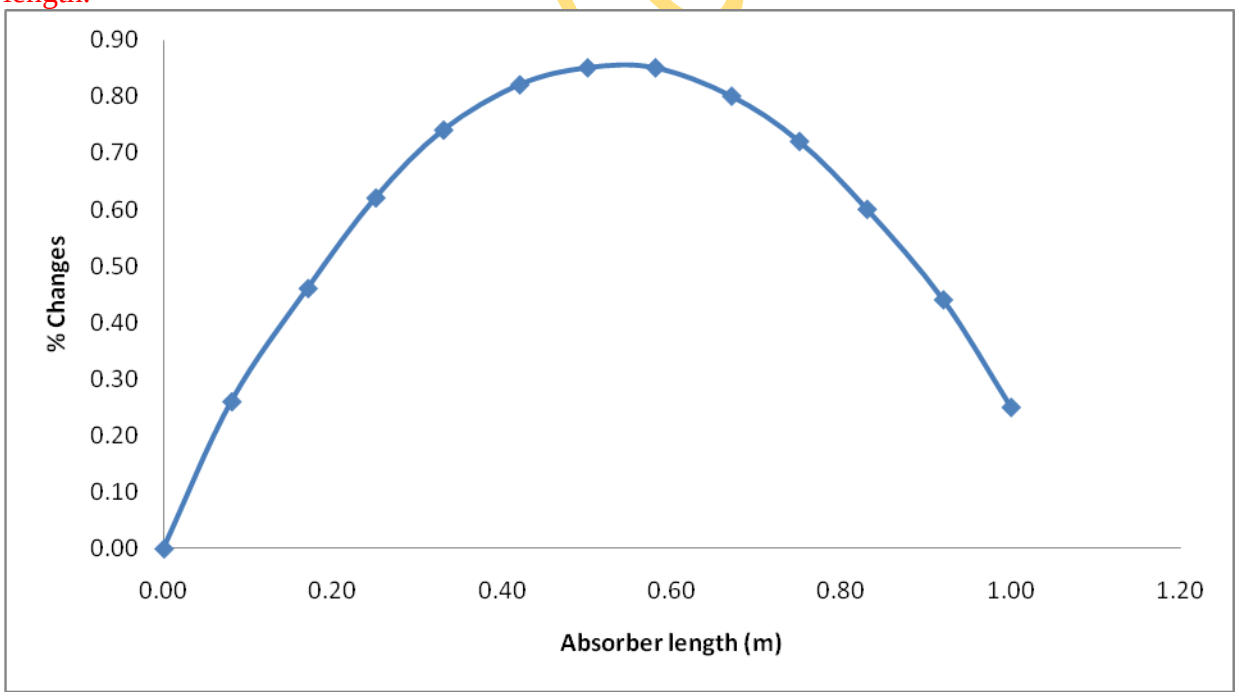

Fig.4.7.6: % Velocity Changes within the Film in X-direction from 0.0 to 1.4Tesla, X = Absorber length.

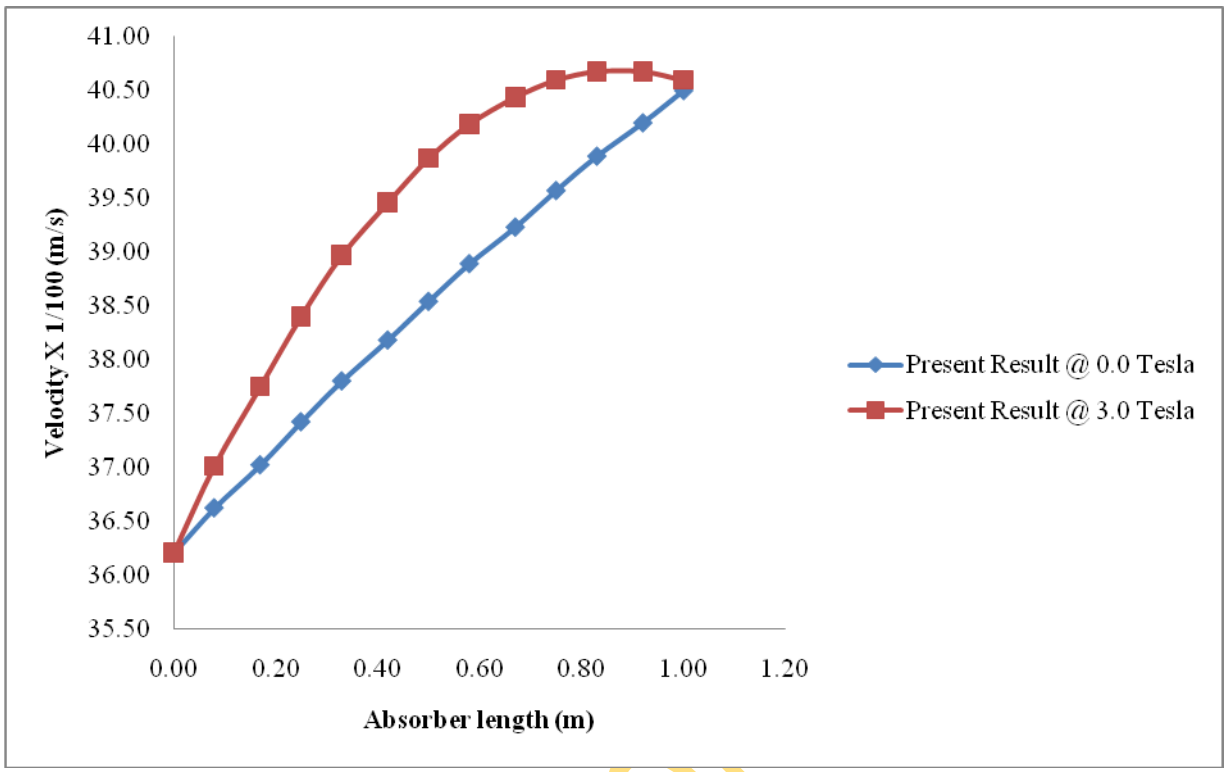

Fig.4.7.7: Velocity Changes within the Film in X-direction at 0.0 & 3.0 Tesla, X = Absorber length.

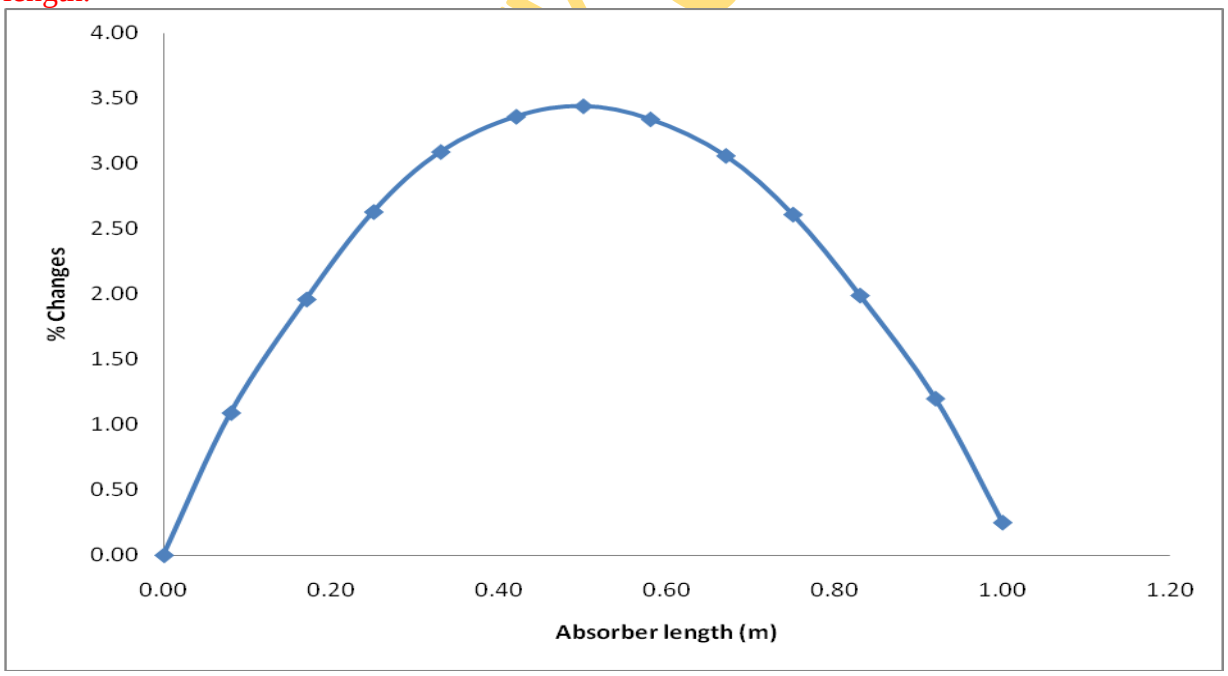

Fig.4.7.8: % Velocity Changes within the Film in X-direction at 0.0 & 3.0Tesla, X = Absorber length.

Table 4.4.5: LiCl-H_2O Velocity Changes within the film in X-direction, X = Absorber length.

Absorber length X (m)	Interface					
	Present Result @ 0.0 Tesla	Present. Result @ 1.4 Tesla	% Changes in X-dir	Present Result @ 0.0 Tesla	Present Result @3.0 Tesla	% Changes in X-dir
0 or 10^{-6}	0.3620	0.3620	0.00	0.3620	0.3620	0.00
$10^{-5.5}$	0.3662	0.3671	0.26	0.3662	0.3702	1.10
10^{-5}	0.3662	0.3671	0.26	0.3662	0.3702	1.10
$10^{-4.5}$	0.3662	0.3671	0.26	0.3662	0.3702	1.10
10^{-4}	0.3662	0.3671	0.26	0.3662	0.3702	1.10
$10^{-3.5}$	0.3662	0.3671	0.26	0.3662	0.3702	1.10
10^{-3}	0.3662	0.3671	0.26	0.3662	0.3702	1.10
$10^{-2.5}$	0.3662	0.3671	0.26	0.3662	0.3702	1.10
10^{-2}	0.3662	0.3671	0.26	0.3662	0.3702	1.10
$10^{-1.5}$	0.3662	0.3671	0.26	0.3662	0.3702	1.10
10^{-1}	0.3662	0.3671	0.26	0.3662	0.3702	1.10
$10^{-0.5}$	0.3662	0.3671	0.26	0.3662	0.3702	1.10
10^{0}	0.4050	0.4060	0.25	0.4050	0.4060	0.25

UNIVERSITY OF IBADAN

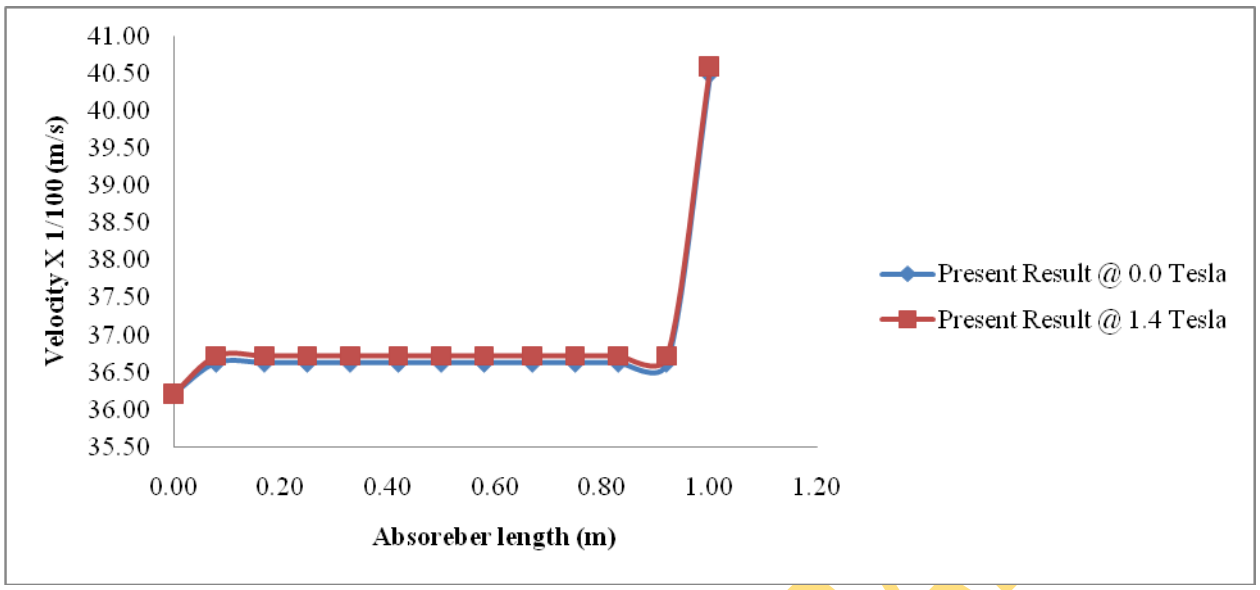

Fig4.7.9: Velocity Changes at the Interface in X-direction at 0.0 & 1.4 Tesla, X = Absorber length.

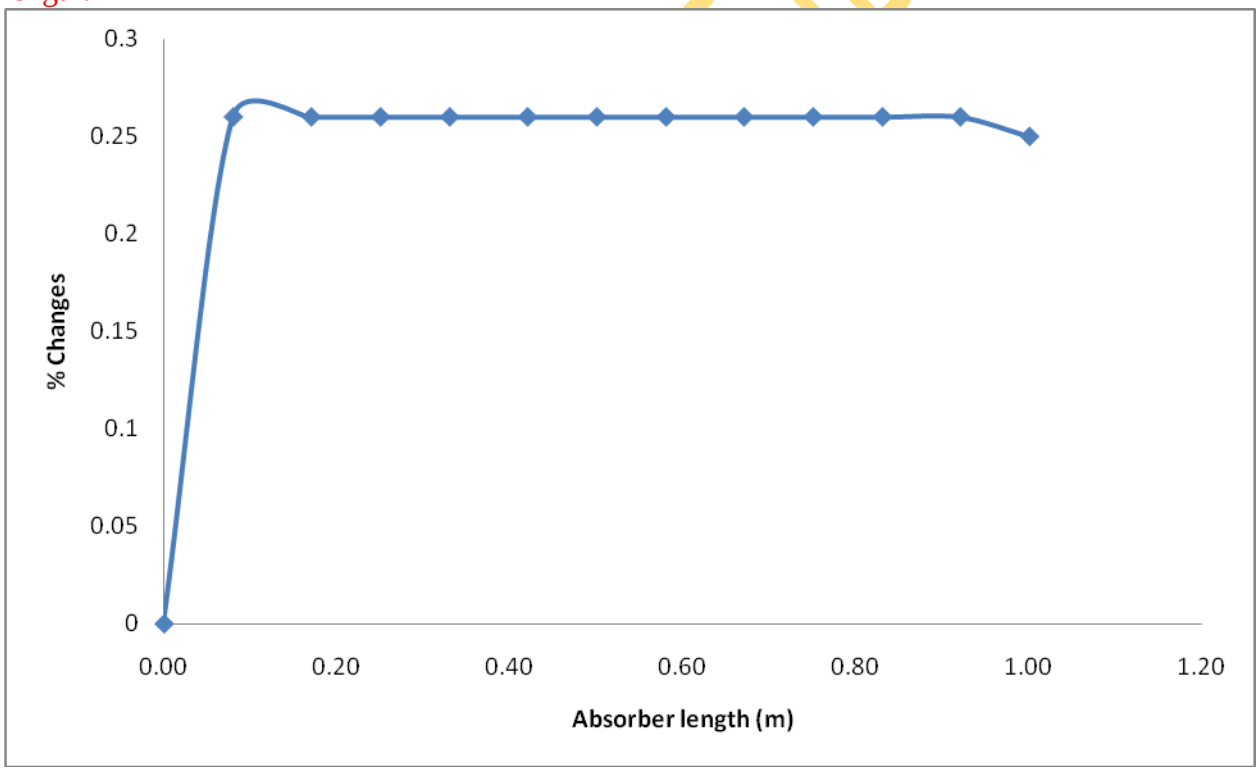

Fig 4.8: % Velocity Changes at the Interface in X-direction at 0.0 & 1.4Tesla, X = Absorber length.

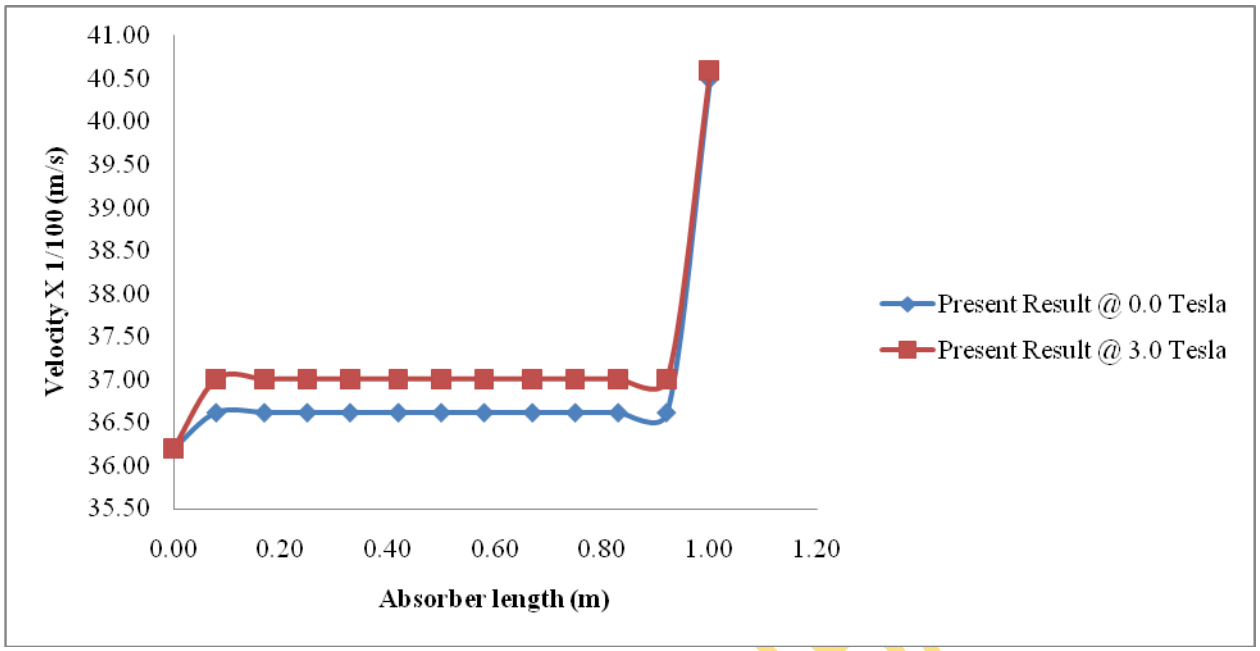

Fig 4.8.1: Velocity Changes at the Interface in X-direction at 0.0 & 3.0Tesla, X = Absorber length.

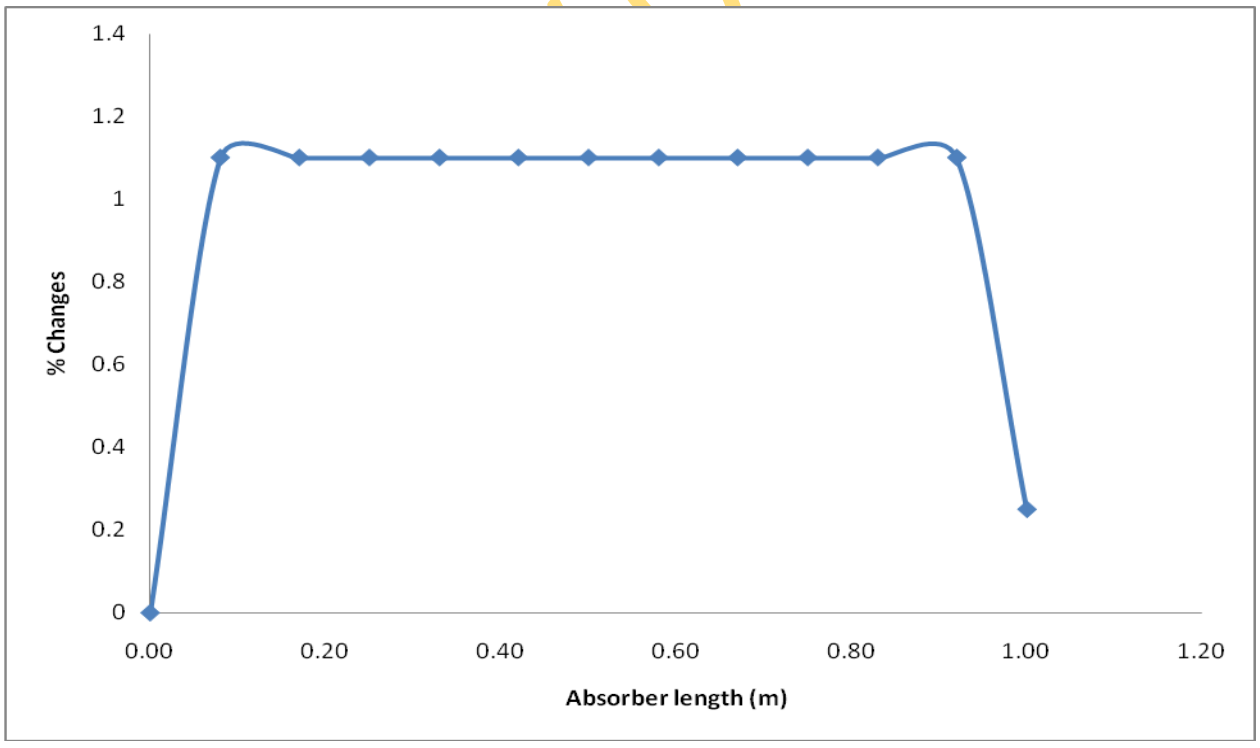

Fig 4.8.2: % Velocity Changes at the Interface in X-direction at 0.0 & 3.0 Tesla, X = Absorber length.

Table 4.4.6: LiCl-H_2O Temperature Changes within the film in X-direction, X = Absorber length.

Absorber length X (m)	Bulk					
	Present Result @ 0.0 Tesla	Present. Result @ 1.4 Tesla	% Changes in X-dir	Present Result @ 0.0 Tesla	Present Result @3.0 Tesla	% Changes in X-dir
0 or 10^{-6}	35.00	35.00	0.00	35.00	35.00	0.00
$10^{-5.5}$	34.74	34.74	0.00	34.74	34.74	0.00
10^{-5}	34.49	34.49	0.00	34.49	34.49	0.00
$10^{-4.5}$	34.23	34.23	0.00	34.23	34.23	0.00
10^{-4}	33.98	33.98	0.00	33.98	33.98	0.00
$10^{-3.5}$	33.73	33.73	0.00	33.73	33.73	0.00
10^{-3}	33.48	33.48	0.00	33.48	33.48	0.00
$10^{-2.5}$	33.24	33.24	0.00	33.24	33.24	0.00
10^{-2}	32.99	32.99	0.00	32.99	32.99	0.00
$10^{-1.5}$	32.75	32.75	0.00	32.75	32.75	0.00
10^{-1}	32.51	32.51	0.00	32.51	32.51	0.00
$10^{-0.5}$	32.27	32.27	0.00	32.27	32.27	0.00
10^{0}	30.00	30.00	0.00	30.00	30.00	0.00

UNIVERSITY OF IBADAN

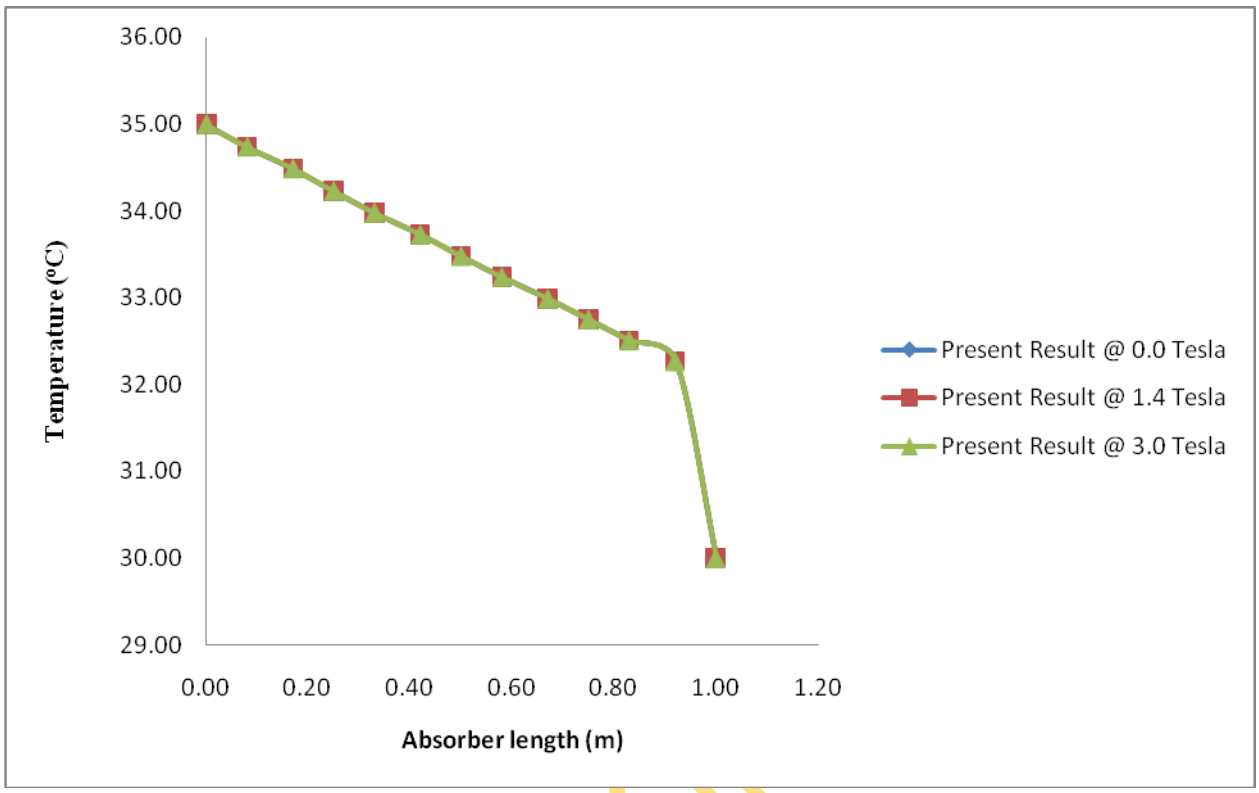

Fig. 4.8.3: Graph of Temperature Changes within the Film in X-direction, X = Absorber length.

Table 4.4.7: LiBr-H_2O Temperature Changes within the film in X-direction, X = Absorber length.

Absorber length X (m)	Interface					
	Present Result @ 0.0 Tesla	**Present. Result @ 1.4 Tesla**	**% Changes in X-dir**	**Present Result @ 0.0 Tesla**	**Present Result @3.0 Tesla**	**% Changes in X-dir**
0 or 10^{-6}	35.00	35.00	0.00	35.00	35.00	0.00
$10^{-5.5}$	38.25	38.25	0.00	38.25	38.25	0.00
10^{-5}	37.50	37.50	0.00	37.50	37.50	0.00
$10^{-4.5}$	36.75	36.75	0.00	36.75	36.75	0.00
10^{-4}	36.00	36.00	0.00	36.00	36.00	0.00
$10^{-3.5}$	35.25	35.25	0.00	35.25	35.25	0.00

UNIVERSITY OF

10^{-3}	34.50	34.50	0.00	34.50	34.50	0.00
$10^{-2.5}$	33.75	33.75	0.00	33.75	33.75	0.00
10^{-2}	33.00	33.00	0.00	33.00	33.00	0.00
$10^{-1.5}$	32.25	32.25	0.00	32.25	32.25	0.00
10^{-1}	31.50	31.50	0.00	31.50	31.50	0.00
$10^{-0.5}$	30.75	30.75	0.00	30.75	30.75	0.00
10^{0}	30.00	30.00	0.00	30.00	30.00	0.00

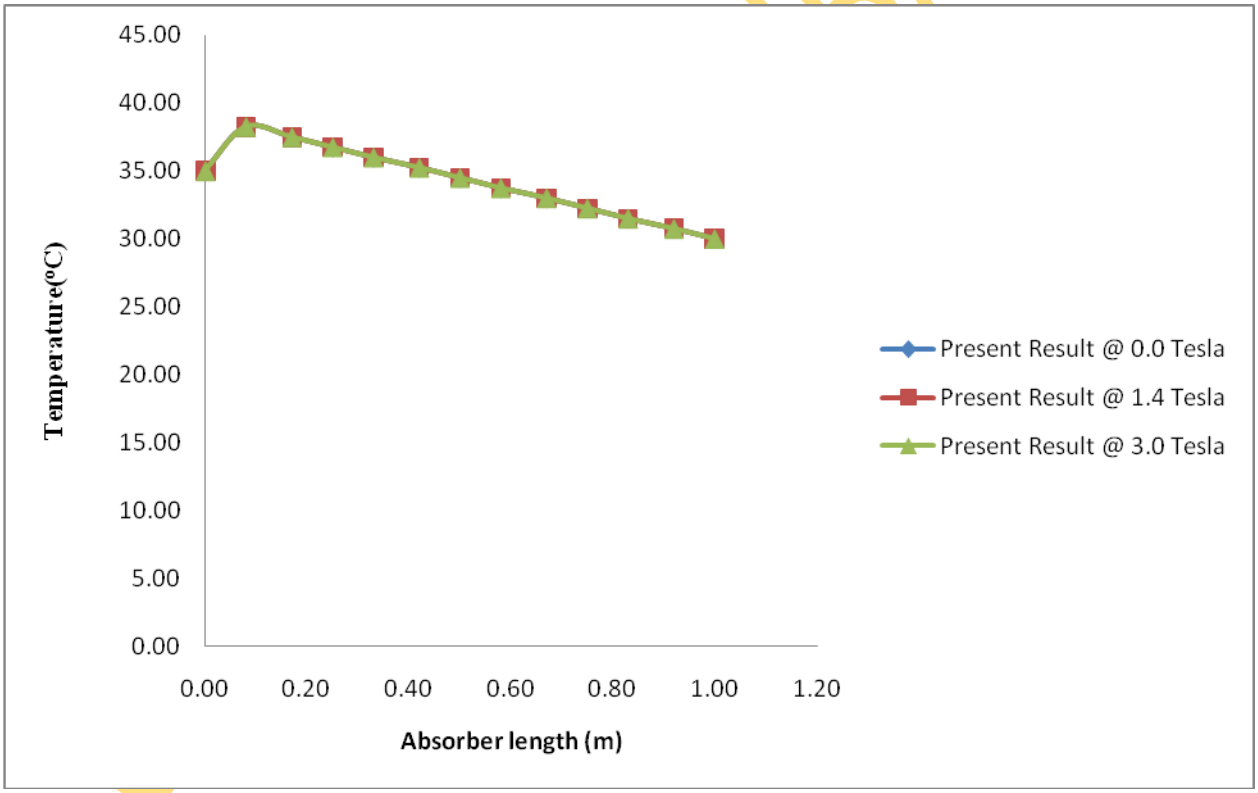

Fig. 4.8.4: Graph of Temperature Changes at the Interface in X-direction, X = Absorber length.

IBADAN

Table 4.4.8: LiCl-H_2O Concentration Changes within the film in X-direction, X = Absorber length.

Absorber length X (m)	Bulk					
	Present Result @ 0.0 Tesla	Present. Result @ 1.4 Tesla	% Changes in X-dir	Present Result @ 0.0 Tesla	Present Result @3.0 Tesla	% Changes in X-dir
0 or 10^{-6}	0.450	0.4500	0.00	0.450	0.4500	0.00
$10^{-5.5}$	0.4453	0.4453	0.005	0.4453	0.4454	0.014
10^{-5}	0.4406	0.4407	0.011	0.4406	0.4408	0.032
$10^{-4.5}$	0.4360	0.4361	0.018	0.4360	0.4362	0.060
10^{-4}	0.4313	0.4314	0.026	0.4313	0.4317	0.090
$10^{-3.5}$	0.4267	0.4268	0.035	0.4267	0.4272	0.124
10^{-3}	0.4221	0.4222	0.045	0.4221	0.4227	0.164
$10^{-2.5}$	0.4174	0.4177	0.053	0.4174	0.4183	0.196
10^{-2}	0.4128	0.4131	0.061	0.4128	0.4138	0.230
$10^{-1.5}$	0.4082	0.4085	0.069	0.4082	0.4093	0.260
10^{-1}	0.4036	0.4039	0.074	0.4036	0.4047	0.283
$10^{-0.5}$	0.3990	0.3993	0.078	0.3990	0.4001	0.293
10^{0}	0.3580	0.3580	0.00	0.3580	0.3580	0.00

UNIVERSITY OF IBADAN

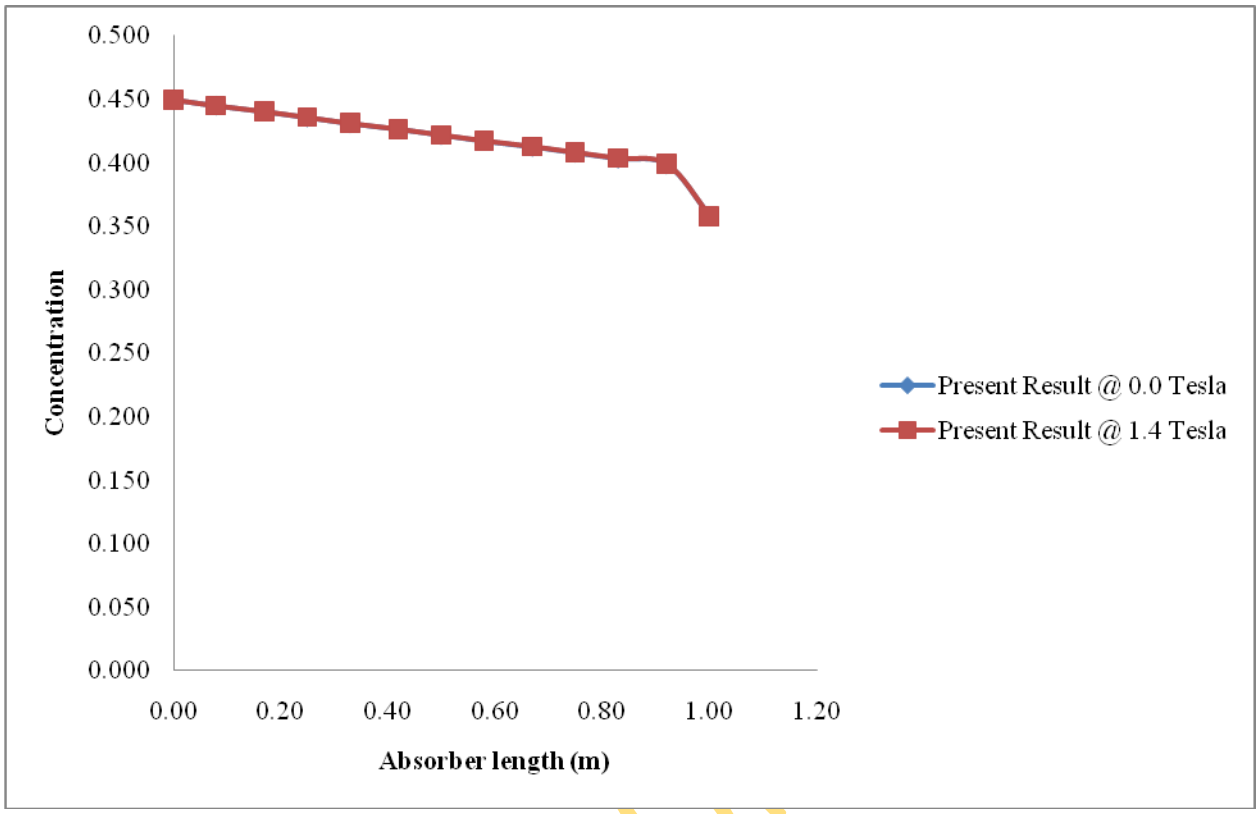

Fig.4.8.5: Concentration Distribution within the Film in X-direction at 0.0 & 1.4 Tesla, X = Absorber length.

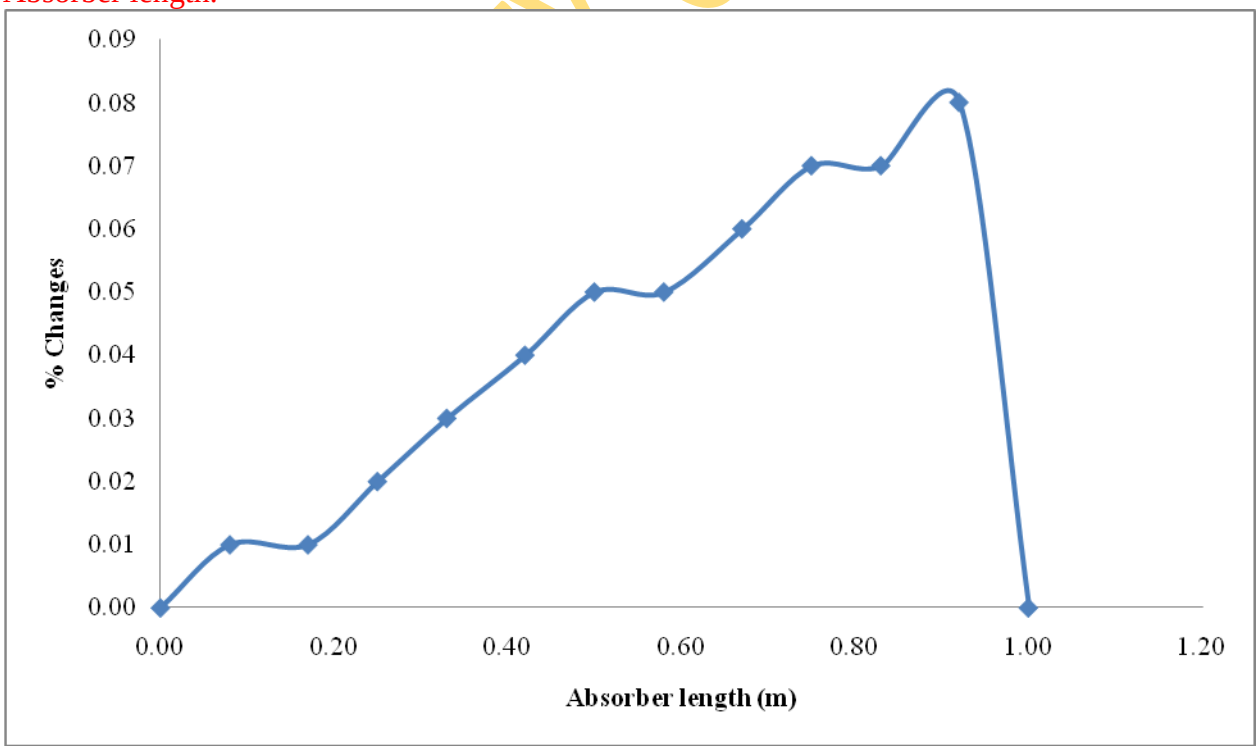

Fig.4.8.6: % Concentration Changes within the Film in X-direction at 0.0 & 1.4Tesla, X = Absorber length.

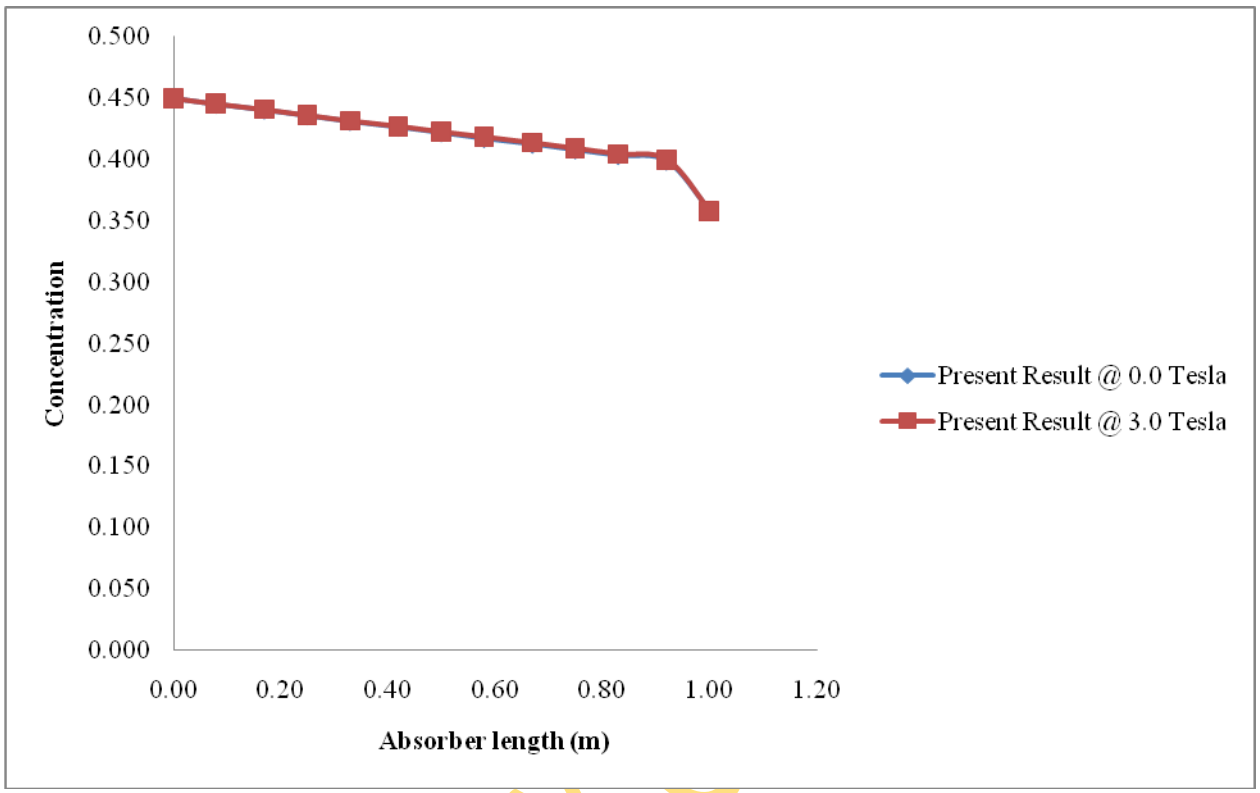

Fig.4.8.7: Concentration Changes within the Film in X-direction at 0.0 & 3.0Tesla, X = Absorber length.

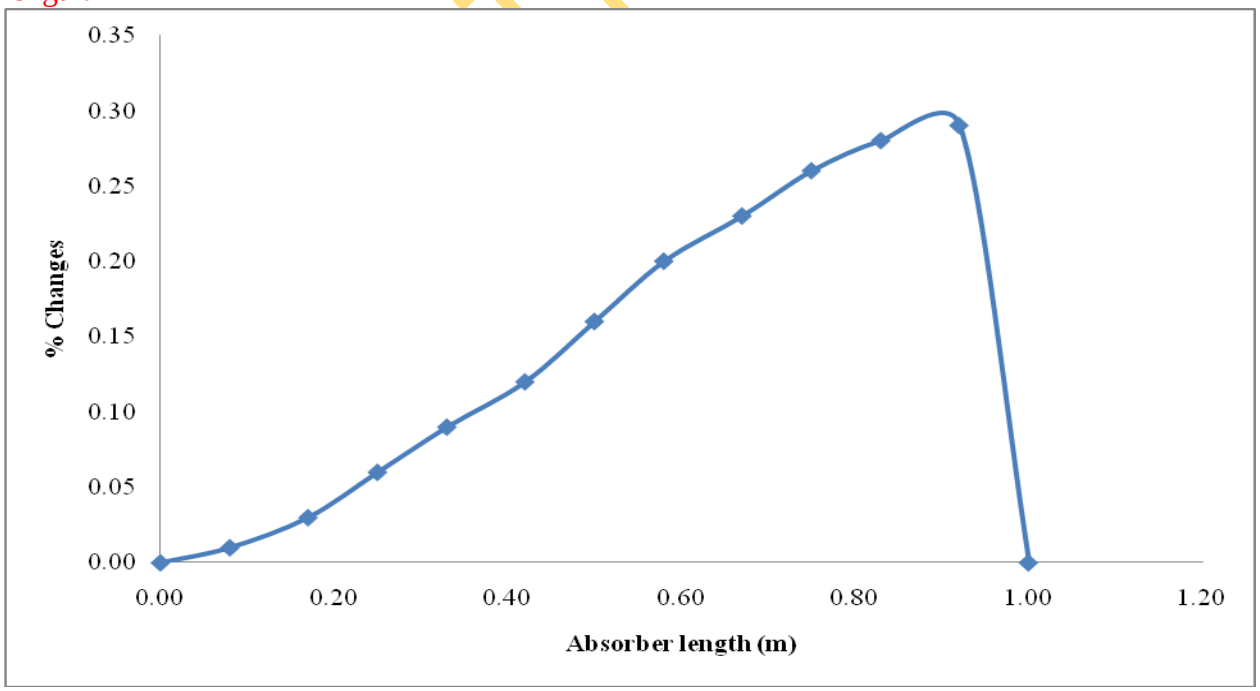

Fig.4.8.8: % Concentration Changes within the Film in X-direction at 0.0 & 3.0T, X = Absorber length.

Table 4.4.9: LiCl-H_2O Concentration Changes within the film in X-direction

Absorber length X (m)	Interface					
	Present Result @ 0.0 Tesla	**Present. Result @ 1.4 Tesla**	**% Changes in X-dir**	**Present Result @ 0.0 Tesla**	**Present Result @3.0 Tesla**	**% Changes in X-dir**
0 or 10^{-6}	0.450	0.4500	0.00	0.450	0.4500	0.00
$10^{-5.5}$	0.44486	0.44487	0.002	0.44486	0.44491	0.011
10^{-5}	0.43978	0.43980	0.005	0.43978	0.43989	0.025
$10^{-4.5}$	0.43476	0.43479	0.007	0.43476	0.43492	0.037
10^{-4}	0.42979	0.42984	0.012	0.42979	0.43000	0.049
$10^{-3.5}$	0.42488	0.42494	0.014	0.42488	0.42514	0.061
10^{-3}	0.42003	0.42010	0.017	0.42003	0.42034	0.074
$10^{-2.5}$	0.41523	0.41531	0.019	0.41523	0.41559	0.087
10^{-2}	0.41049	0.41058	0.022	0.41049	0.41089	0.098
$10^{-1.5}$	0.40580	0.40590	0.025	0.40580	0.40625	0.111
10^{-1}	0.40116	0.40128	0.030	0.40116	0.40166	0.125
$10^{-0.5}$	0.39658	0.39671	0.033	0.39658	0.39712	0.136
10^{0}	0.35800	0.35800	0.00	0.35800	0.35800	0.000

UNIVERSITY OF IBADAN

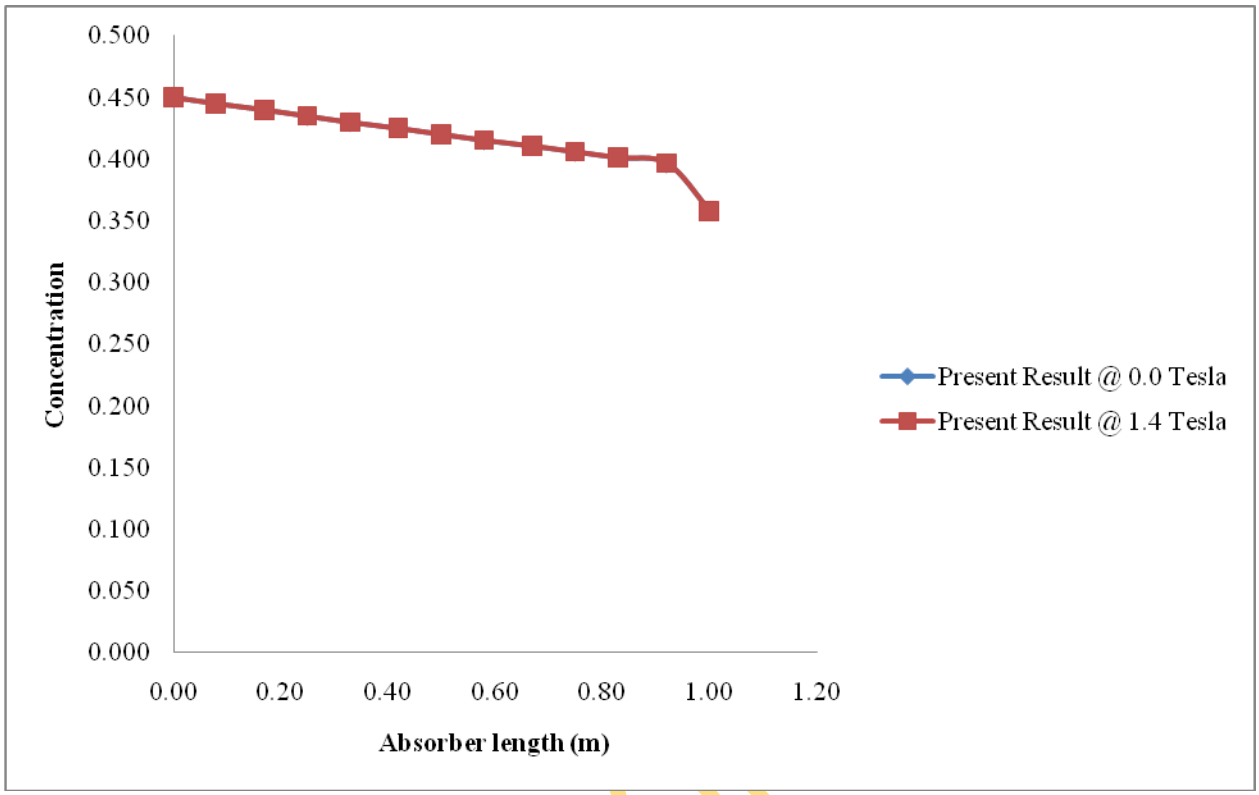

Fig.4.8.9: Concentration Changes at the Interface in X-direction from 0.0 to 1.4 Tesla, X = Absorber length.

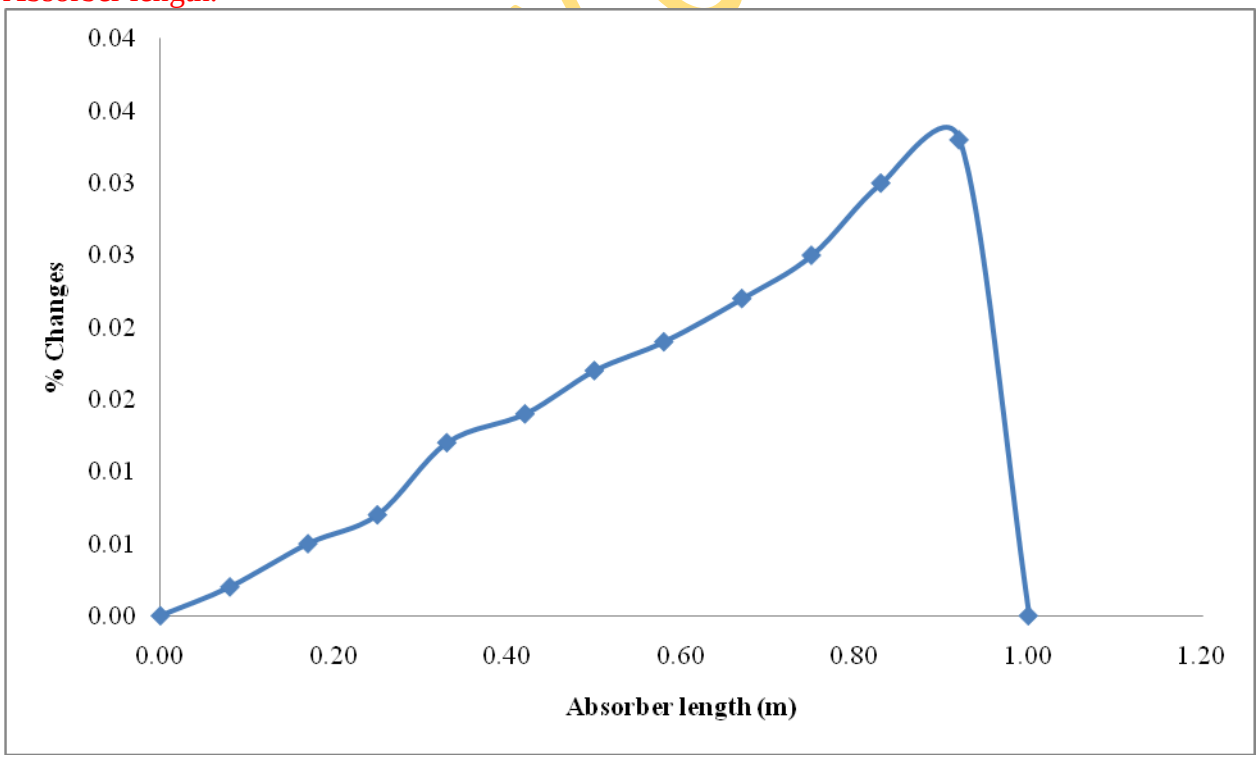

Fig.4.9: % Concentration Changes at the Interface in X-direction at 0.0 & 1.4 Tesla, X = Absorber length.

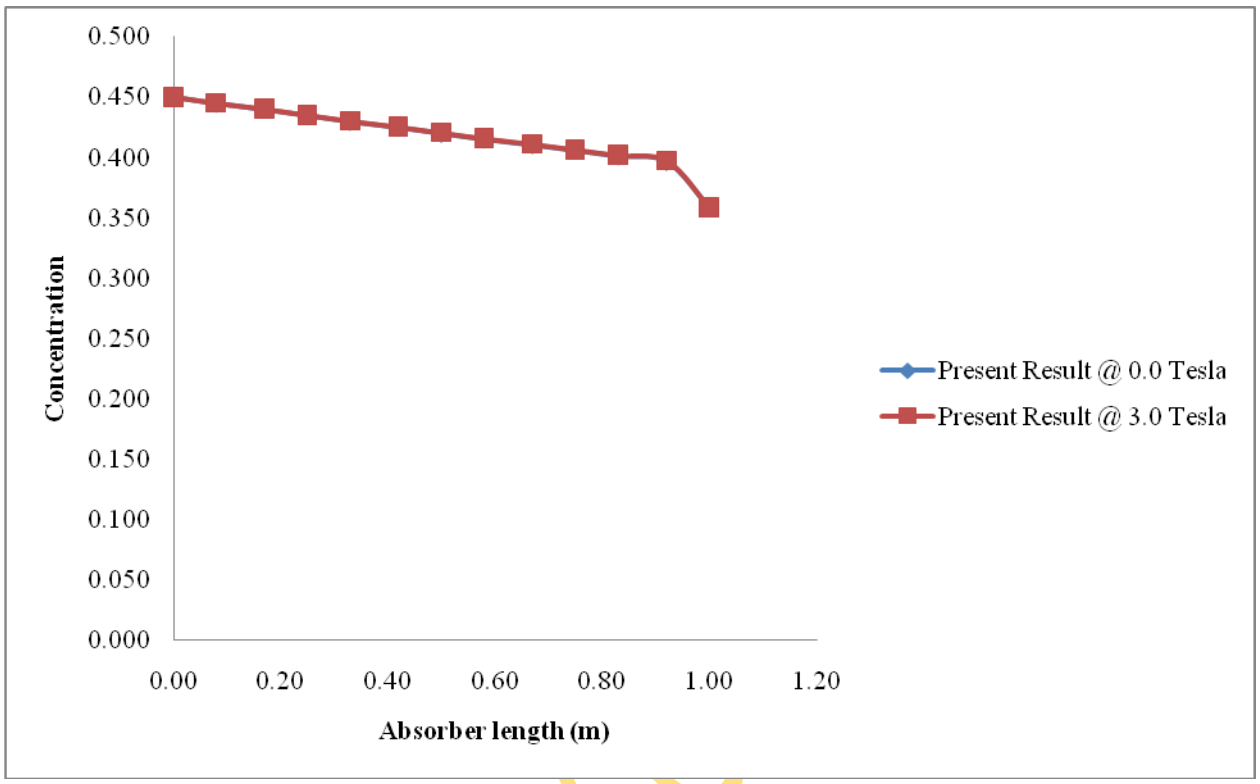

Fig.4.9.1: Concentration Changes at the Interface in X-direction at 0.0 & 3.0Tesla, X = Absorber length.

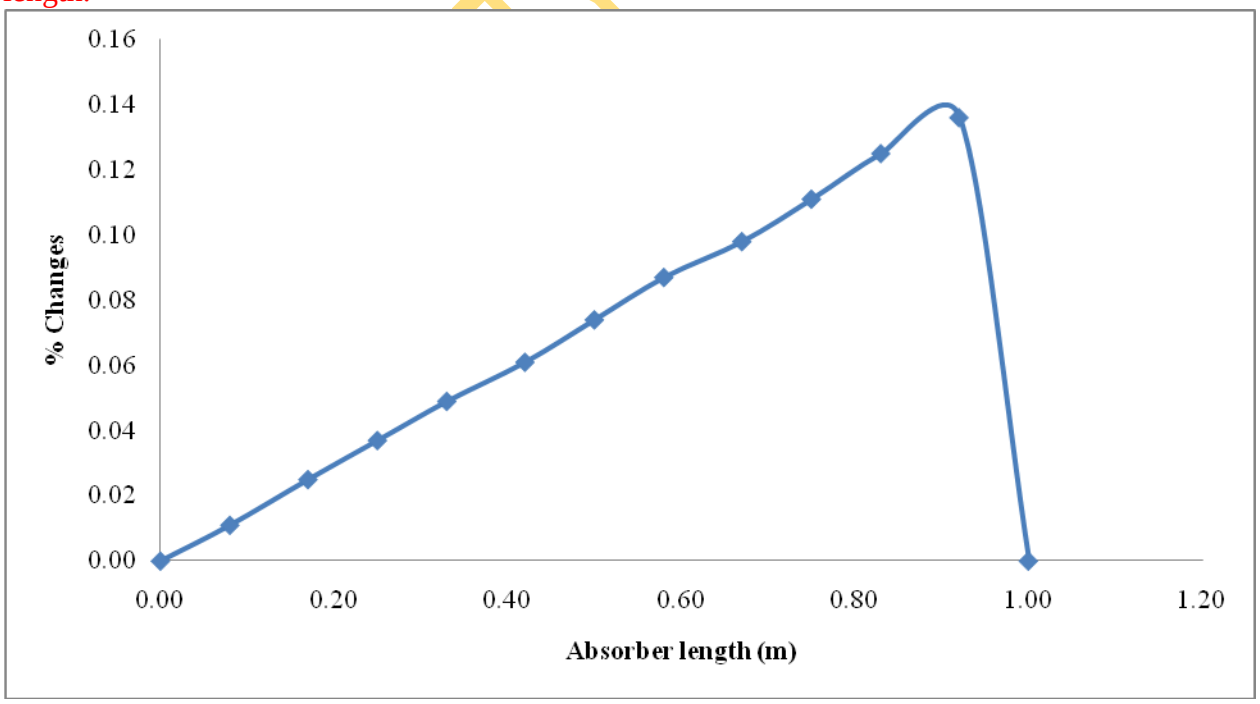

Fig. 4.9.2: % Concentration Changes at the Interface in X-direction from 0.0 to 3.0 Tesla, X = Absorber length.

4.5: Numerical Results in the direction of the film thickness (δ)

One may also be interested in the velocity, temperature and concentration distributions in the direction of the smooth film thickness when enhanced with magnetic intensity. Below are the results of the investigation. The velocity along the liquid film thickness direction at sections X=0.25m, 0.50m and X=0.75m in three different magnetic induction intensities are shown in Tables 4.5.3 to 4.5.5, 4.6.2 to 4.6.4 and Figures 4.9.3 to 4.10.7 and 4.12.6 to 4.14 respectively. A dimensionless parameter of y/ δ is used as the abscissa. It is seen from Tables 4.5.3 to 4.5.5, 4.6.2 to 4.6.4 and Figures 4.9.3 to 4.10.7 and 4.12.6 to 4.14 that with the increase of the magnetic induction (β), the velocity increases at X= 0.25m, 0.5m up to at X= 0.75m for both LiBr and LiCl-water solution. This could be explained as follows; At the inlet section, absorption just began in an intense way and the film thickness is very thin, the absorption enhancement effect by magnetic field is obvious, turbulence in direction of thickness therefore are more intense due to the above mentioned reasons. The turbulence becomes weaker with the increase of the film thickness and the absorption enhancement. Hence, the velocity v is higher in stronger β at X=0.50 and 0.75m respectively. Velocity variations along the thickness direction at the three selected sections have the tendency of increasing from absorber wall to the vapour-liquid interface as established. This indicates that the refrigerants vapour in the two working fluids permeates towards the inner solution from the vapour-liquid interface. When the liquid film drops, the increase in velocity is slowed down. It shows that the absorption has been weakening gradually towards the outlet of the solution resulting in the lower concentration at X= 0.5, 0.75m than at X=0.25m as shown in the Tables 4.5.9 to 4.6.1, 4.6.8 to 4.7 and Figures 4.11.1 to 4.12.5 and 4.14.4 to 4.15.8

For the case of temperature distributions in LiBr-H_2O solution, there was no noticeable temperature change in the temperature apart from the sudden temperature rise at y/ δ = 0.33 within the bulk at absorber wall length X= 0.25, 0.5 and 0.75m levels, perhaps as a result of high inlet temperature than that of absorber wall temperature. However for LiCl-H_2O solution, there was no sudden up-rise of temperature observed at y/ δ = 0.33 within the bulk at absorber wall length X= 0.25, 0.5 and 0.75m levels like that of the LiBr-H_2O solution. This might be due to the same inlet temperature as that of the absorber wall temperature. Tables 4.5.6 to 4.5.8, 4.6.5 to 4.6.7 and Figures 4.10.8 to 4.11 and 4.14.1 to 4.14.3 also show that with the increase of β from 0.0T to 1.4T and from 0.0T to 3.0T velocity increases gradually at X=0.25, 0.5 and 0.75m level

UNIVERSITY OF IBADAN

of the absorber wall length. Concentration distribution for both LiBr-H_2O and LiCl-H_2O solution also increases as the values of β increase from 0.0T to 1.4T and from 0.0T to 3.0Tesla. It also increases from the wall length up to y/δ = 0.58 film thickness before undergoing a reduction at the interface. Tables 4.5.3 to 4.5.5, 4.6.2 to 4.6.4 and Figures 4.9.3 to 4.10.7 and 4.12.6 to 4.14 also show the percentage velocity changes in the film thickness direction for both LiBr-H_2O and LiCl-H_2O solution at X=0.25, 0.5 and 0.75m. The percentage velocity changes when β was increased from 0.0 to 1.4T also increase from 0.0 suddenly up to 0.85 before gradually dying down to 0.71 at the interface. When the magnetic induction was increased from 0.0 to 3.0T, percentage velocity change rises from 0.0 suddenly to 2.22 and reduced down to 1.86 at the interface. This result confirms the establishment of magnetic field enhancement effect on the two working fluids. For the case of Temperature, there was no percentage changes in Y-direction at X=0.25m, 0.5m and 0.75m absorber length for the two working fluids. Tables 4.5.9 to 4.6.1, 4.6.8 to 4.7 and Figures 4.11.1 to 4.12.5 and 4.14.4 to 4.15.8 show the percentage concentration changes in the film thickness (δ) direction (Y) at X=0.25, 0.5 and 0.75m level for both LiBr–H_2O and LiCl–H_2O solutions. At X=0.25m level percentage concentration changes for LiBr-H_2O solution when magnetic induction was increased from 0.0 to 1.4T rises from 0.00 suddenly to 0.67 due to the intense of the absorption rate as a result of the magnetic field force and gradually reduced to 0.26 at the interface while that of 0.0T to 3.0T also suddenly rises from 0.0 to 1.77as a result of the same above mentioned reasons and gradually dying down to 0.67 at the interface. A closer look at the Tables shows that the absorption rate increases tremendously when the magnetic induction increase from 0.0 to 1.4T and up to 3.0T respectively. Thus the result establishes positive influence of the magnetic field enhancement on the working fluids. This same remark also applies to the LiCl-H_2O solution. For Temperature distribution in LiCl–H_2O solution shown in Tables 4.5.6 to 4.5.8, 4.6.5 to 4.6.7 and Figures 4.10.8 to 4.11 and 4.14.1 to 4.14.3, there was no percentage Temperature change. This, in addition to the earlier mentioned reason might also be due to non-inclusion of heat in the magnetism effect. Tables 4.5 to 4.5.2 summarized the COP analysis of both the LiBr and LiCl solutions absorption Refrigeration systems.

UNIVERSITY OF IBADAN

4.5.1: COP analysis of LiBr and LiCl solutions absorption Refrigeration systems

Coefficient of Performance (COP) for LiBr-water absorption Refrigeration

From Table 4.2.9 above

At 0.0 Tesla, COP = $\frac{0.549}{0.600}$ = 0.9152

At 1.4 Tesla, COP = $\frac{0.5501}{0.600}$ = 0.9166

At 3.0 Tesla, COP = $\frac{0.551}{0.600}$ = 0.918

Increment at 1.4 Tesla= 0.9166 – 0.9152 = 0.0014 = 0.1%

Increment at 3.0 Tesla = 0.9186 – 0.9152 = 0.0034 = 0.3%

Coefficient of Performance (COP) for LiCl-water absorption Refrigeration

From Table 4.3.6 above

At 0.0 Tesla, COP = $\frac{0.339}{0.450}$ = 0.8867

At 1.4 Tesla, COP= $\frac{0.3993}{0.450}$ = 0.8873

At 3.0 Tesla, COP = $\frac{0.400}{0.450}$ = 0.8890

Increment at 1.4Tesla = 0.8873 – 0.8867 = 0.0006 = 0.1%

Increment at 3.0Tesla = 0.889 – 0.887 = 0.002 = 0.2%

UNIVERSITY OF IBADAN

Comparison of COP increment of LiBr and LiCl Solutions at 1.4 and 3.0Tesla

Table 4.5: Percentage increment of coefficient of Performance (COP) @ 1.4 Tesla

	LiBr Solution % increment of COP at 1.4 Tesla	LiCl Solution % increment of COP at 1.4 Tesla
	0.1	0.1

Table 4.5.1: Percentage increment of coefficient of Performance (COP) @ 3.0 Tesla

	LiBr Solution % increment of COP at 3.0 Tesla	LiCl Solution % increment of COP at 3.0 Tesla
	0.3	0.2

Table 4.5.2: LiBr & LiCl COP increments at 3.0 Tesla T-Test analysis

Independent Samples Test

		Levene's Test for Equality of Variances		t-test for Equality of Means						
									95% Confidence Interval of the Difference	
		F	Sig.	t	df	Sig. (2-tailed)	Mean Difference	Std. Error Difference	Lower	Upper
Percentage Increment of COP @ 3.0 Tesla	Equal variances assumed	113.293	.000	1.123E16	24	.000	.1000	.0000	.1000	.1000
	Equal variances not assumed			1.123E16	23.361	.000	.1000	.0000	.1000	.1000

UNIVERSITY OF IBADAN

4.5.3: Tabular and Graphical representation of the results in the direction of film thickness

Table.4.5.3: LiBr-H_20: Velocity Changes in the direction of film thickness (δ) @ X=0.25m

Y/δ	BULK					
	Present Result @ 0.0 Tesla	**Present. Result @ 1.4 Tesla**	**% Changes in Y-dir**	**Present Result @ 0.0 Tesla**	**Present Result @3.0 Tesla**	**% Changes in Y-dir**
0.00	0.0000	0.00	0.00	0.0000	0.0000	0.00
0.08	0.0113	0.0116	2.72	0.0113	0.0127	12.24
0.17	0.0222	0.0228	2.63	0.0222	0.0248	11.84
0.25	0.0325	0.0333	2.55	0.0325	0.0362	11.48
0.33	0.0421	0.0431	2.49	0.0421	0.0468	11.18
0.42	0.0508	0.0520	2.43	0.0579	0.0563	10.93
0.50	0.0585	0.0599	2.39	0.0585	0.0648	10.73
0.58	0.0650	0.0666	2.35	0.0650	0.0719	10.56
0.67	0.0704	0.0720	2.33	0.0704	0.0777	10.43
0.75	0.0744	0.0762	2.30	0.0744	0.0821	10.34
0.83	0.0772	0.0789	2.29	0.0771	0.0851	10.29
0.92	0.0785	0.0803	2.29	0.0785	0.0866	10.26
1.00	0.0785	0.0803	2.29	0.0785	0.0866	10.26

UNIVERSITY OF IBADAN

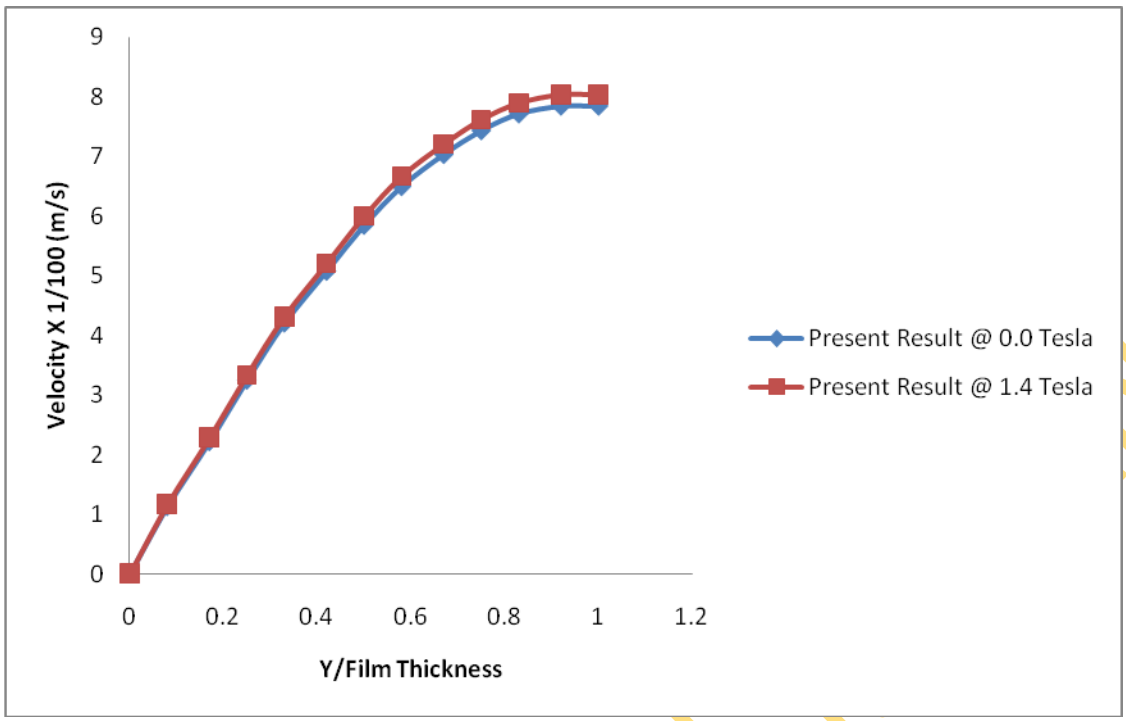

Fig.4.9.3: Graph of Velocity Changes in the Direction of Film Thickness at X=0.25m

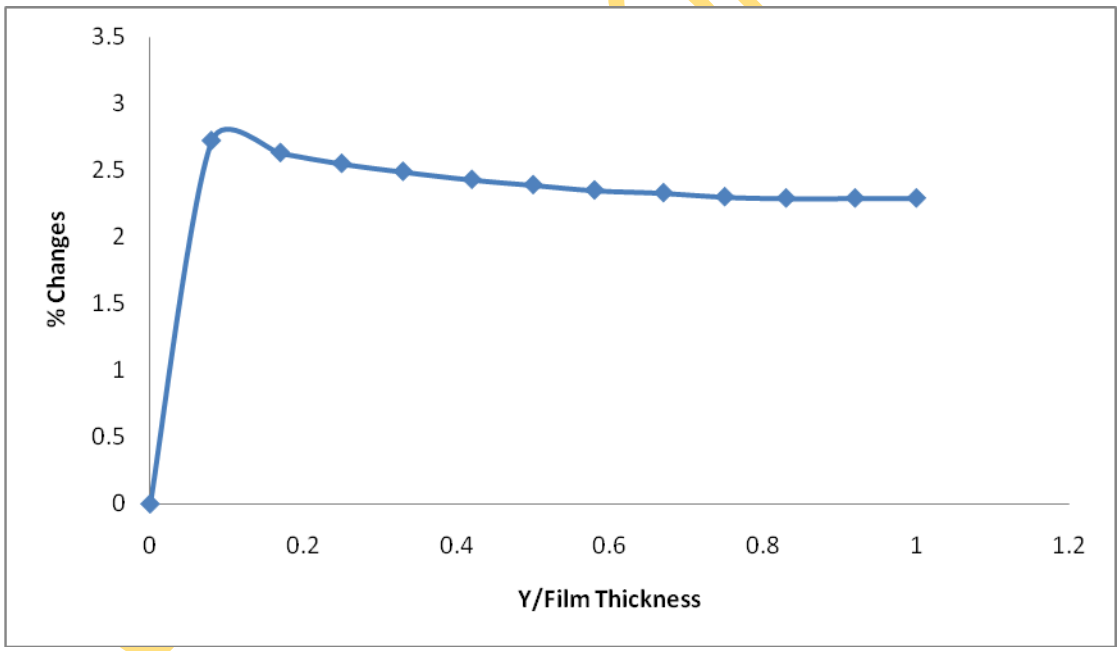

Fig. 4.9.4: Graph of % Velocity Changes in the Direction of Film Thickness at X= 0.25m

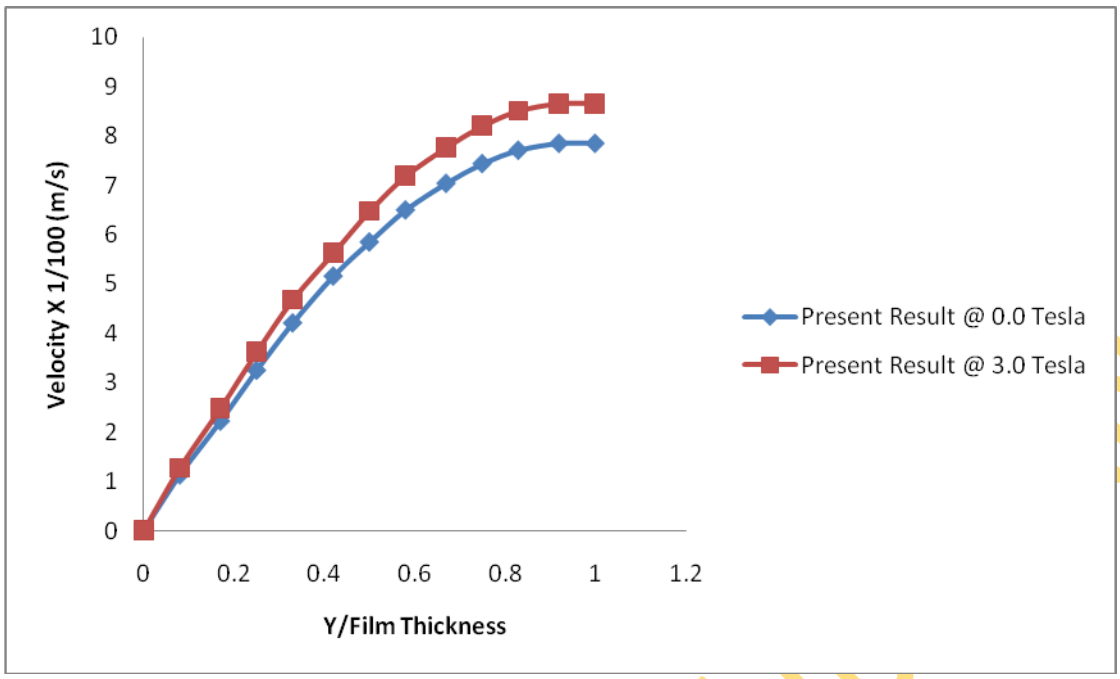

Fig.4.9.5: Graph of Velocity Changes in the Direction of Film Thickness at X= 0.25m

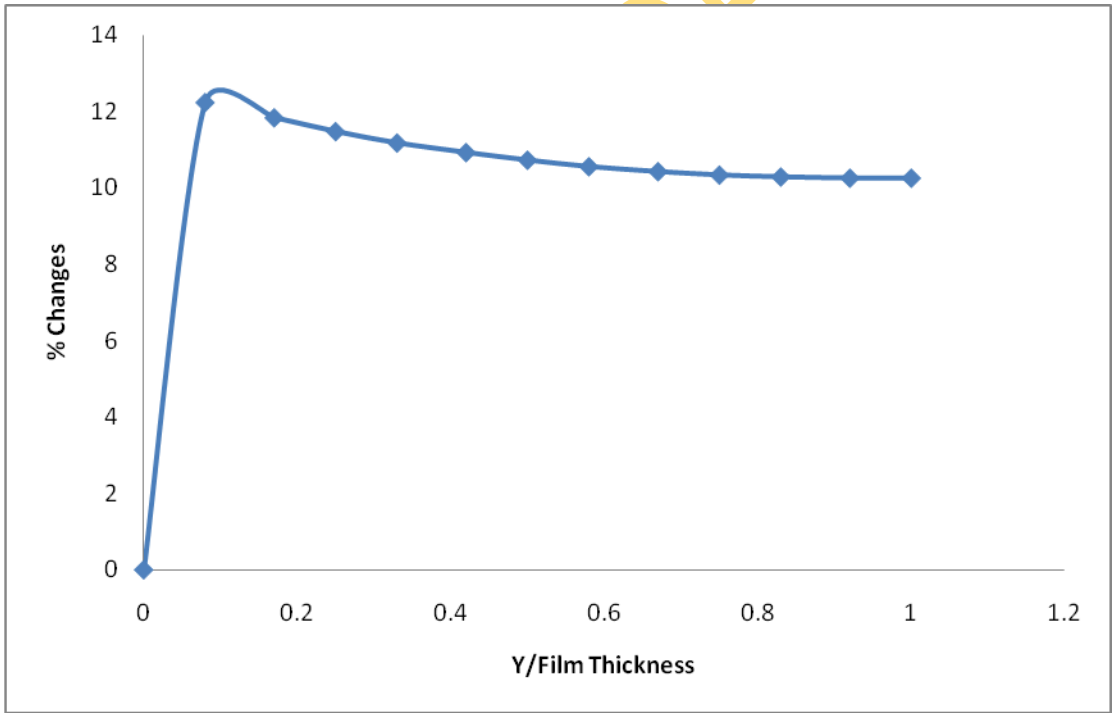

Fig.4.9.6: Graph of % Velocity Changes in the Direction of Film Thickness at X=0.25m

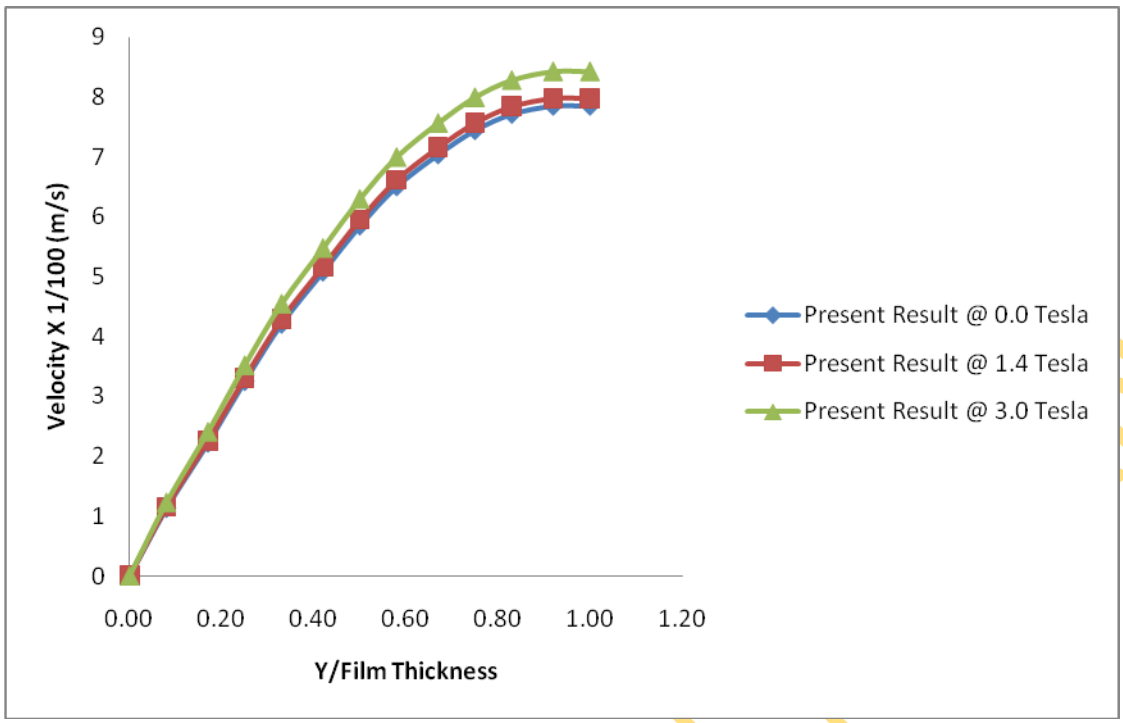

Fig.4.9.7: Graph of Velocity Distribution in the Direction of Film Thickness at X=0.25m

Table 4.5.4: LiBr-H_20: Velocity Changes within the direction of film thickness (δ) at X=0.50m

Y/δ	BULK					
	Present Result @ 0.0 Tesla	**Present. Result @ 1.4 Tesla**	**% Changes in Y-dir**	**Present Result @ 0.0 Tesla**	**Present Result @3.0 Tesla**	**% Changes in Y-dir**
0.00	0.0000	0.0000	0.00	0.000	0.0000	0.00
0.08	0.0113	0.0116	2.72	0.0113	0.0126	12.24
0.17	0.0222	0.0228	2.63	0.0222	0.0248	11.83
0.25	0.0325	0.0330	2.55	0.0325	0.0362	11.48
0.33	0.0421	0.0431	2.49	0.0421	0.0468	11.18
0.42	0.0508	0.0520	2.43	0.0508	0.0564	10.93

UNIVERSITY OF

0.50	0.0585	0.0599	2.39	0.0585	0.0647	10.72
0.58	0.0650	0.0666	2.35	0.0650	0.0719	10.56
0.67	0.0704	0.0720	2.33	0.0704	0.0777	10.43
0.75	0.0744	0.0762	2.31	0.0744	0.0821	10.34
0.83	0.0772	0.0789	2.29	0.0772	0.0851	10.29
0.92	0.0785	0.0803	2.29	0.0785	0.0866	10.26
1.00	0.0785	0.0803	2.29	0.0785	0.0866	10.26

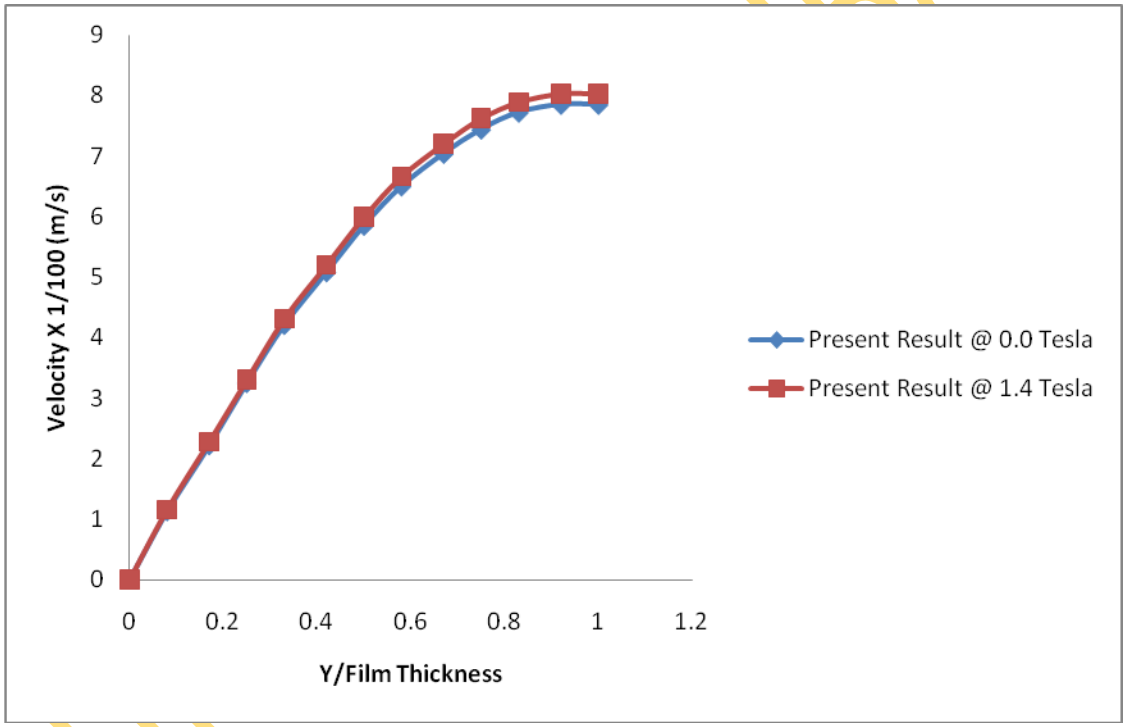

Fig.4.9.8: Graph of Velocity of Changes within the Film in the Direction of Film Thickness at X=0.50m

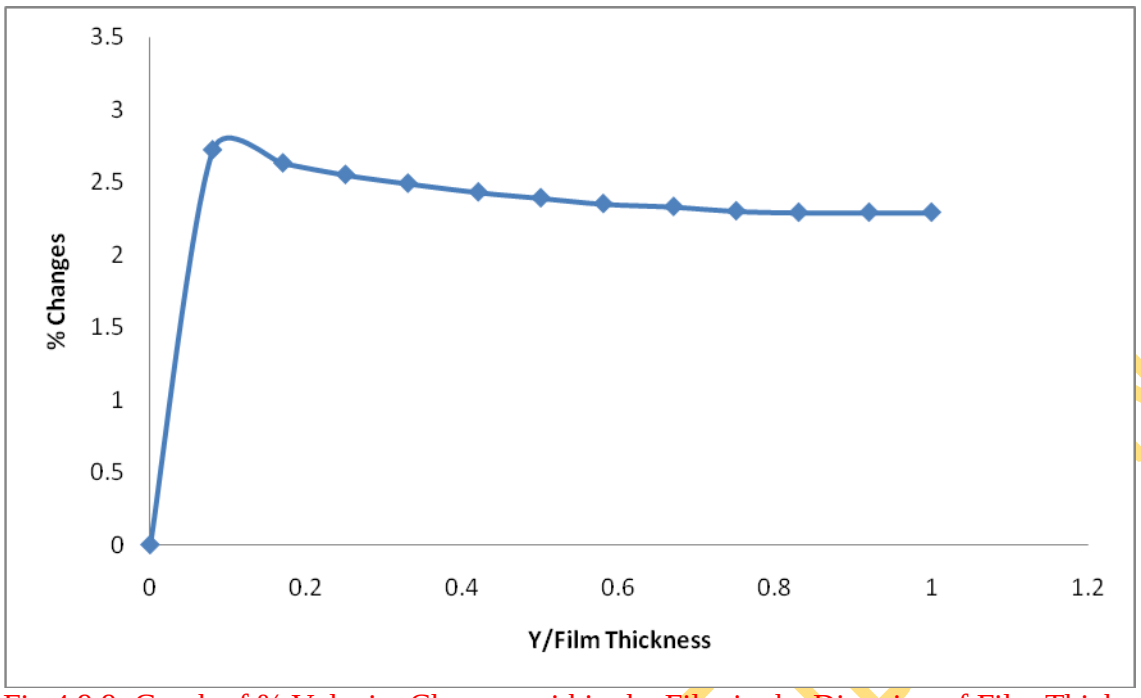

Fig.4.9.9: Graph of % Velocity Changes within the Film in the Direction of Film Thickness at X= 0.50m

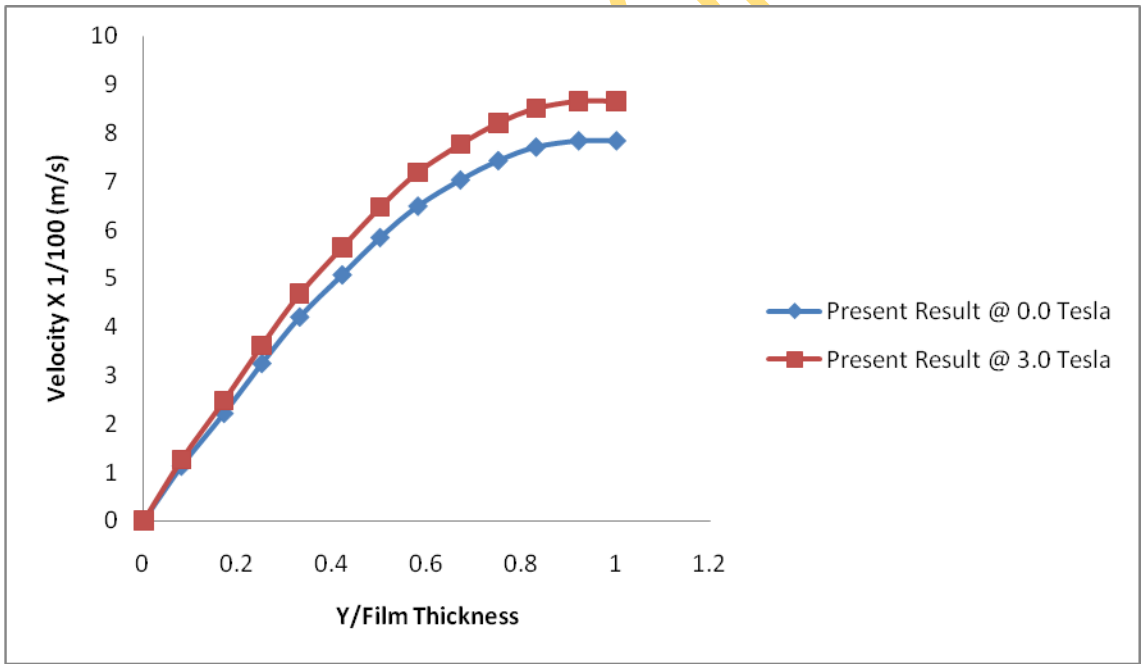

Fig.4.10: Graph of Velocity Changes within the Film in the Direction of Film Thickness at X=0.50m

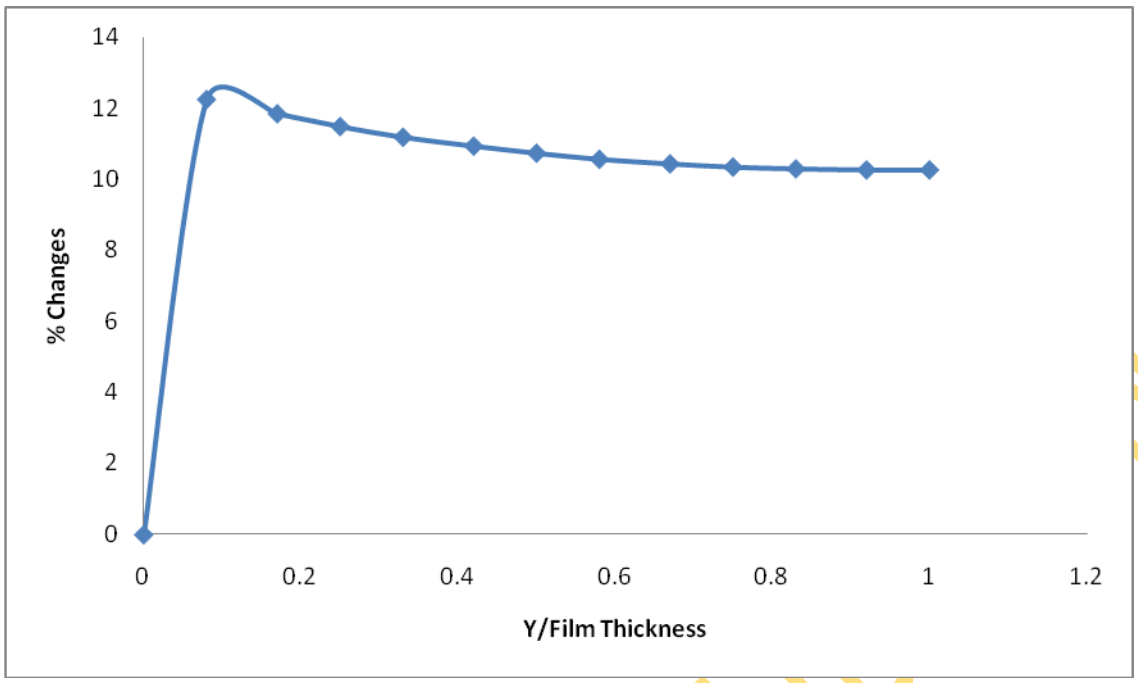

Fig.4.10.1: Graph of % Velocity Change within the Film in the Direction of Film Thickness at X=0.50m

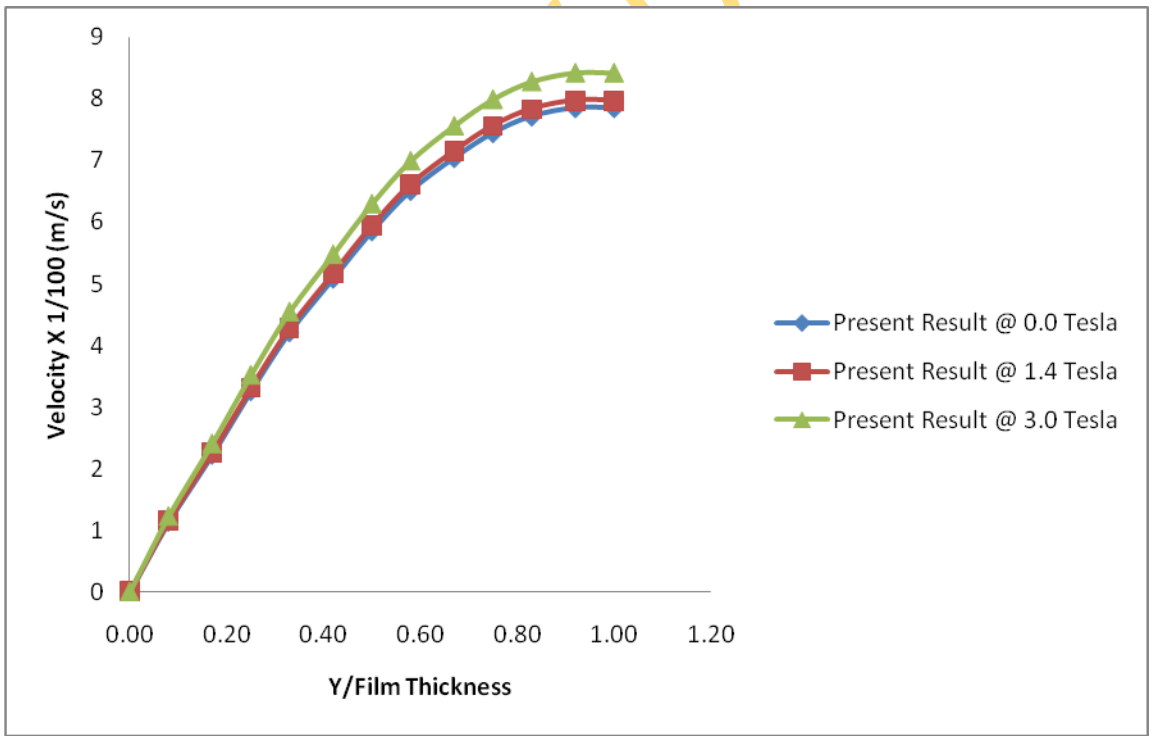

Fig.4.10.2: Graph of Velocity Distribution in the Direction of Film Thickness at X =0.50m

Table 4.5.5: LiBr-H_20: Velocity Changes within the direction of film thickness (δ) at X=0.75m

Y/δ	BULK					
	Present Result @ 0.0 Tesla	**Present. Result @ 1.4 Tesla**	**% Changes in Y-dir**	**Present Result @ 0.0 Tesla**	**Present Result @3.0 Tesla**	**% Changes in Y-dir**
0.00	0.0000	0.0000	0.00	0.000	0.0000	0.00
0.08	0.0113	0.0116	2.72	0.0113	0.0126	12.24
0.17	0.0222	0.0228	2.63	0.0222	0.0248	11.83
0.25	0.0325	0.0330	2.55	0.0325	0.0362	11.48
0.33	0.0421	0.0431	2.49	0.0421	0.0468	11.18
0.42	0.0508	0.0520	2.43	0.0508	0.0564	10.93
0.50	0.0585	0.0599	2.39	0.0585	0.0647	10.72
0.58	0.0650	0.0666	2.35	0.0650	0.0719	10.56
0.67	0.0704	0.0720	2.33	0.0704	0.0777	10.43
0.75	0.0744	0.0762	2.31	0.0744	0.0821	10.34
0.83	0.0772	0.0789	2.29	0.0772	0.0851	10.29
0.92	0.0785	0.0803	2.29	0.0785	0.0866	10.26
1.00	0.0785	0.0803	2.29	0.0785	0.0866	10.26

UNIVERSITY OF IBADAN

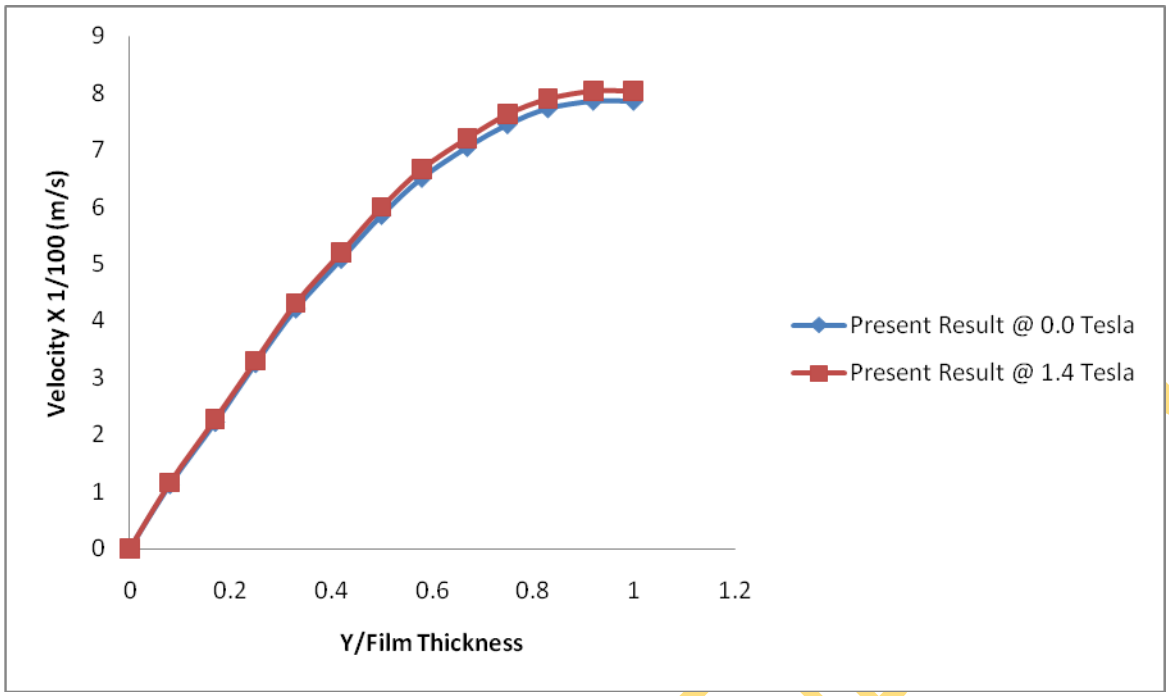

Fig.4.10.3: Graph of Velocity Changes within the Film in the direction of Film Thickness at X= 0.75m

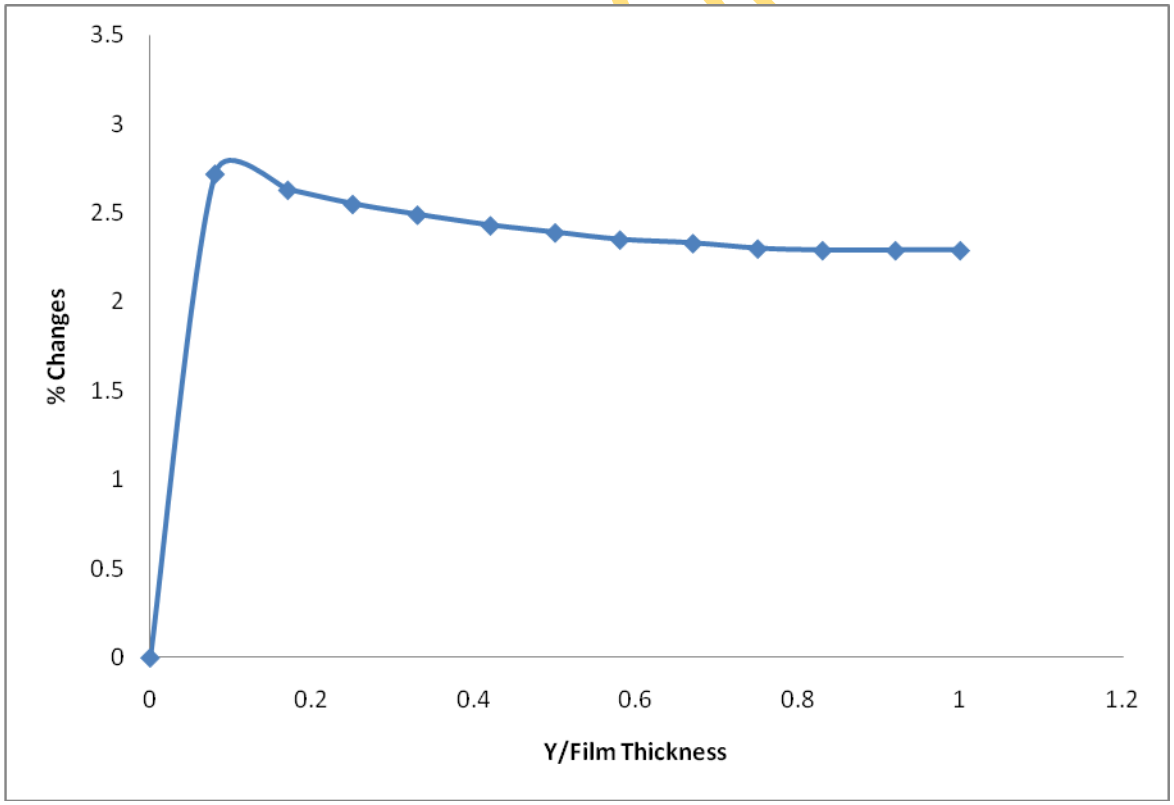

Fig.4.10.4: Graph of % Velocity Changes within the Film in the Direction of Film Thickness at X= 0.75m

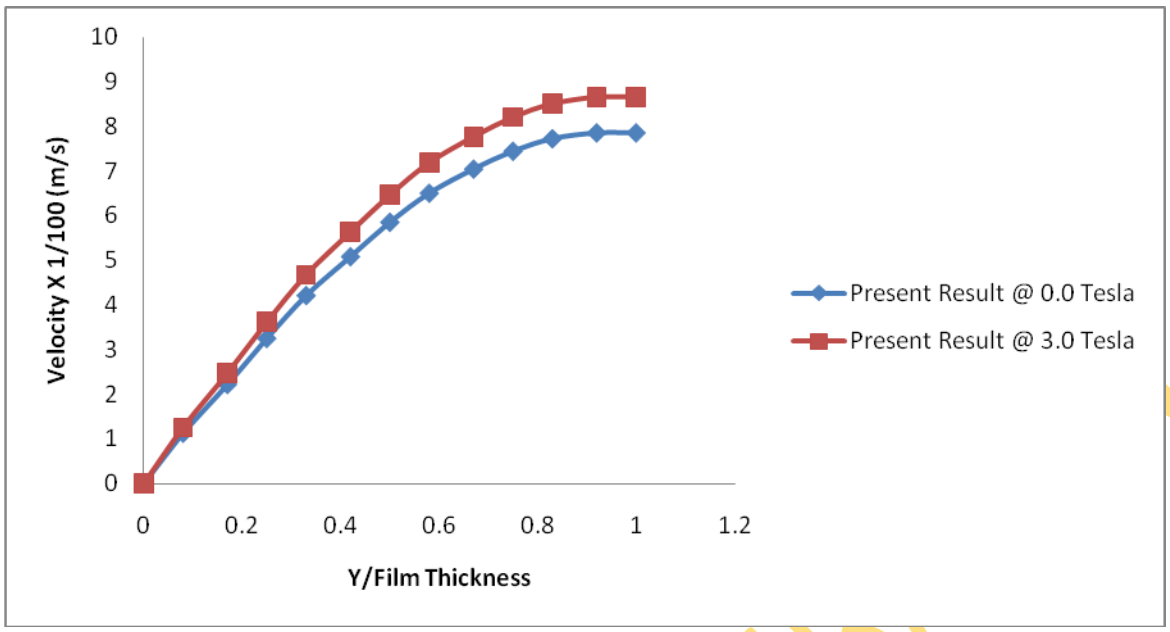

Fig.4.10.5: Graph of Velocity Changes within the Film in the Direction of Film Thickness at X=0.75m

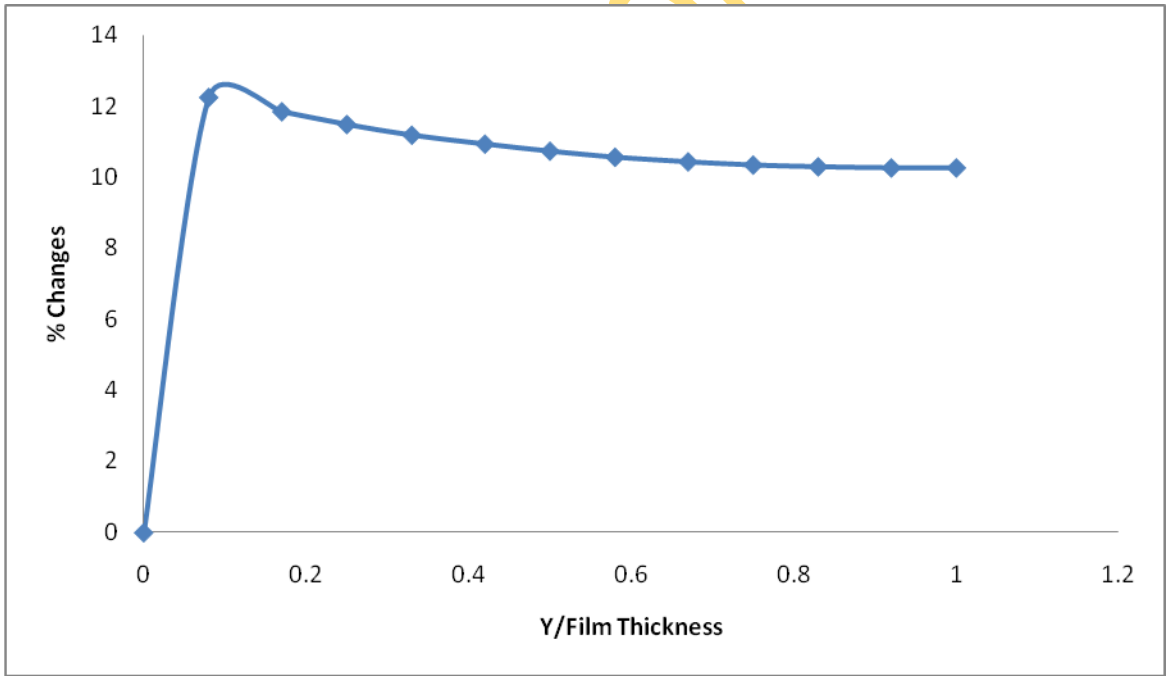

Fig.4.10.6: Graph of % Velocity Change within the Film in the Direction of Film Thickness at X=0.75m

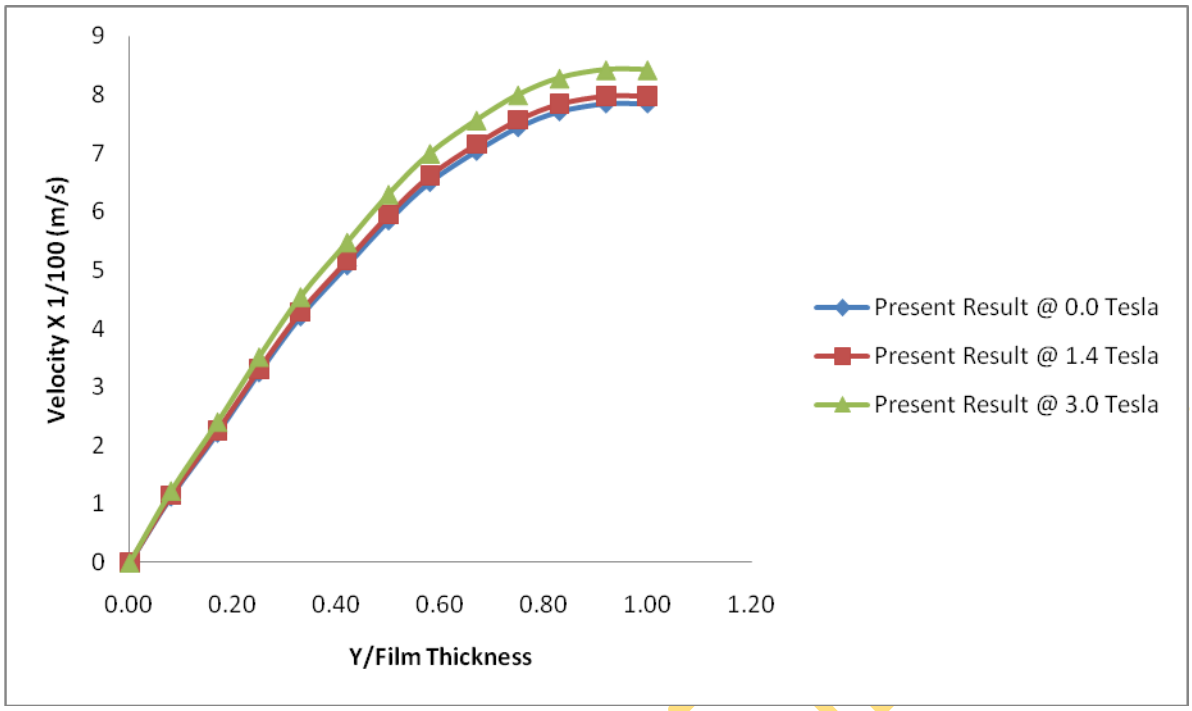

Fig.4.10.7: Graph of Velocity Distribution in the Direction of Film Thickness at X=0.75m

Table 4.5.6: LiBr-H_20: Temperature Changes in the direction of film thickness (δ) at X=0.25m

Y/δ	BULK					
	Present Result @ 0.0 Tesla	**Present. Result @ 1.4 Tesla**	**% Changes in Y-dir**	**Present Result @ 0.0 Tesla**	**Present Result @3.0 Tesla**	**% Changes in Y-dir**
0.00	35.00	35.00	0.00	35.00	35.00	0.00
0.08	35.19	35.19	0.00	35.19	35.19	0.00
0.17	35.19	35.19	0.00	35.19	35.19	0.00
0.25	35.19	35.19	0.00	35.19	35.19	0.00
0.33	37.55	37.55	0.00	37.55	37.55	0.00
0.42	35.19	35.19	0.00	35.19	35.19	0.00

UNIVERSITY OF

0.50	35.19	35.19	0.00	35.19	35.19	0.00
0.58	35.19	35.19	0.00	35.19	35.19	0.00
0.67	35.19	35.19	0.00	35.19	35.19	0.00
0.75	35.19	35.19	0.00	35.19	35.19	0.00
0.83	35.19	35.19	0.00	35.19	35.19	0.00
0.92	35.19	35.19	0.00	35.19	35.19	0.00
1.00	35.19	35.19	0.00	35.19	35.19	0.00

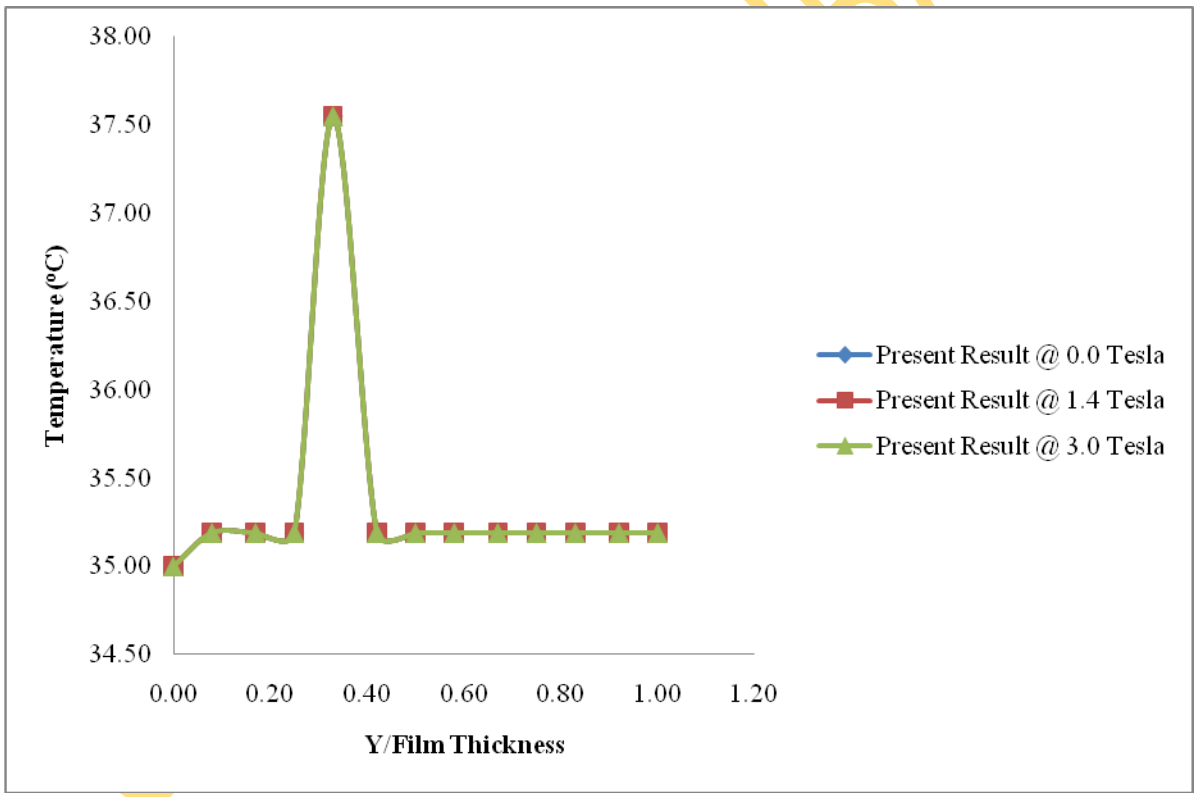

Fig.4.10.8: Graph of Temperature Changes within the Film in the Direction of Film Thickness at X=0.25m

Table 4.5.7: LiBr-H_20: Temperature Changes in the direction of film thickness (δ) at X=0.50m

Y/δ	BULK					
	Present Result @ 0.0 Tesla	**Present. Result @ 1.4 Tesla**	**% Changes in Y-dir**	**Present Result @ 0.0 Tesla**	**Present Result @3.0 Tesla**	**% Changes in Y-dir**
0.00	35.00	35.00	0.00	35.00	35.00	0.00
0.08	35.13	35.13	0.00	35.13	35.13	0.00
0.17	35.13	35.13	0.00	35.13	35.13	0.00
0.25	35.13	35.13	0.00	35.13	35.13	0.00
0.33	36.70	36.70	0.00	36.70	36.70	0.00
0.42	35.13	35.13	0.00	35.13	35.13	0.00
0.50	35.13	35.13	0.00	35.13	35.13	0.00
0.58	35.13	35.13	0.00	35.13	35.13	0.00
0.67	35.13	35.13	0.00	35.13	35.13	0.00
0.75	35.13	35.13	0.00	35.13	35.13	0.00
0.83	35.13	35.13	0.00	35.13	35.13	0.00
0.92	35.13	35.13	0.00	35.13	35.13	0.00
1.00	35.13	35.13	0.00	35.13	35.13	0.00

UNIVERSITY OF IBADAN

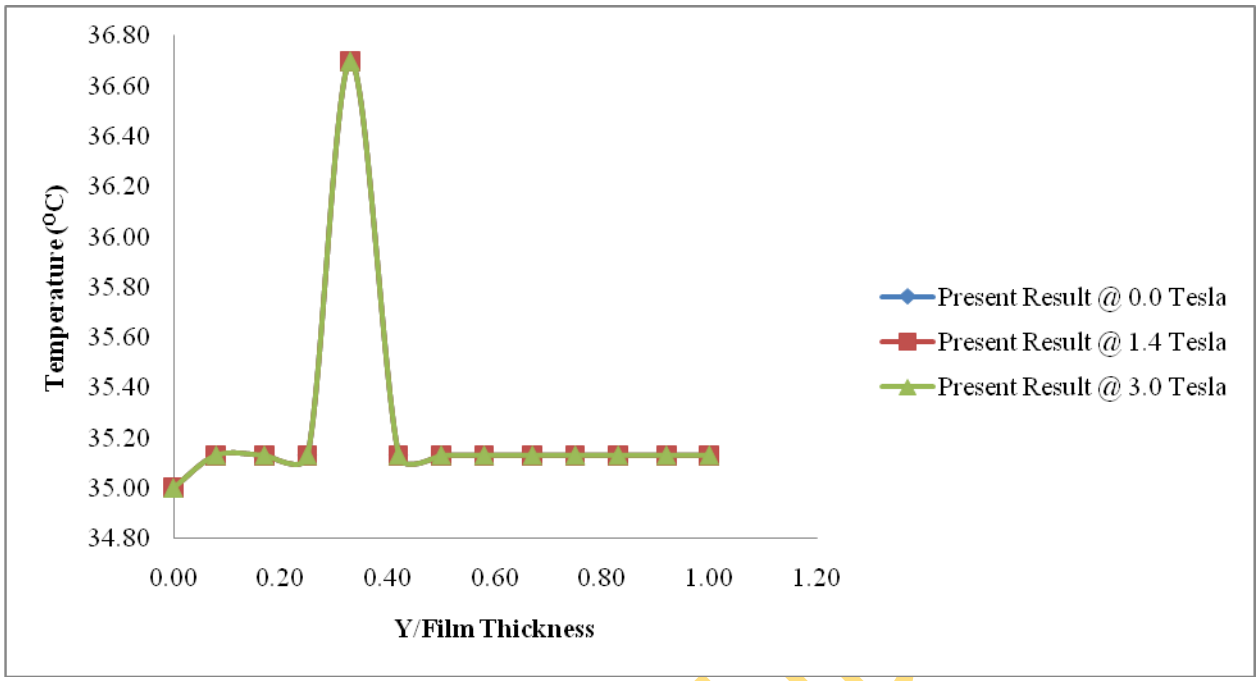

Fig.4.10.9: Graph of Temperature Changes within the Film in the Direction of Film Thickness at X= 0.50m

Table 4.5.8: LiBr-H_20: Temperature Changes in the direction of film thickness (δ) at X=0.75m

Y/δ	BULK					
	Present Result @ 0.0 Tesla	**Present. Result @ 1.4 Tesla**	**% Changes in Y-dir**	**Present Result @ 0.0 Tesla**	**Present Result @3.0 Tesla**	**% Changes in Y-dir**
0.00	35.00	35.00	0.00	35.00	35.00	0.00
0.08	35.06	35.06	0.00	35.06	35.06	0.00
0.17	35.06	35.06	0.00	35.06	35.06	0.00
0.25	35.06	35.06	0.00	35.06	35.06	0.00
0.33	35.85	35.85	0.00	35.85	35.85	0.00
0.42	35.06	35.06	0.00	35.06	35.06	0.00
0.50	35.06	35.06	0.00	35.06	35.06	0.00

UNIVERSITY OF

0.58	35.06	35.06	0.00	35.06	35.06	0.00
0.67	35.06	35.06	0.00	35.06	35.06	0.00
0.75	35.06	35.06	0.00	35.06	35.06	0.00
0.83	35.06	35.06	0.00	35.06	35.06	0.00
0.92	35.06	35.06	0.00	35.06	35.06	0.00
1.00	35.06	35.06	0.00	35.06	35.06	0.00

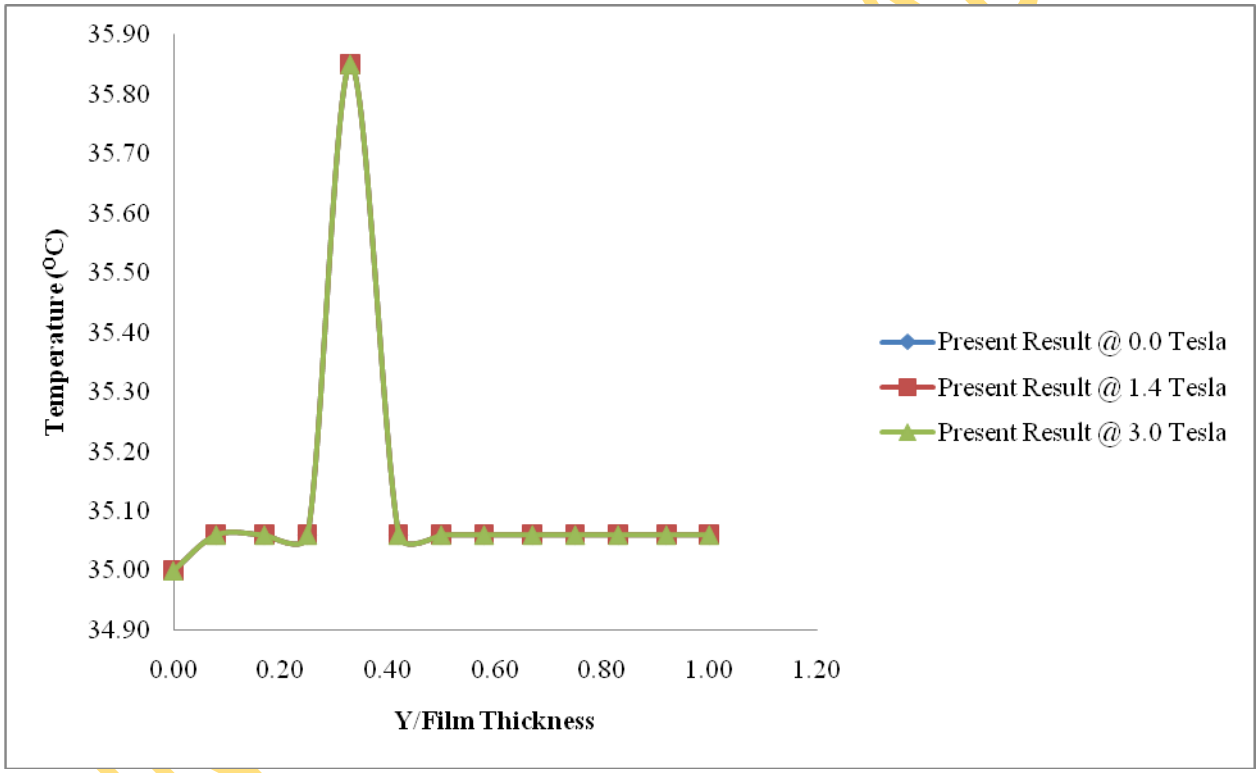

Fig.4.11: Graph of Temperature Changes within the Film in the Direction of Film Thickness at X=0.75m

Table 4.5.9: LiBr-H_20: Concentration Changes in the direction of film thickness (δ) at X=0.25m

Y/δ	BULK					
	Present Result @ 0.0 Tesla	**Present. Result @ 1.4 Tesla**	**% Changes in Y-dir**	**Present Result @ 0.0 Tesla**	**Present Result @3.0 Tesla**	**% Changes in Y-dir**
0.00	0.0000	0.0000	0.00	0.0000	0.0000	0.00
0.08	0.0859	0.0879	2.33	0.0859	0.0948	10.31
0.17	0.1483	0.1512	1.96	0.1483	0.1611	8.65
0.25	0.1949	0.1982	1.71	0.1949	0.2095	7.47
0.33	0.2303	0.2338	1.52	0.2303	0.2455	6.60
0.42	0.2575	0.2610	1.38	0.2575	0.2728	5.96
0.50	0.2784	0.2819	1.27	0.2784	0.2936	5.48
0.58	0.2943	0.2978	1.18	0.2943	0.3093	5.11
0.67	0.3061	0.3095	1.13	0.3061	0.3209	4.85
0.75	0.3145	0.3179	1.08	0.3145	0.3291	4.67
0.83	0.3198	0.3232	1.06	0.3198	0.3344	4.55
0.92	0.3224	0.3258	1.04	0.3224	0.3369	4.50
1.00	0.3224	0.3258	1.05	0.3224	0.3369	4.50

UNIVERSITY OF IBADAN

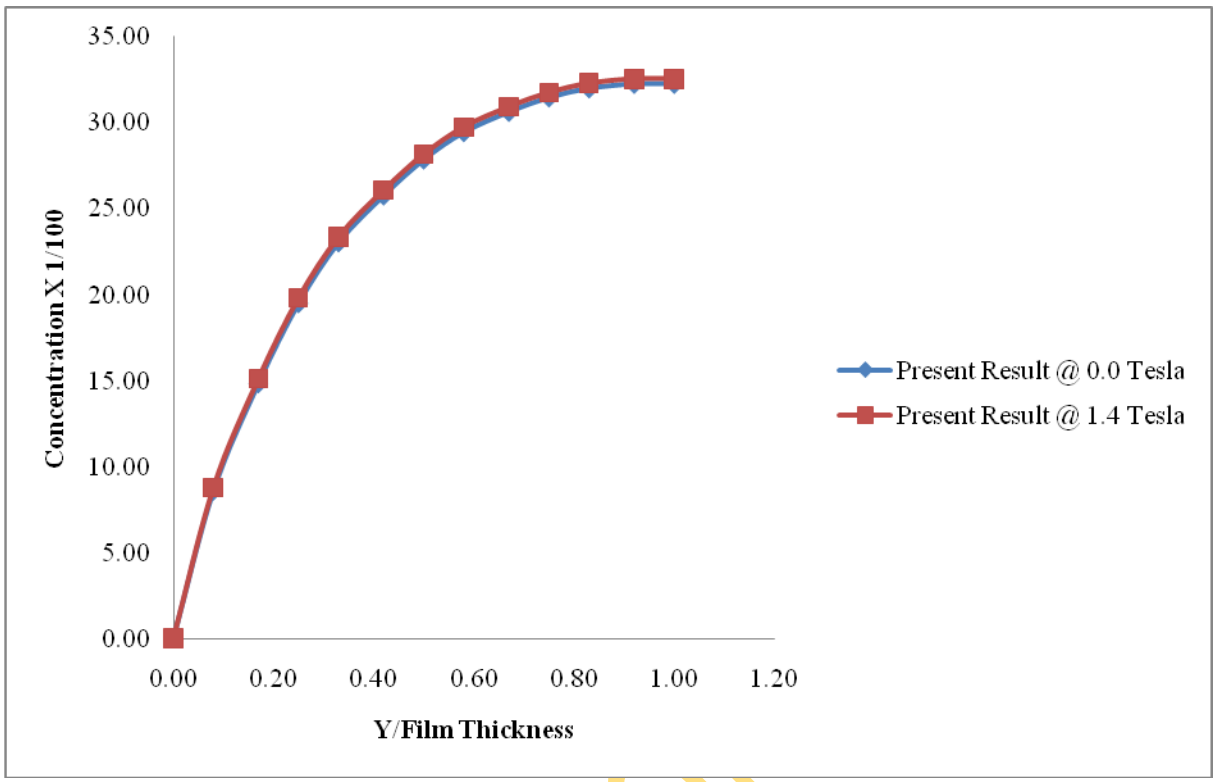

Fig.4.11.1: Graph of Concentration Changes within the Film in the direction of Film Thickness at X= 0.25m

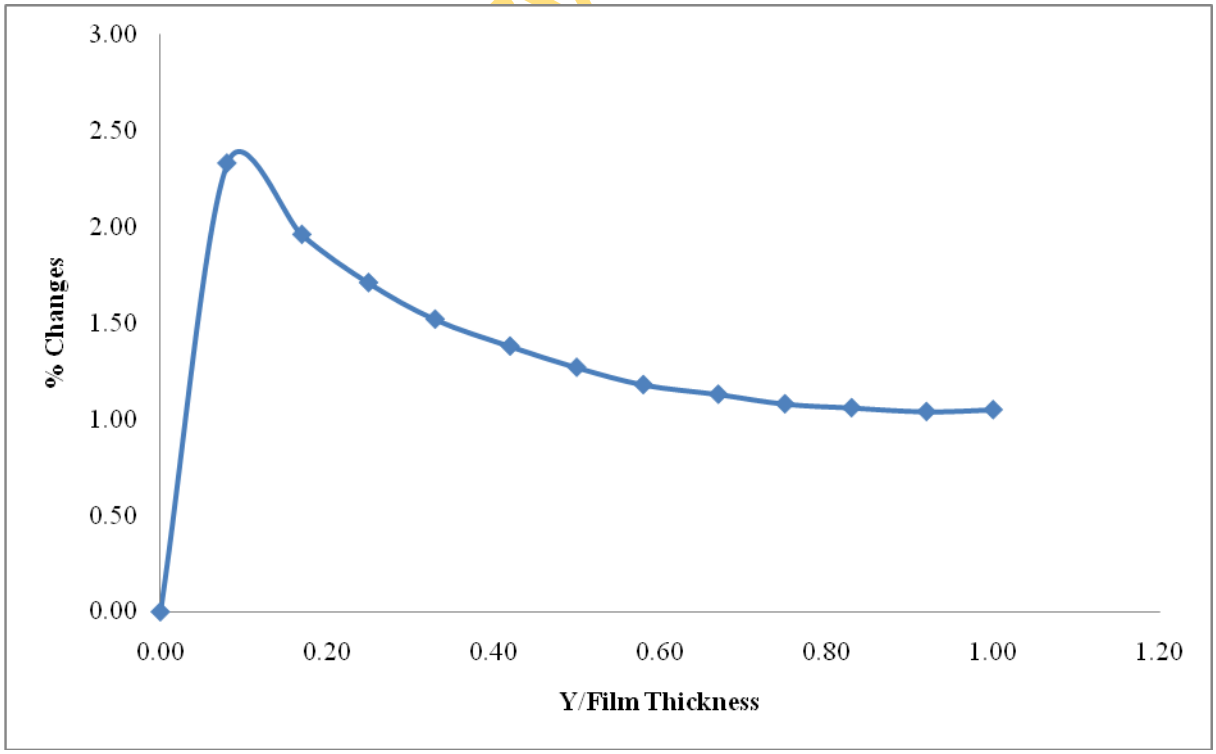

Fig.4.11.2: Graph of % Concentration Changes within the Film in the direction of Film Thickness at X= 0.25m

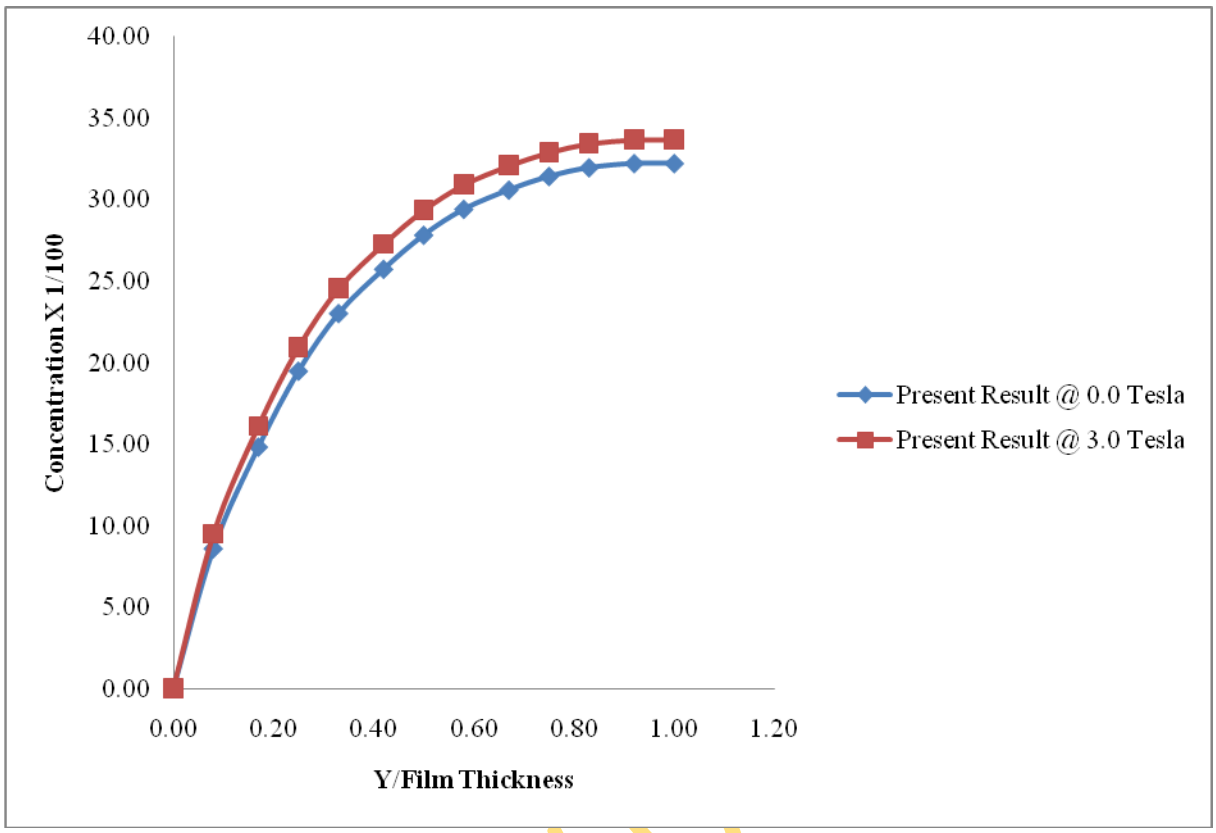

Fig.4.11.3: Graph of Concentration Changes within the Film in the Direction of Film Thickness at X=0.25m

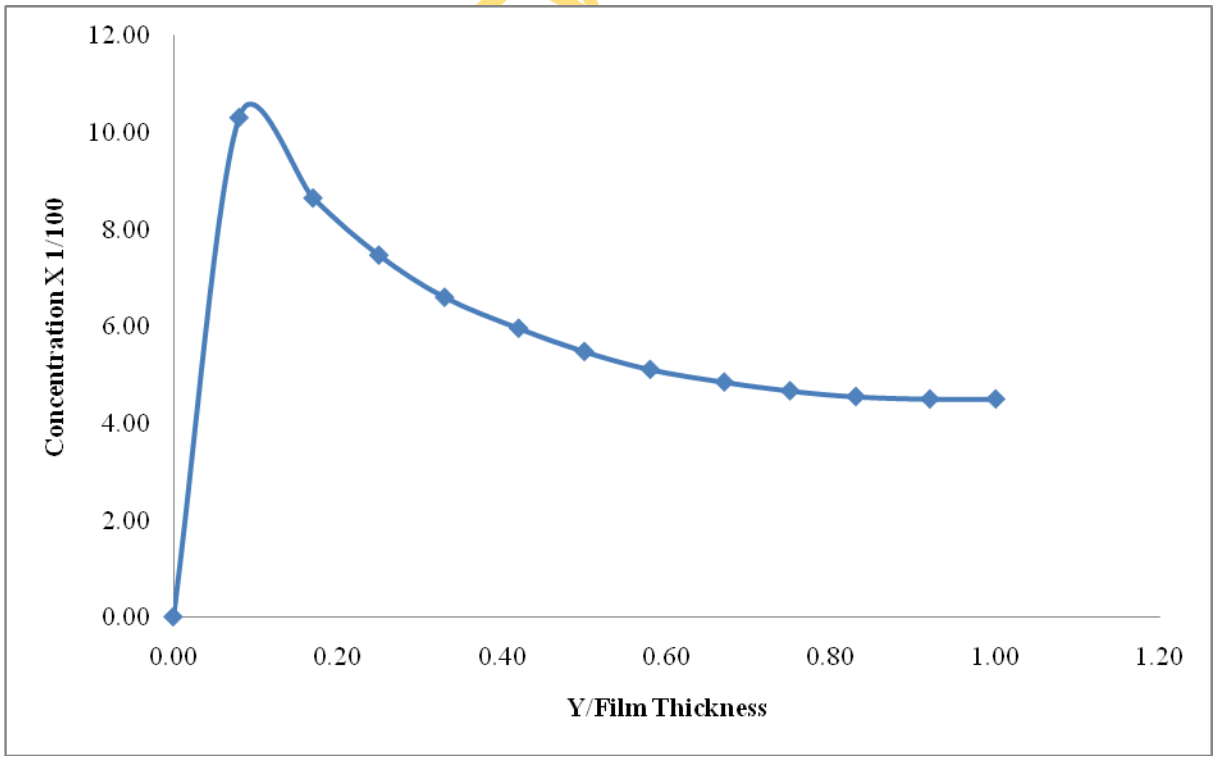

Fig.4.11.4: Graph of % Concentration Changes within the Film in the Direction of Film Thickness at X= 0.25m

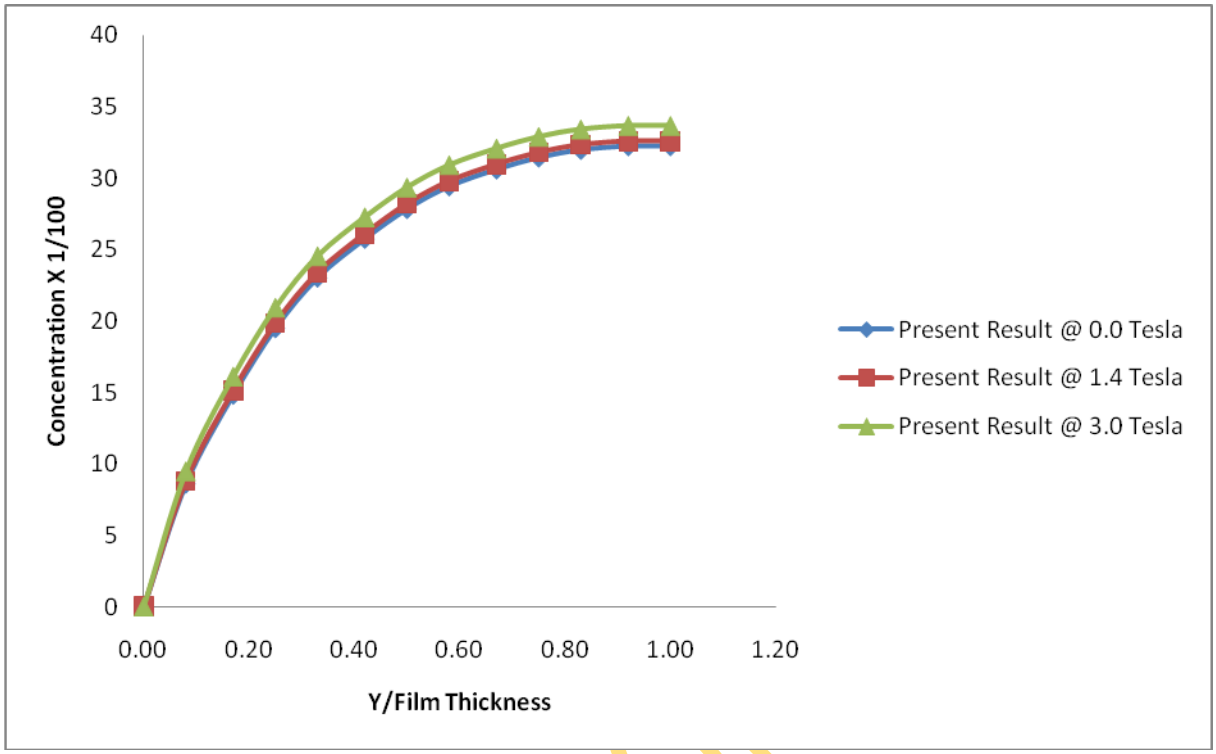

Fig.4.11.5: Graph of Concentration Distribution in the Direction of Film Thickness at X=0.25m

Table 4.6: LiBr-H_20: Concentration Changes in the direction of film thickness (δ) at X=0.50m

Y/δ	BULK					
	Present Result @ 0.0 Tesla	**Present. Result @ 1.4 Tesla**	**% Changes in Y-dir**	**Present Result @ 0.0 Tesla**	**Present Result @3.0 Tesla**	**% Changes in Y-dir**
0.00	0.0000	0.0000	0.00	0.0000	0.0000	0.00
0.08	0.0123	0.0129	4.72	0.0123	0.0150	21.72
0.17	0.0367	0.0381	3.96	0.0367	0.0433	18.04
0.25	0.0633	0.0655	3.46	0.0633	0.0731	15.50
0.33	0.0884	0.0911	3.06	0.0884	0.1005	13.64
0.42	0.1105	0.1135	2.77	0.1105	0.1240	12.27

UNIVERSITY

0.50	0.1291	0.1324	2.55	0.1291	0.1437	11.25
0.58	0.1443	0.1478	2.38	0.1443	0.1595	10.49
0.67	0.1561	0.1597	2.26	0.1561	0.1717	9.94
0.75	0.1648	0.1684	2.19	0.1648	0.1806	9.56
0.83	0.1705	0.1741	2.13	0.1705	0.1863	9.32
0.92	0.1732	0.1769	2.10	0.1732	0.1892	9.20
1.00	0.1732	0.1769	2.10	0.1732	0.1892	9.20

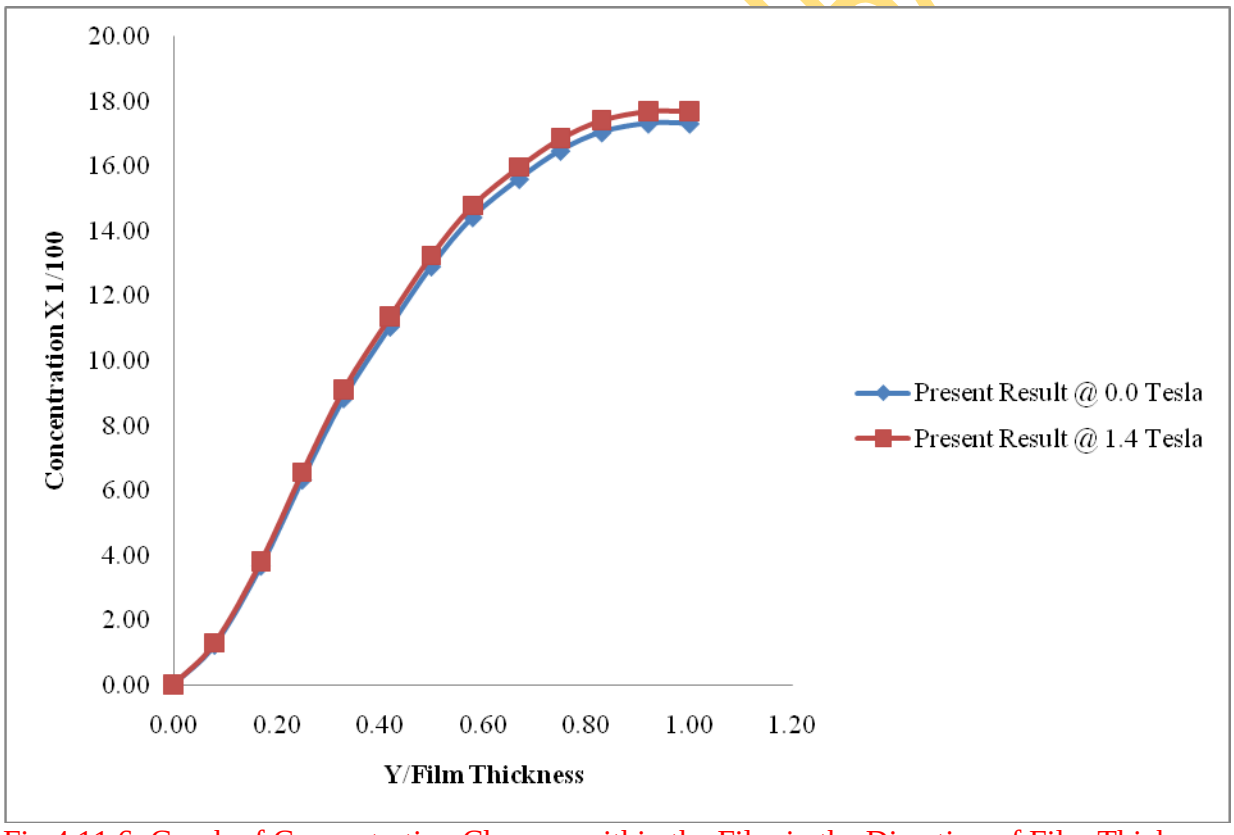

Fig.4.11.6: Graph of Concentration Changes within the Film in the Direction of Film Thickness at X=0.50m

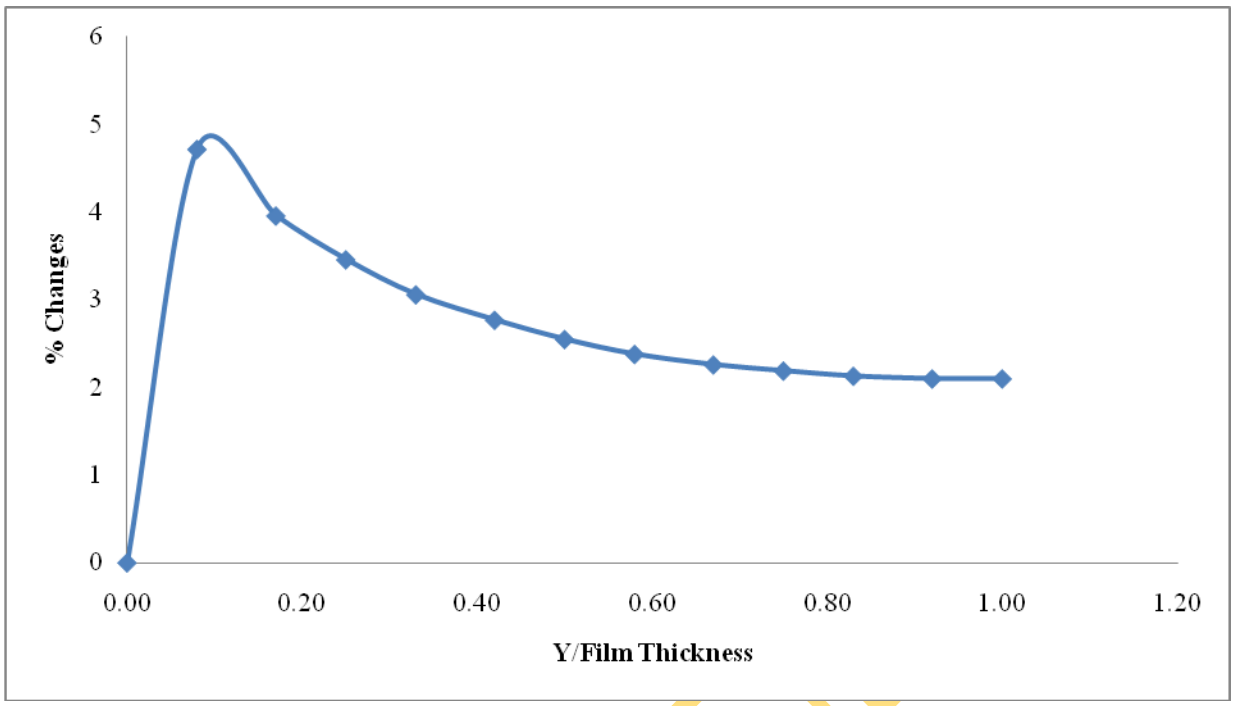

Fig.4.11.7: Graph of % Concentration Changes within the Film in the Direction of Film Thickness at 0.0 & 1.4Tesla

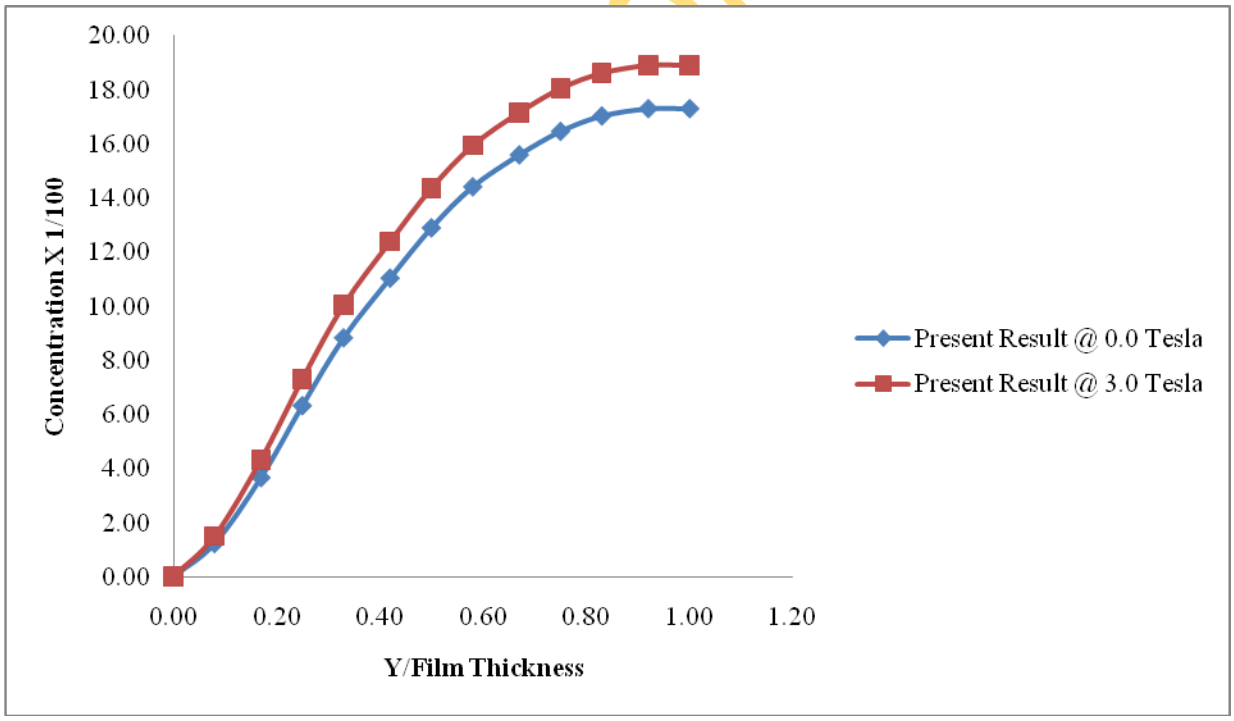

Fig.4.11.8: Graph of Concentration Changes within the Film in the Direction of Film Thickness at X=0.50m

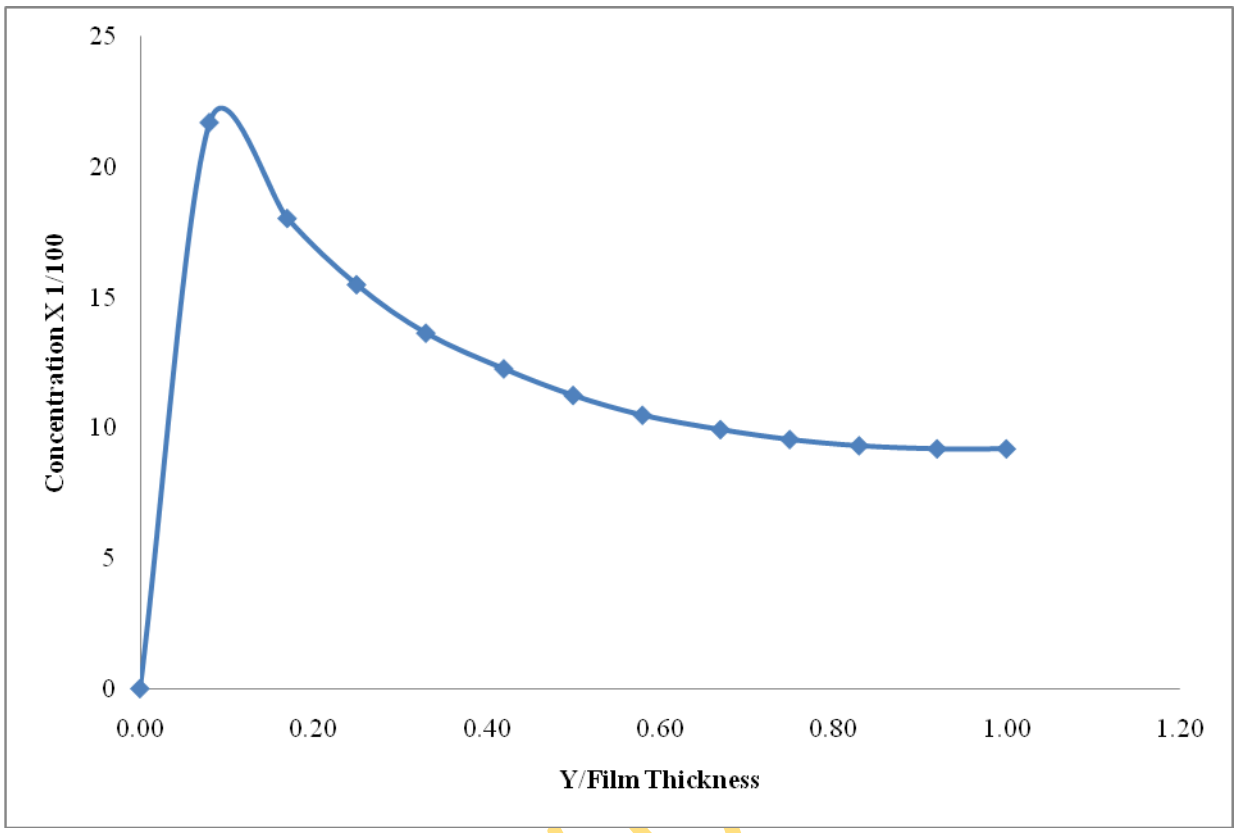

Fig.4.11.9: Graph of % Concentration Changes within the Film in the Direction of Film Thickness at 0.0 & 3.0Tesla

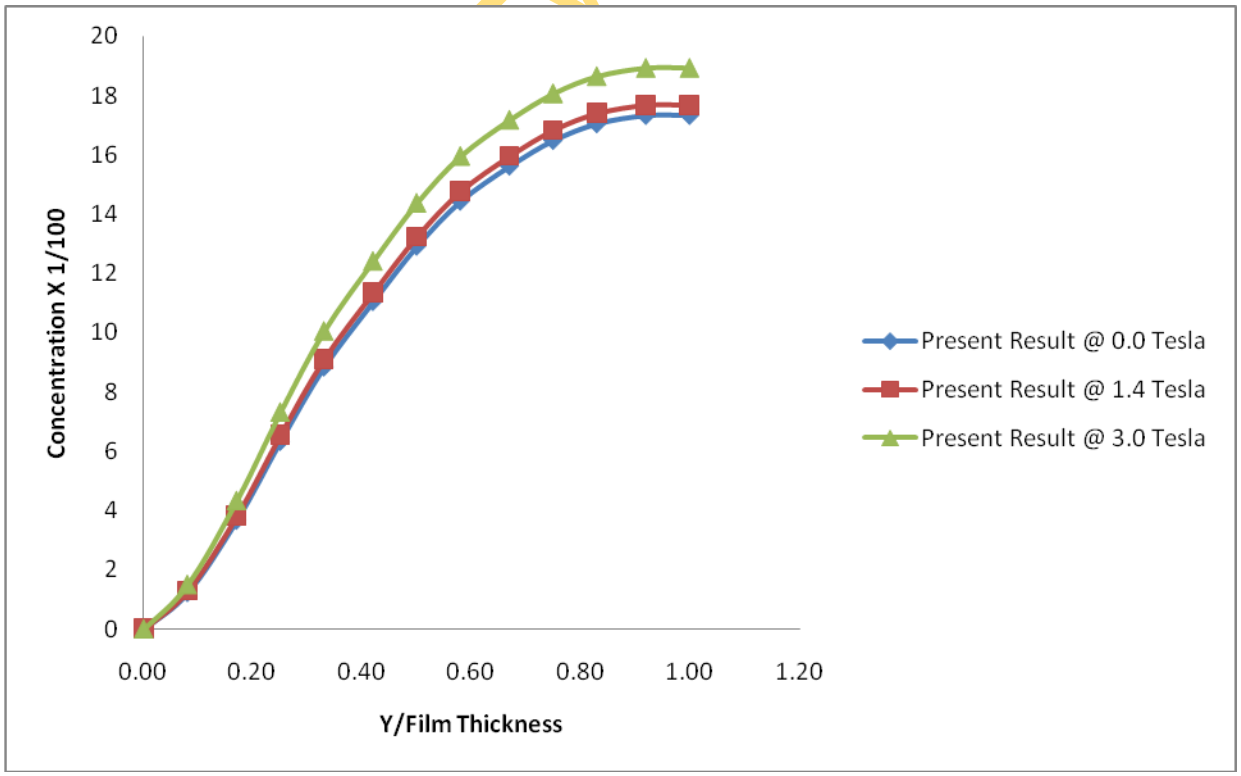

Fig.4.12: Graph of Concentration Distribution in the Direction of Film Thickness at X=0.50m

Table 4.6.1: LiBr-H_20: Concentration Changes in the direction of film thickness (δ) X=0.75m

Y/δ	BULK					
	Present Result @ 0.0 Tesla	**Present. Result @ 1.4 Tesla**	**% Changes in Y-dir**	**Present Result @ 0.0 Tesla**	**Present Result @3.0 Tesla**	**% Changes in Y-dir**
0.00	0.0000	0.0000	0.00	0.0000	0.0000	0.00
0.08	0.0018	0.0019	6.82	0.0018	0.0024	34.09
0.17	0.0091	0.0096	6.08	0.0091	0.0116	28.29
0.25	0.0206	0.0216	5.21	0.0206	0.0255	24.14
0.33	0.0339	0.0355	4.63	0.0339	0.0411	21.17
0.42	0.0474	0.0494	4.18	0.0474	0.0564	18.97
0.50	0.0599	0.0622	3.86	0.0599	0.0703	17.35
0.58	0.0708	0.0733	3.60	0.0708	0.0822	16.14
0.67	0.0796	0.0824	3.42	0.0796	0.0918	15.28
0.75	0.0864	0.0892	3.28	0.0864	0.0990	14.67
0.83	0.0909	0.0938	3.21	0.0909	0.1038	14.30
0.92	0.0931	0.0960	3.16	0.0931	0.1062	14.11
1.00	0.0931	0.0960	3.17	0.0931	0.1062	14.11

UNIVERSITY OF IBADAN

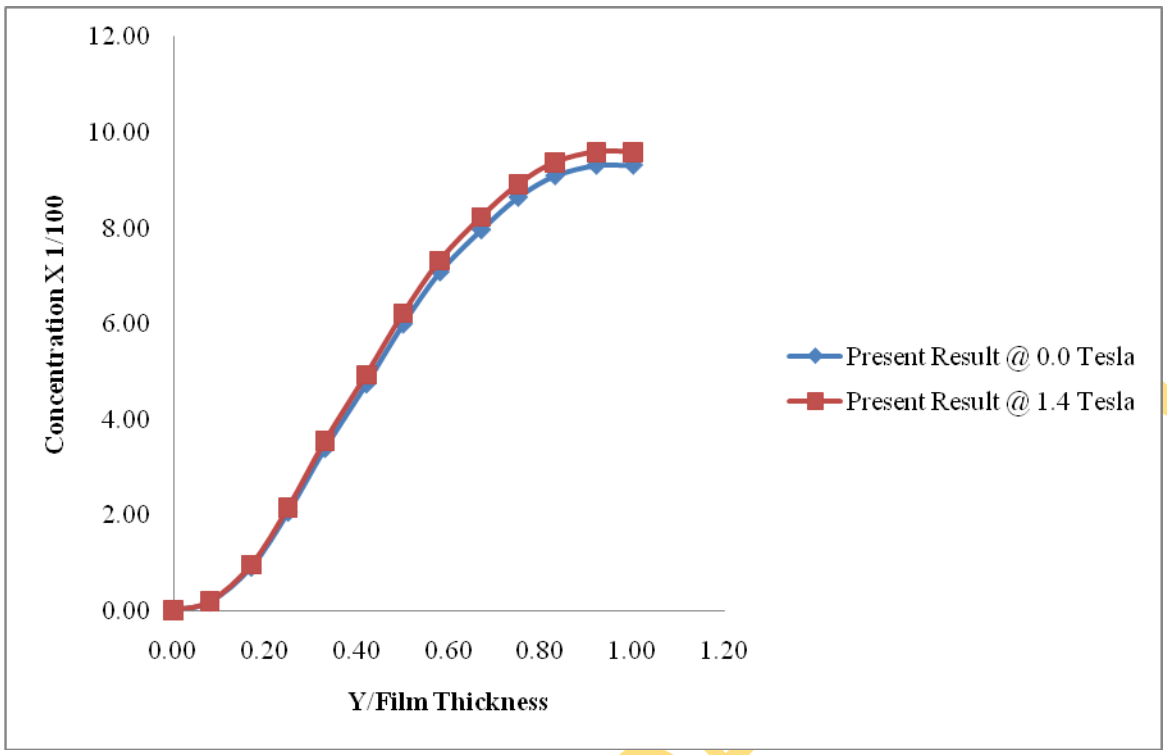

Fig.4.12.1: Graph of Concentration Changes within the Film in the Direction of Film Thickness at X=0.75m

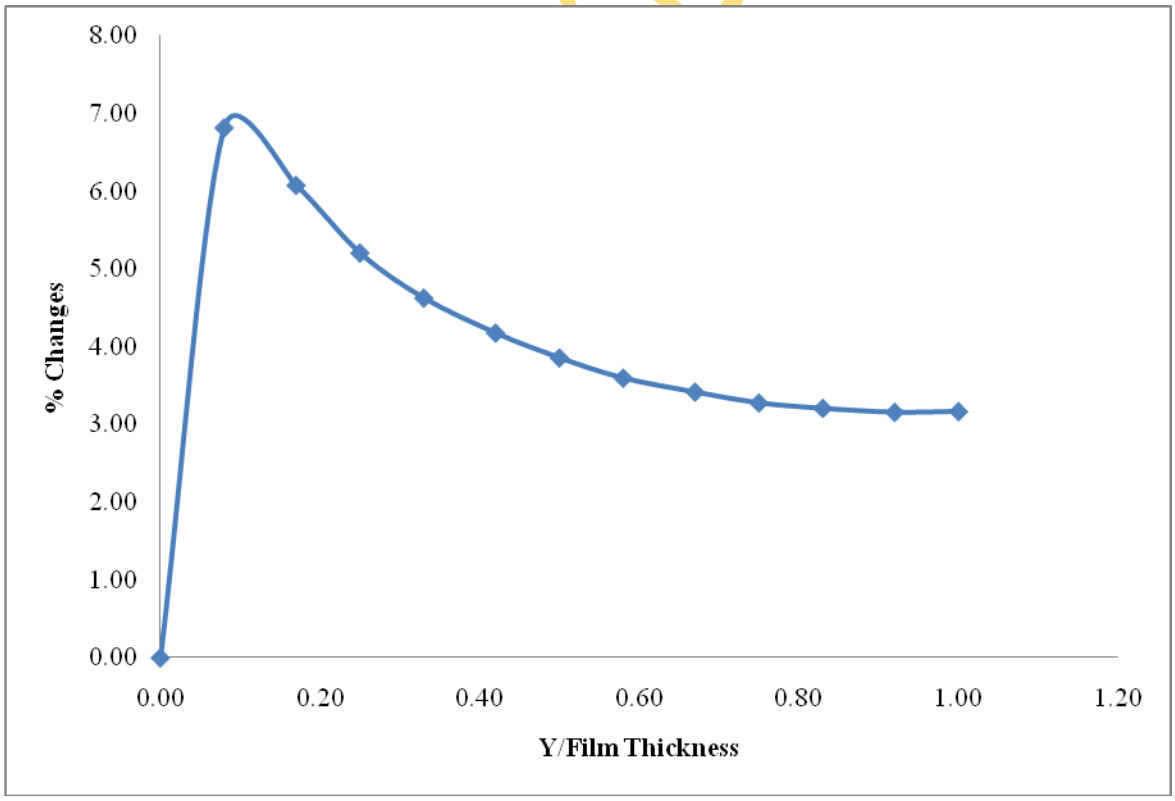

Fig.4.12.2: Graph of % Concentration Changes within the Film in the Direction of Film Thickness at 0.0 & 1.4Tesla

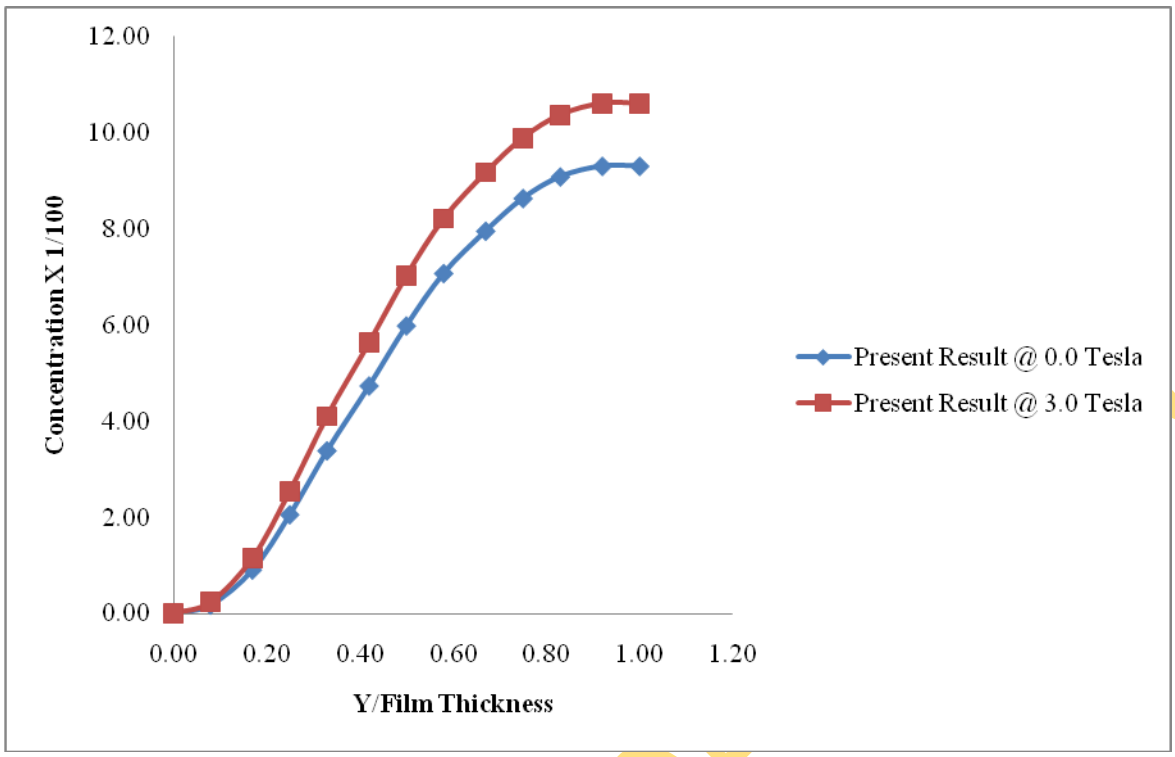

Fig.4.12.3: Graph of Concentration Changes within the Film in the Direction of Film Thickness at X=0.75m

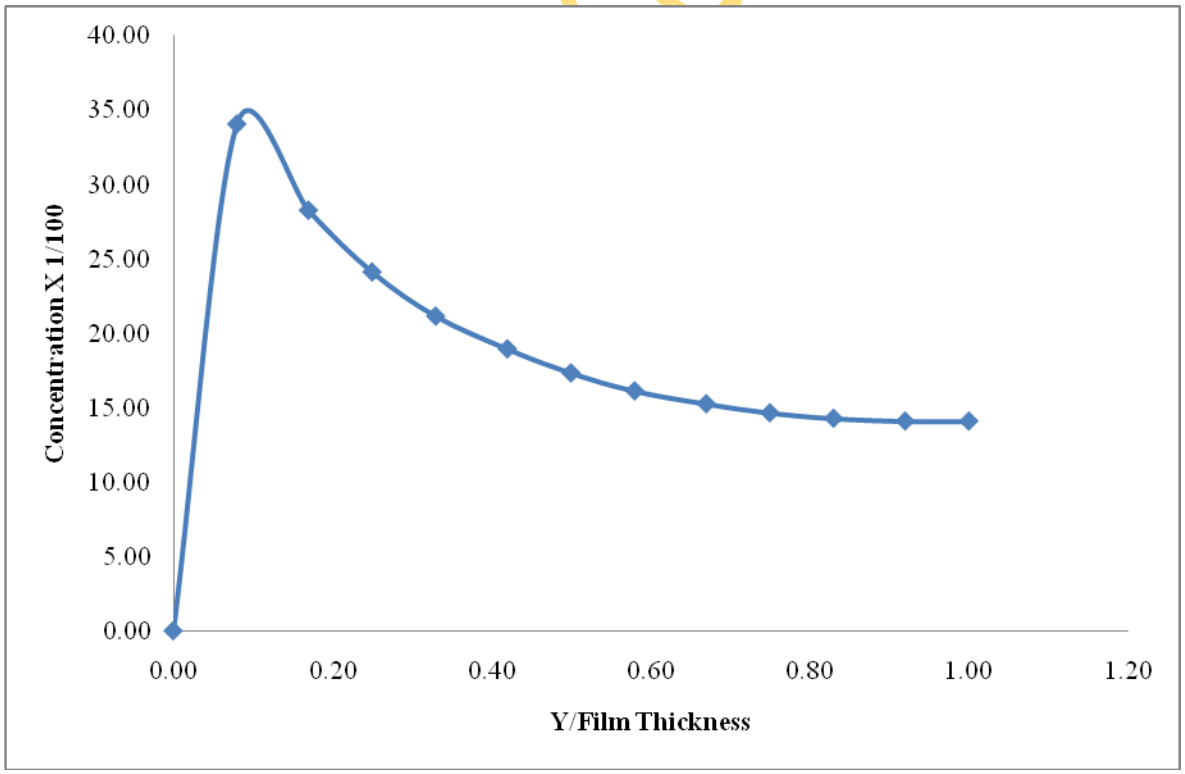

Fig.4.12.4: Graph of % Concentration Changes within the Film Thickness at 0.0 & 3.0 Tesla

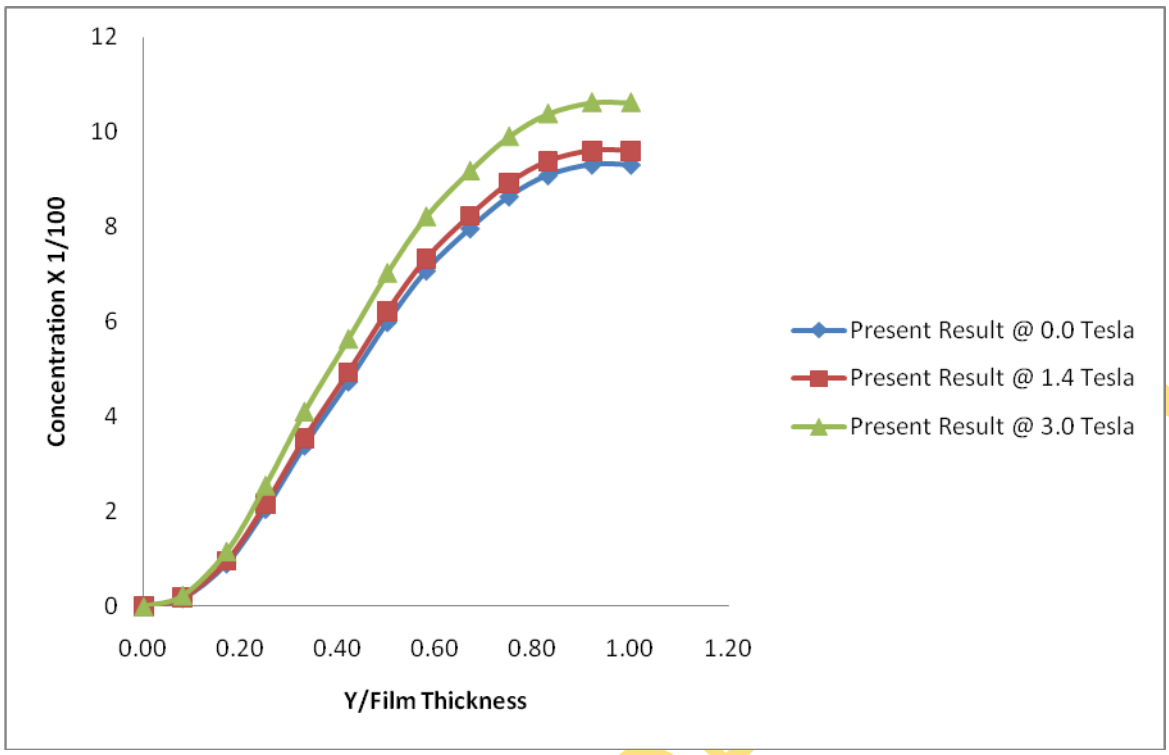

Fig.4.12.5: Graph of Concentration Distribution in the Direction of Film Thickness at X=0.75m

Table 4.6.2: LiCl-H_20: Velocity Changes in the direction of film thickness (δ) at X=0.25m

Y/δ	BULK					
	Present Result @ 0.0 Tesla	**Present. Result @ 1.4 Tesla**	**% Changes in Y-dir**	**Present Result @ 0.0 Tesla**	**Present Result @3.0 Tesla**	**% Changes in Y-dir**
0.00	0.0000	0.0000	0.00	0.000	0.0000	0.00
0.08	0.0113	0.0115	1.88	0.0113	0.0122	8.69
0.17	0.0222	0.0226	1.82	0.0222	0.0240	8.40
0.25	0.0325	0.0331	1.76	0.0325	0.0351	8.15
0.33	0.0421	0.0428	1.72	0.0421	0.0454	7.94
0.42	0.0508	0.0516	1.68	0.0508	0.0547	7.76

UNIVERSITY OF

0.50	0.0585	0.0594	1.65	0.0585	0.0629	7.62
0.58	0.0650	0.0661	1.62	0.0650	0.0699	7.50
0.67	0.0704	0.0715	1.60	0.0704	0.0756	7.41
0.75	0.0744	0.0756	1.59	0.0744	0.0799	7.35
0.83	0.0772	0.0784	1.58	0.0772	0.0828	7.31
0.92	0.0785	0.0797	1.57	0.0785	0.0842	7.29
1.00	0.0785	0.0797	1.57	0.0785	0.0842	7.29

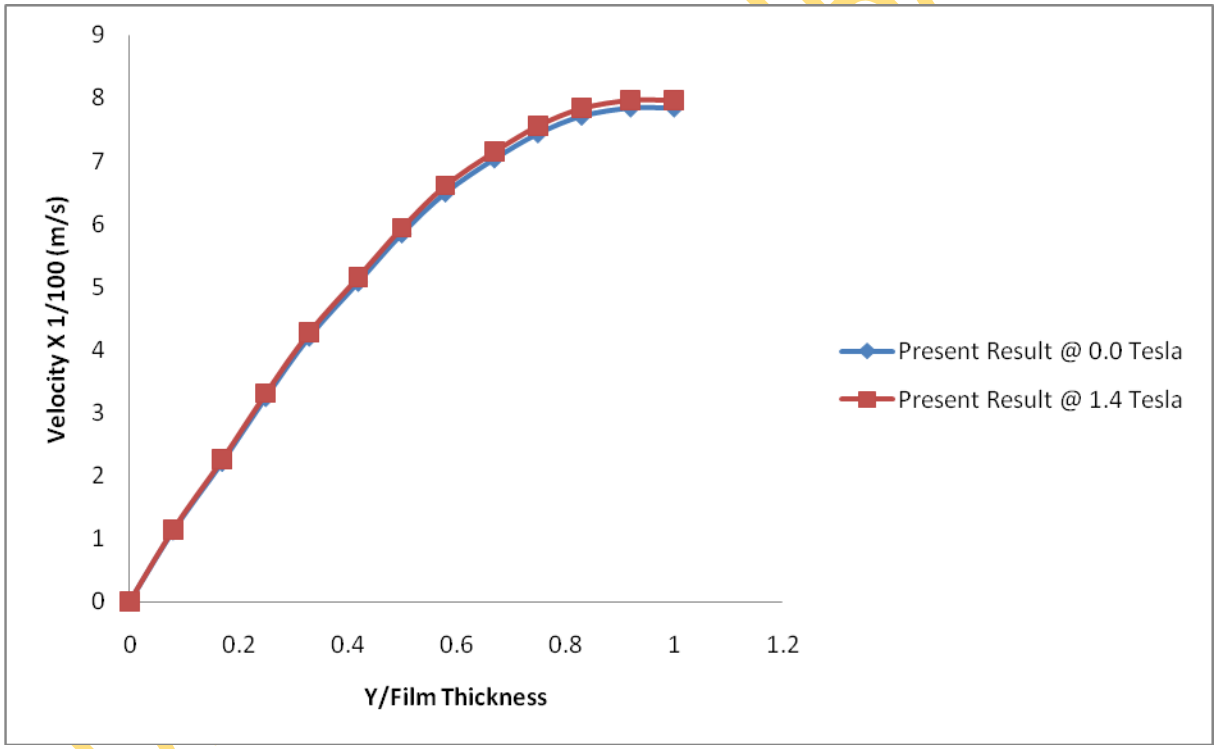

Fig.4.12.6: Graph of Velocity Changes within the Film in the Direction of Film Thickness at X =0.25m

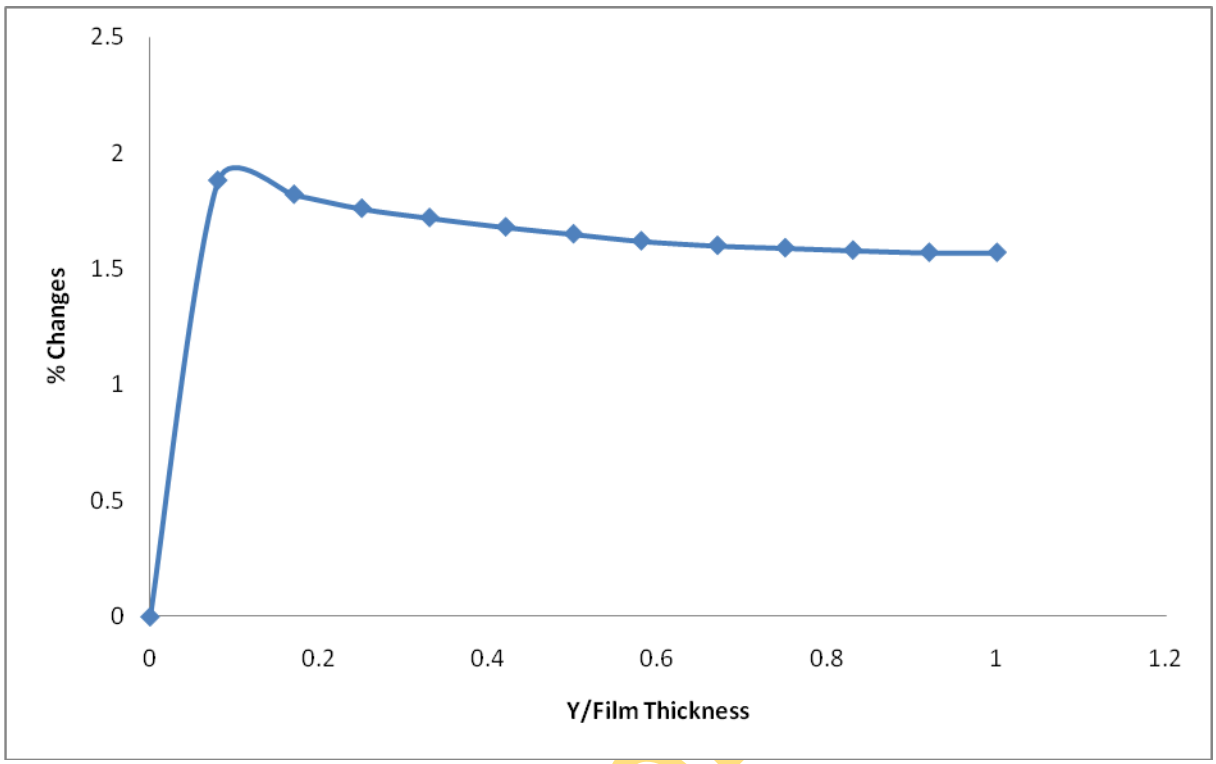

Fig.4.12.7: Graph of Velocity Changes within the Film in the Direction of Film Thickness at 0.0 & 1.4 Tesla

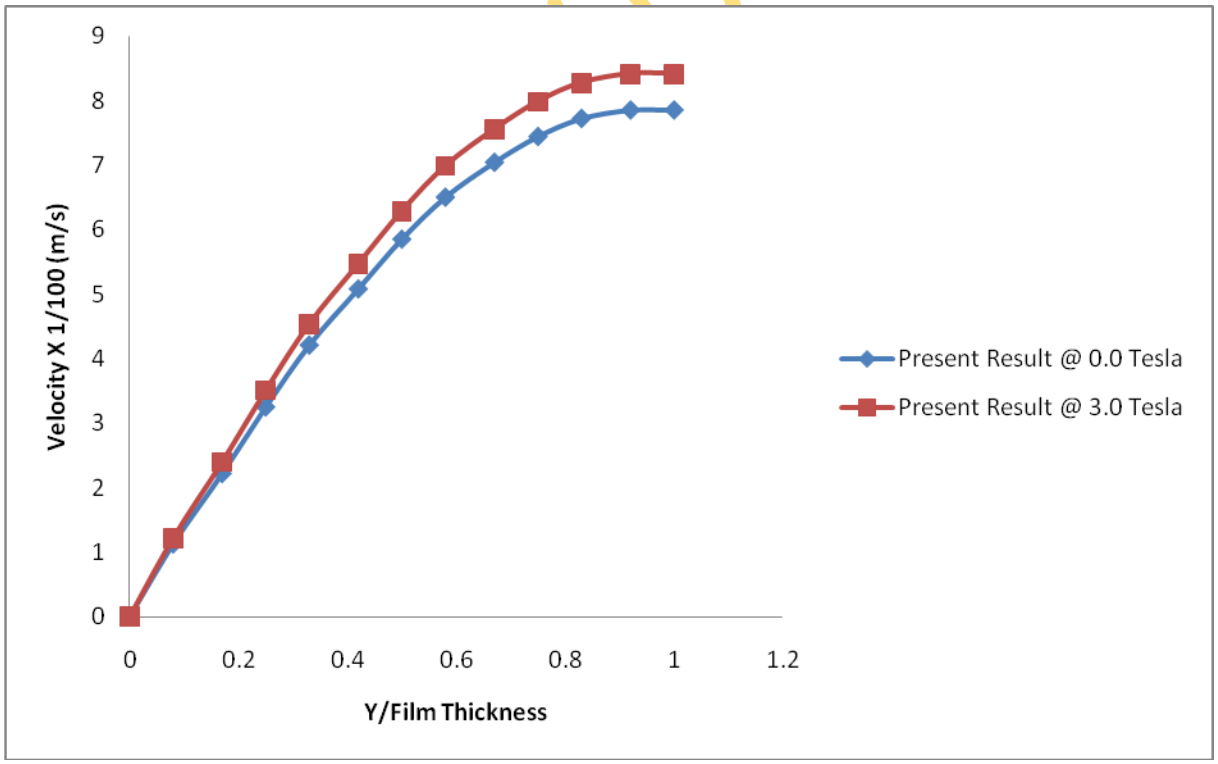

Fig.4.12.8: Graph of Velocity Changes within the Film in the Direction of Film Thickness at X=0.25m

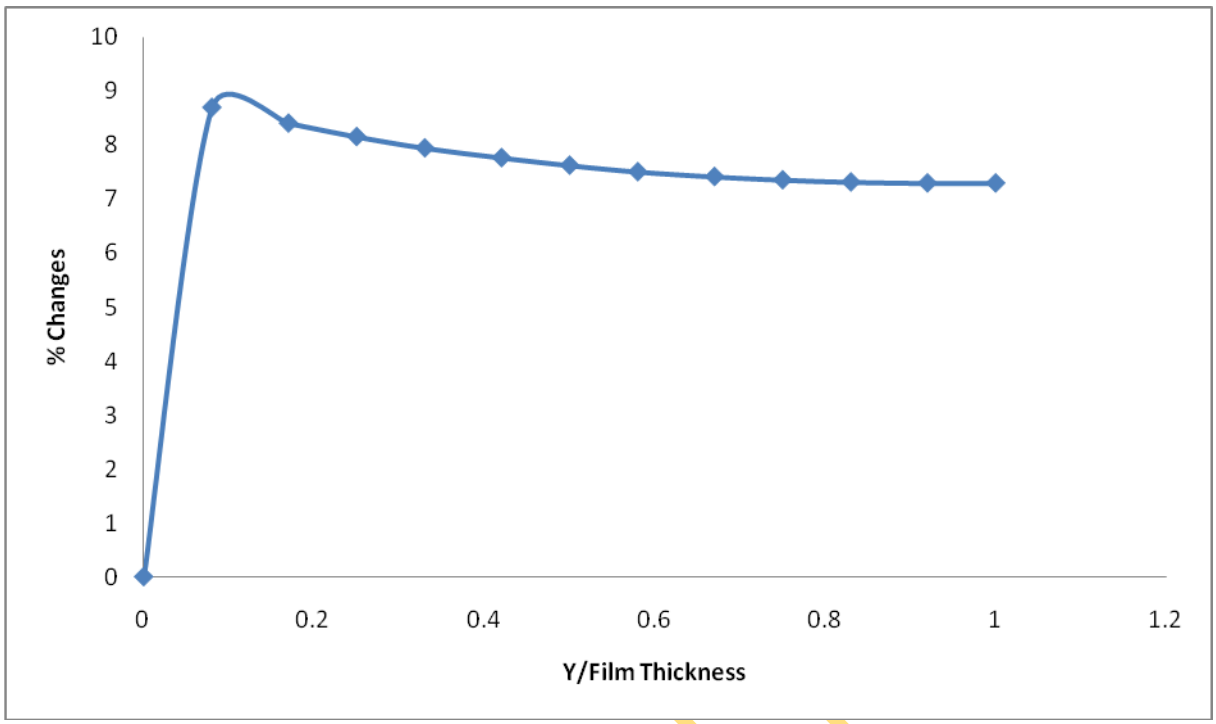

Fig.4.12.9: Graph of % Velocity Changes within the Film in the Direction of Film Thickness at 0.0 & 3.0Tesla

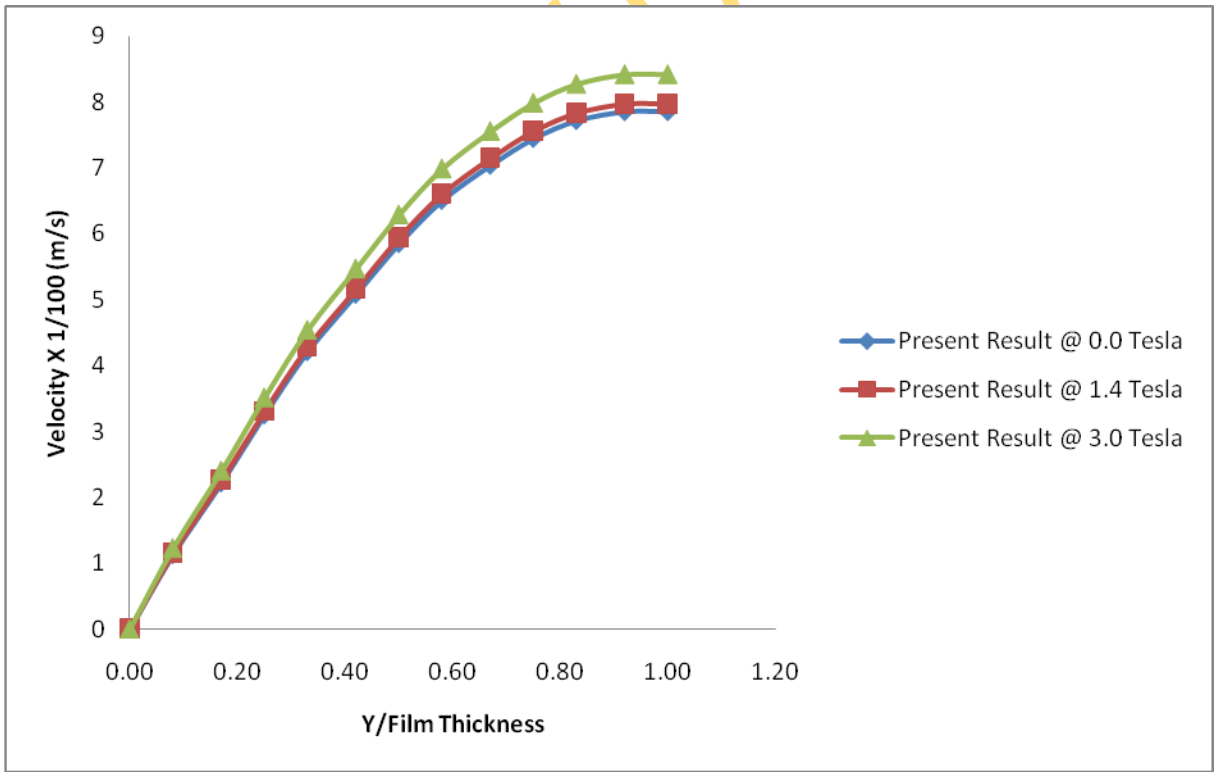

Fig.4.13: Graph of Velocity Distribution in the Direction of Film Thickness at X=0.25m

Table 4.6.3: LiCl-H_20: Velocity Changes in the direction of film thickness (δ) at X=0.50m

Y/δ	BULK					
	Present Result @ 0.0 Tesla	**Present. Result @ 1.4 Tesla**	**% Changes in Y-dir**	**Present Result @ 0.0 Tesla**	**Present Result @3.0 Tesla**	**% Changes in Y-dir**
0.00	0.0000	0.0000	0.00	0.000	0.0000	0.00
0.08	0.0113	0.0115	1.88	0.0113	0.0122	8.70
0.17	0.0222	0.0226	1.82	0.0222	0.0240	8.40
0.25	0.0325	0.0331	1.76	0.0325	0.0351	8.15
0.33	0.0421	0.0428	1.71	0.0421	0.0454	7.94
0.42	0.0508	0.0517	1.68	0.0508	0.0547	7.76
0.50	0.0585	0.0594	1.65	0.0585	0.0629	7.62
0.58	0.0650	0.0661	1.62	0.0650	0.0699	7.50
0.67	0.0704	0.0715	1.60	0.0704	0.0756	7.41
0.75	0.0744	0.0756	1.59	0.0744	0.0799	7.35
0.83	0.0772	0.0784	1.58	0.0772	0.0828	7.31
0.92	0.0785	0.0797	1.57	0.0785	0.0842	7.29
1.00	0.0785	0.0797	1.57	0.0785	0.0842	7.29

UNIVERSITY OF IBADAN

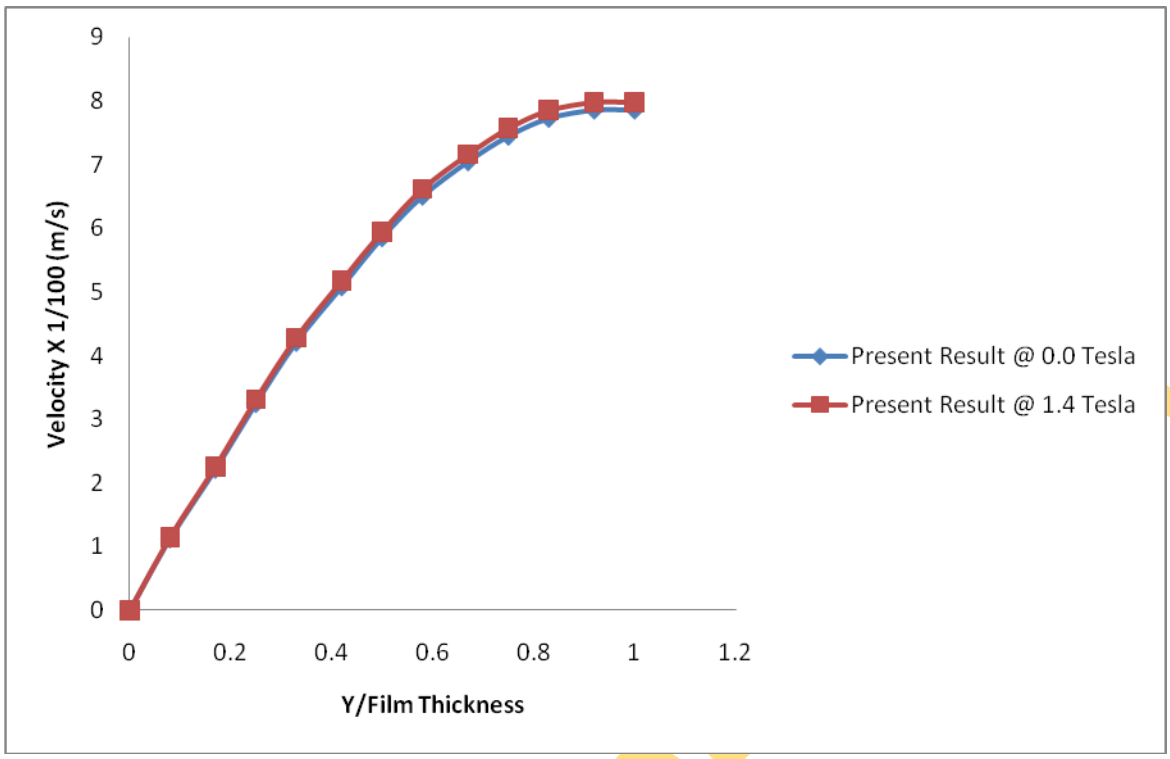

Fig.4.13.1: Graph of Velocity Changes within the Film in the Direction of Film Thickness at X=0.50m

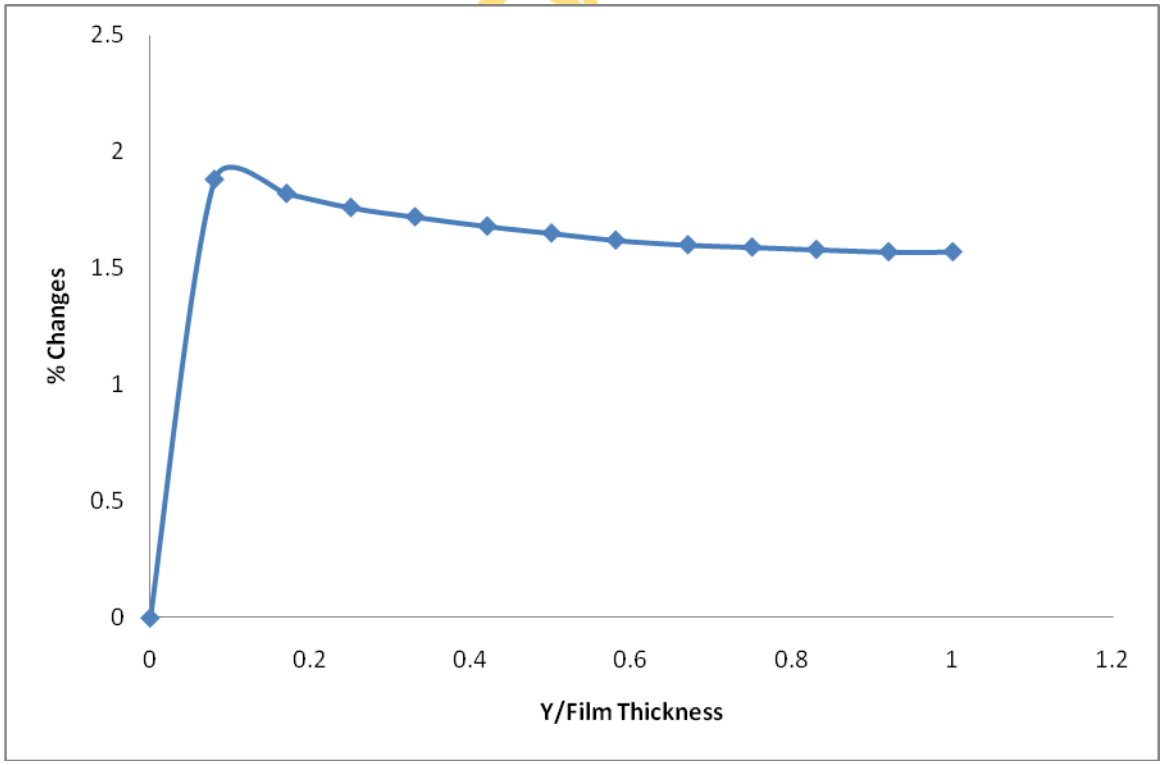

Fig.4.13.2: Graph of % Velocity Changes within the Film in the Direction of Film Thickness at 0.0 & 1.4Tesla

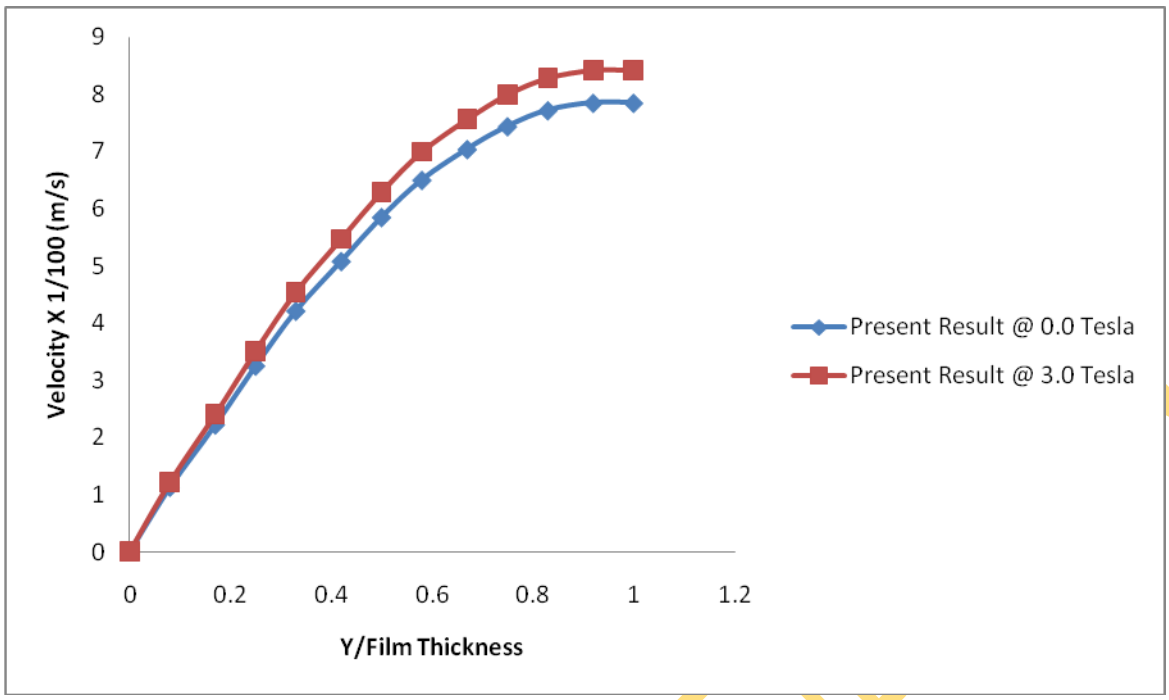

Fig.4.13.3: Graph of Velocity Changes within the Film in the Direction of Film Thickness at X=0.50m

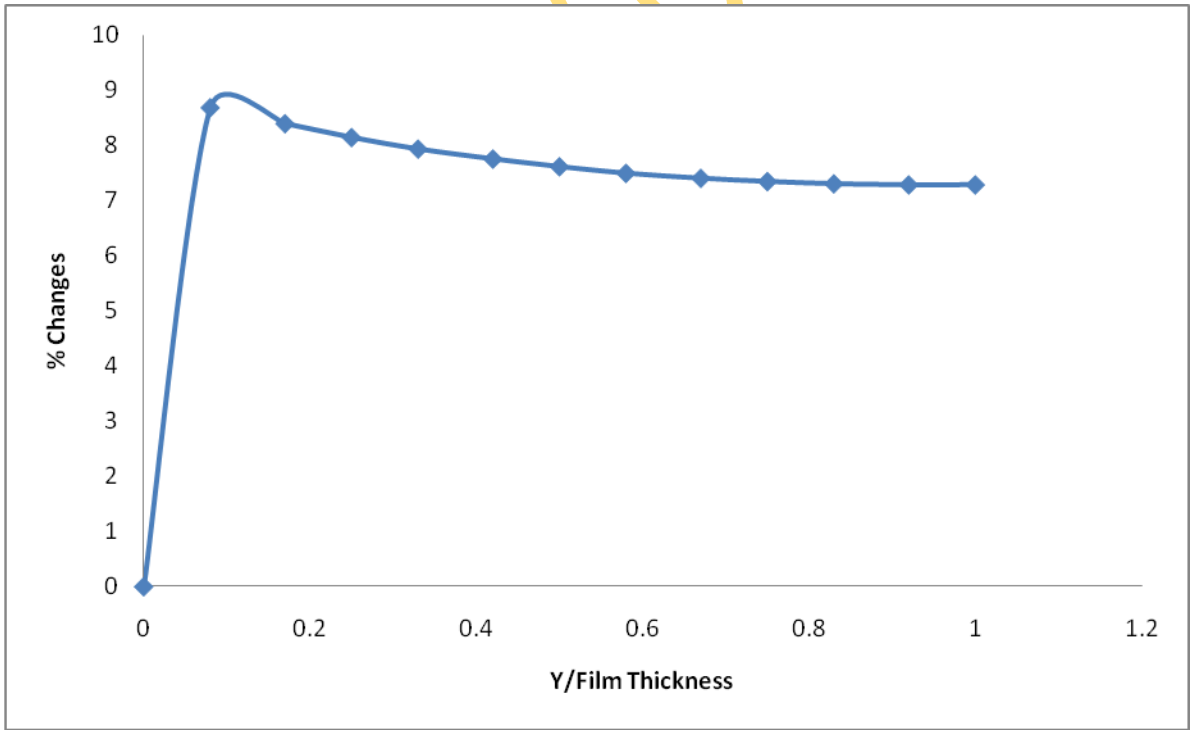

Fig.4.13.4: Graph of % Velocity Changes within the Film in the Direction of Film Thickness at 0.0 & 3.0 Tesla

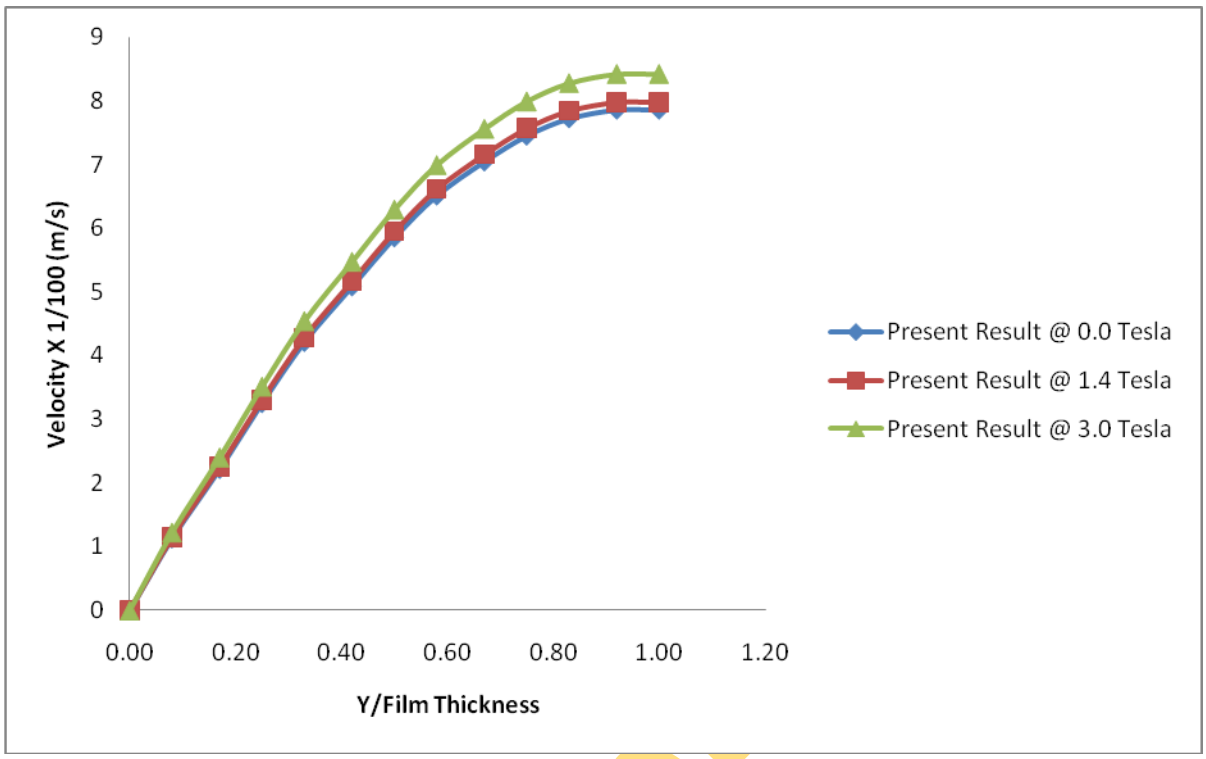

Fig.4.13.5: Graph of Velocity Distribution in the Direction of Film Thickness at X=0.50m

Table 4.6.4: LiCl-H_20: Velocity Changes in the direction of film thickness (δ) at X=0.75m

Y/ δ	BULK					
	Present Result @ 0.0 Tesla	**Present. Result @ 1.4 Tesla**	**% Changes in Y-dir**	**Present Result @ 0.0 Tesla**	**Present Result @3.0 Tesla**	**% Changes in Y-dir**
0.00	0.000	0.0000	0.00	0.000	0.0000	0.00
0.08	0.0113	0.0115	1.88	0.0113	0.0122	8.70
0.17	0.0222	0.0226	1.82	0.0222	0.0240	8.40
0.25	0.0325	0.0331	1.76	0.0325	0.0351	8.15
0.33	0.0421	0.0428	1.71	0.0421	0.0454	7.94
0.42	0.0508	0.0517	1.68	0.0508	0.0547	7.76

UNIVERSITY OF

0.50	0.0585	0.0594	1.65	0.0585	0.0629	7.62
0.58	0.0650	0.0661	1.62	0.0650	0.0699	7.50
0.67	0.0704	0.0715	1.60	0.0704	0.0756	7.41
0.75	0.0744	0.0756	1.59	0.0744	0.0799	7.35
0.83	0.0772	0.0784	1.58	0.0772	0.0828	7.31
0.92	0.0785	0.0797	1.57	0.0785	0.0842	7.29
1.00	0.0785	0.0797	1.57	0.0785	0.0842	7.29

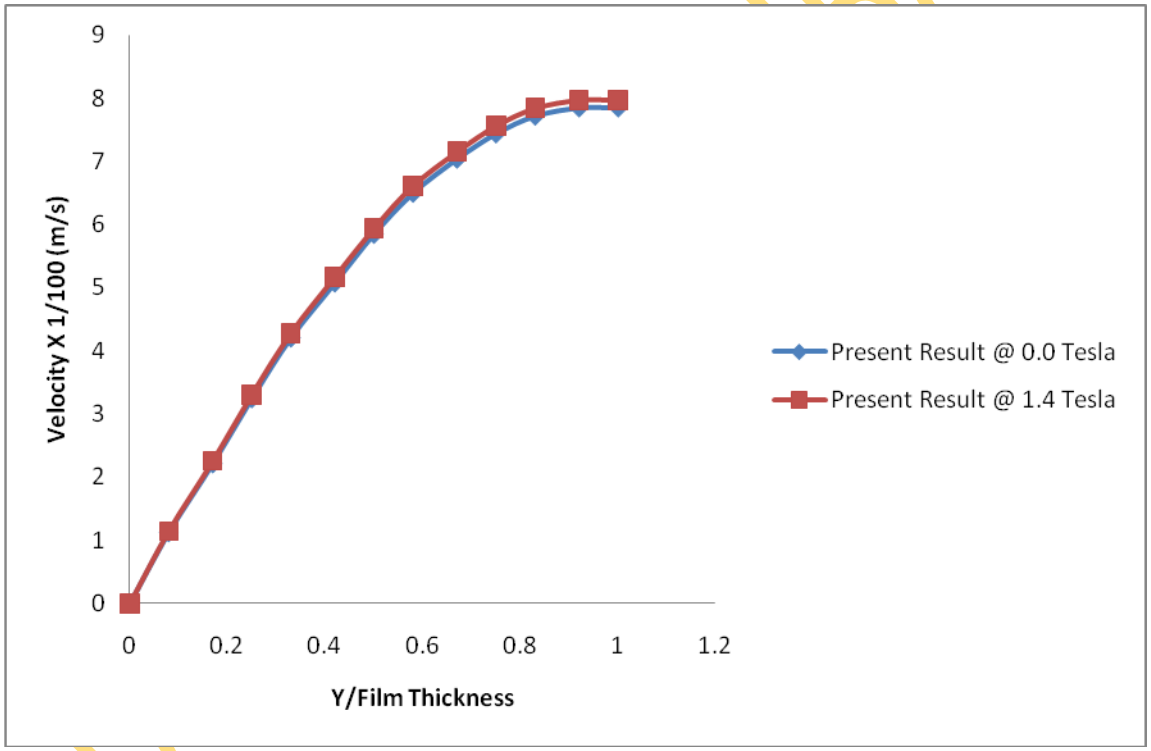

Fig.4.13.6: Graph of Velocity Changes within the Film in the Direction of Film Thickness at X=0.75m

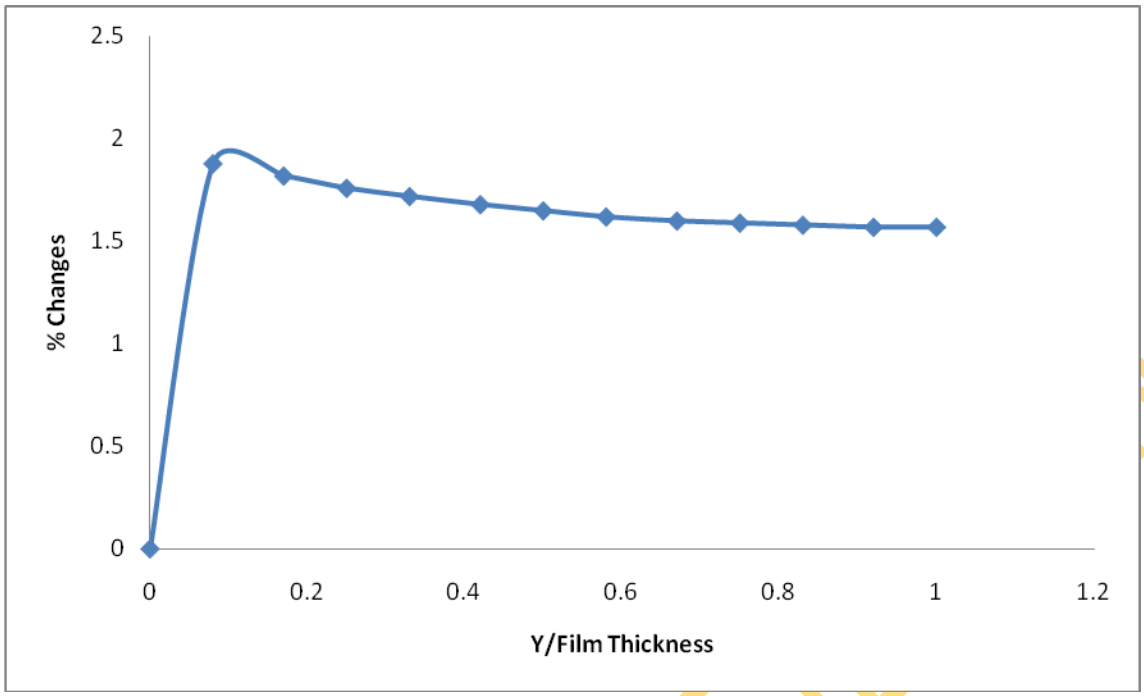

Fig.4.13.7: Graph of % Velocity Changes within the Film in the Direction of Film Thickness at 0.0 & 1.4 Tesla

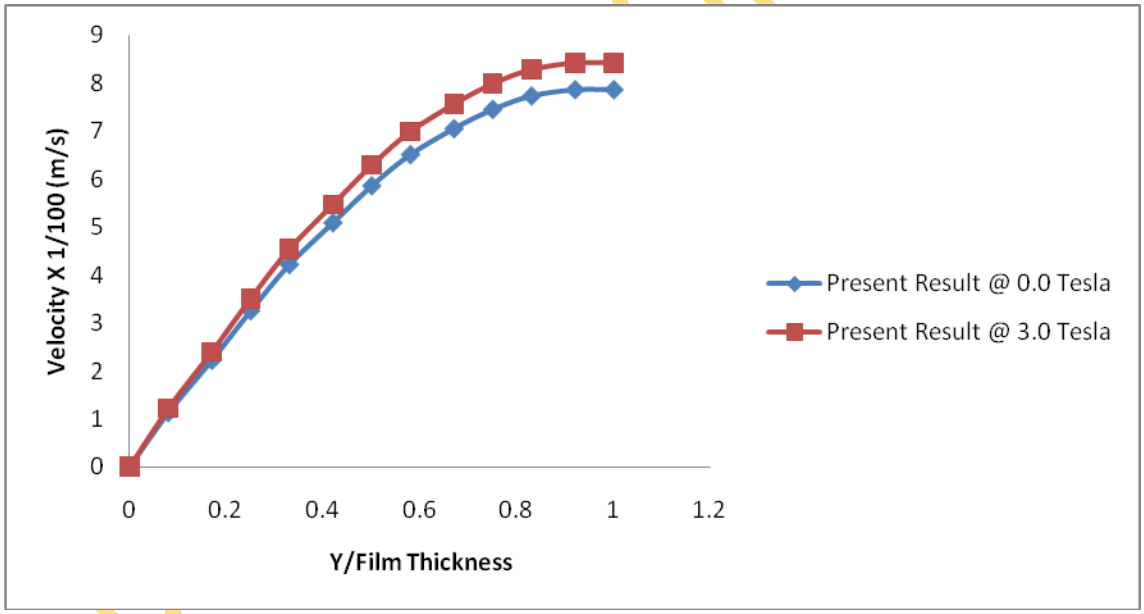

Fig.4.13.8: Graph of Velocity Changes within the Film in the direction of Film Thickness at X=0.75m

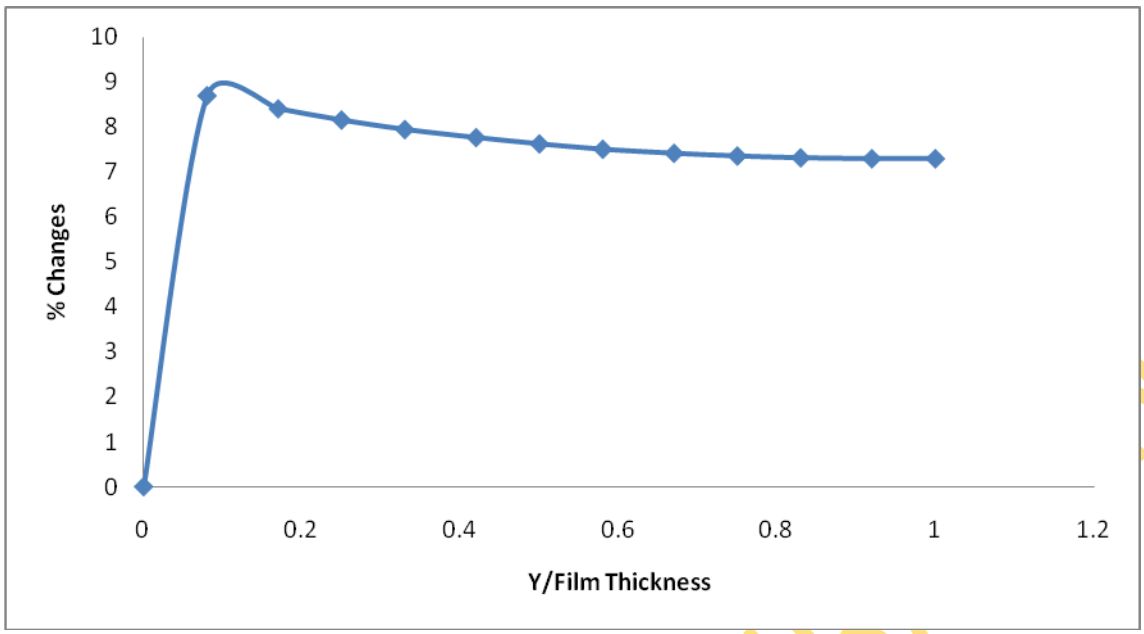

Fig.4.13.9: Graph of % Velocity Changes within the Film in the Direction of Film Thickness at 0.0 & 3.0Tesla

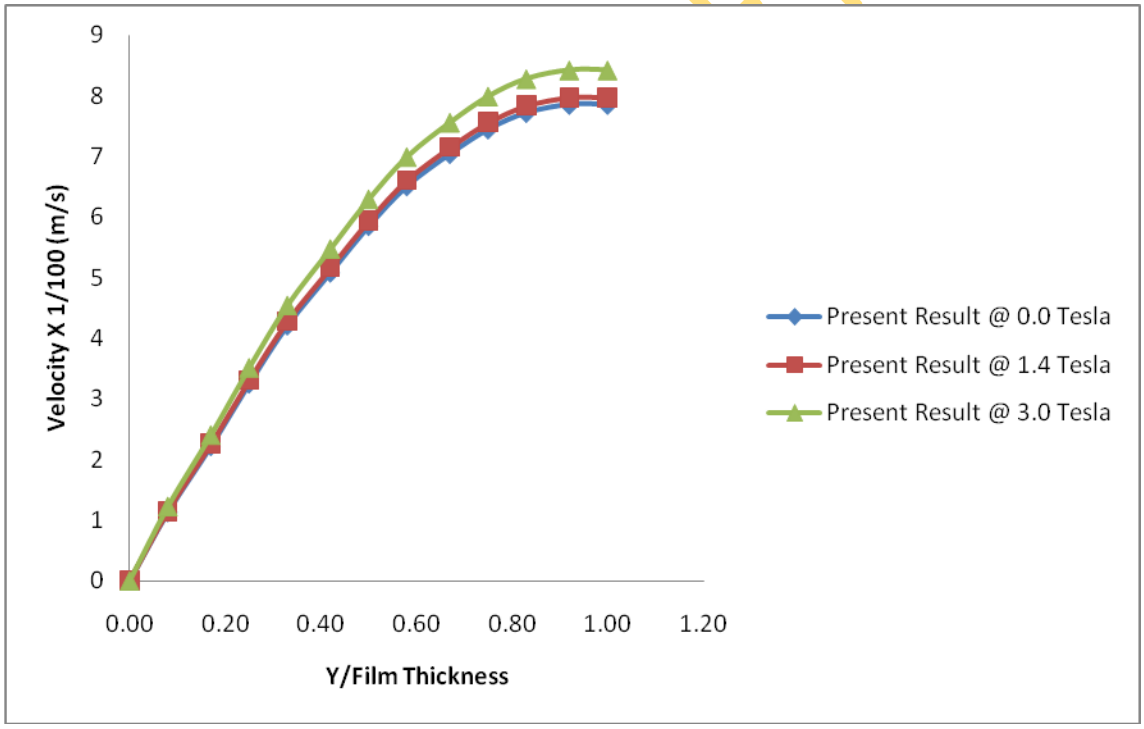

Fig.4.14: Graph of Velocity Distribution in the Direction of Film Thickness at 0.75m

Table 4.6.5: LiCl-H_20: Temperature Changes in the direction of film thickness (δ) at X=0.25m

Y/δ	BULK					
	Present Result @ 0.0 Tesla	**Present. Result @ 1.4 Tesla**	**% Changes in Y-dir**	**Present Result @ 0.0 Tesla**	**Present Result @3.0 Tesla**	**% Changes in Y-dir**
0.00	35.00	35.00	0.00	35.00	35.00	0.00
0.08	30.17	30.17	0.00	30.17	30.17	0.00
0.17	30.17	30.17	0.00	30.17	30.17	0.00
0.25	30.17	30.17	0.00	30.17	30.17	0.00
0.33	30.17	30.17	0.00	30.17	30.17	0.00
0.42	30.17	30.17	0.00	30.17	30.17	0.00
0.50	30.17	30.17	0.00	30.17	30.17	0.00
0.58	30.17	30.17	0.00	30.17	30.17	0.00
0.67	30.17	30.17	0.00	30.17	30.17	0.00
0.75	30.17	30.17	0.00	30.17	30.17	0.00
0.83	30.17	30.17	0.00	30.17	30.17	0.00
0.92	30.17	30.17	0.00	30.17	30.17	0.00
1.00	32.25	32.25	0.00	32.25	32.25	0.00

UNIVERSITY OF IBADAN

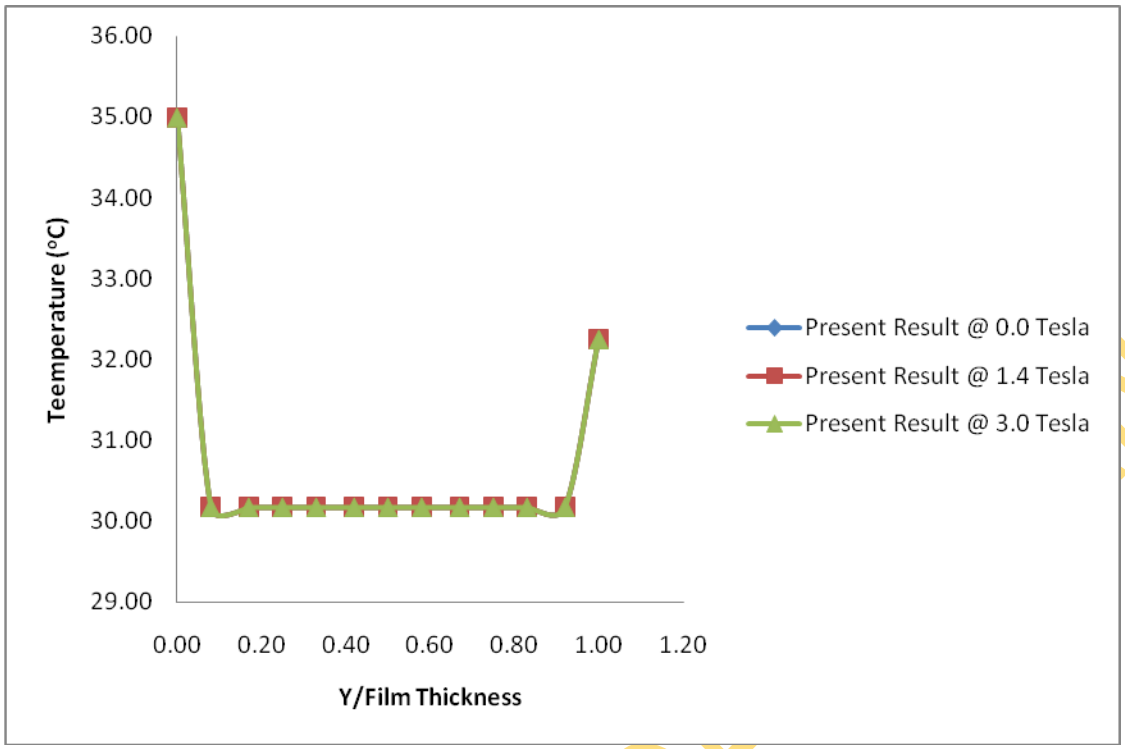

Fig.4.14.1: Graph of Temperature Distribution in the Direction of Film Thickness at X=0.25m

Table 4.6.6: LiCl-H_20: Temperature Changes in the direction of film thickness (δ) at X=0.50m

Y/δ	BULK					
	Present Result @ 0.0 Tesla	**Present. Result @ 1.4 Tesla**	**% Changes in Y-dir**	**Present Result @ 0.0 Tesla**	**Present Result @3.0 Tesla**	**% Changes in Y-dir**
0.00	35.00	35.00	0.00	35.00	35.00	0.00
0.08	30.11	30.11	0.00	30.11	30.11	0.00
0.17	30.11	30.11	0.00	30.11	30.11	0.00
0.25	30.11	30.11	0.00	30.11	30.11	0.00
0.33	30.11	30.11	0.00	30.11	30.11	0.00
0.42	30.11	30.11	0.00	30.11	30.11	0.00
0.50	30.11	30.11	0.00	30.11	30.11	0.00

UNIVERSITY OF

0.58	30.11	30.11	0.00	30.11	30.11	0.00
0.67	30.11	30.11	0.00	30.11	30.11	0.00
0.75	30.11	30.11	0.00	30.11	30.11	0.00
0.83	30.11	30.11	0.00	30.11	30.11	0.00
0.92	30.11	30.11	0.00	30.11	30.11	0.00
1.00	31.50	31.50	0.00	31.50	31.50	0.00

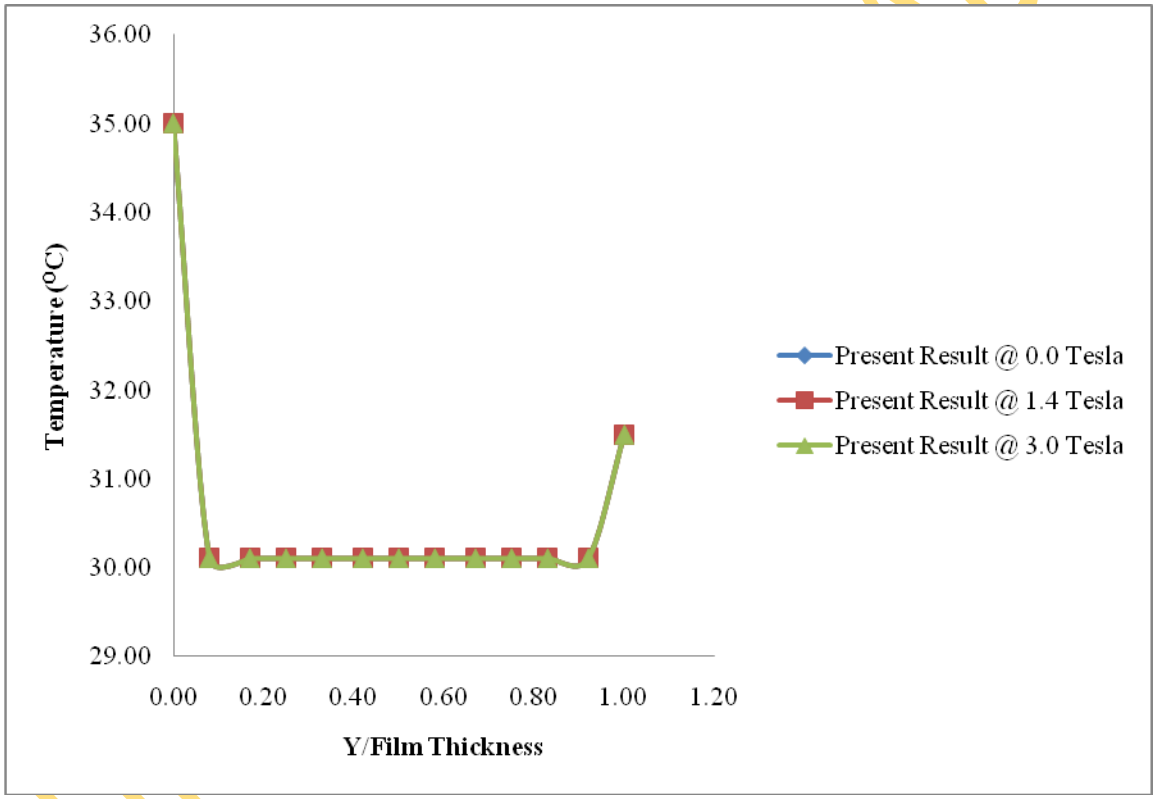

Fig.4.14.2: Graph of Temperature Changes within the Film in the Direction of Film Thickness at X=0.50m

Table 4.6.7 LiCl-H_20: Temperature Changes in the direction of film thickness (δ) at X=0.75m

Y/δ	BULK					
	Present Result @ 0.0 Tesla	**Present. Result @ 1.4 Tesla**	**% Changes in Y-dir**	**Present Result @ 0.0 Tesla**	**Present Result @3.0 Tesla**	**% Changes in Y-dir**
0.00	35.00	35.00	0.00	35.00	35.00	0.00
0.08	30.05	30.05	0.00	30.05	30.05	0.00
0.17	30.05	30.05	0.00	30.05	30.05	0.00
0.25	30.05	30.05	0.00	30.05	30.05	0.00
0.33	30.05	30.05	0.00	30.05	30.05	0.00
0.42	30.05	30.05	0.00	30.05	30.05	0.00
0.50	30.05	30.05	0.00	30.05	30.05	0.00
0.58	30.05	30.05	0.00	30.05	30.05	0.00
0.67	30.05	30.05	0.00	30.05	30.05	0.00
0.75	30.05	30.05	0.00	30.05	30.05	0.00
0.83	30.05	30.05	0.00	30.05	30.05	0.00
0.92	30.05	30.05	0.00	30.05	30.05	0.00
1.00	30.75	30.75	0.00	30.75	30.75	0.00

UNIVERSITY OF IBADAN

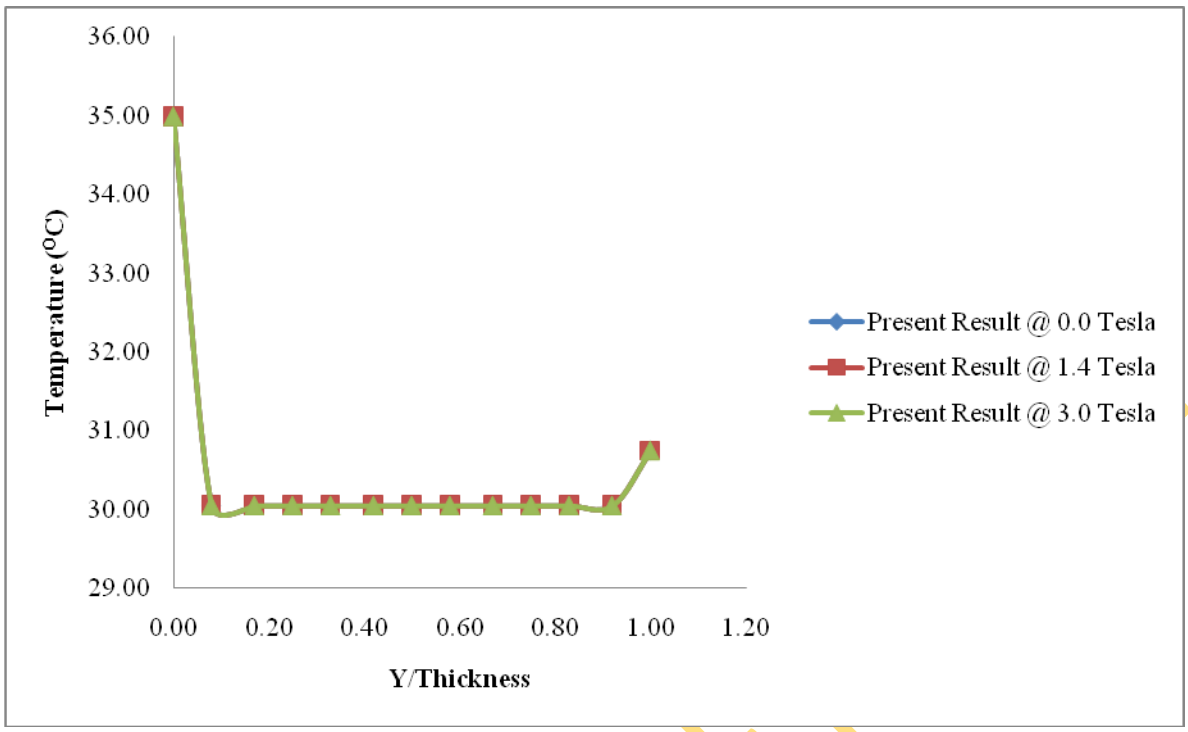

Fig.4.14.3: Graph of Temperature Changes within the Film in the Direction of Film Thickness at X=0.75m

Table 4.6.8: LiCl-H_20: Concentration Changes in the direction of film thickness (δ) at X=0.25m

Y/δ	BULK					
	Present Result @ 0.0 Tesla	**Present. Result @ 1.4 Tesla**	**% Changes in Y-dir**	**Present Result @ 0.0 Tesla**	**Present Result @3.0 Tesla**	**% Changes in Y-dir**
0.00	0.0000	0.0000	0.00	0.0000	0.0000	0.00
0.08	0.0593	0.0603	1.64	0.0593	0.0638	7.47
0.17	0.1034	0.1050	1.39	0.1034	0.1101	6.35
0.25	0.1369	0.1386	1.22	0.1369	0.1445	5.53
0.33	0.1627	0.1645	1.09	0.1627	0.1707	4.92
0.42	0.1827	0.1845	0.99	0.1827	0.1909	4.47

UNIVERSITY OF

0.50	0.1982	0.1999	0.91	0.1982	0.2063	4.12
0.58	0.2100	0.2118	0.86	0.2100	0.2181	3.86
0.67	0.2186	0.2206	0.81	0.2186	0.2269	3.67
0.75	0.2251	0.2269	0.77	0.2251	0.2331	3.55
0.83	0.2292	0.2309	0.77	0.2292	0.2371	3.46
0.92	0.2311	0.2329	0.76	0.2311	0.2391	3.42
1.00	0.2311	0.2329	0.76	0.2311	0.2390	3.42

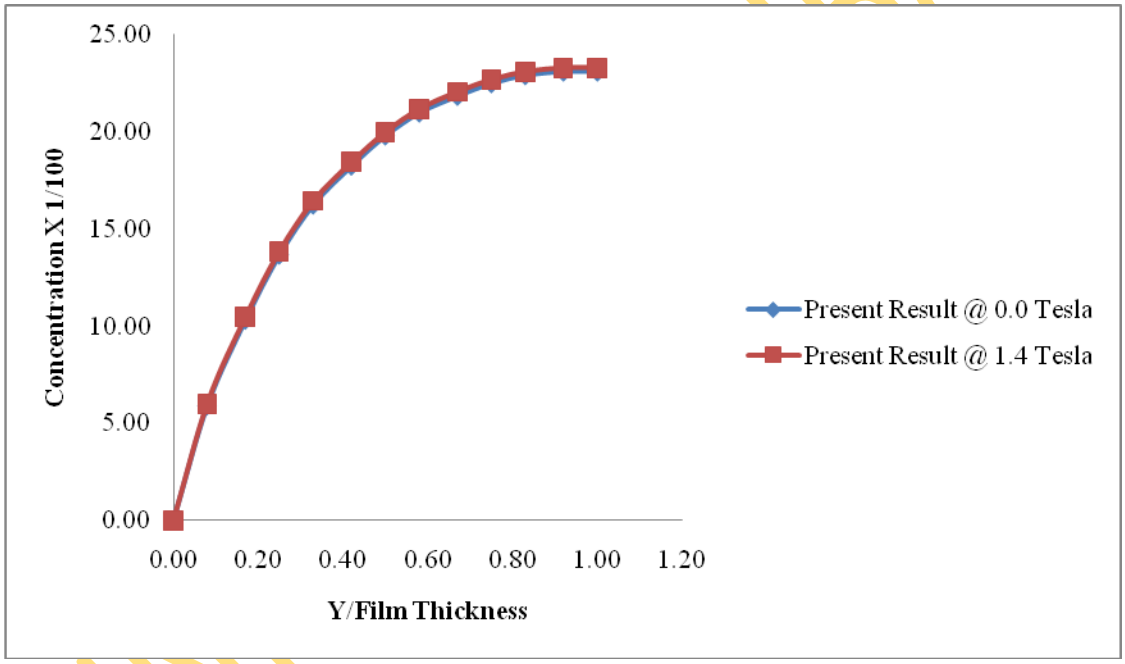

Fig.4.14.4: Graph of Concentration Changes within the Film in the Direction of Film Thickness at X=0.25m

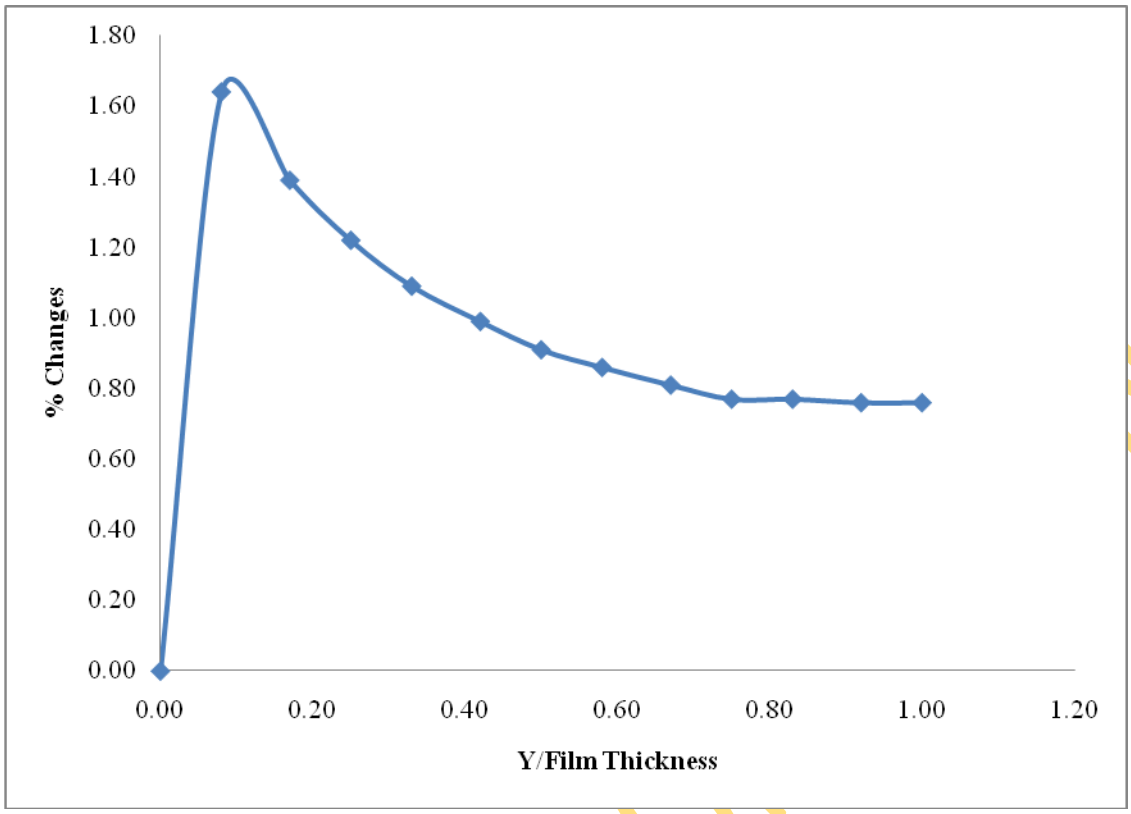

Fig.4.14.5: Graph of % Concentration Changes within the Film in the Direction of Film Thickness at 0.0 & 1.4Tesla

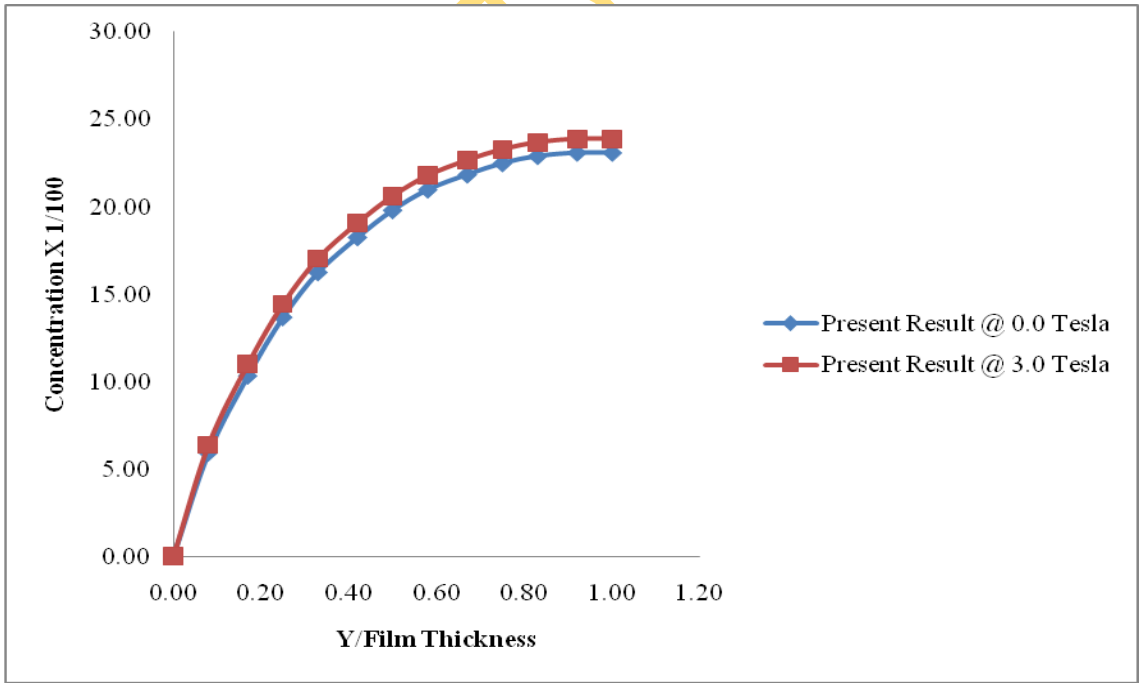

Fig.4.14.6: Graph of Concentration Changes within the Film in the Direction of Film Thickness at X=0.25m

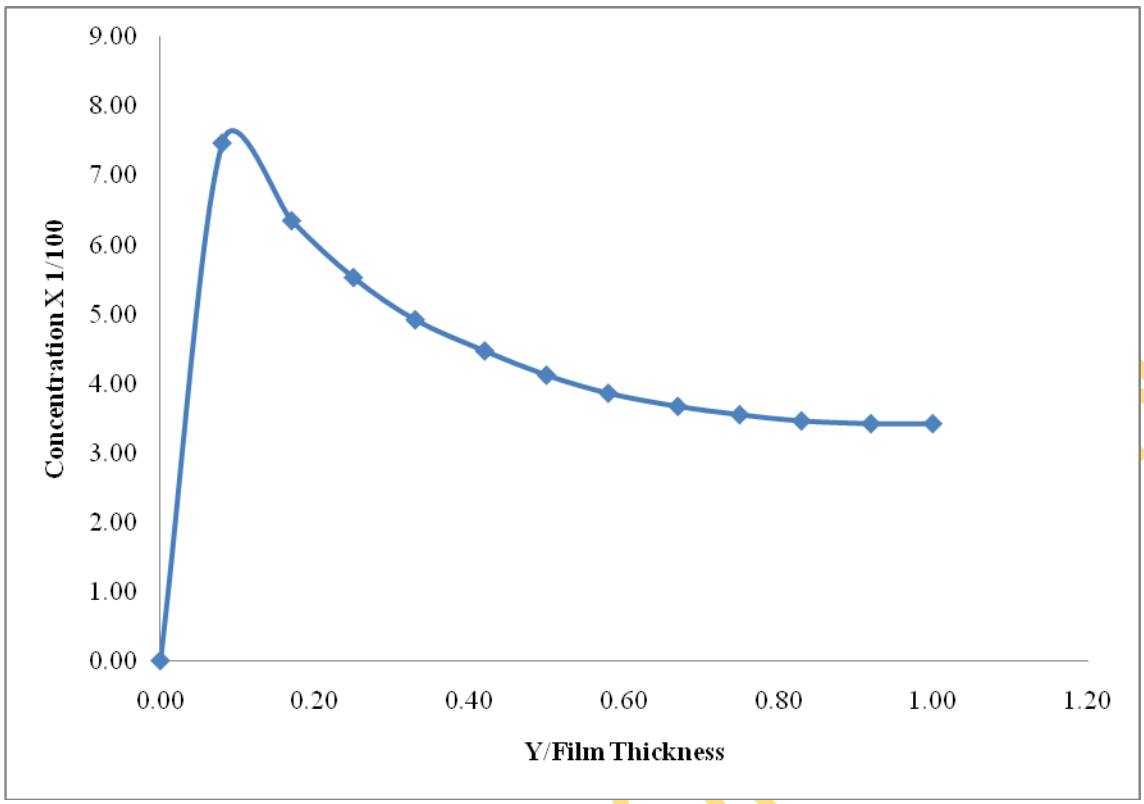

Fig.4.14.7: Graph of % Concentration Changes within the Film in the Direction of Film Thickness at 0.0 & 3.0Tesla

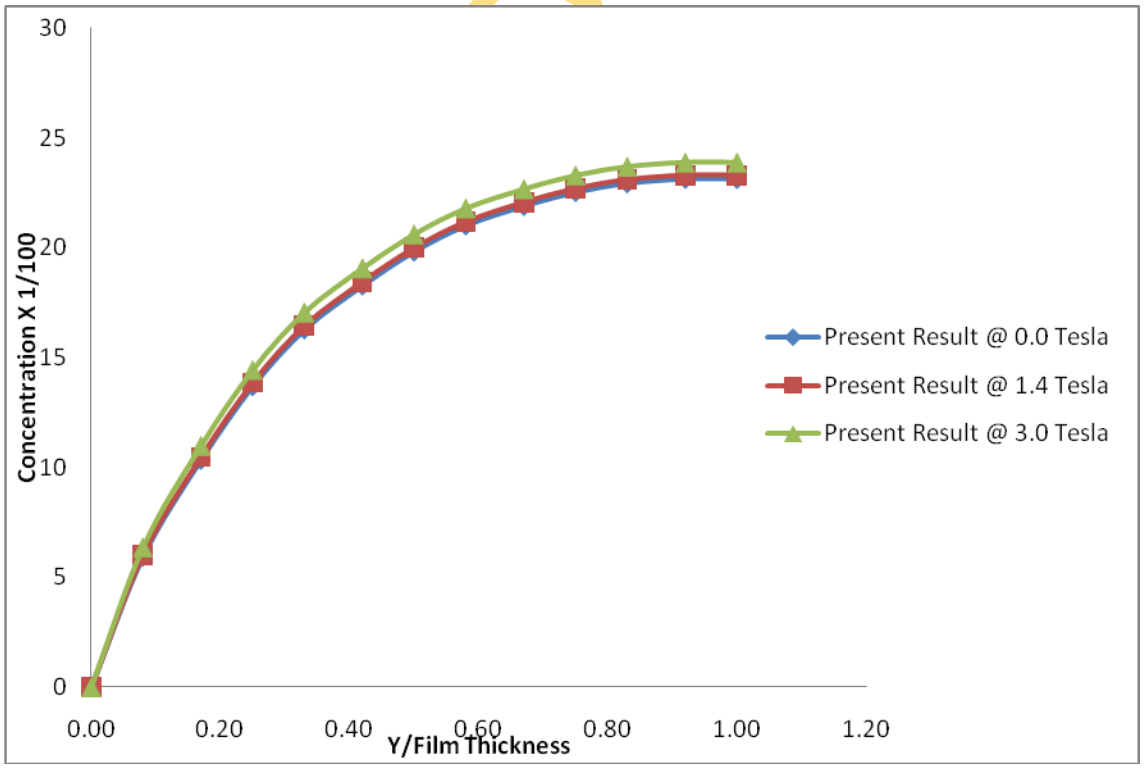

Fig.4.14.8: Graph of Concentration Distribution in the Direction of Film Thickness at X=0.25m

Table 4.6.9: LiCl-H_20: Concentration Changes in the direction of film thickness (δ) at X=0.50m

Y/δ	BULK					
	Present Result @ 0.0 Tesla	**Present. Result @ 1.4 Tesla**	**% Changes in Y-dir**	**Present Result @ 0.0 Tesla**	**Present Result @3.0 Tesla**	**% Changes in Y-dir**
0.00	0.0000	0.0000	0.00	0.0000	0.0000	0.00
0.08	0.0078	0.0081	3.33	0.0078	0.0090	15.47
0.17	0.0238	0.0244	2.82	0.0238	0.0269	13.13
0.25	0.0417	0.0427	2.45	0.0417	0.0464	11.35
0.33	0.0588	0.0601	2.19	0.0588	0.0648	10.10
0.42	0.0742	0.0756	2.00	0.0742	0.0809	9.14
0.50	0.0872	0.0888	1.83	0.0872	0.0946	8.43
0.58	0.0979	0.0997	1.73	0.0979	0.1057	7.88
0.67	0.1064	0.1082	1.64	0.1064	0.1144	7.49
0.75	0.1126	0.1144	1.58	0.1126	0.1207	7.20
0.83	0.1167	0.1185	1.54	0.1167	0.1249	7.04
0.92	0.1187	0.1205	1.53	0.1187	0.1269	6.95
1.00	0.1187	0.1205	1.52	0.1187	0.1269	6.94

UNIVERSITY OF IBADAN

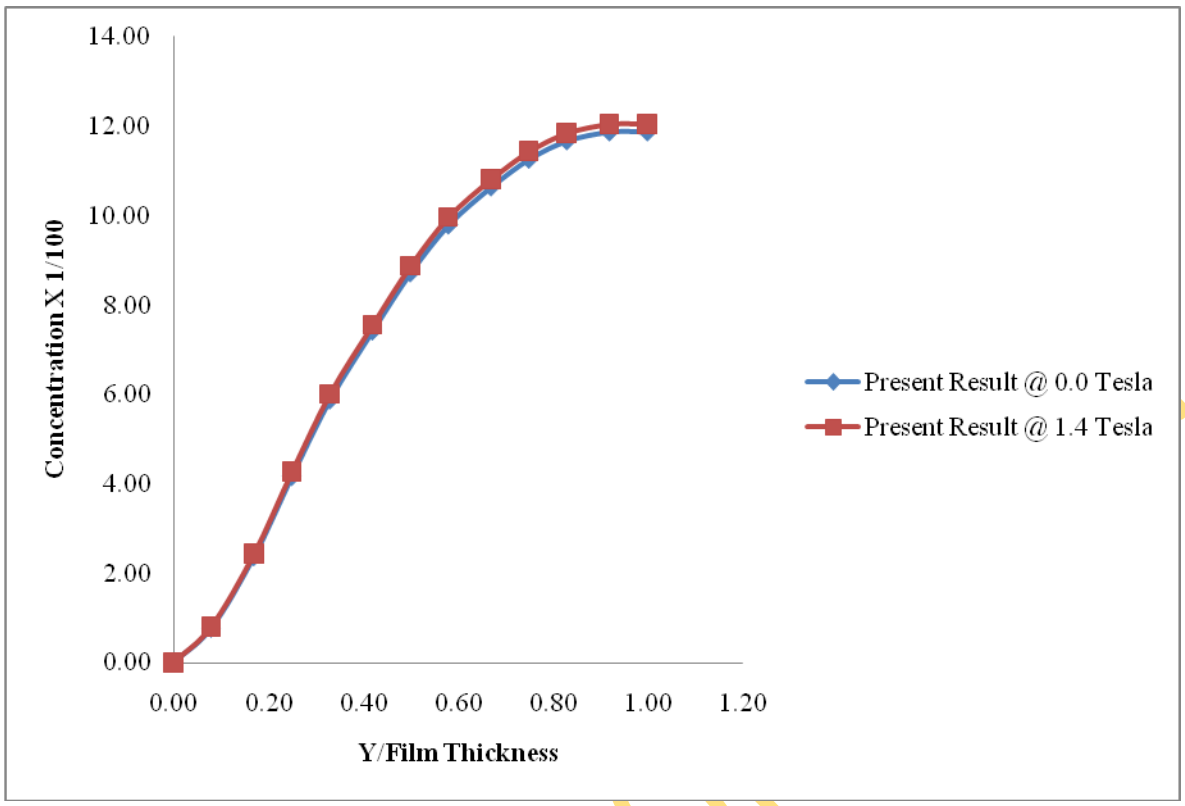

Fig.4.14.9: Graph of Concentration Changes within the Film in the Direction of Film Thickness at X=0.50m

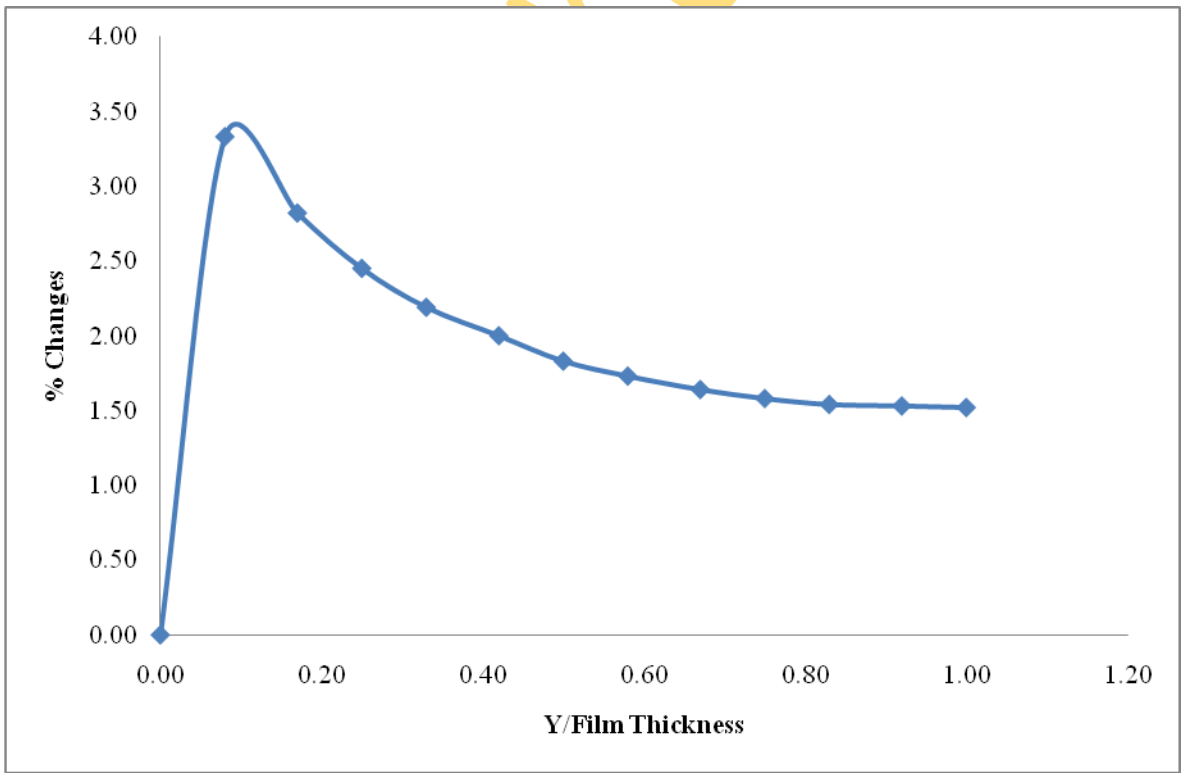

Fig.4.15: Graph of % Concentration Changes within the Film in the Direction of Film Thickness at 0.0 & 1.4Tesla

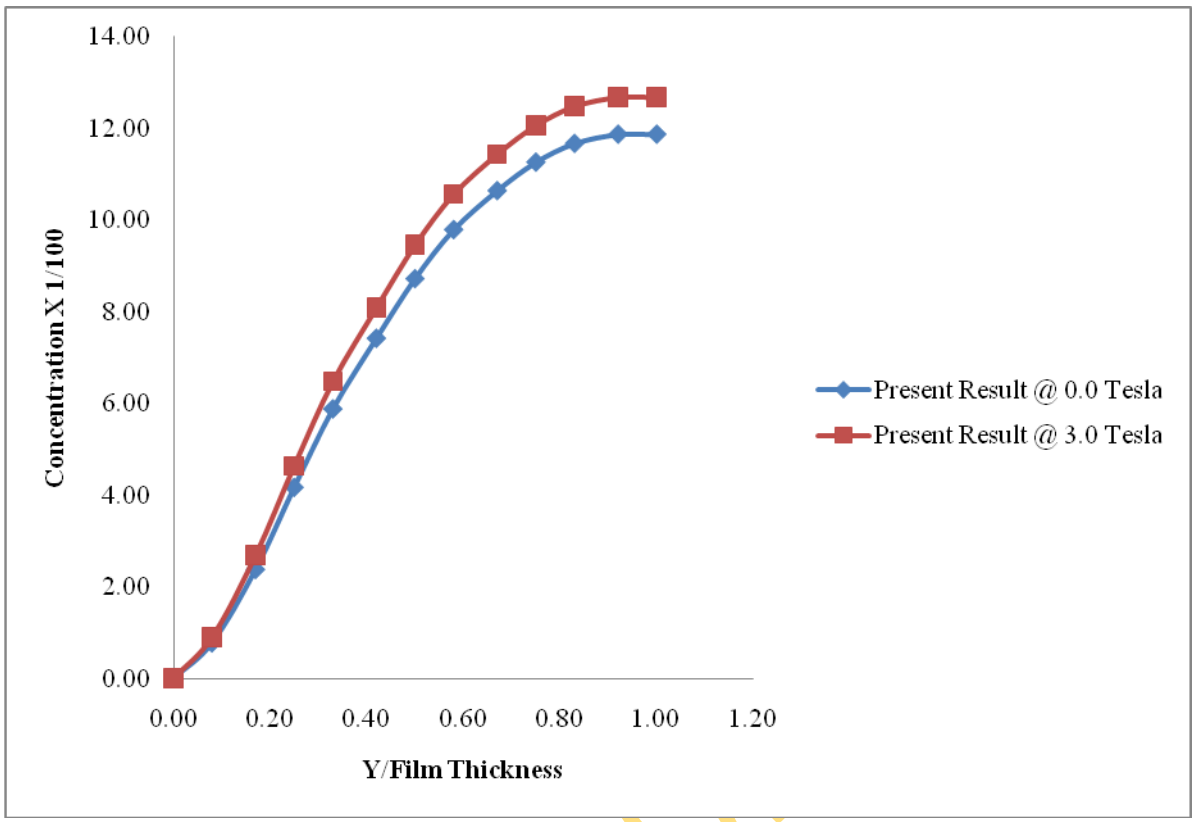

Fig.4.15.1: Graph of Concentration Changes within the Film in the Direction of Film Thickness at X=0.50m

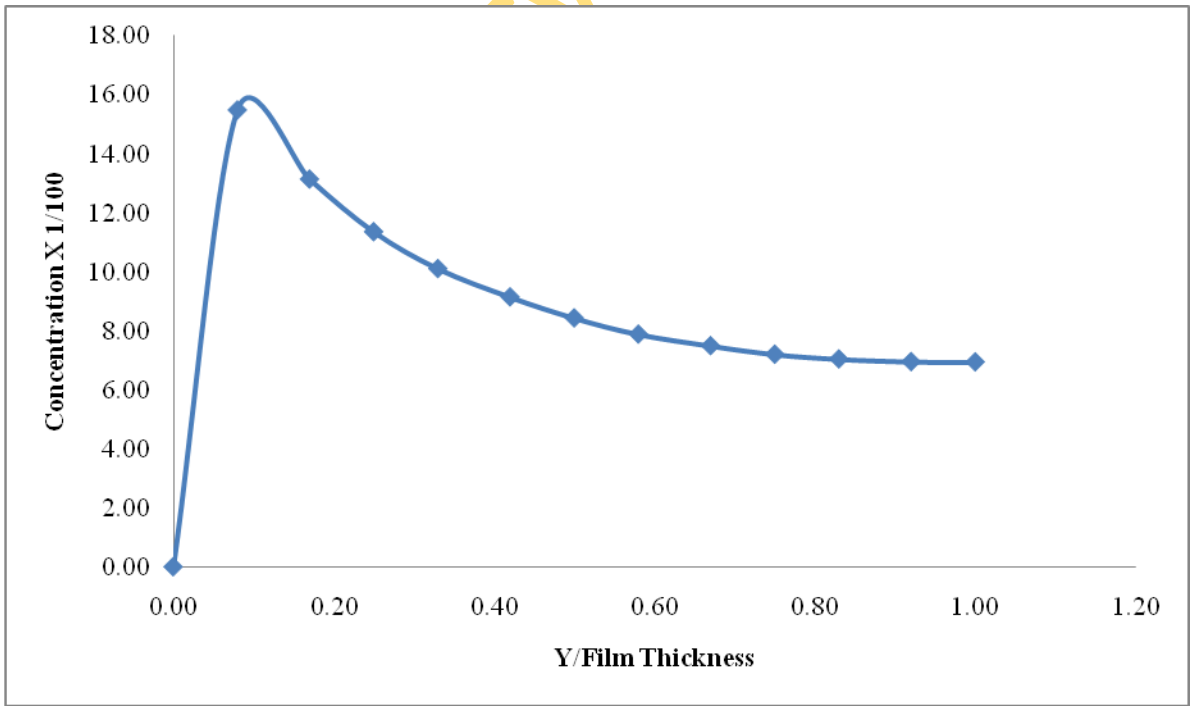

Fig.4.15.2: Graph of % Concentration Changes within the Film in the Direction of Film Thickness at 0.0 & 3.0Tesla

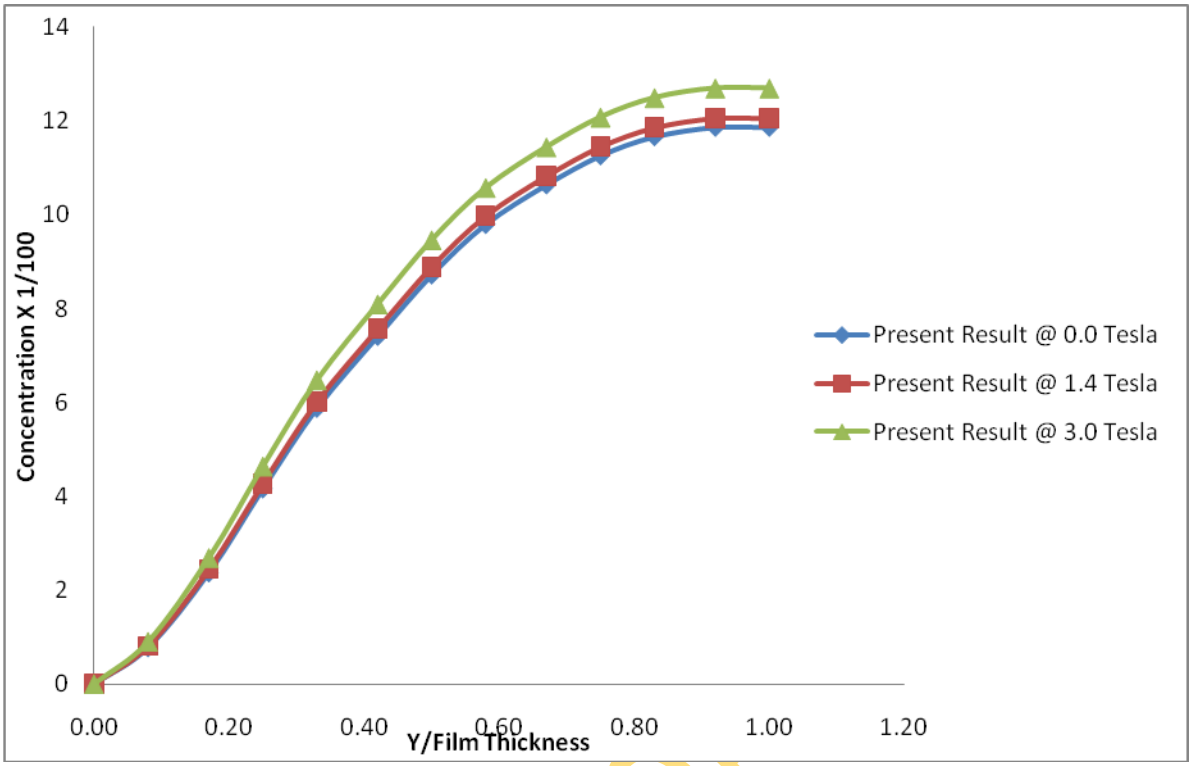

Fig.4.15.3: Graph of Concentration Distribution in the Direction of Film Thickness at X=0.50m

Table 4.7: LiCl-H_20: Concentration Changes in the direction of film thickness (δ) at X=0.75m

Y/δ	BULK					
	Present Result @ 0.0 Tesla	**Present. Result @ 1.4 Tesla**	**% Changes in Y-dir**	**Present Result @ 0.0 Tesla**	**Present Result @3.0 Tesla**	**% Changes in Y-dir**
0.00	0.0000	0.0000	0.00	0.0000	0.0000	0.00
0.08	0.0010	0.0011	4.85	0.0010	0.0013	24.27
0.17	0.0055	0.0057	4.21	0.0055	0.0066	20.33
0.25	0.0127	0.0131	3.71	0.0127	0.0149	17.52
0.33	0.0213	0.0220	3.29	0.0213	0.0246	15.52
0.42	0.0301	0.0310	3.02	0.0301	0.0343	14.03

UNIVERSITY OF

0.50	0.0384	0.0395	2.76	0.0384	0.0434	12.89
0.58	0.0457	0.0469	2.58	0.0457	0.0512	12.05
0.67	0.0518	0.0530	2.45	0.0518	0.0577	11.42
0.75	0.0563	0.0577	2.38	0.0563	0.0625	11.01
0.83	0.0594	0.0608	2.32	0.0594	0.0658	10.74
0.92	0.0610	0.0624	2.28	0.0610	0.0674	10.60
1.00	0.0610	0.0624	2.30	0.0610	0.0674	10.62

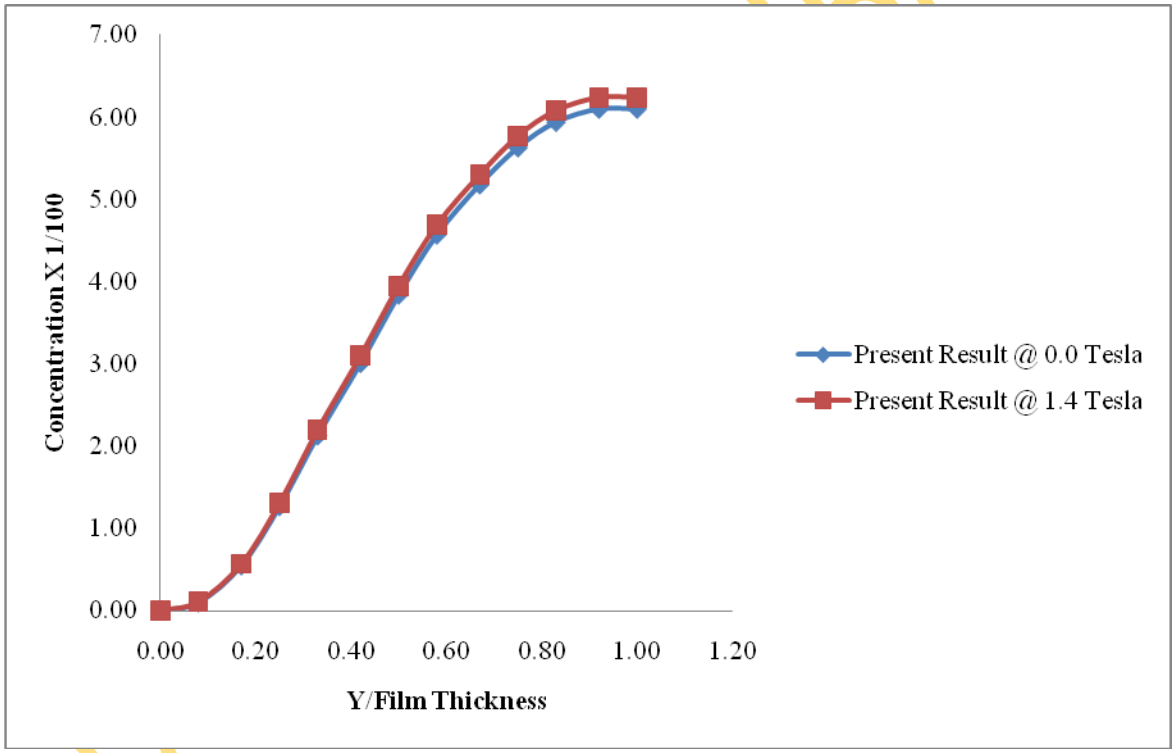

Fig.4.15.4: Graph of Concentration Changes within the Film in the Direction of Film Thickness at X=0.75m

IBADAN

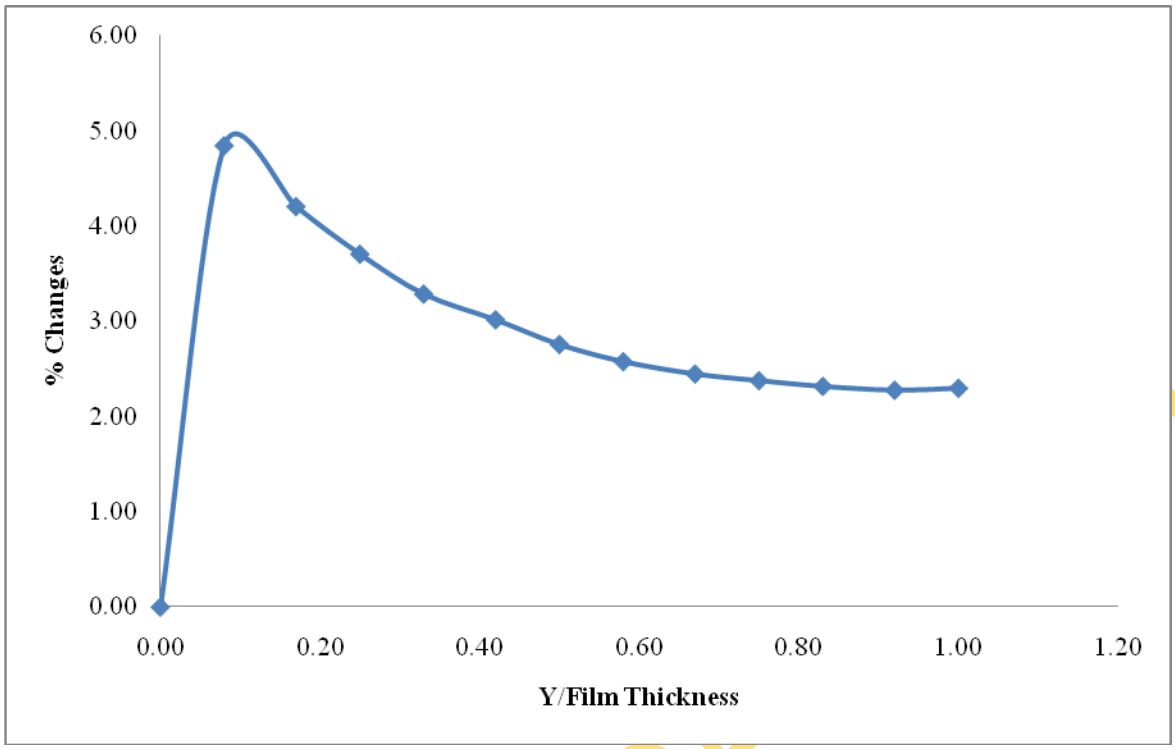

Fig.4.15.5: Graph of % Concentration Changes within the Film in the Direction of Film Thickness at 0.0 & 1.4Tesla

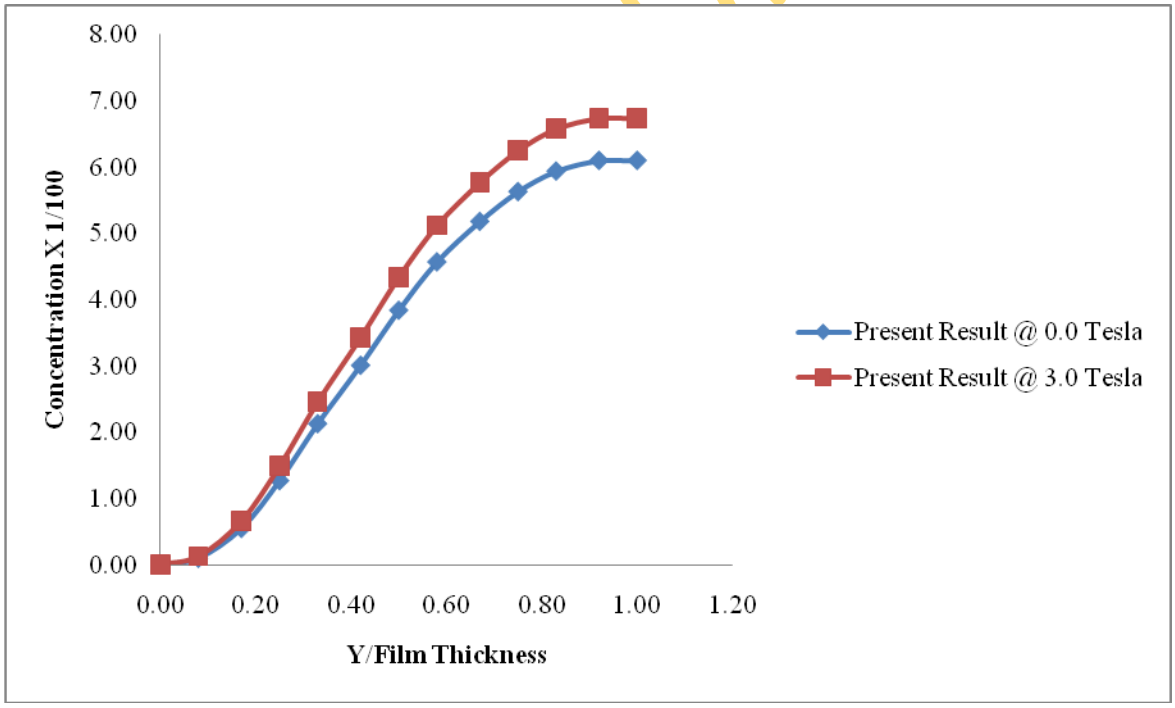

Fig.4.15.6: Graph of Concentration Changes within the Film in the Direction of Film Thickness at X=0.75m

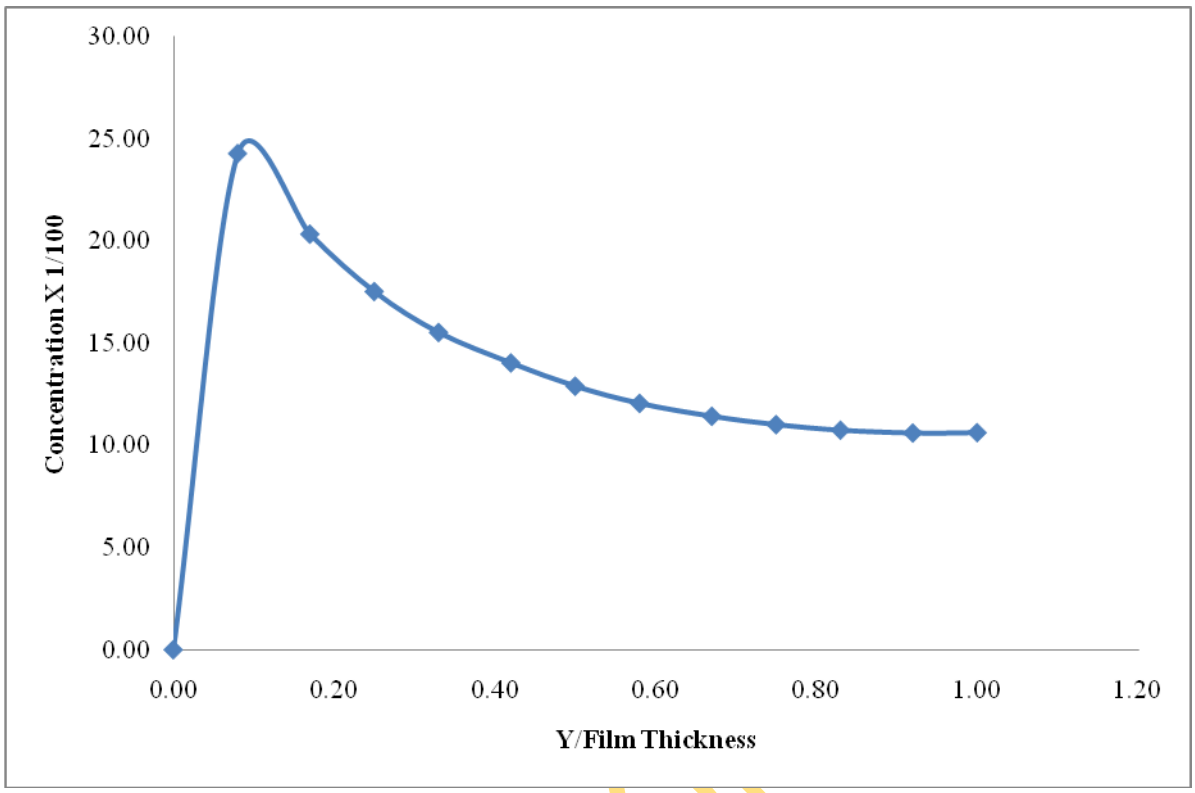

Fig.4.15.7: Graph of % Concentration Changes within the Film in the Direction of Film Thickness at 0.0 & 3.0Tesla

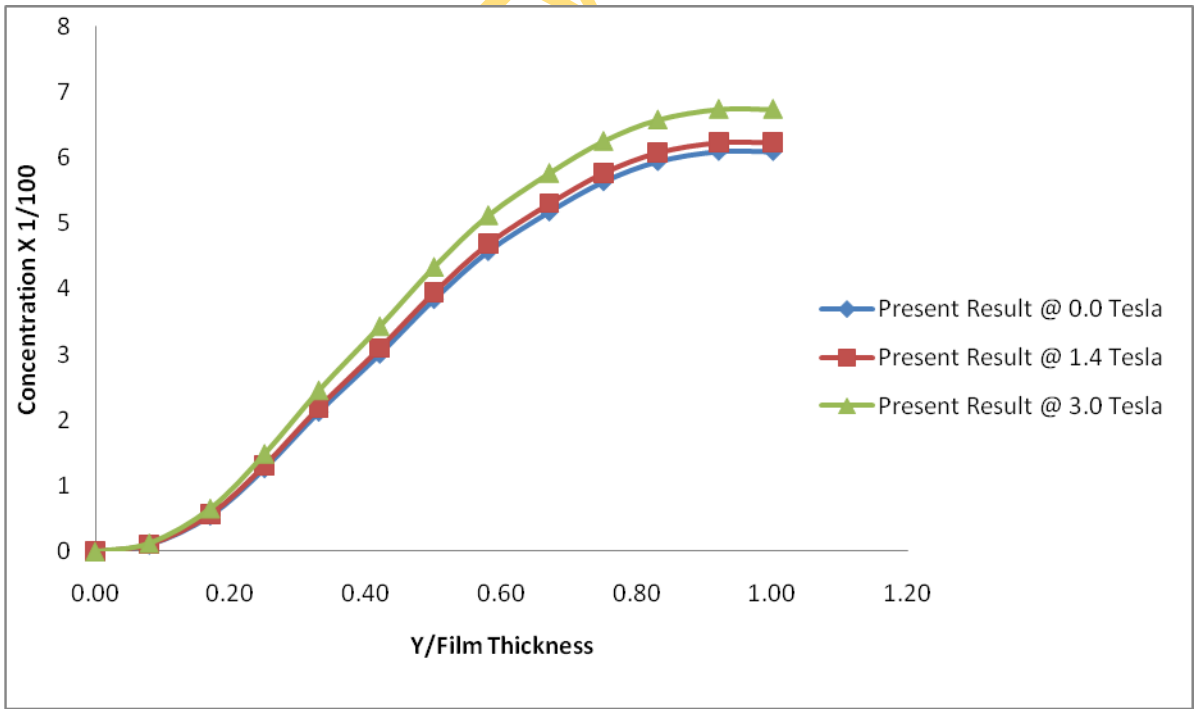

Fig.4.15.8: Graph of Concentration Distribution in the Direction of Film Thickness at 0.75m

CHAPTER FIVE
CONCLUSIONS AND RECOMMENDATIONS

5.1: Conclusions

The absorption process modeling of a smooth thin-liquid falling-film in a cooling system using Lithium bromide-water and Lithium chloride-water solutions in a magnetic field enhancement medium has been undertaken. The physical model for the magnetic field enhancement of the absorption cooling-system using lithium bromide water and lithium chloride water has been developed. The ensuing equations were developed from the conservation laws for mass, momentum, energy, concentration or species and the mass transport equations. The changes in physical properties of the two working fluids in the absorption process, the variation of falling film within the smooth thin-liquid film thickness along falling and the convection in the direction of thickness of liquid film were considered in the modeling. Distributions of parameters in falling-film absorption, such as velocity, temperature and concentration in the application of magnetic field were obtained. The distributions of the parameters were obtained in both the direction of falling-film and across the film thickness.

The numerical results obtained show that magnetic field can improve the performance of lithium bromide-water and lithium chloride-water falling film absorption, and the absorption strengthening effect increases with the enhancement of magnetic intensity. In this work the strengthening effect is limited within the magnetic field intensity of 0-3Tesla, but there are trends of absorption strengthening effect increasing more in stronger magnetic fields. Macroscopic magnetic field force was introduced in the mathematical model to reflect the influence of magnetic field on lithium bromide water and lithium chloride water absorption, while the microcosmic impact of magnetic field was not considered in this work.

UNIVERSITY OF IBADAN

5.2: Recommendations

This work has limited its scope of study to only two working fluid-pairs i.e lithium bromide and lithium chloride solutions out of numerous available absorption working fluids pairs. A few of such additional working fluid pairs are Ammonia-water solution, HFC-dimethylethylenurea [DMEU], NH_3-$SrCl_2$, ethylene glycol solution and Ammonia-water sodium hydroxide mixtures, although the literature survey indicated that of all these absorption working-fluid pairs, the working fluid pairs used in the present study were rated the best. It has also limited its scope in the adopted solution method used to only finite difference method out of all the available numerical methods such as finite element method, finite volume, boundary element method, Monte Carlo technique, vortex method etc; due to the fact that finite difference had been proved reliable from the literature and quite adequate for the flow under consideration.

Out of the three kinds of methods of absorption enhancement and five different categories of researchable areas on nano-fluids/nano-particles in absorbent form of absorption enhancement study which falls under the third kind of enhancement, magnetic field form of enhancement is seldom mentioned in the literature, this work has limited its scope to this seldom mentioned form of absorption enhancement in the investigation.

With earlier mentioned objectives of this work, the followings recommendations are being made.

- The model developed in this work for the magnetic field enhancement of the absorption cooling-system using lithium bromide-water and lithium chloride-water has been established and therefore recommended for usage in investigating the magnetic field effect on other available working fluids in absorption refrigeration.
- Improvement in the performance of lithium bromide-water and lithium chloride-water falling film absorption, and absorption strengthening increasing with the enhancement of magnetic induction intensity has also been established.
- Positive effect of macroscopic magnetic field force on the two working fluids used was also demonstrated.
- The Coefficient of Performance (COP) of LiBr and LiCl solutions absorption refrigeration systems was established to have increased by 0.3% and 0.2%, respectively, when magnetic induction was 3.0 Tesla.

UNIVERSITY OF IBADAN

The following areas are therefore worthy of further research work:

- Experimental validation of the developed model for the magnetic field enhancement of the absorption cooling-system using lithium bromide-water and lithium chloride-water
- Investigation of microcosmic impact of magnetic field on lithium bromide-water and lithium chloride-water absorption refrigeration.
- Development of magnetic field enhancement absorption process model using any other absorption refrigeration working fluids apart from lithium bromide, lithium chloride-water and ammonia-water solutions.
- Adoption of any other numerical solution method such as finite element method, finite volume, boundary element method, Monte Carlo technique, vortex method etc on absorption enhancement modeling study.

UNIVERSITY OF IBADAN

REFERENCES

Arora, C.P (2006). Refrigeration and Air-Conditioning, Sixteenth reprint edition;

ASHRAE Inc. Fundamentals (1985), American Society of Heating, Refrigerating and air- conditioning Engineers (ASHRAE)

Andberg, J.W. and Vliet, G.C. (1983).Design guildlines for water Libr absorbers, A*SHRAE Transactions* 89, 220

Andberg, G.W. (1982). Non-Isothermal absorption of gases into falling liquid film, M.Sc Thesis, University of Texas at Austin, Austin TX

Ali R. and El-Ghalban, (2002). Operational results of an intermittent absorption cooling unit *Inter. Journal of Energy Research* (2002) 26:825-835

Argiriou A.A., Balaras C.A., Kontoyiannidis, S, and Michel, E.(2004). Numerical Simulation and performance assessment of a low capacity solar assisted absorption heat pump coupled with a sub-floor system *Solar Energy* 79 (2005) 290-301

Amanie, N. A, Abdulwahab A, Mohammad A and Jay Munson.(2005). An Experimental Absorption Refrigeration Cycle *4th Int. Conference on Heat Transfer, Fluid Mechanics and Thermodynamics* (HEFAT) 2005

Bruno, J.C., Vidal, A., San Roman, M.F., Ortiz, I. and Coronas, A.(2004). Modeling of absorption refrigeration plants using ammonia-water-sodium hydroxide mixtures *3rd Int. Conference on Heat and powered Cycles* (HPC), Cyprus, 2004

Bohdal, T and Matysko, R.(2005). Condensation of Refrigeration medium with Non-condensable gas *4th Int. Conference on Heat Transfer, Fluid Mechanics and Thermodynamics* (HEFAT) 2005

UNIVERSITY OF IBADAN

Balghouthi, M., Chahbani, M.H and Guizani, A.(2007). Feasibility of Solar absorption air- conditioning in Tunisia, *Int. Journal of Building and Environment.*43 (2008) 1459-1470

Bird, E.B., Steward, W.E and Lightfoot, E.N.(1960). Transport phenomena, Wiley, New York

El May, S and Bellagi, A (2005). Modular Simulation Program for Absorption Machines 4th *Int. Conference on Heat Transfer, Fluid Mechanics and Thermodynamics* (HEFAT) 2005

Fagbenle, R.'L., James, R.W and Karayiannis, T. G.(1994). Technical implications of the 1987 Montreal Protocol for developing countries, *Int. J. of Environment and Polution* Vol. 4 No ¾, pp 214-228.

Fan, Y., Luo, L., Souyri, B.(2006). Review of solar sorption refrigeration technologies: Development and applications *Renewable and Sustainable Energy Reviews 11*(2007) 1758-1775

Forsythe, G. E and Wasow, W. R. Finite Difference Method for partial Differential Equations, New York; John Wiley&Sons.Inc.1960 p 247, Eq.22.4

Grossman, G. (1983). Simultaneous heat and mass transfer in film absorption under laminar flow. *Inter. Journal Heat and Mass transfer* 26,357

Ghaddar, N.K., Shihab, M and Bdeir, F.(1996). Modeling and Simulation of Solar Absorption System Performance in Beirut *Renewable Energy, Vol.10***,** No.4, pp 539-558, (1977)

Gu Yaxiu,Wu Yuyuan and Ke Xin. (2007).Experimental research on a new solar pump-free lithium bromide absorption refrigeration system with a second generator *Solar Energy* 82 (2008) 33-42

UNIVERSITY OF IBADAN

Gustavo, R. F, Mahmoud, B and Alberto, C.(2007). Thermodynamic modelling of a Two-stage absorption chiller driven at two-temperature levels *Applied Thermal Engineering* xxx (2007) xxx-xxx

Icksoo Kyung, Keith, E. H and Yong Tae Kang. (2006).Model for absorption of water vapor into aqueous LiBr flowing over a horizontal smooth tube *Int. Journal of Refrigeration* 30 (2007) 591-600

Icksoo Kyung, Keith, E. Hand Yong Tae Kang. (2006). Experimental verification of H2O/LiBr absorber bundle performance with smooth horizontal tubes;*Int. Journal of Refrigeration* 30 (2007) 582-590

James, M.L., Smith, G.M. and Wolford, J.C. Applied Numerical Methods for Digital Computation with FORTRAN

Jelinek, M., Levy, A and Borde, I.(2008). The performance of a triple pressure level absorption cycle(TPLAC)with working fluids based on the absorbent DMEU and the refrigerants R22, R32, R124, R125,R134a and R152a *Applied Thermal Engineering* **28**(2008) 1551-1555

Kim, D.S and Infante Ferreira, C.A.(2007). Solar refrigeration options- a state-of-the-art review *International Journal of Refrigeration* 31(2008) 3-15

Lazarus, G., Raja, B., Mohan Lal, D and Wongwises, S.(2009). Enhancement of Heat Transfer using nanofluids- An overview. *Renewable and Sustainable Energy Reviews* 14 (2010) 629-641

Li, G.D.(1999) Contemporary Magnetism, University of Science & Technology of China Press, pp 3-33

Li, Y and Yang, H.(2007). Investigation on Solar desiccant dehumidification process for

UNIVERSITY OF IBADAN

energy conservation of central air-conditioning system *Applied Thermal Engineering* 28(2008) 1118-1126

Muhsin Kilic and Omer Kaynakli.(2004). Second law-based thermodynamic analysis of Water - lithium bromide absorption refrigeration system *Energy* 32 (2007) 1502-1512

Muthu, V., Saravanan, R., Renganarayanan, S.(2007). Experimental studies on R134a-DMAC hot water based vapour absorption refrigeration systems *International Journal of Thermal Sciences* 47(2008) 175-181)

Mauran, S., Lahmidi, H and Goetz, V.(2008). Solar heating and cooling by a thermo-chemical process. First experiments of a prototype storing 60kWh by a solid/gas reaction *Solar Energy* 82 (2008) 623-636

Niu, X., Du Kai and Du Shunxiang.(2006). Numerical analysis of falling film absorption with ammonia–water in magnetic field *Applied Thermal Engineering* 27 (2007) 2059-2065

Okon, (1990). Finite element analysis of 2-dimensional stress problems using isoparametric Element, M.Sc Thesis, University of Ibadan at Ibadan, Nigeria

Ortega, N., Garcia-Valladares, O., Best, R and Gomez, V.H.(2008). Two-phase flow modeling of a solar concentrator applied as ammonia vapor generator in an absorption refrigerator *Renewable Energy* 33 (2008) 2064-2076

Parsons, K., Ahmad A., Pesaran, Desikan, Bharathan and Benjamin Shelpuk. (1987). Evaluation of Thermally Activated Heat-Pump/Desiccant Air-Conditioning Systems and Components

Pongsid, S, Satha, A and Supachart. (2001). A review of absorption refrigeration technologies *Renewable and Sustainable Energy Reviews* 5 (2001) 343-372

UNIVERSITY OF IBADAN

Safarik, M., Lutz Richter and Mike Otto. (2004). Solar Powered H_2O/LiBr-Absorption Chiller with low Capacity *3rd Int. Conference on Heat and powered Cycles* (HPC), Cyprus, 2004

Stavocia, M.D and Isvoranu, D.(2005). Model of the Water/Lithium Bromide Absorption / generation processes in a Marangoni Convection Cell, using the Two-Part-Theory (TPT) of mass and Heat Transfer *4th Int. Conference on Heat Transfer, Fluid Mechanics and Thermodynamics* (HEFAT) 2005

Sieres, J., Fernandez-Seara, J., Uhia, FJ and Vazquez, M.(2005). Solution of the Simultaneous heat and mass transfer equation in ammonia-water Absorption system Processes *4th Int. Conference on Heat Transfer, Fluid Mechanics and Thermodynamics* (HEFAT) 2005

Tatiana Morosuk and George Tsatsaronis.(2007). A new approach to the exergy analysis of absorption refrigeration machines *Energy* 33 (2008) 890-907

Wen-Long. C., Kouich, H., Ze-Shao , C., Atsushi, A.,Peng , H. and Takao Kashiwagi (2003). Heat Transfer enhancement by additive in vertical falling film absorption of H_2O/LiBr

Xiao, F.N.,Kai, D and Xiao, F. (2009) Experimental study on ammonia-water falling film absorption in External magnetic fields *International Journal of Refrigeration xxx* (2010) 1-9

Xu, S.M., Zhang, L., Xu, C.H., Liang, J and Du, R.(2006). Numerical simulation of an advanced energy storage system using H2O-LiBr as working fluid, Part 1: System design and modeling *Int. Journal of Refrigeration* 30 (2007) 364-376

Xu, S.M., Zhang, L., Xu, C.H., Liang, J and Du, R.(2006). Numerical simulation of an advanced energy storage system using H2O-LiBr as working fluid, Part 2: System simulation and analysis *Int. Journal of Refrigeration 30* (2007) 354-363.

UNIVERSITY OF IBADAN

Yang, R and Wood, B.D.(1992). A numerical modeling of an absorption process on a liquid falling film *Solar Energy Vol.* 48, No3,pp 195-198

Yong, T.K., Hyun, J.K and Kang I,L.(2007). Heat and mass transfer enhancement of binary nanofluids for H2O/LiBr falling absorption process *International Journal of Refrigeration 31* (2008) 850-856

Zohar, A, Jelinek, M, Levy, A and Borde, I.(2005). The influence of diffusion absorption Refrigeration cycle configuration on the performance *Applied Thermal Engineering* 27 (2007) 2213-2219

Zheng, G.S and Worek,W.M. (1996). Method of heat and mass transfer enhancement in film evaporation *International Journal of Heat and Mass Transfer.* Vol.39, No. 1 pp.97-108

Ziegler, F and Grossman, G. (1996).Heat Transfer enhancement by additives *International Journal of Refrigeration* Vol.19, No. 5 pp.301-309

UNIVERSITY OF IBADAN

APPENDICES

UNIVERSITY OF IBADAN

APPENDIX A

DEVELOPMENT OF THE MODEL EQUATIONS

a. Development of Magnetic field enhanced velocity field equation in smooth thin liquid falling film using mass transport relationship

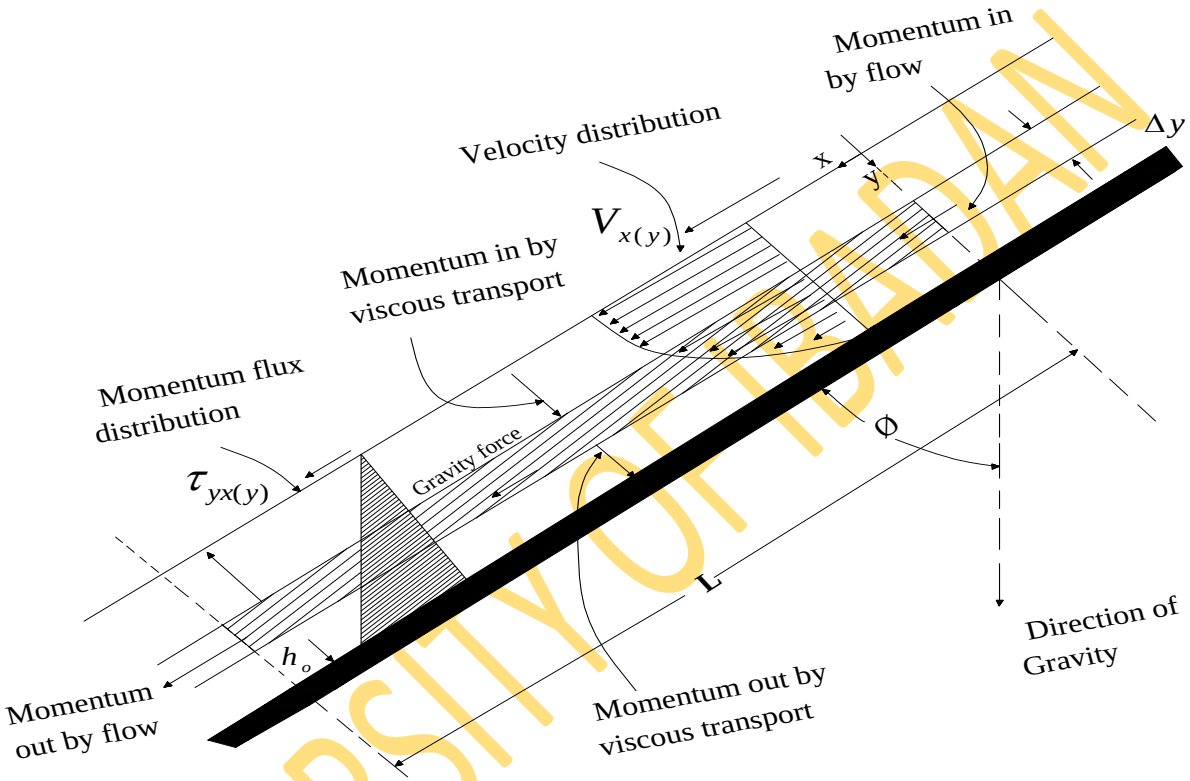

Fig. 1

Momentum balances over a thin "shell" of fluid for a steady-state flow is given as

{Rate of momentum in} – {rate of momentum out} + {sum of forces acting on systems} = 0 1

From Fig. 1

rate of x- momentum in across surface at y	$(LW)((\tau_{yx})\|_y$	i
rate of x- momentum out across surface at $y + \Delta y$	$(LW)((\tau_{yx})\|_{y+\Delta y}$	ii
rate of x-momentum in across surface at x = 0	$(W\Delta y\, V_x)(\rho V_X)\|_x = 0$	iii

UNIVERSITY OF IBADAN

rate of x-momentum out across surface at x = L | $(W\,\Delta y\,V_x)(\rho V_X)|_x = L$ | iv

gravity force acting on fluid | $(LW\,\Delta y)(\rho g\cos\phi)$ | v

Substitute equations (i) to (v) in the momentum balances equation 1

$(LW)((\tau_{yx})|_y - (LW)((\tau_{yx})|_{y+}\,\Delta y + (W\,\Delta y\,V_x)(\rho V_X)|_x - (W\,\Delta y\,V_x)(\rho V_X)|_x + (LW\,\Delta y)(\rho g\cos\phi) = 0$

V_x is the same at x = 0 as it is at x = L

Dividing through with $LW\,\Delta y$ and taken the limit as Δy approaches zero

$$\lim_{\Delta y \to 0}\left(\frac{\tau_{yx}|_{y+\Delta y} - \tau_{yx}|_y}{\Delta y}\right) = \rho g\cos\phi \qquad \text{vi}$$

$$\frac{\partial}{\partial}\tau_{yx} = \rho g\cos\phi \qquad \text{vii}$$

Integrating

$$\tau_{yyx} = \rho g\cos\phi + C_1 \qquad \text{viii}$$

B. C. 1: at y = 0, $\tau_{yx} = 0$

Substituting

$$\tau_{yx} = \rho g y\cos\phi \qquad \text{ix}$$

For Newtonian fluid, the momentum flux is related to the velocity gradient according to

$$\tau_{yx} = -u\frac{\partial v_x}{\partial y} \qquad \text{x}$$

Substitute for τ_{yx}

Therefore $$\frac{\partial v_x}{\partial y} = -\left(\frac{\rho g\cos\phi}{\mu}\right)y \qquad \text{xi}$$

In this model ϕ is 0^0, $\cos 0 = 1$

Therefore $$\frac{\partial v_x}{\partial y} = -\left(\frac{\rho g}{\mu}\right)y \qquad \text{xii}$$

Since $v_x = u$, Therefore $$\frac{\partial u}{\partial y} = -\left(\frac{\rho g}{\mu}\right)y \qquad \text{xiia}$$

UNIVERSITY OF IBADAN

Mean velocity in the liquid film $V_o = \frac{\rho g h_o^2}{3\mu}$ or $\rho g = \frac{3\mu V_0}{h_o^2}$

Substitution for ρg in equation (xiia)

Therefore $\frac{\partial u}{\partial y} = -3\frac{V_O}{h_o^2} y$ xiii

Second derivative

$\frac{\partial^2 u}{\partial y^2} = -3\frac{V_o}{h_o^2}$ Implies

$\frac{\partial^2 u}{\partial y^2} + 3\frac{V_o}{h_o^2} = 0$ xix

This is the velocity field equation in the thin film. The magnetic force in the falling film is given as $\int_{mag}$.

In this model the magnetic force coupled with the body weight acts in the direction of the falling-film.

Therefore the complete magnetic enhanced velocity field equation will be

$\frac{\partial^2 u}{\partial y^2} + 3\frac{V_o}{h_o^2} + \rho g + \int_{mag} = 0$ xx

$\int_{mag} = \frac{\rho \chi^{\beta^2}}{l\mu_o}$ is the magnetic force which the falling-film solution experienced per unit volume

Finally, Magnetic enhanced Model Equation is

$\frac{\partial^2 u}{\partial y^2} + 3\frac{V_o}{h_o^2} + \rho g + \frac{\rho \chi^{\beta^2}}{l\mu_o} = 0$ xxi

Equation (xxi) is the developed model magnetic field enhanced velocity field equation in the smooth thin liquid film

b. Development of Boundary conditions/equations

Temperature

Fig 3.2, the quantity of heat flowing into the three faces of the half element in time dt is given by the following equations:

UNIVERSITY OF IBADAN

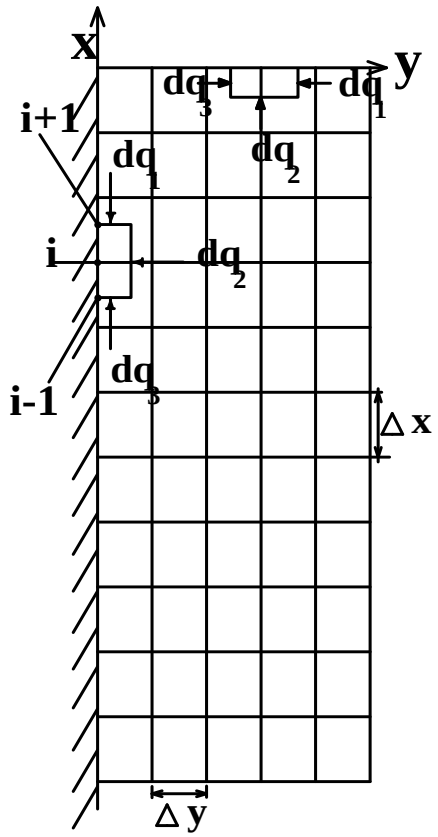

Fig. 2 Temperature boundary conditions analysis

$$dq_1 = \left(\frac{khd}{2}\right)\frac{\partial T}{\partial x}_{i+\frac{1}{2}} dt = \left(\frac{khd}{2}\right)\frac{(T_{i+1,j} - T_{i,j})}{h} dt$$

$$dq_2 = (khd)\frac{\partial T}{\partial y}_{j+\frac{1}{2}} dt = (khd)\frac{(T_{i,J+1} - T_{i,j})}{h} dt \qquad \text{(xxii)}$$

$$dq_3 = -\left(\frac{khd}{2}\right)\frac{\partial T}{\partial x}_{i-\frac{1}{2}} dt = -\left(\frac{khd}{2}\right)$$

Substituting Eq. (xxii) into the heat balance equation for the half element

$dq_1 + dq_2 + dq_3 = 0$

yields

$$\text{(Left)}\quad T_{i+1,j} + 2T_{i,j+1} + T_{i-1,j} - 4T_{i,j} = 0 \qquad \text{(xxiii)}$$

Following the same procedure above, the difference equations which apply on the right, upper and lower could be obtained.

$$\text{(Right)}\quad T_{i+1,j} + 2T_{i,j-1} + T_{i-1,j} - 4T_{i,j} = 0 \qquad \text{(xxiv)}$$

$$\text{(Upper)}\quad T_{i,j-1} + 2T\,i-1, j + T_{i,j+1} - 4T_{i,j} = 0 \qquad \text{(xxv)}$$

UNIVERSITY OF IBADAN

(Lower) $T_{i,j-1} + 2T_{i+1,j} + T_{i,j+1} - 4T_{i,j} = 0$ (xxvi)

Concentration

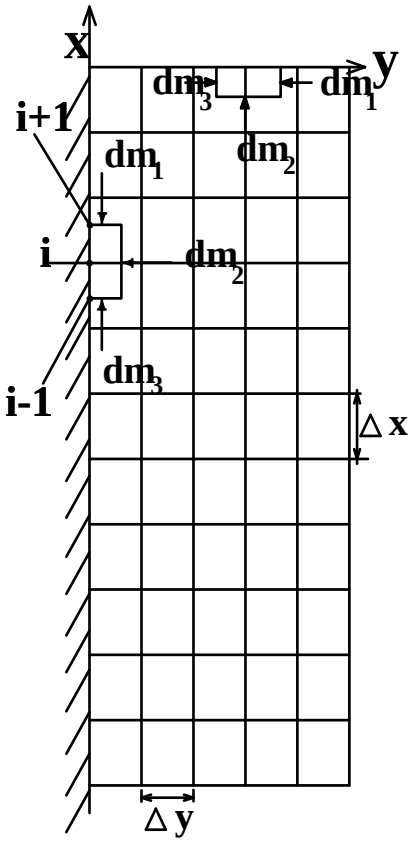

Fig. 3 Concentration boundary conditions analysis

The net mass flowing into this element must be equal to zero when considering steady-state condition in the liquid-film. The quantity of mass flowing into the three faces of the half-element in time dt are given by the following equations.

$$dm_1 = \left(\frac{\rho hd}{2}\right)\frac{\partial \xi}{\partial x}_{i+\frac{1}{2}} dt = \left(\frac{\rho hd}{2}\right)\frac{\left(\xi_{i+1,j} - \xi_{i,j}\right)}{h} dt$$

$$dm_2 = \left(\rho hd\right)\frac{\partial \xi}{\partial y}_{j+\frac{1}{2}} dt = \left(\rho hd\right)\frac{\left(\xi_{i,j+1} - \xi_{i,j}\right)}{h} dt \quad \text{(xxvii)}$$

$$dm_3 = -\left(\frac{\rho hd}{2}\right)\frac{\partial \xi}{\partial x}_{i-\frac{1}{2}} dt = -\left(\frac{\rho hd}{2}\right)\frac{\left(\xi_{i,j} - \xi_{i-1,j}\right)}{h} dt$$

Substituting Eq. (xxvii) into the mass balance equation for the half-element

$dm_1 + dm_2 + dm_3 = 0$

yields

UNIVERSITY OF IBADAN

(Left) $\xi_{i+1,j} + 2\xi_{i,j+1} + \xi_{i-1,j} - 4\xi_{i,j} = 0$ (xxviii)

Following the same procedure above, the difference equations which apply on the right, upper and lower could be obtained.

(Right) $\xi_{i+1,j} + 2\xi_{i,j-1} + \xi_{i-1,j} - 4\xi_{i,j} = 0$ (xxix)

(Upper) $\xi_{i,j-1} + 2\xi_{i-1,j} + \xi_{i,j+1} - 4\xi_{i,j} = 0$ (xxx)

(Lower) $\xi_{i,j-1} + 2\xi_{i+1,j} + \xi_{i,j+1} - 4\xi_{i,j} = 0$ (xxxi)

UNIVERSITY OF IBADAN

APPENDIX B

Source Code

C: LiBr-H2O Parameter distribution in the direction of falling

```
C: ABSORPTION PROCESS MODELING ON A LIQUID FALLING FILM
CCCCCCCCCCCCCCCCCCCCCCCCCCCCCCCCCCCCCCCCCCCCCCCCCCC
C                                                 C
C          Ph.D FINITE DIFFERENCE MODEL           C
C                                                 C
C                     FOR                         C
C                                                 C
C          ABSORPTION PROCESS MODELING ON A       C
C                                                 C
C                                                 C
C              LIQUID FALLING FILM                C
C                                                 C
C                                                 C
C              K.M ODUNFA (44113)                 C
C                                                 C
C                 SUPERVISED BY                   C
C            PROFESSOR FAGBENLE, R O              C
C                                                 C
C                 JANUARY 2009                    C
CCCCCCCCCCCCCCCCCCCCCCCCCCCCCCCCCCCCCCCCCCCCCCCCCCC

      COMMON/XL1/AVISC,DENS,TMMSUC, FMAG,AMAGIND,VT,VB,AGRAV
C     COMMON/XL2/RH,RL,NEX,NEY,UT,UB,EPSI,CT,CB,NN,S,NMAX
      COMMON/XL2/RH,RL,NEX,NEY,UT,UB,EPSI,CT,CB,NN,NMAX
      COMMON/XL3/NX,NY,IB,IA,VELM,FILMT,ALPHA,TAMAC,SDIFU,V(14,10)
      DIMENSION XCO(13),YCO(5)

      OPEN(UNIT = 4,FILE = 'FINAL RESULT.OUT')
      OPEN(UNIT = 6,FILE = 'LiBr Data.IN',STATUS='OLD')
C
C     INPUT THE PROBLEM DATA
C
      READ(6,2)IA,IB,NMAX,UT,UB,CT,CB,VT,VB,AVISC,TMMSUC,EPSI
  2   FORMAT(2I3,I4,F6.2,F6.0,2F6.4,2F6.4,F8.5,F10.7,F5.2)
      WRITE(*,2)IA,IB,NMAX,UT,UB,CT,CB,VT,VB,AVISC,TMMSUC,EPSI
      READ(*,2)
      READ(6,*)RH,RL
 105  FORMAT(2(F8.5,1X))
      WRITE(*,105)RH,RL
      READ(6,*)VELM,VELM1,FILMT,AMAGIND,AGRAV
```


UNIVERSITY OF IBADAN

```
 102    FORMAT(3(F9.6,1X),F3.1, F5.3)
        WRITE(*,102)VELM,VELM1,FILMT,AMAGIND, AGRAV
        READ(6,*)ALPHA,TAMAC,SDIFU,HITAB,CONEQ,DENS
 104    FORMAT(6(F9.5,1X))
        WRITE(*,*)ALPHA,TAMAC,SDIFU,HITAB,CONEQ,DENS
        READ(6,*)NEX,NEY
 205    FORMAT(2(I3,1X))
        WRITE(*,205)NEX,NEY
C
        DY= RL/NEY
        DX= RH/NEX
        NX=NEX+1
        NY=NEY+1
        NNT=NX*NY
C
    DO 101 I = 1,NX
        DO 101 J = 1,NY
        NNC= (J-1)*NX+I
        YCO(NNC)=(J-1)*DY
        XCO(NNC)=(I-1)*DX
  101 CONTINUE
C
C       COMPUTE TEMPERATURE DISTRIBUTION IN THE FILM
C
        CALL SOLUTION1
C
C       COMPUTE CONCENTRATION DISTRIBUTION IN THE FILM

        CALL SOLUTION2
C
        STOP
        END
C
        SUBROUTINE VELOCITY
        COMMON/XL1/AVISC,DENS,TMMSUC,FMAG,AMAGIND,VT,VB,AGRAV
c       COMMON/XL2/RH,RL,NEX,NEY,UT,UB,EPSI,CT,CB,NN,S,NMAX
        COMMON/XL2/RH,RL,NEX,NEY,UT,UB,EPSI,CT,CB,NN,NMAX
        COMMON/XL3/NX,NY,IB,IA,VELM,FILMT,ALPHA,TAMAC,SDIFU,V(14,10)
        DIMENSION XCO(13),YCO(5)
C
        DY= RL/NEY
        DX= RH/NEX
        NX=NEX+1
        NY=NEY+1
        NNT=NX*NY
C
```

UNIVERSITY OF IBADAN

```
      DO 101 I = 1,NX
      DO 101 J = 1,NY
      NNC= (J-1)*NX+I
      YCO(NNC)=(J-1)*DY
      XCO(NNC)=(I-1)*DX
 101 CONTINUE

      WRITE(4,3)
3     FORMAT(47H1VEL.DIST ON A FILM BY GAUSS-SEIDEL ITERATION//)
      DO 4 I=1,13
      DO 4 J=1,5
      A=I
4     V(I,J)=VB+(VT-VB)*(A-1.)/12.
      N=0
5     K=0
      DO 16 J=1,5
      DO 16 I=2,12
      IF(J-1)9,6,9
6     IF(IA-I)7,7,8
7     UVEL = VT
      GO TO 14
C8    UTEMP = (V(I+1,J)+2.*V(I,J+1)+V(I-1,J))/4.
8     UVEL = 0.0
      GO TO 14
9     IF(J-5)13,10,13
10    IF(I-IB)12,11,11
11    UVEL = VT
      GO TO 14
c12   UTEMP=(V(I+1,J)+2.*V(I,J-1)+V(I-1,J))/4
c
12    V(I,J)= V(I,J+1)
      GO TO 14
13    UVEL = ((V(I+1,J)+V(I-1,J)+(3*VELM/FILMT**2)*DY**2
     .+DY**2*DENS*AGRAV+((DENS*TMMSUC*AMAGIND*AMAGIND)
     ./0.000001257)*DY**2))/2.0
C
14    DIFF=UVEL-V(I,J)
      IF(ABS(DIFF)-EPSI)16,15,15
15    K=K+1
16    V(I,J)=UVEL
C     write(*,*)((V(I,J),I=2,11),J=1,5)
C     read(*,*)
      N=N+1
      IF(N-NMAX)17,20,20
17    IF(K)18,20,18
18    WRITE(4,19)N,K
```

UNIVERSITY OF IBADAN

```
19      FORMAT(7H IT NO.,I4,4H K= ,I4)
        GOTO 5
20      WRITE(4,19)N,K
21      FORMAT(///10F9.6)
        DO 22 M= 1,13
        I=14-M
22      WRITE(4,21)(V(I,J),J=1,5)
        RETURN
        END

C
        SUBROUTINE SOLUTION1
        COMMON/XL1/AVISC,DENS,TMMSUC,FMAG,AMAGIND,VT,VB,AGRAV
c       COMMON/XL2/RH,RL,NEX,NEY,UT,UB,EPSI,CT,CB,NN,S,NMAX
        COMMON/XL2/RH,RL,NEX,NEY,UT,UB,EPSI,CT,CB,NN,NMAX
        COMMON/XL3/NX,NY,IB,IA,VELM,FILMT,ALPHA,TAMAC,SDIFU,V(14,10)
        DIMENSION XCO(13),YCO(5),U(13,5)
c       S(100)
C
        DY= RL/NEY
        DX= RH/NEX
        NX=NEX+1
        NY=NEY+1
        NNT=NX*NY
c
        DO 102 I = 1,NX
        DO 102 J = 1,NY
        NNC= (J-1)*NX+I
        YCO(NNC)=(J-1)*DY
        XCO(NNC)=(I-1)*DX
  102 CONTINUE

C       COMPUTE VELOCITY DISTRIBUTION IN THE FILM
        CALL VELOCITY
C
        WRITE(4,3)
3       FORMAT(47H1TEMP DIST ON A FILM BY GAUSS-SEIDEL ITERATION//)
        DO 4 I=1,13
        DO 4 J=1,5
        A=I
4       U(I,J)=UB+(UT-UB)*(A-1.)/12.

        N=0
5       K=0
        DO 16 J=1,5
        DO 16 I=2,12
```

UNIVERSITY OF IBADAN

```
      IF(J-1)9,6,9
6     IF(IA-I)7,7,8
7     UTEMP = UT
      GO TO 14
C8    UTEMP = (U(I+1,J)+2.*U(I,J+1)+U(I-1,J))/4.
8     UTEMP = 35
      GO TO 14
9     IF(J-5)13,10,13
10    IF(I-IB)12,11,11
11    UTEMP = UT
      GO TO 14
12    UTEMP=(U(I-1,J)+0.85)
      GO TO 14
C
      UVEL=V(I,J)
C
13    UTEMP=(ALPHA*DX*(U(I+1,J)+U(I-1,J))+(UVEL*DY*DY*U(I-1,J))/
     .(2*ALPHA*DX-(UVEL*DY*DY)))


14    DIFF=UTEMP-U(I,J)
      IF(ABS(DIFF)-EPSI)16,15,15
15    K=K+1
16    U(I,J)=UTEMP
C
      N=N+1
      IF(N-NMAX)17,20,20
17    IF(K)18,20,18

18    WRITE(4,19)N,K
19    FORMAT(7H IT NO.,I4,4H K= ,I4)
      GOTO 5
20    WRITE(4,19)N,K
C
21    FORMAT(///10F7.2)
      DO 22 M= 1,13
      I=14-M
22    WRITE(4,21)(U(I,J),J=1,5)
      RETURN
      END
C
      SUBROUTINE SOLUTION2
      COMMON/XL1/AVISC,DENS,TMMSUC,FMAG,AMAGIND,VT,VB,AGRAV
c     COMMON/XL2/RH,RL,NEX,NEY,UT,UB,EPSI,CT,CB,NN,S,NMAX
      COMMON/XL2/RH,RL,NEX,NEY,UT,UB,EPSI,CT,CB,NN,NMAX
      COMMON/XL3/NX,NY,IB,IA,VELM,FILMT,ALPHA,TAMAC,SDIFU,V(14,10),
```

UNIVERSITY OF IBADAN

```
C       COMMON/XL4/V(11,5),S(110)
        DIMENSION XCO(14),YCO(10),C(14,10),CSTORE(50,20),DIFFD(50,
        &20)
        Open(unit=273,file='SalauOdunfasolution2.out')

        DY= RL/NEY
        DX= RH/NEX
        NX=NEX+1
        NY=NEY+1
        NNT=NX*NY

        DO 103 I = 1,NX
        DO 103 J = 1,NY
        NNC= (J-1)*NX+I
        YCO(NNC)=(J-1)*DY
        XCO(NNC)=(I-1)*DX
 103  CONTINUE

C       COMPUTE VELOCITY DISTRIBUTION IN THE FILM

        CALL VELOCITY

        do 121 i=1,5
        do 121 j=1,13
c       write(4,*) 'when',v(i,j)
 121  continue

        WRITE(4,3)
3       FORMAT(47H1CONC DIST ON A FILM BY GAUSS-SEIDEL ITERATION//)

        DO 4 J=1,5
        DO 4 I=1,13
        A=I
C       IF(J.EQ.5)GOTO 4
         C(I,J)=5

4       CONTINUE



7       DO  116  J=1,5
        DO  116  I=1,13

        IF ( I.EQ.1) C(I,J)=CT
        IF(I.EQ.1) GOTO 6
        IF(I.EQ.13)C(I,J) = CB
```

UNIVERSITY OF IBADAN

```
          IF(I.EQ.13) GOTO 6
C         IF(J.EQ.1) C(I,J)=CB+(CT-CB)*(A-1.)/10
C         IF(J.EQ.1) GOTO 14
          IF(J.EQ.5) CONC= C(I,J)+0.0035
          IF(J.EQ.5) GOTO 6
 6        CSTORE(I,J)=C(I,J)
116       CONTINUE
          DO 16 J=1,5
          DO 16 I=2,12
          Do 275 k=13,1,-1
          WRITE(273,274)k,(V(k,kj),kj=1,5)
274       Format(i3,2x,5(f12.5,2x))
275       Continue
c         READ(*,*)
c         WRITE(*,*)I,J
C
13    c(i,j)=(sdifu*dx*(c(1+1,j)+c(1-1,j))+(v(i,j)*dy*dy*c(i-1,j))/
     .(2*sdifu*dx+(v(i,j)*dy*dy)))

c         READ(*,*)
16        CONTINUE
          DO 22 J=1,5
          DO 22 I=1,13


          DIFFD(I,J)=ABS( CSTORE(I,J)-C(I,J))
22         CONTINUE

          DIFF= DIFFD(1,1)
          DO  12  J =1,5
          DO  12  I =1,13

          IF(DIFFD(I,J).LT.DIFF)DIFF=DIFFD(I,J)
 12      CONTINUE

c         WRITE(*,*)'DFF',DIFF,EPSI
c         READ(*,*)

          IF(DIFF.LE.EPSI)GOTO 18
          K=K+1

          GOTO 7
C         DO 101 N=1,11
C         I=12-N
C101      WRITE(*,*)(V(I,J),J=1,5)
```

UNIVERSITY OF IBADAN

```
      N=N+1
      IF(N-NMAX)17,20,20
17    IF(K)18,20,18
18    WRITE(4,19)N,K
19    FORMAT(7H IT NO.,I4,4H K= ,I4)
C     GOTO 5
20    WRITE(4,19)N,K
21    FORMAT(///10F10.5)
      DO 232 M= 13,1,-1
      I=14-M
C     IF(C(1,5))EQ((C(1,4)+C(2,5))/2)GOTO 22
232   WRITE(4,274)i,(C(I,J),J=1,5)
      RETURN
      END
```

UNIVERSITY OF IBADAN

C: LiBr-H_2O: Parameter's distribution in the direction of film thickness
C: ABSORPTION PROCESS MODELING ON A LIQUID FALLING FILM

```
CCCCCCCCCCCCCCCCCCCCCCCCCCCCCCCCCCCCCCCCCCCCCCCCCCCCCCCCCCCCCCCC
C                                                               C
C              Ph.D FINITE DIFFERENCE MODEL                     C
C                                                               C
C                          FOR                                  C
C                                                               C
C              ABSORPTION PROCESS MODELING ON A                 C
C                                                               C
C                                                               C
C                   LIQUID FALLING FILM                         C
C                                                               C
C                                                               C
C                    K.M ODUNFA (44113)                         C
C                                                               C
C                      SUPERVISED BY                            C
C                   PROFESSOR FAGBENLE, R O                     C
C                                                               C
C                      JANUARY 2009                             C
CCCCCCCCCCCCCCCCCCCCCCCCCCCCCCCCCCCCCCCCCCCCCCCCCCCCCCCCCCCCCCCC
      COMMON/XL1/AVISC,DENS, TMMSUC,FMAG,AMAGIND,VT,VB,AGRAV
c     COMMON/XL2/RH,RL,NEX,NEY,UT,UB,EPSI,CT,CB,NN,S,NMAX
      COMMON/XL2/RH,RL,NEX,NEY,UT,UB,EPSI,CT,CB,NN,NMAX
      COMMON/XL3/NX,NY,IB,IA,VELM,FILMT,ALPHA,TAMAC,SDIFU,V(14,10)
      DIMENSION XCO(5),YCO(13)

      OPEN(UNIT = 4,FILE = 'FINAL RESULT.OUT')
      OPEN(UNIT = 6,FILE = 'LiBr2Data.IN',STATUS='OLD')
C
C     INPUT THE PROBLEM DATA
C
      READ(6,2)IA,IB,NMAX,UT,UB,CT,CB,VT,VB,AVISC,TMMSUC,EPSI
 2    FORMAT(2I3,I4,F6.2,F6.0,2F6.4,2F6.4,F8.5,F10.7,F5.2)
      WRITE(*,2)IA,IB,NMAX,UT,UB,CT,CB,VT,VB,AVISC,TMMSUC,EPSI
      READ(*,2)
      READ(6,*)RH,RL
 105  FORMAT(2(F8.5,1X))
      WRITE(*,105)RH,RL
      READ(6,*)VELM,VELM1,FILMT,AMAGIND,AGRAV
 102  FORMAT(3(F9.6,1X),F3.1, F5.3)
      WRITE(*,102)VELM,VELM1,FILMT,AMAGIND, AGRAV
      READ(6,*)ALPHA,TAMAC,SDIFU,HITAB,CONEQ,DENS
 104  FORMAT(6(F9.5,1X))
      WRITE(*,*)ALPHA,TAMAC,SDIFU,HITAB,CONEQ,DENS
```

UNIVERSITY OF IBADAN

```
      READ(6,*)NEX,NEY
 205  FORMAT(2(I3,1X))
      WRITE(*,205)NEX,NEY
C
      DY= RL/NEY
      DX= RH/NEX
      NX=NEX+1
      NY=NEY+1
      NNT=NX*NY
C
      DO 101 I = 1,NX
      DO 101 J = 1,NY
      NNC= (J-1)*NX+I
      YCO(NNC)=(J-1)*DY
      XCO(NNC)=(I-1)*DX
 101  CONTINUE
C
C     COMPUTE TEMPERATURE DISTRIBUTION IN THE FILM
C
      CALL SOLUTION1
C
C     COMPUTE CONCENTRATION DISTRIBUTION IN THE FILM

      CALL SOLUTION2
C
      STOP
      END
C
      SUBROUTINE VELOCITY
      COMMON/XL1/AVISC,DENS,TMMSUC,FMAG,AMAGIND,VT,VB,AGRAV
c     COMMON/XL2/RH,RL,NEX,NEY,UT,UB,EPSI,CT,CB,NN,S,NMAX
      COMMON/XL2/RH,RL,NEX,NEY,UT,UB,EPSI,CT,CB,NN,NMAX
      COMMON/XL3/NX,NY,IB,IA,VELM,FILMT,ALPHA,TAMAC,SDIFU,V(14,10)
      DIMENSION XCO(5),YCO(13)
C
      DY= RL/NEY
      DX= RH/NEX
      NX=NEX+1
      NY=NEY+1
      NNT=NX*NY
C
      DO 101 I = 1,NX
      DO 101 J = 1,NY
      NNC= (J-1)*NX+I
      YCO(NNC)=(J-1)*DY
      XCO(NNC)=(I-1)*DX
```

UNIVERSITY OF IBADAN

```
 101    CONTINUE

        WRITE(4,3)
3       FORMAT(47H1VEL.DIST ON A FILM BY GAUSS-SEIDEL ITERATION//)
        DO 4 I=1,5
        DO 4 J=1,13
        A=I
4       V(I,J)=VB+(VT-VB)*(A-1.)/4.
        N=0
5       K=0
        DO 16 J=1,13
        DO 16 I=2,4
        IF(J-1)9,6,9
6       IF(IA-I)7,7,8
7       UVEL = VT
        GO TO 14
C8      UTEMP = (V(I+1,J)+2.*V(I,J+1)+V(I-1,J))/4.
8       UVEL = 0.0
        GO TO 14
9       IF(J-13)13,10,13
10      IF(I-IB)12,11,11
11      UVEL = VT
        GO TO 14
c12     UTEMP=(V(I+1,J)+2.*V(I,J-1)+V(I-1,J))/4
c
12      V(I,J)= V(I,J+1)
        GO TO 14
13      UVEL = ((V(I,J+1)+V(I,J-1)+(3*VELM/FILMT**2)*DY**2
     .+DY**2*DENS*AGRAV+((DENS*TMMSUC*AMAGIND*AMAGIND)
     ./0.000001257)*DY**2))/2.0
c
14      DIFF=UVEL-V(I,J)
        IF(ABS(DIFF)-EPSI)16,15,15
15      K=K+1
16      V(I,J)=UVEL
C       write(*,*)((V(I,J),I=2,11),J=1,5)
C       read(*,*)
        N=N+1
        IF(N-NMAX)17,20,20
17      IF(K)18,20,18
18      WRITE(4,19)N,K
19      FORMAT(7H IT NO.,I4,4H K= ,I4)
        GOTO 5
20      WRITE(4,19)N,K
21      FORMAT(10F9.6)
        DO 22 M= 1,5
```

UNIVERSITY OF IBADAN

```
      I=6-M
22    WRITE(4,21)(V(I,J),J=1,13)
      RETURN
      END

C
      SUBROUTINE SOLUTION1
      COMMON/XL1/AVISC,DENS, TMMSUC,FMAG,AMAGIND,VT,VB,AGRAV
c     COMMON/XL2/RH,RL,NEX,NEY,UT,UB,EPSI,CT,CB,NN,S,NMAX
      COMMON/XL2/RH,RL,NEX,NEY,UT,UB,EPSI,CT,CB,NN,NMAX
      COMMON/XL3/NX,NY,IB,IA,VELM,FILMT,ALPHA,TAMAC,SDIFU,V(14,10)
      DIMENSION XCO(5),YCO(13),U(5,13)
c     S(100)
C
      DY= RL/NEY
      DX= RH/NEX
      NX=NEX+1
      NY=NEY+1
      NNT=NX*NY
c
      DO 102 I = 1,NX
      DO 102 J = 1,NY
      NNC= (J-1)*NX+I
      YCO(NNC)=(J-1)*DY
      XCO(NNC)=(I-1)*DX
 102  CONTINUE

C     COMPUTE VELOCITY DISTRIBUTION IN THE FILM
      CALL VELOCITY
C
      WRITE(4,3)
3     FORMAT(47H1TEMP DIST ON A FILM BY GAUSS-SEIDEL ITERATION//)
      DO 4 I=1,5
      DO 4 J=1,13
      A=I
4     U(I,J)=UB+(UT-UB)*(A-1.)/4.

      N=0
5     K=0
      DO 16 J=1,13
      DO 16 I=2,4
      IF(J-1)9,6,9
6     IF(IA-I)7,7,8
7     UTEMP = UT
      GO TO 14
C8    UTEMP = (U(I+1,J)+2.*U(I,J+1)+U(I-1,J))/4.
```

UNIVERSITY OF IBADAN

```
8       UTEMP = 35
        GO TO 14
9       IF(J-5)13,10,13
10      IF(I-IB)12,11,11
11      UTEMP = UT
        GO TO 14
c12     UTEMP=(U(I+1,J)+2.*U(I,J-1)+U(I-1,J))/4
12      UTEMP=(U(I-1,J)+0.85)
        GO TO 14
C
        UVEL=V(I,J)
13      UTEMP=(ALPHA*DX*(U(I+1,J)+U(I-1,J))-(UVEL*DY*DY*U(I-1,J))/
     .(2*ALPHA*DX-(UVEL*DY*DY)))

c
14      DIFF=UTEMP-U(I,J)
        IF(ABS(DIFF)-EPSI)16,15,15
15      K=K+1
16      U(I,J)=UTEMP
C
        N=N+1
        IF(N-NMAX)17,20,20
17      IF(K)18,20,18

18      WRITE(4,19)N,K
19      FORMAT(7H IT NO.,I4,4H K= ,I4)
        GOTO 5
20      WRITE(4,19)N,K
C
21      FORMAT(10F7.2)
        DO 22 M= 1,5
        I=6-M
22      WRITE(4,21)(U(I,J),J=1,13)
        RETURN
        END
C
        SUBROUTINE SOLUTION2
        COMMON/XL1/AVISC,DENS,TMMSUC,FMAG,AMAGIND,VT,VB,AGRAV
c       COMMON/XL2/RH,RL,NEX,NEY,UT,UB,EPSI,CT,CB,NN,S,NMAX
        COMMON/XL2/RH,RL,NEX,NEY,UT,UB,EPSI,CT,CB,NN,NMAX
        COMMON/XL3/NX,NY,IB,IA,VELM,FILMT,ALPHA,TAMAC,SDIFU,V(14,10),
C       COMMON/XL4/V(11,5),S(110)
        DIMENSION XCO(10),YCO(13),C(13,10),CSTORE(50,20),DIFFD(50,
        &20)
        Open(unit=273,file='SalauOdunfasolution2.out')
```

UNIVERSITY OF IBADAN

```
      DY= RL/NEY
      DX= RH/NEX
      NX=NEX+1
      NY=NEY+1
      NNT=NX*NY

      DO 103 I = 1,NX
      DO 103 J = 1,NY
      NNC= (J-1)*NX+I
      YCO(NNC)=(J-1)*DY
      XCO(NNC)=(I-1)*DX
103   CONTINUE

C     COMPUTE VELOCITY DISTRIBUTION IN THE FILM

      CALL VELOCITY

      do 121 i=1,13
      do 121 j=1,5
c     write(4,*) 'when',v(i,j)
121   continue

      WRITE(4,3)
3     FORMAT(47H1CONC DIST ON A FILM BY GAUSS-SEIDEL ITERATION//)

      DO 4 J=1,13
      DO 4 I=1,5
      A=I
C     IF(J.EQ.5)GOTO 4
       C(I,J)=0.5965

4     CONTINUE

7     DO  116  J=1,13
      DO  116  I=1,5

      IF ( I.EQ.1) C(I,J)=CT
      IF(I.EQ.1) GOTO 6
      IF(I.EQ.5)C(I,J) = CB
      IF(I.EQ.5) GOTO 6
C     IF(J.EQ.1) C(I,J)=CB+(CT-CB)*(A-1.)/10
C     IF(J.EQ.1) GOTO 14
      IF(J.EQ.13) CONC= C(I,J)+0.0035
      IF(J.EQ.13) GOTO 6
 6    CSTORE(I,J)=C(I,J)
116   CONTINUE
```

UNIVERSITY OF IBADAN

```
        DO 16 J=1,13
        DO 16 I=2,4
        Do 275 k=13,1,-1
       WRITE(273,274)k,(V(k,kj),kj=1,13)
274     Format(i3,2x,13(f12.5,2x))
275     Continue
c       READ(*,*)
c       WRITE(*,*)I,J

13    c(i,j)=(sdifu*dx*(c(1+1,j)+c(1-1,j))+(v(i,j)*dy*dy*c(i-1,j))/
     .(2*sdifu*dx+(v(i,j)*dy*dy)))

c       write(*,*)I,J,'conc',c(i,j)
c       READ(*,*)
16      CONTINUE
c       WRITE(*,*)'OUTTT'
        DO 22 J=1,13
        DO 22 I=1,5


         DIFFD(I,J)=ABS( CSTORE(I,J)-C(I,J))
22       CONTINUE

        DIFF= DIFFD(1,1)
        DO  12  J =1,13
        DO  12  I =1,5

        IF(DIFFD(I,J).LT.DIFF)DIFF=DIFFD(I,J)
 12     CONTINUE

c       WRITE(*,*)'DFF',DIFF,EPSI
c       READ(*,*)

        IF(DIFF.LE.EPSI)GOTO 18
        K=K+1

        GOTO 7
C       DO 101 N=1,11
C       I=12-N
C101    WRITE(*,*)(V(I,J),J=1,5)
C        READ(*,*)

        N=N+1
        IF(N-NMAX)17,20,20
17      IF(K)18,20,18
18      WRITE(4,19)N,K
```

UNIVERSITY OF IBADAN

```
19      FORMAT(7H IT NO.,I4,4H K= ,I4)
C       GOTO 5
20      WRITE(4,19)N,K
21      FORMAT(10F10.5)
        DO 232 M= 5,1,-1
        I=6-M
C       IF(C(1,5))EQ((C(1,4)+C(2,5))/2)GOTO 22
232     WRITE(4,274)i,(C(I,J),J=1,13)
        RETURN
        END
```

UNIVERSITY OF IBADAN

C: LiCl-H_2O Parameters distribution in the direction of falling

```
C: ABSORPTION PROCESS MODELING ON A LIQUID FALLING FILM
CCCCCCCCCCCCCCCCCCCCCCCCCCCCCCCCCCCCCCCCCCCCCCCCCCCCC
C                                                     C
C           Ph.D FINITE DIFFERENCE MODEL              C
C                                                     C
C                       FOR                           C
C                                                     C
C           ABSORPTION PROCESS MODELING ON A          C
C                                                     C
C                                                     C
C               LIQUID FALLING FILM                   C
C                                                     C
C                                                     C
C               K.M ODUNFA (44113)                    C
C                                                     C
C                 SUPERVISED BY                       C
C             PROFESSOR FAGBENLE, R O                 C
C                                                     C
C                  JANUARY 2009                       C
CCCCCCCCCCCCCCCCCCCCCCCCCCCCCCCCCCCCCCCCCCCCCCCCCCCCC
      COMMON/XL1/AVISC,DENS, TMMSUC,FMAG,AMAGIND,VT,VB,AGRAV
      COMMON/XL2/RH,RL,NEX,NEY,UT,UB,EPSI,CT,CB,NN,NMAX
      COMMON/XL3/NX,NY,IB,IA,VELM,FILMT,ALPHA,TAMAC,SDIFU,V(14,10)
      DIMENSION XCO(13),YCO(5)

      OPEN(UNIT = 4,FILE = 'FINAL RESULT.OUT')
      OPEN(UNIT = 6,FILE = 'LiCl Data.IN',STATUS='OLD')
C
C     INPUT THE PROBLEM DATA
C
      READ(6,2)IA,IB,NMAX,UT,UB,CT,CB,VT,VB,AVISC,TMMSUC,EPSI
 2    FORMAT(2I3,I4,F6.2,F6.0,2F6.4,2F6.4,F8.5,F10.7,F5.2)
      WRITE(*,2)IA,IB,NMAX,UT,UB,CT,CB,VT,VB,AVISC,TMMSUC,EPSI
      READ(*,2)
      READ(6,*)RH,RL
105   FORMAT(2(F8.5,1X))
      WRITE(*,105)RH,RL
      READ(6,*)VELM,VELM1,FILMT,AMAGIND,AGRAV
102   FORMAT(3(F9.6,1X),F3.1, F5.3)
      WRITE(*,102)VELM,VELM1,FILMT,AMAGIND, AGRAV
      READ(6,*)ALPHA,TAMAC,SDIFU,HITAB,CONEQ,DENS
104   FORMAT(6(F9.5,1X))
      WRITE(*,*)ALPHA,TAMAC,SDIFU,HITAB,CONEQ,DENS
      READ(6,*)NEX,NEY
```

UNIVERSITY OF IBADAN

```
 205    FORMAT(2(I3,1X))
        WRITE(*,205)NEX,NEY
C
        DY= RL/NEY
        DX= RH/NEX
        NX=NEX+1
        NY=NEY+1
        NNT=NX*NY
C
        DO 101 I = 1,NX
        DO 101 J = 1,NY
        NNC= (J-1)*NX+I
        YCO(NNC)=(J-1)*DY
        XCO(NNC)=(I-1)*DX
 101    CONTINUE
C
C       COMPUTE TEMPERATURE DISTRIBUTION IN THE FILM
C
        CALL SOLUTION1
C
C       COMPUTE CONCENTRATION DISTRIBUTION IN THE FILM

        CALL SOLUTION2
C
        STOP
        END
C
        SUBROUTINE VELOCITY
        COMMON/XL1/AVISC,DENS, TMMSUC,FMAG,AMAGIND,VT,VB,AGRAV
        COMMON/XL2/RH,RL,NEX,NEY,UT,UB,EPSI,CT,CB,NN,NMAX
        COMMON/XL3/NX,NY,IB,IA,VELM,FILMT,ALPHA,TAMAC,SDIFU,V(14,10)
        DIMENSION XCO(13),YCO(5)
C
        DY= RL/NEY
        DX= RH/NEX
        NX=NEX+1
        NY=NEY+1
        NNT=NX*NY
C
        DO 101 I = 1,NX
        DO 101 J = 1,NY
        NNC= (J-1)*NX+I
        YCO(NNC)=(J-1)*DY
        XCO(NNC)=(I-1)*DX
 101    CONTINUE
```

UNIVERSITY OF IBADAN

```
      WRITE(4,3)
3     FORMAT(47H1VEL.DIST ON A FILM BY GAUSS-SEIDEL ITERATION//)
      DO 4 I=1,13
      DO 4 J=1,5
      A=I
4     V(I,J)=VB+(VT-VB)*(A-1.)/12.
      N=0
5     K=0
      DO 16 J=1,5
      DO 16 I=2,12
      IF(J-1)9,6,9
6     IF(IA-I)7,7,8
7     UVEL = VT
      GO TO 14
C8    UTEMP = (V(I+1,J)+2.*V(I,J+1)+V(I-1,J))/4.
8     UVEL = 0.0
      GO TO 14
9     IF(J-5)13,10,13
10    IF(I-IB)12,11,11
11    UVEL = VT
      GO TO 14
c12   UTEMP=(V(I+1,J)+2.*V(I,J-1)+V(I-1,J))/4
c
12    V(I,J)= V(I,J+1)
      GO TO 14
13    UVEL = ((V(I+1,J)+V(I-1,J)+(3*VELM/FILMT**2)*DY**2
     .+ DY**2*DENS*AGRAV+((DENS*TMMSUC*AMAGIND*AMAGIND)
     ./0.000001257)*DY**2))/2.0
14    DIFF=UVEL-V(I,J)
      IF(ABS(DIFF)-EPSI)16,15,15
15    K=K+1
16    V(I,J)=UVEL
C     write(*,*)((V(I,J),I=2,11),J=1,5)
C     read(*,*)
      N=N+1
      IF(N-NMAX)17,20,20
17    IF(K)18,20,18
18    WRITE(4,19)N,K
19    FORMAT(7H IT NO.,I4,4H K= ,I4)
      GOTO 5
20    WRITE(4,19)N,K
21    FORMAT(///10F9.6)
      DO 22 M= 1,13
      I=14-M
22    WRITE(4,21)(V(I,J),J=1,5)
      RETURN
```

UNIVERSITY OF IBADAN

```
      END
C
      SUBROUTINE SOLUTION1
      COMMON/XL1/AVISC,DENS, TMMSUC,FMAG,AMAGIND,VT,VB,AGRAV
      COMMON/XL2/RH,RL,NEX,NEY,UT,UB,EPSI,CT,CB,NN,NMAX
      COMMON/XL3/NX,NY,IB,IA,VELM,FILMT,ALPHA,TAMAC,SDIFU,V(14,10)
      DIMENSION XCO(13),YCO(5),U(13,5)
C
      DY= RL/NEY
      DX= RH/NEX
      NX=NEX+1
      NY=NEY+1
      NNT=NX*NY
c
      DO 102 I = 1,NX
      DO 102 J = 1,NY
      NNC= (J-1)*NX+I
      YCO(NNC)=(J-1)*DY
      XCO(NNC)=(I-1)*DX
  102 CONTINUE

C     COMPUTE VELOCITY DISTRIBUTION IN THE FILM
      CALL VELOCITY
C
      WRITE(4,3)
3     FORMAT(47H1TEMP DIST ON A FILM BY GAUSS-SEIDEL ITERATION//)
      DO 4 I=1,13
      DO 4 J=1,5
      A=I
4     U(I,J)=UB+(UT-UB)*(A-1.)/12.

      N=0
5     K=0
      DO 16 J=1,5
      DO 16 I=2,12
      IF(J-1)9,6,9
6     IF(IA-I)7,7,8
7     UTEMP = UT
      GO TO 14
C8    UTEMP = (U(I+1,J)+2.*U(I,J+1)+U(I-1,J))/4.
8     UTEMP = 35
      GO TO 14
9     IF(J-5)13,10,13
10    IF(I-IB)12,11,11
11    UTEMP = UT
      GO TO 14
```

UNIVERSITY OF IBADAN

```
c12     UTEMP=(U(I+1,J)+2.*U(I,J-1)+U(I-1,J))/4
12      UTEMP=(U(I-1,J)+0.75)
        GO TO 14
C
        UVEL=V(I,J)
C
13      UTEMP=(ALPHA*DX*(U(I+1,J)+U(I-1,J))+(UVEL*DY*DY*U(I+1,J))/
   .(2*ALPHA*DX-(UVEL*DY*DY)))
c
14      DIFF=UTEMP-U(I,J)
        IF(ABS(DIFF)-EPSI)16,15,15
15      K=K+1
16      U(I,J)=UTEMP
C
        N=N+1
        IF(N-NMAX)17,20,20
17      IF(K)18,20,18

18      WRITE(4,19)N,K
19      FORMAT(7H IT NO.,I4,4H K= ,I4)
        GOTO 5
20      WRITE(4,19)N,K
C
21      FORMAT(///10F7.2)
        DO 22 M= 1,13
        I=14-M
22      WRITE(4,21)(U(I,J),J=1,5)
        RETURN
        END
C
        SUBROUTINE SOLUTION2
        COMMON/XL1/AVISC,DENS, TMMSUC,FMAG,AMAGIND,VT,VB,AGRAV
        COMMON/XL2/RH,RL,NEX,NEY,UT,UB,EPSI,CT,CB,NN,NMAX
        COMMON/XL3/NX,NY,IB,IA,VELM,FILMT,ALPHA,TAMAC,SDIFU,V(14,10),
        DIMENSION XCO(13),YCO(10),C(13,10),CSTORE(50,20),DIFFD(50,
        &20)
        Open(unit=273,file='SalauOdunfasolution2.out')

        DY= RL/NEY
        DX= RH/NEX
        NX=NEX+1
        NY=NEY+1
        NNT=NX*NY

       DO 103 I = 1,NX
       DO 103 J = 1,NY
```

UNIVERSITY OF IBADAN

```
      NNC= (J-1)*NX+I
      YCO(NNC)=(J-1)*DY
      XCO(NNC)=(I-1)*DX
 103  CONTINUE

C     COMPUTE VELOCITY DISTRIBUTION IN THE FILM

      CALL VELOCITY

      do 121 i=1,5
      do 121 j=1,13
c     write(4,*) 'when',v(i,j)
 121   continue

      WRITE(4,3)
3     FORMAT(47H1CONC DIST ON A FILM BY GAUSS-SEIDEL ITERATION//)

      DO 4 J=1,5
      DO 4 I=1,13
      A=I
C     IF(J.EQ.5)GOTO 4
      C(I,J)=0.358
c     V(I,J)=VB+(VT-VB)*(A-1.)/10.

4     CONTINUE

7     DO  116  J=1,5
      DO  116  I=1,13

      IF ( I.EQ.1) C(I,J)=CT
      IF(I.EQ.1) GOTO 6
      IF(I.EQ.11)C(I,J) = CB
      IF(I.EQ.11) GOTO 6
C     IF(J.EQ.1) C(I,J)=CB+(CT-CB)*(A-1.)/10
C     IF(J.EQ.1) GOTO 14
      IF(J.EQ.5) CONC= C(I,J)+0.0040
      IF(J.EQ.5) GOTO 6
 6    CSTORE(I,J)=C(I,J)
116   CONTINUE
      DO 16 J=1,5
      DO 16 I=2,12
      Do 275 k=13,1,-1
      WRITE(273,274)k,(V(k,kj),kj=1,5)
274   Format(i3,2x,5(f12.5,2x))
275   Continue
c     READ(*,*)
```

UNIVERSITY OF IBADAN

```
c       WRITE(*,*)I,J
C
13   c(i,j)=(sdifu*dx*(c(1+1,j)+c(1-1,j))+(v(i,j)*dy*dy*c(i-1,j))/
    .(2*sdifu*dx+(v(i,j)*dy*dy)))

c       write(*,*)I,J,'conc',c(i,j)
c       READ(*,*)
16      CONTINUE
c       WRITE(*,*)'OUTTT'
        DO 22 J=1,5
        DO 22 I=1,13
         DIFFD(I,J)=ABS( CSTORE(I,J)-C(I,J))
22       CONTINUE

        DIFF= DIFFD(1,1)
        DO  12  J =1,5
        DO  12  I =1,13

        IF(DIFFD(I,J).LT.DIFF)DIFF=DIFFD(I,J)
 12     CONTINUE

c       WRITE(*,*)'DFF',DIFF,EPSI
c       READ(*,*)

        IF(DIFF.LE.EPSI)GOTO 18
        K=K+1

        GOTO 7
C       DO 101 N=1,11
C       I=12-N
C101    WRITE(*,*)(V(I,J),J=1,5)
C       READ(*,*)

        N=N+1
        IF(N-NMAX)17,20,20
17      IF(K)18,20,18
18      WRITE(4,19)N,K
19      FORMAT(7H IT NO.,I4,4H K= ,I4)
C       GOTO 5
20      WRITE(4,19)N,K
21      FORMAT(///10F10.5)
        DO 232 M= 13,1,-1
        I=14-M
C       IF(C(1,5))EQ((C(1,4)+C(2,5))/2)GOTO 22
232     WRITE(4,274)i,(C(I,J),J=1,5)
        RETURN
```

UNIVERSITY OF IBADAN

```
      END
C: LiCl2-H2O Parameter's distribution in the direction of film thickness
C: ABSORPTION PROCESS MODELING ON A LIQUID FALLING FILM
CCCCCCCCCCCCCCCCCCCCCCCCCCCCCCCCCCCCCCCCCCCCCCCCCC
C                                                  C
C              Ph.D FINITE DIFFERENCE MODEL        C
C                                                  C
C                         FOR                      C
C                                                  C
C         ABSORPTION PROCESS MODELING ON A         C
C                                                  C
C                                                  C
C                 LIQUID FALLING FILM              C
C                                                  C
C                                                  C
C                  K.M ODUNFA (44113)              C
C                                                  C
C                    SUPERVISED BY                 C
C              PROFESSOR FAGBENLE, R O             C
C                                                  C
C                    JANUARY 2009                  C
CCCCCCCCCCCCCCCCCCCCCCCCCCCCCCCCCCCCCCCCCCCCCCCCCC

      COMMON/XL1/AVISC,DENS, TMMSUC,FMAG,AMAGIND,VT,VB,AGRAV
      COMMON/XL2/RH,RL,NEX,NEY,UT,UB,EPSI,CT,CB,NN,NMAX
      COMMON/XL3/NX,NY,IB,IA,VELM,FILMT,ALPHA,TAMAC,SDIFU,V(10,14)
      DIMENSION XCO(5),YCO(13)

      OPEN(UNIT = 4,FILE = 'FINAL RESULT.OUT')
      OPEN(UNIT = 6,FILE = 'LiCl2 Data.IN',STATUS='OLD')
C
C     INPUT THE PROBLEM DATA
C
      READ(6,2)IA,IB,NMAX,UT,UB,CT,CB,VT,VB,AVISC,TMMSUC,EPSI
 2    FORMAT(2I3,I4,F6.2,F6.0,2F6.4,2F6.4,F7.5,F10.7,F5.2)
      WRITE(*,2)IA,IB,NMAX,UT,UB,CT,CB,VT,VB,AVISC,TMMSUC,EPSI
      READ(*,2)
      READ(6,*)RH,RL
 105  FORMAT(2(F8.5,1X))
      WRITE(*,105)RH,RL
      READ(6,*)VELM,VELM1,FILMT,AMAGIND,AGRAV
 102  FORMAT(3(F9.6,1X),F3.1, F5.3)
      WRITE(*,102)VELM,VELM1,FILMT,AMAGIND, AGRAV
      READ(6,*)ALPHA,TAMAC,SDIFU,HITAB,CONEQ,DENS
 104  FORMAT(6(F9.5,1X))
      WRITE(*,*)ALPHA,TAMAC,SDIFU,HITAB,CONEQ,DENS
```

```
      READ(6,*)NEX,NEY
 205  FORMAT(2(I3,1X))
      WRITE(*,205)NEX,NEY
C
      DY= RL/NEY
      DX= RH/NEX
      NX=NEX+1
      NY=NEY+1
      NNT=NX*NY
C
      DO 101 I = 1,NX
      DO 101 J = 1,NY
      NNC= (J-1)*NX+I
      YCO(NNC)=(J-1)*DY
      XCO(NNC)=(I-1)*DX
 101  CONTINUE
C
C     COMPUTE TEMPERATURE DISTRIBUTION IN THE FILM
C
      CALL SOLUTION1
C
C     COMPUTE CONCENTRATION DISTRIBUTION IN THE FILM

      CALL SOLUTION2
C
      STOP
      END
C
      SUBROUTINE VELOCITY
      COMMON/XL1/AVISC,DENS,TMMSUC,FMAG,AMAGIND,VT,VB,AGRAV
      COMMON/XL2/RH,RL,NEX,NEY,UT,UB,EPSI,CT,CB,NN,NMAX
      COMMON/XL3/NX,NY,IB,IA,VELM,FILMT,ALPHA,TAMAC,SDIFU,V(10,14)
      DIMENSION XCO(5),YCO(13)
C
      DY= RL/NEY
      DX= RH/NEX
      NX=NEX+1
      NY=NEY+1
      NNT=NX*NY
C
      DO 101 I = 1,NX
      DO 101 J = 1,NY
      NNC= (J-1)*NX+I
      YCO(NNC)=(J-1)*DY
      XCO(NNC)=(I-1)*DX
 101  CONTINUE
```

UNIVERSITY OF IBADAN

```
      WRITE(4,3)
3     FORMAT(47H1VEL.DIST ON A FILM BY GAUSS-SEIDEL ITERATION//)
      DO 4 I=1,5
      DO 4 J=1,13
      A=I
4     V(I,J)=VB+(VT-VB)*(A-1.)/4.
      N=0
5     K=0
      DO 16 J=1,13
      DO 16 I=2,4
      IF(J-1)9,6,9
6     IF(IA-I)7,7,8
7     UVEL = VT
      GO TO 14
C8    UTEMP = (V(I+1,J)+2.*V(I,J+1)+V(I-1,J))/4.
8     UVEL = 0.0
      GO TO 14
9     IF(J-13)13,10,13
10    IF(I-IB)12,11,11
11    UVEL = VT
      GO TO 14
c12   UTEMP=(V(I+1,J)+2.*V(I,J-1)+V(I-1,J))/4

12    V(I,J)= V(I,J+1)
      GO TO 14
13    UVEL = ((V(I,J+1)+V(I,J-1)+(3*VELM/FILMT**2)*DY**2
     .+DY**2*DENS*AGRAV+((DENS*TMMSUC*AMAGIND*AMAGIND)
     ./0.000001257)*DY**2))/2.0
c
14    DIFF=UVEL-V(I,J)
      IF(ABS(DIFF)-EPSI)16,15,15
15    K=K+1
16    V(I,J)=UVEL
C     write(*,*)((V(I,J),I=2,11),J=1,5)
C     read(*,*)
      N=N+1
      IF(N-NMAX)17,20,20
17    IF(K)18,20,18
18    WRITE(4,19)N,K
19    FORMAT(7H IT NO.,I4,4H K= ,I4)
      GOTO 5
20    WRITE(4,19)N,K
21    FORMAT(10F9.6)
      DO 22 M= 1,5
      I=6-M
```

UNIVERSITY OF IBADAN

```
22      WRITE(4,21)(V(I,J),J=1,13)
C22     WRITE(4,*)(V(I,J),J=1,13)

        RETURN
        END

C
        SUBROUTINE SOLUTION1
        COMMON/XL1/AVISC,DENS, TMMSUC,FMAG,AMAGIND,VT,VB,AGRAV
        COMMON/XL2/RH,RL,NEX,NEY,UT,UB,EPSI,CT,CB,NN,NMAX
        COMMON/XL3/NX,NY,IB,IA,VELM,FILMT,ALPHA,TAMAC,SDIFU,V(10,14)
        DIMENSION XCO(5),YCO(13),U(5,13)
C
        DY= RL/NEY
        DX= RH/NEX
        NX=NEX+1
        NY=NEY+1
        NNT=NX*NY
c
        DO 102 I = 1,NX
        DO 102 J = 1,NY
        NNC= (J-1)*NX+I
        YCO(NNC)=(J-1)*DY
        XCO(NNC)=(I-1)*DX
 102    CONTINUE

C       COMPUTE VELOCITY DISTRIBUTION IN THE FILM
        CALL VELOCITY
C
        WRITE(4,3)
3       FORMAT(47H1TEMP DIST ON A FILM BY GAUSS-SEIDEL ITERATION//)
        DO 4 I=1,5
        DO 4 J=1,13
        A=I
4       U(I,J)=UB+(UT-UB)*(A-1.)/4.

        N=0
5       K=0
        DO 16 J=1,13
        DO 16 I=2,4
        IF(J-1)9,6,9
6       IF(IA-I)7,7,8
7       UTEMP = UT
        GO TO 14
C8      UTEMP = (U(I+1,J)+2.*U(I,J+1)+U(I-1,J))/4.
8       UTEMP = 35
```

UNIVERSITY OF IBADAN

```
      GO TO 14
9     IF(J-13)13,10,13
10    IF(I-IB)12,11,11
11    UTEMP = UT
      GO TO 14
c12   UTEMP=(U(I+1,J)+2.*U(I,J-1)+U(I-1,J))/4
12    UTEMP=(U(I-1,J)+0.75)
      GO TO 14
C
      UVEL=V(I,J)
C
13    UTEMP=(ALPHA*DX*(U(I+1,J)+U(I-1,J))-(UVEL*DY*DY*U(I-1,J))/
     .(2*ALPHA*DX-(UVEL*DY*DY)))
c
14    DIFF=UTEMP-U(I,J)
      IF(ABS(DIFF)-EPSI)16,15,15
15    K=K+1
16    U(I,J)=UTEMP
C
      N=N+1
      IF(N-NMAX)17,20,20
17    IF(K)18,20,18

18    WRITE(4,19)N,K
19    FORMAT(7H IT NO.,I4,4H K= ,I4)
      GOTO 5
20    WRITE(4,19)N,K
C
21    FORMAT(10F7.2)
      DO 22 M= 1,5
      I=6-M
22    WRITE(4,21)(U(I,J),J=1,13)
      RETURN
      END
C
      SUBROUTINE SOLUTION2
      COMMON/XL1/AVISC,DENS,TMMSUC,FMAG,AMAGIND,VT,VB,AGRAV
      COMMON/XL2/RH,RL,NEX,NEY,UT,UB,EPSI,CT,CB,NN,NMAX
      COMMON/XL3/NX,NY,IB,IA,VELM,FILMT,ALPHA,TAMAC,SDIFU,V(10,14),
      DIMENSION XCO(10),YCO(13),C(13,10),CSTORE(50,20),DIFFD(50,
      &20)
      Open(unit=273,file='SalauOdunfasolution2.out')

      DY= RL/NEY
      DX= RH/NEX
      NX=NEX+1
```

UNIVERSITY OF IBADAN

```
      NY=NEY+1
      NNT=NX*NY

      DO 103 I = 1,NX
      DO 103 J = 1,NY
      NNC= (J-1)*NX+I
      YCO(NNC)=(J-1)*DY
      XCO(NNC)=(I-1)*DX
 103  CONTINUE

C     COMPUTE VELOCITY DISTRIBUTION IN THE FILM

      CALL VELOCITY

      do 121 i=1,13
      do 121 j=1,5
c     write(4,*) 'when',v(i,j)
 121  continue

      WRITE(4,3)
3     FORMAT(47H1CONC DIST ON A FILM BY GAUSS-SEIDEL ITERATION//)

      DO 4 J=1,13
      DO 4 I=1,5
      A=I
C     IF(J.EQ.5)GOTO 4
      C(I,J)=0.446

4     CONTINUE

7     DO  116  J=1,13
      DO  116  I=1,5

      IF ( I.EQ.1) C(I,J)=CT
      IF(I.EQ.1) GOTO 6
      IF(I.EQ.5)C(I,J) = CB
      IF(I.EQ.5) GOTO 6
C     IF(J.EQ.1) C(I,J)=CB+(CT-CB)*(A-1.)/10
C     IF(J.EQ.1) GOTO 14
      IF(J.EQ.13) CONC= C(I,J)+0.0040
      IF(J.EQ.13) GOTO 6
 6    CSTORE(I,J)=C(I,J)
116   CONTINUE
      DO 16 J=1,13
      DO 16 I=2,4
      Do 275 k=13,1,-1
```

UNIVERSITY OF IBADAN

```
      WRITE(273,274)k,(V(k,kj),kj=1,13)
274   Format(i3,x,13(f12.5,x))
275   Continue
c     READ(*,*)
c     WRITE(*,*)I,J

C
13   c(i,j)=(sdifu*dx*(c(1+1,j)+c(1-1,j))+(v(i,j)*dy*dy*c(i-1,j))/
    .(2*sdifu*dx+(v(i,j)*dy*dy)))

c     write(*,*)I,J,'conc',c(i,j)
c     READ(*,*)
16    CONTINUE
c     WRITE(*,*)'OUTTT'
      DO 22 J=1,13
      DO 22 I=1,5


      DIFFD(I,J)=ABS( CSTORE(I,J)-C(I,J))
22     CONTINUE

      DIFF= DIFFD(1,1)
      DO  12  J =1,13
      DO  12  I =1,5

      IF(DIFFD(I,J).LT.DIFF)DIFF=DIFFD(I,J)
 12   CONTINUE

c     WRITE(*,*)'DFF',DIFF,EPSI
c     READ(*,*)

      IF(DIFF.LE.EPSI)GOTO 18
      K=K+1

      GOTO 7
C     DO 101 N=1,11
C     I=12-N
C     READ(*,*)

      N=N+1
      IF(N-NMAX)17,20,20
17    IF(K)18,20,18
18    WRITE(4,19)N,K
19    FORMAT(7H IT NO.,I4,4H K= ,I4)
C     GOTO 5
20    WRITE(4,19)N,K
```

UNIVERSITY OF IBADAN

```
21      FORMAT(///10F10.5)
        DO 232 M= 5,1,-1
        I=6-M
C       IF(C(1,5))EQ((C(1,4)+C(2,5))/2)GOTO 22
232     WRITE(4,274)i,(C(I,J),J=1,13)
        RETURN
        END
```

UNIVERSITY OF IBADAN

APPENDIX C

COMPUTER RESULTS

LiBr-H_2O

IN THE DIRECTION OF FALLING

LiBr-H_2O
At B= 0.0

1VEL.DIST ON A FILM BY GAUSS-SEIDEL ITERATION//
IT NO. 1 K= 22
IT NO. 2 K= 11
IT NO. 3 K= 11
IT NO. 4 K= 11
IT NO. 5 K= 11
IT NO. 6 K= 11
IT NO. 7 K= 11
IT NO. 8 K= 11
IT NO. 9 K= 11
IT NO. 10 K= 11
IT NO. 11 K= 11
IT NO. 12 K= 11
IT NO. 13 K= 11
IT NO. 14 K= 11
IT NO. 15 K= 11
IT NO. 16 K= 11
IT NO. 17 K= 11
IT NO. 18 K= 11
IT NO. 19 K= 11
IT NO. 20 K= 11
IT NO. 21 K= 11
IT NO. 22 K= 11
IT NO. 23 K= 11
IT NO. 24 K= 11
IT NO. 25 K= 11
IT NO. 26 K= 11
IT NO. 27 K= 11
IT NO. 28 K= 11
IT NO. 29 K= 11
IT NO. 30 K= 11
IT NO. 31 K= 11
IT NO. 32 K= 11
IT NO. 33 K= 11

UNIVERSITY OF IBADAN

IT NO. 34 K= 11
IT NO. 35 K= 11
IT NO. 36 K= 11
IT NO. 37 K= 11
IT NO. 38 K= 11
IT NO. 39 K= 11
IT NO. 40 K= 11
IT NO. 41 K= 11
IT NO. 42 K= 11
IT NO. 43 K= 11
IT NO. 44 K= 11
IT NO. 45 K= 11
IT NO. 46 K= 11
IT NO. 47 K= 11
IT NO. 48 K= 11
IT NO. 49 K= 11
IT NO. 50 K= 11
IT NO. 51 K= 11
IT NO. 52 K= 11
IT NO. 53 K= 11
IT NO. 54 K= 11
IT NO. 55 K= 11
IT NO. 56 K= 11
IT NO. 57 K= 11
IT NO. 58 K= 11
IT NO. 59 K= 11
IT NO. 60 K= 11
IT NO. 61 K= 11
IT NO. 62 K= 11
IT NO. 63 K= 11
IT NO. 64 K= 11
IT NO. 65 K= 11
IT NO. 66 K= 11
IT NO. 67 K= 11
IT NO. 68 K= 11
IT NO. 69 K= 11
IT NO. 70 K= 11
IT NO. 71 K= 11
IT NO. 72 K= 11
IT NO. 73 K= 11
IT NO. 74 K= 11
IT NO. 75 K= 11
IT NO. 76 K= 11
IT NO. 77 K= 11
IT NO. 78 K= 11
IT NO. 79 K= 11

UNIVERSITY OF IBADAN

IT NO. 80 K= 11
IT NO. 81 K= 11
IT NO. 82 K= 11
IT NO. 83 K= 11
IT NO. 84 K= 11
IT NO. 85 K= 11
IT NO. 86 K= 11
IT NO. 87 K= 11
IT NO. 88 K= 11
IT NO. 89 K= 11
IT NO. 90 K= 11
IT NO. 91 K= 11
IT NO. 92 K= 11
IT NO. 93 K= 11
IT NO. 94 K= 11
IT NO. 95 K= 11
IT NO. 96 K= 11
IT NO. 97 K= 11
IT NO. 98 K= 11
IT NO. 99 K= 11
IT NO. 100 K= 11

.362000 .362000 .362000 .362000 .362000

.000000 .366245 .366245 .366245 .366245

.000000 .370384 .370384 .370384 .366245

.000000 .374418 .374418 .374418 .366245

.000000 .378348 .378348 .378348 .366245

.000000 .382172 .382172 .382172 .366245

UNIVERSITY OF IBADAN

.000000 .385891 .385891 .385891 .366245

.000000 .389505 .389505 .389505 .366245

.000000 .393014 .393014 .393014 .366245

.000000 .396418 .396418 .396418 .366245

.000000 .399717 .399717 .399717 .366245

.000000 .402911 .402911 .402911 .366245

.406000 .406000 .406000 .406000 .406000
1TEMP DIST ON A FILM BY GAUSS-SEIDEL ITERATION/

IT NO. 1 K= 43
IT NO. 2 K= 0

44.44 44.44 44.44 44.44 44.44

35.00 44.40 44.40 44.40 44.35

35.00 43.45 43.45 43.45 43.50

UNIVERSITY OF IBADAN

35.00 42.52 42.52 42.52 42.65

35.00 41.61 41.61 41.61 41.80

35.00 40.72 40.72 40.72 40.95

35.00 39.85 39.85 39.85 40.10

35.00 39.00 39.00 39.00 39.25

35.00 38.16 38.16 38.16 38.40

35.00 37.35 37.35 37.35 37.55

35.00 36.55 36.55 36.55 36.70

35.00 35.77 35.77 35.77 35.85

35.00 35.00 35.00 35.00 35.00

1CONC DIST ON A FILM BY GAUSS-SEIDEL ITERATION/

IT NO. 0 K= 0
IT NO. 0 K= 0

1	.60000	.60000	.60000	.60000	.60000
2	.00000	.59545	.59545	.59545	.59500
3	.00000	.59090	.59090	.59090	.59004
4	.00000	.58635	.58635	.58635	.58513

UNIVERSITY OF IBADAN

5	.00000	.58180	.58180	.58180	.58025
6	.00000	.57724	.57724	.57724	.57542
7	.00000	.57267	.57267	.57267	.57063
8	.00000	.56810	.56810	.56810	.56587
9	.00000	.56352	.56352	.56352	.56116
10	.00000	.55892	.55892	.55892	.55648
11	.00000	.55432	.55432	.55432	.55185
12	.00000	.54970	.54970	.54970	.54725
13	.54500	.54500	.54500	.54500	.54500

At B=1.4

1VEL.DIST ON A FILM BY GAUSS-SEIDEL ITERATION//

.362000 .362000 .362000 .362000 .362000

.000000 .367444 .367444 .367444 .367444

.000000 .372564 .372564 .372564 .367444

.000000 .377361 .377361 .377361 .367444

.000000 .381835 .381835 .381835 .367444

.000000 .385986 .385986 .385986 .367444

.000000 .389814 .389814 .389814 .367444

.000000 .393319 .393319 .393319 .367444

UNIVERSITY OF IBADAN

.000000 .396501 .396501 .396501 .367444

.000000 .399360 .399360 .399360 .367444

.000000 .401897 .401897 .401897 .367444

.000000 .404110 .404110 .404110 .367444

.406000 .406000 .406000 .406000 .406000
1TEMP DIST ON A FILM BY GAUSS-SEIDEL ITERATION/

IT NO. 1 K= 43
IT NO. 2 K= 0

44.44 44.44 44.44 44.44 44.44

35.00 44.40 44.40 44.40 44.35

35.00 43.45 43.45 43.45 43.50

35.00 42.52 42.52 42.52 42.65

35.00 41.61 41.61 41.61 41.80

UNIVERSITY OF IBADAN

35.00 40.72 40.72 40.72 40.95

35.00 39.85 39.85 39.85 40.10

35.00 39.00 39.00 39.00 39.25

35.00 38.16 38.16 38.16 38.40

35.00 37.35 37.35 37.35 37.55

35.00 36.55 36.55 36.55 36.70

35.00 35.77 35.77 35.77 35.85

35.00 35.00 35.00 35.00 35.00

1CONC DIST ON A FILM BY GAUSS-SEIDEL ITERATION/

IT NO. 0 K= 0
IT NO. 0 K= 0

1	.60000	.60000	.60000	.60000	.60000
2	.00000	.59547	.59547	.59547	.59502
3	.00000	.59094	.59094	.59094	.59008
4	.00000	.58642	.58642	.58642	.58518
5	.00000	.58191	.58191	.58191	.58032
6	.00000	.57739	.57739	.57739	.57550
7	.00000	.57287	.57287	.57287	.57072
8	.00000	.56834	.56834	.56834	.56598
9	.00000	.56380	.56380	.56380	.56128
10	.00000	.55924	.55924	.55924	.55662
11	.00000	.55465	.55465	.55465	.55200
12	.00000	.55005	.55005	.55005	.54741

UNIVERSITY OF IBADAN

13 .54500 .54500 .54500 .54500 .54500

At B=3.0

1VEL.DIST ON A FILM BY GAUSS-SEIDEL ITERATION//

.362000 .362000 .362000 .362000 .362000

.000000 .371751 .371751 .371751 .371751

.000000 .380396 .380396 .380396 .371751

.000000 .387933 .387933 .387933 .371751

.000000 .394364 .394364 .394364 .371751

.000000 .399689 .399689 .399689 .371751

.000000 .403908 .403908 .403908 .371751

.000000 .407021 .407021 .407021 .371751

.000000 .409029 .409029 .409029 .371751

.000000 .409930 .409930 .409930 .371751

UNIVERSITY OF IBADAN

.000000 .409726 .409726 .409726 .371751

.000000 .408416 .408416 .408416 .371751

.406000 .406000 .406000 .406000 .406000
1TEMP DIST ON A FILM BY GAUSS-SEIDEL ITERATION/

IT NO. 1 K= 43
IT NO. 2 K= 0

44.44 44.44 44.44 44.44 44.44

35.00 44.40 44.40 44.40 44.35

35.00 43.45 43.45 43.45 43.50

35.00 42.52 42.52 42.52 42.65

35.00 41.61 41.61 41.61 41.80

35.00 40.72 40.72 40.72 40.95

35.00 39.85 39.85 39.85 40.10

UNIVERSITY OF IBADAN

35.00 39.00 39.00 39.00 39.25

35.00 38.16 38.16 38.16 38.40

35.00 37.35 37.35 37.35 37.55

35.00 36.55 36.55 36.55 36.70

35.00 35.77 35.77 35.77 35.85

35.00 35.00 35.00 35.00 35.00

1CONC DIST ON A FILM BY GAUSS-SEIDEL ITERATION/

IT NO. 0 K= 0
IT NO. 0 K= 0

1	.60000	.60000	.60000	.60000	.60000
2	.00000	.59551	.59551	.59551	.59507
3	.00000	.59107	.59107	.59107	.59019
4	.00000	.58667	.58667	.58667	.58535
5	.00000	.58229	.58229	.58229	.58054
6	.00000	.57792	.57792	.57792	.57577
7	.00000	.57355	.57355	.57355	.57105
8	.00000	.56917	.56917	.56917	.56636
9	.00000	.56476	.56476	.56476	.56171
10	.00000	.56032	.56032	.56032	.55710
11	.00000	.55582	.55582	.55582	.55253
12	.00000	.55126	.55126	.55126	.54799
13	.54500	.54500	.54500	.54500	.54500

LiCl-H_2O

At B=0.0

1VEL.DIST ON A FILM BY GAUSS-SEIDEL ITERATION//
IT NO. 1 K= 22
IT NO. 2 K= 11

UNIVERSITY OF IBADAN

IT NO. 3 K= 11
IT NO. 4 K= 11
IT NO. 5 K= 11
IT NO. 6 K= 11
IT NO. 7 K= 11
IT NO. 8 K= 11
IT NO. 9 K= 11
IT NO. 10 K= 11
IT NO. 11 K= 11
IT NO. 12 K= 11
IT NO. 13 K= 11
IT NO. 14 K= 11
IT NO. 15 K= 11
IT NO. 16 K= 11
IT NO. 17 K= 11
IT NO. 18 K= 11
IT NO. 19 K= 11
IT NO. 20 K= 11
IT NO. 21 K= 11
IT NO. 22 K= 11
IT NO. 23 K= 11
IT NO. 24 K= 11
IT NO. 25 K= 11
IT NO. 26 K= 11
IT NO. 27 K= 11
IT NO. 28 K= 11
IT NO. 29 K= 11
IT NO. 30 K= 11
IT NO. 31 K= 11
IT NO. 32 K= 11
IT NO. 33 K= 11
IT NO. 34 K= 11
IT NO. 35 K= 11
IT NO. 36 K= 11
IT NO. 37 K= 11
IT NO. 38 K= 11
IT NO. 39 K= 11
IT NO. 40 K= 11
IT NO. 41 K= 11
IT NO. 42 K= 11
IT NO. 43 K= 11
IT NO. 44 K= 11
IT NO. 45 K= 11
IT NO. 46 K= 11
IT NO. 47 K= 11
IT NO. 48 K= 11

UNIVERSITY OF IBADAN

IT NO. 49 K= 11
IT NO. 50 K= 11
IT NO. 51 K= 11
IT NO. 52 K= 11
IT NO. 53 K= 11
IT NO. 54 K= 11
IT NO. 55 K= 11
IT NO. 56 K= 11
IT NO. 57 K= 11
IT NO. 58 K= 11
IT NO. 59 K= 11
IT NO. 60 K= 11
IT NO. 61 K= 11
IT NO. 62 K= 11
IT NO. 63 K= 11
IT NO. 64 K= 11
IT NO. 65 K= 11
IT NO. 66 K= 11
IT NO. 67 K= 11
IT NO. 68 K= 11
IT NO. 69 K= 11
IT NO. 70 K= 11
IT NO. 71 K= 11
IT NO. 72 K= 11
IT NO. 73 K= 11
IT NO. 74 K= 11
IT NO. 75 K= 11
IT NO. 76 K= 11
IT NO. 77 K= 11
IT NO. 78 K= 11
IT NO. 79 K= 11
IT NO. 80 K= 11
IT NO. 81 K= 11
IT NO. 82 K= 11
IT NO. 83 K= 11
IT NO. 84 K= 11
IT NO. 85 K= 11
IT NO. 86 K= 11
IT NO. 87 K= 11
IT NO. 88 K= 11
IT NO. 89 K= 11
IT NO. 90 K= 11
IT NO. 91 K= 11
IT NO. 92 K= 11
IT NO. 93 K= 11
IT NO. 94 K= 11

UNIVERSITY OF IBADAN

IT NO. 95 K= 11
IT NO. 96 K= 11
IT NO. 97 K= 11
IT NO. 98 K= 11
IT NO. 99 K= 11
IT NO. 100 K= 11

.362000 .362000 .362000 .362000 .362000

.000000 .366245 .366245 .366245 .366245

.000000 .370384 .370384 .370384 .366245

.000000 .374418 .374418 .374418 .366245

.000000 .378348 .378348 .378348 .366245

.000000 .382172 .382172 .382172 .366245

.000000 .385891 .385891 .385891 .366245

.000000 .389505 .389505 .389505 .366245

.000000 .393014 .393014 .393014 .366245

.000000 .396418 .396418 .396418 .366245

UNIVERSITY OF IBADAN

.000000 .399717 .399717 .399717 .366245

.000000 .402911 .402911 .402911 .366245

.406000 .406000 .406000 .406000 .406000
1TEMP DIST ON A FILM BY GAUSS-SEIDEL ITERATION/

IT NO. 1 K= 55
IT NO. 2 K= 30
IT NO. 3 K= 27
IT NO. 4 K= 24
IT NO. 5 K= 21
IT NO. 6 K= 18
IT NO. 7 K= 15
IT NO. 8 K= 12
IT NO. 9 K= 9
IT NO. 10 K= 6
IT NO. 11 K= 3
IT NO. 12 K= 0

35.00 35.00 35.00 35.00 35.00

35.00 34.74 34.74 34.74 38.25

35.00 34.49 34.49 34.49 37.50

35.00 34.23 34.23 34.23 36.75

35.00 33.98 33.98 33.98 36.00

UNIVERSITY OF IBADAN

35.00 33.73 33.73 33.73 35.25

35.00 33.48 33.48 33.48 34.50

35.00 33.24 33.24 33.24 33.75

35.00 32.99 32.99 32.99 33.00

35.00 32.75 32.75 32.75 32.25

35.00 32.51 32.51 32.51 31.50

35.00 32.27 32.27 32.27 30.75

30.00 30.00 30.00 30.00 30.00

1CONC DIST ON A FILM BY GAUSS-SEIDEL ITERATION/

IT NO. 0 K= 0
IT NO. 0 K= 0

1	.45000	.45000	.45000	.45000	.45000
2	.00000	.44532	.44532	.44532	.44486
3	.00000	.44066	.44066	.44066	.43978
4	.00000	.43601	.43601	.43601	.43476
5	.00000	.43136	.43136	.43136	.42979
6	.00000	.42673	.42673	.42673	.42489
7	.00000	.42210	.42210	.42210	.42003
8	.00000	.41748	.41748	.41748	.41524
9	.00000	.41286	.41286	.41286	.41049
10	.00000	.40825	.40825	.40825	.40581
11	.00000	.40364	.40364	.40364	.40117
12	.00000	.39903	.39903	.39903	.39659

UNIVERSITY OF IBADAN

13 .35800 .35800 .35800 .35800 .35800

At B=1.4

1VEL.DIST ON A FILM BY GAUSS-SEIDEL ITERATION//

.362000 .362000 .362000 .362000 .362000

.000000 .367094 .367094 .367094 .367094

.000000 .371929 .371929 .371929 .367094

.000000 .376503 .376503 .376503 .367094

.000000 .380819 .380819 .380819 .367094

.000000 .384874 .384874 .384874 .367094

.000000 .388671 .388671 .388671 .367094

.000000 .392207 .392207 .392207 .367094

.000000 .395485 .395485 .395485 .367094

.000000 .398503 .398503 .398503 .367094

UNIVERSITY OF IBADAN

.000000 .401261 .401261 .401261 .367094

.000000 .403760 .403760 .403760 .367094

.406000 .406000 .406000 .406000 .406000
1TEMP DIST ON A FILM BY GAUSS-SEIDEL ITERATION/

IT NO. 1 K= 55
IT NO. 2 K= 30
IT NO. 3 K= 27
IT NO. 4 K= 24
IT NO. 5 K= 21
IT NO. 6 K= 18
IT NO. 7 K= 15
IT NO. 8 K= 12
IT NO. 9 K= 9
IT NO. 10 K= 6
IT NO. 11 K= 3
IT NO. 12 K= 0

35.00 35.00 35.00 35.00 35.00

35.00 34.74 34.74 34.74 38.25

35.00 34.49 34.49 34.49 37.50

35.00 34.23 34.23 34.23 36.75

35.00 33.98 33.98 33.98 36.00

UNIVERSITY OF IBADAN

35.00 33.73 33.73 33.73 35.25

35.00 33.48 33.48 33.48 34.50

35.00 33.24 33.24 33.24 33.75

35.00 32.99 32.99 32.99 33.00

35.00 32.75 32.75 32.75 32.25

35.00 32.51 32.51 32.51 31.50

35.00 32.27 32.27 32.27 30.75

30.00 30.00 30.00 30.00 30.00

1CONC DIST ON A FILM BY GAUSS-SEIDEL ITERATION/

IT NO. 0 K= 0
IT NO. 0 K= 0

1	.45000	.45000	.45000	.45000	.45000
2	.00000	.44533	.44533	.44533	.44487
3	.00000	.44069	.44069	.44069	.43980
4	.00000	.43606	.43606	.43606	.43479
5	.00000	.43144	.43144	.43144	.42984
6	.00000	.42684	.42684	.42684	.42494
7	.00000	.42224	.42224	.42224	.42010
8	.00000	.41765	.41765	.41765	.41531
9	.00000	.41306	.41306	.41306	.41058
10	.00000	.40847	.40847	.40847	.40590
11	.00000	.40388	.40388	.40388	.40128

UNIVERSITY OF IBADAN

12	.00000	.39928	.39928	.39928	.39671
13	.35800	.35800	.35800	.35800	.35800

At B=3.0

1VEL.DIST ON A FILM BY GAUSS-SEIDEL ITERATION//

.362000 .362000 .362000 .362000 .362000

.000000 .370146 .370146 .370146 .370146

.000000 .377477 .377477 .377477 .370146

.000000 .383993 .383993 .383993 .370146

.000000 .389695 .389695 .389695 .370146

.000000 .394582 .394582 .394582 .370146

.000000 .398655 .398655 .398655 .370146

.000000 .401914 .401914 .401914 .370146

.000000 .404360 .404360 .404360 .370146

.000000 .405991 .405991 .405991 .370146

UNIVERSITY OF IBADAN

.000000 .406808 .406808 .406808 .370146

.000000 .406811 .406811 .406811 .370146

.406000 .406000 .406000 .406000 .406000
1TEMP DIST ON A FILM BY GAUSS-SEIDEL ITERATION/

IT NO. 1 K= 55
IT NO. 2 K= 30
IT NO. 3 K= 27
IT NO. 4 K= 24
IT NO. 5 K= 21
IT NO. 6 K= 18
IT NO. 7 K= 15
IT NO. 8 K= 12
IT NO. 9 K= 9
IT NO. 10 K= 6
IT NO. 11 K= 3
IT NO. 12 K= 0

35.00 35.00 35.00 35.00 35.00

35.00 34.74 34.74 34.74 38.25

35.00 34.49 34.49 34.49 37.50

35.00 34.23 34.23 34.23 36.75

35.00 33.98 33.98 33.98 36.00

UNIVERSITY OF IBADAN

35.00 33.73 33.73 33.73 35.25

35.00 33.48 33.48 33.48 34.50

35.00 33.24 33.24 33.24 33.75

35.00 32.99 32.99 32.99 33.00

35.00 32.75 32.75 32.75 32.25

35.00 32.51 32.51 32.51 31.50

35.00 32.27 32.27 32.27 30.75

30.00 30.00 30.00 30.00 30.00

1CONC DIST ON A FILM BY GAUSS-SEIDEL ITERATION/

IT NO. 0 K= 0
IT NO. 0 K= 0

1	.45000	.45000	.45000	.45000	.45000
2	.00000	.44537	.44537	.44537	.44491
3	.00000	.44078	.44078	.44078	.43989
4	.00000	.43624	.43624	.43624	.43492
5	.00000	.43172	.43172	.43172	.43000
6	.00000	.42722	.42722	.42722	.42514
7	.00000	.42274	.42274	.42274	.42034
8	.00000	.41825	.41825	.41825	.41559
9	.00000	.41376	.41376	.41376	.41089
10	.00000	.40925	.40925	.40925	.40625

UNIVERSITY OF IBADAN

11	.00000	.40472	.40472	.40472	.40166
12	.00000	.40014	.40014	.40014	.39712
13	.35800	.35800	.35800	.35800	.35800

IN THE DIRECTION OF FILM THICKNESS
LiBr-H_2O

At B = 0.0

1VEL.DIST ON A FILM BY GAUSS-SEIDEL ITERATION//
IT NO. 1 K= 12
IT NO. 2 K= 3
IT NO. 3 K= 3
IT NO. 4 K= 3
IT NO. 5 K= 3
IT NO. 6 K= 3
IT NO. 7 K= 3
IT NO. 8 K= 3
IT NO. 9 K= 3
IT NO. 10 K= 3
IT NO. 11 K= 3
IT NO. 12 K= 3
IT NO. 13 K= 3
IT NO. 14 K= 3
IT NO. 15 K= 3
IT NO. 16 K= 3
IT NO. 17 K= 3
IT NO. 18 K= 3
IT NO. 19 K= 3
IT NO. 20 K= 3
IT NO. 21 K= 3
IT NO. 22 K= 3
IT NO. 23 K= 3
IT NO. 24 K= 3
IT NO. 25 K= 3
IT NO. 26 K= 3
IT NO. 27 K= 3
IT NO. 28 K= 3
IT NO. 29 K= 3
IT NO. 30 K= 3
IT NO. 31 K= 3
IT NO. 32 K= 3
IT NO. 33 K= 3
IT NO. 34 K= 3
IT NO. 35 K= 3
IT NO. 36 K= 3

UNIVERSITY OF IBADAN

IT NO. 37 K= 3
IT NO. 38 K= 3
IT NO. 39 K= 3
IT NO. 40 K= 3
IT NO. 41 K= 3
IT NO. 42 K= 3
IT NO. 43 K= 3
IT NO. 44 K= 3
IT NO. 45 K= 3
IT NO. 46 K= 3
IT NO. 47 K= 3
IT NO. 48 K= 3
IT NO. 49 K= 3
IT NO. 50 K= 3
IT NO. 51 K= 3
IT NO. 52 K= 3
IT NO. 53 K= 3
IT NO. 54 K= 3
IT NO. 55 K= 3
IT NO. 56 K= 3
IT NO. 57 K= 3
IT NO. 58 K= 3
IT NO. 59 K= 3
IT NO. 60 K= 3
IT NO. 61 K= 3
IT NO. 62 K= 3
IT NO. 63 K= 3
IT NO. 64 K= 3
IT NO. 65 K= 3
IT NO. 66 K= 3
IT NO. 67 K= 3
IT NO. 68 K= 3
IT NO. 69 K= 3
IT NO. 70 K= 3
IT NO. 71 K= 3
IT NO. 72 K= 3
IT NO. 73 K= 3
IT NO. 74 K= 3
IT NO. 75 K= 3
IT NO. 76 K= 3
IT NO. 77 K= 3
IT NO. 78 K= 3
IT NO. 79 K= 3
IT NO. 80 K= 3
IT NO. 81 K= 3
IT NO. 82 K= 3

UNIVERSITY OF IBADAN

IT NO. 83 K=   3
IT NO. 84 K=   3
IT NO. 85 K=   3
IT NO. 86 K=   2
IT NO. 87 K=   2
IT NO. 88 K=   2
IT NO. 89 K=   2
IT NO. 90 K=   2
IT NO. 91 K=   2
IT NO. 92 K=   2
IT NO. 93 K=   2
IT NO. 94 K=   2
IT NO. 95 K=   2
IT NO. 96 K=   2
IT NO. 97 K=   2
IT NO. 98 K=   2
IT NO. 99 K=   2
IT NO. 100 K=   2
.362000 .362000 .362000 .362000 .362000 .362000 .362000 .362000 .362000 .362000
.362000 .362000 .362000
.000000 .011294 .022194 .032522 .042115 .050824 .058517 .065081 .070426 .074480
.077199 .078558 .078558
.000000 .011299 .022202 .032534 .042129 .050839 .058532 .065095 .070437 .074490
.077205 .078562 .078558
.000000 .011303 .022211 .032545 .042142 .050853 .058546 .065109 .070449 .074499
.077212 .078565 .078558
.406000 .406000 .406000 .406000 .406000 .406000 .406000 .406000 .406000 .406000
.406000 .406000 .406000

1TEMP DIST ON A FILM BY GAUSS-SEIDEL ITERATION/

IT NO.   1 K=   39
IT NO.   2 K=   0
 44.44 44.44 44.44 44.44 44.44 44.44 44.44 44.44 44.44 44.44
 44.44 44.44 44.44
 35.00 35.19 35.19 35.19 37.55 35.19 35.19 35.19 35.19 35.19
 35.19 35.19 35.19
 35.00 35.13 35.13 35.13 36.70 35.13 35.13 35.13 35.13 35.13
 35.13 35.13 35.13
 35.00 35.06 35.06 35.06 35.85 35.06 35.06 35.06 35.06 35.06
 35.06 35.06 35.06
 35.00 35.00 35.00 35.00 35.00 35.00 35.00 35.00 35.00 35.00
 35.00 35.00 35.00

UNIVERSITY OF IBADAN

1CONC DIST ON A FILM BY GAUSS-SEIDEL ITERATION/

IT NO. 0 K= 0
IT NO. 0 K= 0
.60000.60000.60000.60000.60000.60000.60000.60000.60000.60000.60000 .60000.60000
.00000.08595.14838.19499.23041.25759.27847.29437.30619.31457.31991 .32251.32249
.00000.01231.03669.06335.08846.11057.12922.14441.15624.16491.17057.17335 .17334
.00000.00176.00907.02058.03396.04745.05996.07083 .07972.08645.09094.09317.09317
.54500.54500.54500.54500.54500.54500.54500.54500.54500.54500.54500.54500 .54500

At B= 1.4Tesla
1VEL.DIST ON A FILM BY GAUSS-SEIDEL ITERATION//
.362000.362000.362000.362000.362000.362000.362000.362000.362000.362000
.362000.362000.362000
.000000.011594.022762.033330.043134.052026.059875.066568.072015.076146
.078916.080301.080301
.000000.011598.022771.033342 .043148.052041.059889.066581.072027.076156
.078923.080304.080301
.000000.011603.022779.033353.043161.052055.059904 .066595.072038.076165
.078929.080308.080301
.406000.406000.406000.406000.406000.406000.406000.406000.406000.406000
.406000.406000.406000

1TEMP DIST ON A FILM BY GAUSS-SEIDEL ITERATION/
IT NO. 1 K= 39
IT NO. 2 K= 0
44.44 44.44 44.44 44.44 44.44 44.44 44.44 44.44 44.44 44.44
44.44 44.44 44.44
35.00 35.19 35.19 35.19 37.55 35.19 35.19 35.19 35.19 35.19
35.19 35.19 35.19
35.00 35.13 35.13 35.13 36.70 35.13 35.13 35.13 35.13 35.13
35.13 35.13 35.13
35.00 35.06 35.06 35.06 35.85 35.06 35.06 35.06 35.06 35.06
35.06 35.06 35.06
35.00 35.00 35.00 35.00 35.00 35.00 35.00 35.00 35.00 35.00
35.00 35.00 35.00

1CONC DIST ON A FILM BY GAUSS-SEIDEL ITERATION/
IT NO. 0 K= 0
IT NO. 0 K= 0
.60000.60000.60000.60000.60000.60000.60000.60000.60000.60000.60000.60000
.00000.08790.15122.19823.23381.26103.28189.29775.30954.31787.32319.32577.32576
.00000.01287.03810.06548.09109.11354.13242.14775.15967.16840.17409.17688.17687
.00000.00188.00960.02162.03548.04938.06220.07331.08236.08920.09377.09603.09603
.54500.54500.54500.54500.54500.54500.54500.54500.54500.54500.54500.54500.54500

UNIVERSITY OF IBADAN

At B=3.0Tesla

1VEL.DIST ON A FILM BY GAUSS-SEIDEL ITERATION//
.362000.362000.362000.362000.362000.362000.362000.362000.362000.362000
.362000.362000.362000
.000000.012669.024804.036232.046793.056342.064750.071906.077722.082129
.085083.086559.086559
.000000.012673.024812.036244.046807.056357.064764.071920.077734.082139
.085089.086562.086559
.000000.012678.024821.036255.046821.056371.064779.071933.077745.082148
.085095.086566 .086559
.406000.406000.406000.406000.406000.406000.406000.406000.406000.406000
.406000.406000.406000

1TEMP DIST ON A FILM BY GAUSS-SEIDEL ITERATION/
IT NO. 1 K= 39
IT NO. 2 K= 0
44.44 44.44 44.44 44.44 44.44 44.44 44.44 44.44 44.44 44.44
44.44 44.44 44.44
35.00 35.19 35.19 35.19 37.55 35.19 35.19 35.19 35.19 35.19
35.19 35.19 35.19
35.00 35.13 35.13 35.13 36.70 35.13 35.13 35.13 35.13 35.13
35.13 35.13 35.13
35.00 35.06 35.06 35.06 35.85 35.06 35.06 35.06 35.06 35.06
35.06 35.06 35.06
35.00 35.00 35.00 35.00 35.00 35.00 35.00 35.00 35.00 35.00
35.00 35.00 35.00

1CONC DIST ON A FILM BY GAUSS-SEIDEL ITERATION/

IT NO. 0 K= 0
IT NO. 0 K= 0
.60000.60000.60000.60000.60000.60000.60000.60000.60000.60000.60000 .60000
.00000.09476.16114.20946.24552.27283.29361.30932.32094.32914.33437.33691 .33690
.00000.01496.04326.07310.10045.12404.14366.15945.17166.18055.18634.18917 .18916
.00000.00236.01161.02551.04109.05639.07028 .08218.09181.09904.10384.10621.10621
.54500.54500.54500.54500.54500.54500.54500.54500.54500.54500.54500.54500 .54500

UNIVERSITY OF IBADAN

LiCl-H_2O
At B=0.0Tesla

1VEL.DIST ON A FILM BY GAUSS-SEIDEL ITERATION//
IT NO. 1 K= 12
IT NO. 2 K= 3
IT NO. 3 K= 3
IT NO. 4 K= 3
IT NO. 5 K= 3
IT NO. 6 K= 3
IT NO. 7 K= 3
IT NO. 8 K= 3
IT NO. 9 K= 3
IT NO. 10 K= 3
IT NO. 11 K= 3
IT NO. 12 K= 3
IT NO. 13 K= 3
IT NO. 14 K= 3
IT NO. 15 K= 3
IT NO. 16 K= 3
IT NO. 17 K= 3
IT NO. 18 K= 3
IT NO. 19 K= 3
IT NO. 20 K= 3
IT NO. 21 K= 3
IT NO. 22 K= 3
IT NO. 23 K= 3
IT NO. 24 K= 3
IT NO. 25 K= 3
IT NO. 26 K= 3
IT NO. 27 K= 3
IT NO. 28 K= 3
IT NO. 29 K= 3
IT NO. 30 K= 3
IT NO. 31 K= 3
IT NO. 32 K= 3
IT NO. 33 K= 3
IT NO. 34 K= 3
IT NO. 35 K= 3
IT NO. 36 K= 3
IT NO. 37 K= 3
IT NO. 38 K= 3
IT NO. 39 K= 3
IT NO. 40 K= 3
IT NO. 41 K= 3
IT NO. 42 K= 3

UNIVERSITY OF IBADAN

IT NO. 43 K= 3
IT NO. 44 K= 3
IT NO. 45 K= 3
IT NO. 46 K= 3
IT NO. 47 K= 3
IT NO. 48 K= 3
IT NO. 49 K= 3
IT NO. 50 K= 3
IT NO. 51 K= 3
IT NO. 52 K= 3
IT NO. 53 K= 3
IT NO. 54 K= 3
IT NO. 55 K= 3
IT NO. 56 K= 3
IT NO. 57 K= 3
IT NO. 58 K= 3
IT NO. 59 K= 3
IT NO. 60 K= 3
IT NO. 61 K= 3
IT NO. 62 K= 3
IT NO. 63 K= 3
IT NO. 64 K= 3
IT NO. 65 K= 3
IT NO. 66 K= 3
IT NO. 67 K= 3
IT NO. 68 K= 3
IT NO. 69 K= 3
IT NO. 70 K= 3
IT NO. 71 K= 3
IT NO. 72 K= 3
IT NO. 73 K= 3
IT NO. 74 K= 3
IT NO. 75 K= 3
IT NO. 76 K= 3
IT NO. 77 K= 3
IT NO. 78 K= 3
IT NO. 79 K= 3
IT NO. 80 K= 3
IT NO. 81 K= 3
IT NO. 82 K= 3
IT NO. 83 K= 3
IT NO. 84 K= 3
IT NO. 85 K= 3
IT NO. 86 K= 3
IT NO. 87 K= 3
IT NO. 88 K= 3

UNIVERSITY OF IBADAN

IT NO. 89 K=   3
IT NO. 90 K=   3
IT NO. 91 K=   3
IT NO. 92 K=   3
IT NO. 93 K=   3
IT NO. 94 K=   3
IT NO. 95 K=   3
IT NO. 96 K=   3
IT NO. 97 K=   3
IT NO. 98 K=   3
IT NO. 99 K=   3
IT NO. 100 K=   3
.362000 .362000 .362000 .362000 .362000 .362000 .362000 .362000 .362000 .362000
.362000 .362000 .362000
.000000 .011294 .022194 .032522 .042115 .050824 .058517 .065081 .070426 .074480
.077199 .078558 .078558
.000000 .011299 .022202 .032534 .042129 .050839 .058532 .065095 .070437 .074490
.077205 .078562 .078558
.000000 .011303 .022211 .032545 .042142 .050853 .058546 .065109 .070449 .074499
.077212 .078565 .078558
.406000 .406000 .406000 .406000 .406000 .406000 .406000 .406000 .406000 .406000
.406000 .406000 .406000

1TEMP DIST ON A FILM BY GAUSS-SEIDEL ITERATION/

IT NO.   1 K=   39
IT NO.   2 K=   0
 35.00 35.00 35.00 35.00 35.00 35.00 35.00 35.00 35.00 35.00
 35.00 35.00 35.00
 35.00 30.17 30.17 30.17 30.17 30.17 30.17 30.17 30.17 30.17
 30.17 30.17 32.25
 35.00 30.11 30.11 30.11 30.11 30.11 30.11 30.11 30.11 30.11
 30.11 30.11 31.50
 35.00 30.05 30.05 30.05 30.05 30.05 30.05 30.05 30.05 30.05
 30.05 30.05 30.75
 30.00 30.00 30.00 30.00 30.00 30.00 30.00 30.00 30.00 30.00
 30.00 30.00 30.00

1CONC DIST ON A FILM BY GAUSS-SEIDEL ITERATION/

IT NO.   0 K=   0
IT NO.   0 K=   0
.45000.45000.45000.45000.45000.45000.45000.45000.45000.45000.45000 .45000
.00000.05938.10350.13699.16278.18276.19823.21007.21892.22521.22923.23119 .23118
.00000.00783.02380.04169.05887.07421.08731.09806.10650.11270.11677.11877 .11876
.00000.00103.00547.01269.02129.03013.03845.04577.05180.05640.05948.06102 .06101

UNIVERSITY OF IBADAN

.35800.35800.35800.35800.35800.35800.35800.35800.35800.35800.35800.35800 .35800

At B= 1.4Tesla

1VEL.DIST ON A FILM BY GAUSS-SEIDEL ITERATION//

.362000 .362000 .362000 .362000 .362000 .362000 .362000 .362000 .362000 .362000
.362000 .362000 .362000
.000000 .011506 .022596 .033095 .042837 .051676 .059479 .066134 .071551 .075661
.078415 .079793 .079793
.000000 .011511 .022605 .033106 .042851 .051690 .059493 .066148 .071563 .075670
.078422 .079796 .079793
.000000 .011515 .022613 .033118 .042864 .051705 .059508 .066162 .071575 .075679
.078428 .079799 .079793
.406000 .406000 .406000 .406000 .406000 .406000 .406000 .406000 .406000 .406000
.406000 .406000 .406000

1TEMP DIST ON A FILM BY GAUSS-SEIDEL ITERATION/

IT NO. 1 K= 39
IT NO. 2 K= 0
35.00 35.00 35.00 35.00 35.00 35.00 35.00 35.00 35.00 35.00
35.00 35.00 35.00
35.00 30.17 30.17 30.17 30.17 30.17 30.17 30.17 30.17 30.17
30.17 30.17 32.25
35.00 30.11 30.11 30.11 30.11 30.11 30.11 30.11 30.11 30.11
30.11 30.11 31.50
35.00 30.05 30.05 30.05 30.05 30.05 30.05 30.05 30.05 30.05
30.05 30.05 30.75
30.00 30.00 30.00 30.00 30.00 30.00 30.00 30.00 30.00 30.00
30.00 30.00 30.00

1CONC DIST ON A FILM BY GAUSS-SEIDEL ITERATION/

IT NO. 0 K= 0
IT NO. 0 K= 0
.45000.45000.45000.45000.45000.45000.45000.45000.45000.45000.45000.45000 .45000
.00000.06034.10494.13866.16455.18457.20004.21187.22071.22698.23099.23294 .23293
.00000.00809.02446.04272.06016.07569.08891.09974.10824.11448.11857.12058 .12057
.00000.00108.00570.01316.02199.03103.03951.04695.05308.05774.06086.06241 .06241
.35800.35800.35800.35800.35800.35800.35800.35800.35800.35800.35800.35800 .35800

At B= 3.0Tesla

1VEL.DIST ON A FILM BY GAUSS-SEIDEL ITERATION//

UNIVERSITY OF IBADAN

.362000 .362000 .362000 .362000 .362000 .362000 .362000 .362000 .362000 .362000
.362000 .362000 .362000
.000000 .012268 .024043 .035151 .045430 .054733 .062933 .069916 .075595 .079899
.082784 .084227 .084227
.000000 .012273 .024051 .035162 .045443 .054748 .062947 .069930 .075606 .079909
.082791 .084230 .084227
.000000 .012277 .024060 .035173 .045457 .054763 .062962 .069944 .075618 .079918
.082797 .084233 .084227
.406000 .406000 .406000 .406000 .406000 .406000 .406000 .406000 .406000 .406000
.406000 .406000 .406000

1TEMP DIST ON A FILM BY GAUSS-SEIDEL ITERATION/

IT NO. 1 K= 39
IT NO. 2 K= 0
35.00 35.00 35.00 35.00 35.00 35.00 35.00 35.00 35.00 35.00
35.00 35.00 35.00
35.00 30.17 30.17 30.17 30.17 30.17 30.17 30.17 30.17 30.17
30.17 30.17 32.25
35.00 30.11 30.11 30.11 30.11 30.11 30.11 30.11 30.11 30.11
30.11 30.11 31.50
35.00 30.05 30.05 30.05 30.05 30.05 30.05 30.05 30.05 30.05
30.05 30.05 30.75
30.00 30.00 30.00 30.00 30.00 30.00 30.00 30.00 30.00 30.00
30.00 30.00 30.00

1CONC DIST ON A FILM BY GAUSS-SEIDEL ITERATION/

IT NO. 0 K= 0
IT NO. 0 K= 0
.45000.45000.45000.45000.45000.45000.45000.45000.45000.45000.45000 .45000
.00000.06377.11001.14450.17072.19085.20632.21811.22689.23311.23708.23901 .23900
.00000.00903.02689.04639.06476.08093.09459.10571.11439.12074.12490.12694 .12693
.00000.00128.00657.01489.02456.03431.04336.05123.05766.06254.06580.06742 .06742
.35800.35800.35800.35800.35800.35800.35800.35800.35800.35800.35800 .35800

UNIVERSITY OF IBADAN

APPENDIX D

GAUSSIAN ELIMINATION

Gaussian elimination is direct method for solving sets of simultaneous linear algebraic equations of the general form

$$
\begin{aligned}
&a_{11}x_1 + a_{12}x_2 + \ldots\ldots\ldots\ldots\ldots + a_{1n}x_n = b_1 \\
&a_{21}x_1 + a_{22}x_2 + \ldots\ldots\ldots\ldots\ldots + a_{2n}x_n = b_2 \\
&a_{31}x_1 + a_{32}x_2 + \ldots\ldots\ldots\ldots\ldots + a_{3n}x_n = b_3 \qquad \text{(D.1)} \\
&\qquad\qquad \ldots\ldots\ldots\ldots \\
&\qquad\qquad \ldots\ldots\ldots\ldots \\
&\qquad\qquad \ldots\ldots\ldots\ldots \\
&\qquad\qquad \ldots\ldots\ldots\ldots \\
&a_{n1}x_1 + a_{n2}x_2 + \ldots\ldots\ldots\ldots\ldots + a_{nn}x_n = b_n
\end{aligned}
$$

where $x_1, x_2, x_3 \ldots\ldots\ldots x_n$ are the unknowns and the coefficients a_{ij} and b_i are all known constants. This set of equations can be expressed in matrix form as follows

$$
\begin{bmatrix}
a_{11} & a_{12} \ldots\ldots\ldots\ldots\ldots a_{1n} \\
a_{11} & a_{12} \ldots\ldots\ldots\ldots\ldots a_{1n} \\
\ldots\ldots\ldots\ldots\ldots\ldots & \ldots \\
\ldots\ldots\ldots\ldots\ldots\ldots & \ldots \\
\ldots\ldots\ldots\ldots\ldots\ldots & \ldots \\
a_{n1} & a_{n2} \ldots\ldots\ldots\ldots\ldots a_{nn}
\end{bmatrix}
\begin{bmatrix} x_1 \\ x_2 \\ \ldots \\ \ldots \\ \ldots \\ x_n \end{bmatrix}
=
\begin{bmatrix} b_1 \\ b_2 \\ \ldots \\ \ldots \\ \ldots \\ b_n \end{bmatrix}
\qquad \text{(D.2)}
$$

$$
AX = B \qquad \text{(D.3)}
$$

The unknowns are successfully eliminated by algebraic manipulations. The first equation can be used to eliminate x_1 from the remaining n-1 equations. The modified second equation is then used to eliminate x_2 from the remaining n-2 equations and so on until the last equation contains only x_n. Thus x_n may be found, followed by all the other unknowns by back substitution. Let the coefficient shown in equation b_1 and b_2 be given by the notation $a_{ij}^1 = a_i^1$;

UNIVERSITY OF IBADAN

After the K_{th} elimination the modified coefficient are:-

$$a_{ij}^{k+1} = a_{ij}^{k} - \phi a_{kj}^{k}$$

$$b_{1}^{k+1} = b_{1}^{k} - \phi b_{k}^{k}\omega \qquad \text{(D.4)}$$

where j = k, k+1……..n

The final set of equations is

$$a_{11}^{1}x_1 + a_{12}^{1}x_2 + \ldots\ldots\ldots\ldots + a_{1n}^{1}x_n = b_1^1$$

$$a_{22}x_2 + \ldots\ldots\ldots\ldots\ldots\ldots a_{2n}x_n = b_2$$

$$+\ldots\ldots\ldots\ldots + = \ldots$$

$$+\ldots\ldots\ldots + = \ldots \qquad \text{(D.5)}$$

$$+\ldots\ldots + = \ldots$$

$$a_{nn}x_n = b$$

The unknown are obtained in reverse order

$$x_n = \frac{b_n^n}{a_{nn}^n} \qquad \text{(D.6)}$$

$$x_n = \frac{b_i^i - \sum_{j=i+i}^{n} a_{ij}^i x_j}{a_{ii}^i} \qquad \text{(D.7)}$$

UNIVERSITY OF IBADAN